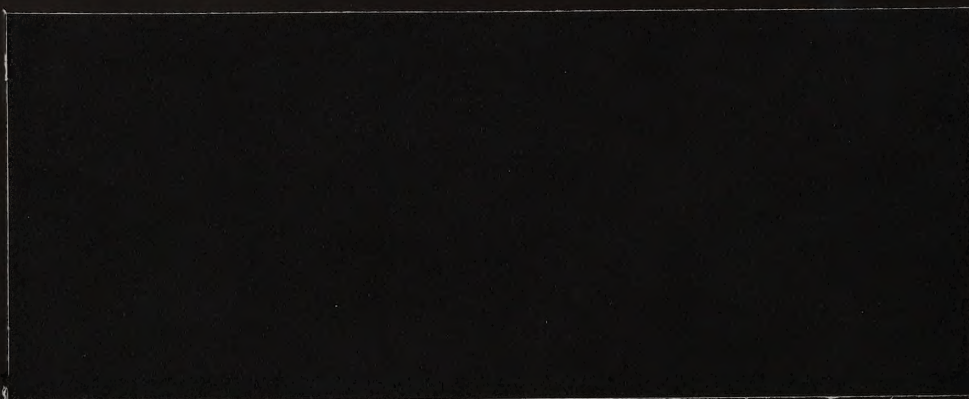


HYDROGEOLOGIC AND CHEMICAL ANALYSES
FOR THE PROPOSED GUADALUPE MOUNTAIN TAILINGS
DISPOSAL SITE GROUND-WATER DISCHARGE PLAN,
TAOS COUNTY, NEW MEXICO

Report to
MolyCorp, Inc., Questa Division
Questa, New Mexico

July 7, 1987

Dames & Moore



#903214778

ID 88068217

TN

321

.N6

D364

1987

HYDROGEOLOGIC AND CHEMICAL ANALYSES
FOR THE PROPOSED GUADALUPE MOUNTAIN TAILINGS
DISPOSAL SITE GROUND-WATER DISCHARGE PLAN,
TAOS COUNTY, NEW MEXICO

Report to
Molycorp, Inc., Questa Division
Questa, New Mexico

July 7, 1987

Dames & Moore

DAMES & MOORE

7500 North Dreamy Draw Drive

Suite 145

Phoenix, Arizona 85020

(602) 371-1110



Summary

Table of Contents

SUMMARY AND DISCUSSION

In May 1985, Dames & Moore was retained by MolyCorp to expand on previous hydrogeologic investigations pertaining to the siting of a new tailings disposal facility at the Questa Division. The focus of Dames & Moore's investigations has been the evaluation of ground-water flow patterns, ambient ground-water quality, and possible impacts of tailings leachate to ambient ground-water quality in the area near the confluence of the Red River and Rio Grande.

The scope of work involved the performance of the following major tasks, each of which included several subtasks:

Task 1: Field Studies:

- o Drilling for geologic and hydrogeologic information.
- o Water-level measurements in wells.
- o Ground- and surface-water sampling.
- o Discharge measurements of springs.
- o Geologic reconnaissance.

Task 2: Laboratory Studies:

- o Adsorption experiments.
- o Leaching experiments.
- o Radioisotope analyses.

Task 3: Office Analyses:

- o Evaluation of the probable direction and movement of ground water and leachate.
- o Establishment of a data base for ambient ground-water quality, leachate chemistry, and ambient surface-water quality.
- o Evaluation of the impact of leachate on ambient ground-water quality.
- o Computer modeling of leachate movement and attenuation in the vadose zone.

In addition, representatives of Vail Engineering, Inc., and MolyCorp geologists studied surface and subsurface geologic units and structural geologic features in the study area and, with Dames & Moore, reviewed seepage-run data for the Red River and Rio Grande.

As a result of the work performed thus far, the following findings have been made:

- 1) Drilling on Guadalupe Mountain identified the ground-water level to be approximately 785 feet below the base of the proposed pond. The upper 644 feet of volcanics show good potential for leachate attenuation and adsorption. Below 644 feet, the rock units are highly fractured and show good potential for significant ground-water flow and eventual leachate dilution below the water table.

- 2) Our analyses indicate that a substantial amount of ground water flows under the proposed tailings pond site. This flow is in a general southwestern direction to the Red River Fault Zone. At this zone, ground-water flow is deflected, in part, by a dacite flow that fills a westerly-trending paleo valley that reaches the Rio Grande gorge near Big Arsenic Springs. As a result, it is anticipated that most of the ground water flowing under the proposed tailings pond site is discharged in the vicinity of the Big Arsenic Springs complex.
- 3) In the Red River Canyon, the river level upstream of approximately the Fish Hatchery is above the regional water table that exists beneath the proposed tailings pond. Therefore, ground water flowing under the proposed tailings pond would not discharge to the Red River upstream of the Fish Hatchery area. Similarly, the elevation of the Rio Grande upstream of approximately Cerro Chiflo is above the regional water table.
- 4) Springs along the Rio Grande are connected to the regional aquifer, as identified by chemical, radioisotope, and flow measurement data.
- 5) Springs along the lower Red River discharge regional aquifer water and water held in stream bank storage. These discharge data are supported by chemical, radioisotope, flow measurement, and river seepage analyses.
- 6) Springs along the upper Red River show a hydraulic connection with the surface-water system as well as with the regional aquifer, as suggested by analyses of chemical, radioisotope, and spring flow measurement data. These springs are not related to ground water flowing under Guadalupe Mountain.
- 7) Average ambient ground-water quality is within New Mexico State Ground Water Standards.
- 8) Average ambient surface-water quality is within New Mexico State Ground Water Standards. However, regional mineralization combined with seasonal precipitation causes short-lived adverse impacts to surface-water quality in some portions of the Red River.
- 9) Results of leaching experiments indicate that tailings-pond leachate will not preferentially leach radioisotopes found in rock units beneath Guadalupe Mountain.
- 10) Adsorption trials indicate excellent leachate constituent adsorption potential, especially for metals, in the vadose zone beneath the proposed tailings pond.
- 11) Computer simulation of leachate movement in the vadose zone and mixing beneath the water table indicates that: 1) Metals are essentially fully adsorbed and attenuated in the vadose zone. Metals concentrations are negligible at the water table. 2) Total dissolved solids and sulphate are not attenuated in the vadose zone. Concentrations of these parameters may exceed New Mexico

State Ground Water Standards at the water table immediately beneath the proposed pond and prior to dilution.

- 12) Average ground-water flow across a line from Cerro Chiflo to the head of Red River Canyon (about a 5-mile straight-line distance) is at least 50 cfs. Therefore, the average ground-water flow is at least 10 cfs per linear mile within the ground-water flow system. Most of this flow is in volcanics.

Based on the findings of this study, there should be no adverse impact to either surface-water or ground-water quality due to seepage from the proposed tailings pond. Supporting evidence is:

- o Tailing leachate toxicity tests using invertebrates found in the Big Arsenic Springs area showed no adverse impacts resulting from exposure of the invertebrates to tailings leachate.
- o The leaching, adsorption, and vadose-zone modeling studies show that metals will essentially be fully absorbed and attenuated in the vadose zone (Section 7.0).
- o Total dissolved solids and sulphates are not expected to be sufficiently attenuated in the vadose zone to meet New Mexico State Ground Water Standards at the water table. Modeling studies (Section 7.0) were based on very conservative estimates of ground-water underflow, which in turn were based on qualitative data from available test holes. These modeling studies, using an underflow estimate of 0.5 cfs, indicated an approximate 1:1 ratio of effluent to underflow. However, subsequent analysis of spring discharge and of available accretion data for the Red River and Rio Grande indicates that over 10 cfs of ground-water underflow is available for dilution (Section 3.0). Thus, total dissolved solids and sulphates should be diluted to well within New Mexico Ground Water Standards near the claim boundary; there, the ratio of underflow to effluent could be greater than 20:1. Thus, there should be no violation of down-gradient water-quality standards.

TABLE OF CONTENTS

	<u>Page</u>
SUMMARY AND DISCUSSION	S-1
LIST OF PLATES	iii
LIST OF FIGURES.	iv
LIST OF TABLES	vii
1.0 INTRODUCTION.	1-1
1.1 PROJECT HISTORY.	1-1
1.2 OVERVIEW OF WORK TO-DATE	1-1
1.3 REGIONAL GEOLOGY	1-2
1.4 REGIONAL HYDROGEOLOGY.	1-3
2.0 GUADALUPE MOUNTAIN TAILINGS DISPOSAL SITE	2-1
2.1 SITE SELECTION AND GENERAL SITE GEOLOGY.	2-1
2.2 GUADALUPE NO. 1 TEST HOLE.	2-2
2.3 GUADALUPE NO. 2 TEST HOLE.	2-5
2.4 GUADALUPE NO. 3 TEST HOLE.	2-6
2.5 EXISTING WELLS	2-8
2.5.1 BLM WELLS	2-8
2.5.2 U.S. ARMY CORPS OF ENGINEERS CHIFLO DAM TEST HOLES	2-9
2.5.3 QUESTA AND CERRO MUNICIPAL PRODUCTION WELLS.	2-9
3.0 GROUND-WATER OCCURRENCE, MOVEMENT, AND DISCHARGE, GUADALUPE MOUNTAIN REGION.	3-1
3.1 GENERAL OCCURRENCE OF GROUND WATER	3-1
3.2 CONTROLS TO GROUND-WATER MOVEMENT	3-2
3.3 DIRECTIONS AND GRADIENTS OF GROUND-WATER FLOW	3-4
3.4 GROUND-WATER DISCHARGE	3-6
3.4.1 ACCRETION MEASUREMENTS.	3-6
3.4.2 ACCRETION TO THE RED RIVER	3-7
3.4.3 ACCRETION TO THE RIO GRANDE	3-11
3.4.4 AGE OF GROUND-WATER DISCHARGING TO SPRINGS.	3-14
3.5 BIG ARSENIC SPRINGS COMPLEX AS A SPECIAL CASE OF GROUND-WATER DISCHARGE	3-16
3.6 DISCUSSION OF GROUND-WATER UNDERFLOW AND DISCHARGE	3-17
4.0 CINDER LEACH TEST	4-1
5.0 ADSORPTION EXPERIMENTS	5-1
5.1 TEST RESULTS	5-3
5.2 X-RAY DIFFRACTION ANALYSIS	5-4
6.0 WATER QUALITY	6-1
6.1 AMBIENT GROUND-WATER QUALITY	6-1
6.2 SURFACE-WATER QUALITY.	6-5

TABLE OF CONTENTS

	<u>Page</u>
6.3 LEACHATE CHEMISTRY	6-7
7.0 SIMULATION OF CONTAMINANT TRANSPORT BENEATH THE PROPOSED GUADALUPE MOUNTAIN TAILINGS DISPOSAL SITE	7-1
7.1 INTRODUCTION	7-1
7.2 TECHNICAL APPROACH	7-2
7.3 SITE-SPECIFIC DATA	7-7
7.4 PREDICTED RESULTS	7-11
7.4.1 SUMMARY OF SIMULATIONS	7-11
7.4.2 PHYSICAL SENSITIVITY ANALYSES	7-16
7.4.3 NUMERICAL SENSITIVITY ANALYSES	7-20
7.5 CONCLUSIONS	7-23
8.0 REFERENCES	8-1
APPENDICES:	
A) GEOLOGIC AND COMPLETION LOGS, GUADALUPE MOUNTAIN AREA WELLS	
B) GRAPHIC SOLUTIONS OF GROUND-WATER FLOW DIRECTION AND GRADIENT	
C) CINDER LEACH TESTS: LABORATORY REPORT OF ANALYSES	
D) ADSORPTION CAPACITY TESTS ON BEDROCK AND BRECCIA SAMPLES: LABORATORY REPORT OF ANALYSES	
E) DESCRIPTION OF WATER QUALITY SAMPLING LOCATIONS	
F) SUMMARY OF TARGET MODELS	
G) CRITICAL REVIEWS OF TARGET MODEL	
H) PREDICTED CONCENTRATION PLUMES	

LIST OF PLATES

(Located in Pocket at Back of Report)

	Geologic Map of the Guadalupe Mountain Area, Taos County, New Mexico	1-1
1	Geologic Map of the Guadalupe Mountain Area, Taos County, New Mexico	1-1
2	Geologic Sections Along the Rio Grande Gorge and Red River Canyon, Taos County, New Mexico	2-2
3	Geologic Cross Section, Guadalupe Mountain Area, Taos County, New Mexico	3-3
4	Geologic Cross Section, Arsenic Springs Area, Taos County, New Mexico	3-10
5	Generalized Ground-Water Flow, Guadalupe Mountain, Taos County, New Mexico	3-3
6.1	Diagram of Average Water Quality Parameters	4-2
7.1	Ground-Water Model Location Map	7-4
7.2	Finite Difference Mesh used in Case 1 (Flow 1)	7-1
7.3	Estimated Unsaturated Properties of Fractured Bedrock	7-11
7.4	Contours of Hydraulic Head During Flood Operation	7-12
7.5	Time History of Concentration as a Function of Adsorption Distribution Coefficient	7-23
	(A) Beneath Pond, Just Below Water Table	
	(B) At Down-Gradient Drain Boundary	
7.6	Time History of Anion Concentrations as a Function of Pond Seepage Rate	7-16
	(A) Beneath Pond, Just Below Water Table	
	(B) At Down-Gradient Drain Boundary	
7.7	Time History of Metal Concentrations as a Function of Pond Seepage Rate	7-24
	(A) Beneath Pond, Just Below Water Table	
	(B) At Down-Gradient Drain Boundary	

LIST OF FIGURES

<u>Figure No.</u>	<u>Follows Page</u>
1.1 Location Map of Guadalupe Tailings Disposal Site . .	1-1
2.1 Map of Guadalupe Mountain Tailings Disposal Site . .	2-1
2.2 Map of Guadalupe Mountain Monitoring Locations . . .	2-2
3.1 Rose Diagram of Ground-Water Flow Direction Solutions, Guadalupe Mountain and Confluence Area .	3-5
3.2 Stiff Diagram of Big Arsenic Spring, Rio Grande, and BLM-Headquarters Water Quality	3-16
5.1 Lead Adsorption Isotherm: Breccia and Solution Concentrations	5-3
5.2 Molybdenum Adsorption Isotherm: Breccia and Solution Concentrations	5-3
6.1 Diagram of Average Water Quality Parameters.	6-2
7.1 Ground-Water Model Location Map	7-4
7.2 Finite Difference Mesh used in Cases 2 thru 16 . . .	7-5
7.3 Estimated Unsaturated Properties of Fractured Bedrock	7-11
7.4 Contours of Hydraulic Head During Pond Operation . .	7-12
7.5 Time History of Concentration as a Function of Adsorption Distribution Coefficient	7-13
(A) Beneath Pond, Just Below Water Table	
(B) At Down-Gradient Claim Boundary	
7.6 Time History of Anion Concentrations as a Function of Pond Seepage Rate	7-16
(A) Beneath Pond, Just Below Water Table	
(B) At Down-Gradient Claim Boundary	
7.7 Time History of Metal Concentrations as a Function of Pond Seepage Rate	7-16
(A) Beneath Pond, Just Below Water Table	
(B) At Down-Gradient Claim Boundary	

LIST OF FIGURES (Continued)

<u>Figure No.</u>		<u>Follows Page</u>
7.8	Time History of Anion Concentrations as a Function of Saturated Thickness	7-17
	(A) Beneath Pond, Just Below Water Table	
	(B) At Down-Gradient Claim Boundary	
7.9	Time History of Anion Concentrations as a Function of Hydraulic Gradient	7-18
	(A) Beneath Pond, Just Below Water Table	
	(B) At Down-Gradient Claim Boundary	
7.10	Time History of Anion Concentrations as a Function of Hydraulic Conductivity Anisotropy	7-19
	(A) Beneath Pond, Just Below Water Table	
	(B) At Down-Gradient Claim Boundary	
7.11	Time History of Metal Concentrations as a Function of Hydraulic Conductivity Anisotropy	7-19
	(A) Beneath Pond, Just Below Water Table	
	(B) At Down-Gradient Claim Boundary	
7.12	Time History of Anion Concentrations as a Function of Hydraulic Conductivity	7-19
	(A) Beneath Pond, Just Below Water Table	
	(B) At Down-Gradient Claim Boundary	
7.13	Time History of Metal Concentrations as a Function of Hydraulic Conductivity	7-19
	(A) Beneath Pond, Just Below Water Table	
	(B) At Down-Gradient Claim Boundary	
7.14	Finite Difference Mesh Used to Test Sensitivity to Boundary Locations	7-20
7.15	Time History of Anion Concentrations as a Function of Boundary Location	7-20
	(A) Beneath Pond, Just Below Water Table	
	(B) At Down-Gradient Claim Boundary	
7.16	Time History of Anion Concentrations as a Function of Timestep	7-21
	(A) Beneath Pond, Just Below Water Table	
	(B) At Down-Gradient Claim Boundary	

LIST OF FIGURES (Continued)

<u>Figure No.</u>	<u>Follows Page</u>
7.17	
Time History of Metal Concentrations as a Function of Timestep	7-21
(A) Beneath Pond, Just Below Water Table	
(B) At Down-Gradient Claim Boundary	
7.18	
Time History of Metal Concentrations as a Function of Relaxation Factor and Convergence Criteria: . . .	7-22
Beneath Pond, Just Below Water Table	
7.19	
Variation of Concentrations at Water Table With Pond Seepage Rate	7-23

LIST OF TABLES

<u>Table No.</u>	<u>Page</u>
3.1 Water-Level Measurements, Guadalupe Mountain Area.	3-5
3.2 Summary of Accretion to Red River and Rio Grande . .	3-9
3.3 Spring Flow Data	3-15
3.4 Analyses of Tritium and of Gross Alpha and Beta Activity for Spring Waters.	3-15
4.1 Results of Gamma Spectral Analysis Results of Cinders and Bedrock, Guadalupe No. 1	4-1
4.2 Cinders Leaching Test Results.	4-3
5.1 Minerals Detected in the Fine Fraction of Bedrock and Breccia Via X-Ray Diffraction Guadalupe No. 1 Test Hole.	5-5
6.1 Mean Water Quality of Ambient Ground Water, Surface Water, and Leachate	6-2
6.2 Comparison of Ambient Ground-Water Quality to New Mexico State Ground-Water Standards.	6-3
6.3 Comparison of Surface-Water Quality to New Mexico State Ground-Water Standards.	6-6
6.4 Comparison of Leachate/Tailing Area Water Quality to New Mexico State Ground-Water Standards.	6-8
7.1 Geologic and Hydrogeologic Data for Units Beneath Guadalupe Mountain	7-8
7.2 Derivation of Adsorption Distribution Coefficients for Medium Kd case	7-9
7.3 Transport Model Case Descriptions	7-12
7.4 (A) Predicted Concentrations for Average Case: At Water Table Beneath Pond	7-14
(B) Predicted Concentrations for Average Case: At Down-Gradient Claim Boundary	7-15
7.5 Comparison of Peak Anion Concentrations with Varying Hydraulic Gradients	7-18

1.0 INTRODUCTION

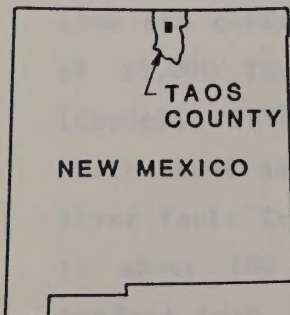
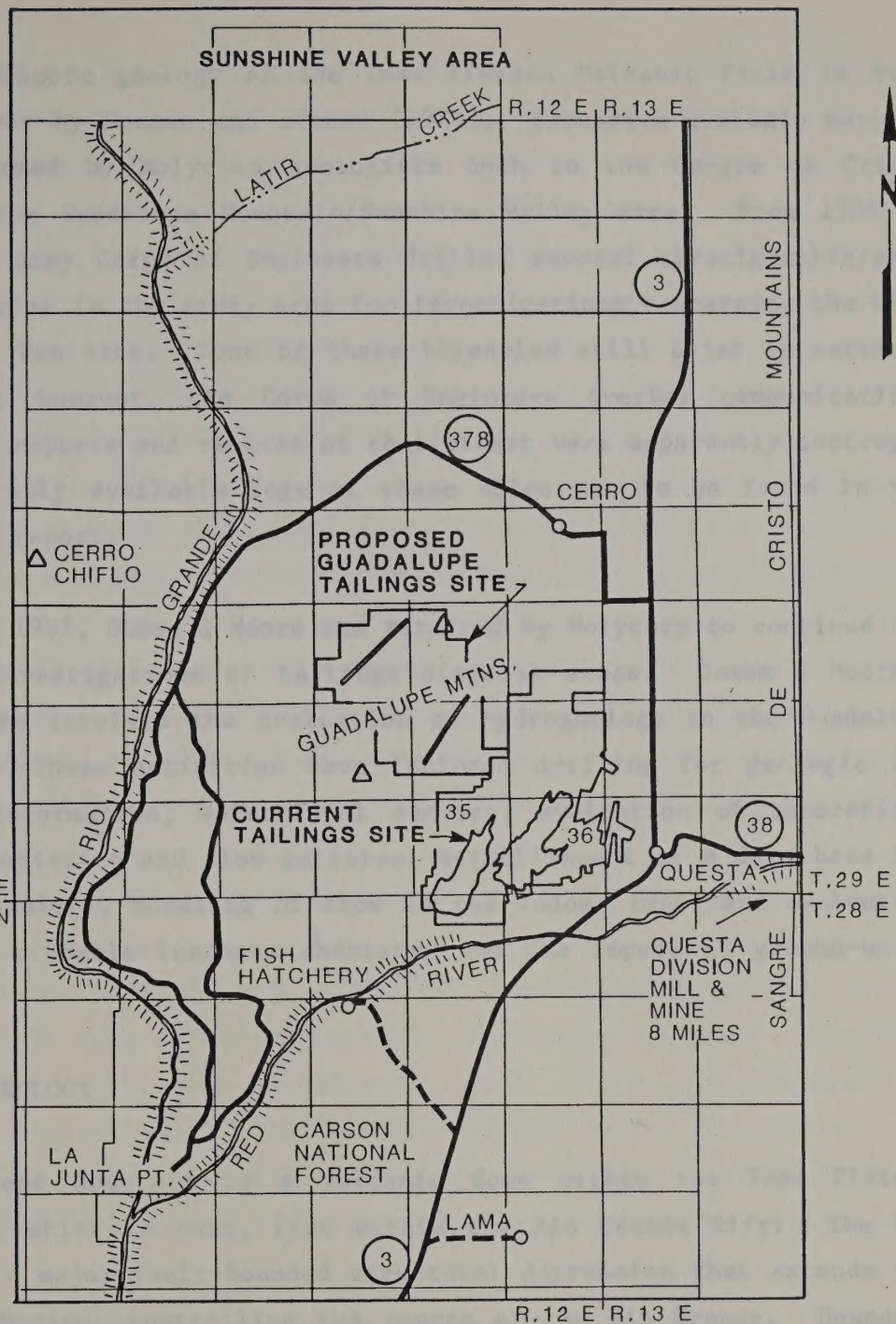
1.1 PROJECT HISTORY

Molycorp has mined molybdenum at the Questa Division since 1965. For most of that time, tailings slurry has been piped approximately 8 miles downstream from the mill along the Red River to the Sections 35 and 36 disposal areas, which are located directly west of the Town of Questa, New Mexico (Figure 1.1). These tailings disposal sites currently encompass approximately 450 acres.

In 1978, Molycorp began a search for a new tailings disposal site. Since then, several consulting firms have been retained by Molycorp to conduct hydrogeologic investigations. In May 1985, Dames & Moore was retained to continue field investigations at the various proposed sites and to refine and supplement the work of previous and current investigators. As of January 1986, Molycorp and the State of New Mexico agreed to investigate one primary potential site located in the saddle of the Guadalupe Mountains northwest of Questa (Figure 1.1). Other potential sites, such as Latir Creek drainage and the Open Pit at the mine site, were rejected for a number of environmental and economic reasons. The focus of recent investigations by Molycorp's consultants has been to evaluate the ground-water flow patterns and possible leachate impacts to water quality in the vicinity of Guadalupe Mountain.

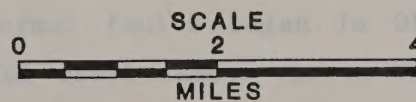
1.2 OVERVIEW OF WORK TO-DATE

Preliminary regional hydrogeologic investigations were conducted for Molycorp by Vail Engineering, Inc. (April 1982) and Water Resources Associates Inc. (June 1984). Information presented in these two reports was derived in part from work done by Winograd (1959). Summers and Hargis, in 1984, presented a paper commenting on Winograd's early work in Sunshine Valley. Winograd (1985) rebutted this paper in August 1985. Geocon (December 1983) investigated the possible leachate seepage rates from the proposed tailings pond.



LEGEND

- CLAIM BOUNDARY
- △ SUMMIT
- 3 HIGHWAY
- GORGE
- CREEK
- TOWN



LOCATION MAP OF GUADALUPE TAILINGS DISPOSAL SITE

Figure 1:1

BASE MAP:
QUESTA QUADRANGLE,
NEW MEXICO STATE HIGHWAY DEPT.
QUADRANGLE MAPS

The Cenozoic geology of the Taos Plateau Volcanic Field is discussed in a paper by Dungan and others (1984). Extensive geologic mapping has been performed by MolyCorp geologists both in the Sangre de Cristo Mountains and the Guadalupe Mountain/Sunshine Valley area. From 1936 to 1946, the U.S. Army Corps of Engineers drilled several stratigraphic/geotechnical boreholes in the study area for investigations concerning the then proposed Chiflo Dam site. Some of these boreholes still exist in serviceable condition; however, the Corps of Engineers (verbal communication) claims that the reports and records of that effort were apparently destroyed in 1978. The only available logs of these holes are to be found in the Winograd (1959) report.

In May 1985, Dames & Moore was retained by MolyCorp to continue the hydrogeologic investigations of tailings disposal areas. Dames & Moore's work to date has involved the evaluation of hydrogeology in the Guadalupe Mountain area. These activities have included drilling for geologic and hydrogeologic information, water-level surveys, evaluation of theoretical aquifer characteristics and flow patterns, establishment of a data base for ambient water quality, modeling of flow in the vadose zone, and evaluation of current and probable leachate chemistry and its impact on ground-water quality.

1.3 REGIONAL GEOLOGY

Guadalupe Mountain is a volcanic dome within the Taos Plateau Volcanic Field, which in turn, lies within the Rio Grande Rift. The Rio Grande Rift is a major fault-bounded structural depression that extends the length of New Mexico, controlling the course of the Rio Grande. Downdrop along the bounding north/south-trending normal faults began in Oligocene time and continued into the Pliocene. Total displacement was on the order of 15,000 feet in the Taos area, as indicated by gravity measurements (Cordell, 1978). In the study area, rifting also generated a subsidiary northwest-trending set of faults (referred to in this report as the Red River Fault Zone). Individual faults in this zone have displacements of up to about 100 feet. Total displacement across the zone may be several hundred feet. Approximately 7 miles east of the Rio Grande, the Sangre de

Cristo Mountains have been up-thrown by north-trending late Miocene (17 to 6 million years before present) high-angle normal faults. These faults probably have displacements in excess of 6,000 feet.

Eruption of numerous volcanic fields accompanied rifting. The Taos Plateau Volcanic Field, which is one of the larger and younger of these fields, has an area of approximately 600 square miles and an age ranging mostly within 4.5 to 2.5 million years before present (Pliocene). Volcanic rocks within the field include minor silicic domes (which are older than the rest of the field); larger andesitic to rhyodacitic domes, including Guadalupe Mountain; and widespread flood basalt flows (the Servilleta Basalt), which were erupted from large shield volcanos. About 2,000 feet of volcanic strata are exposed in the Guadalupe Mountain area. The flood basalts intertongue with the intermediate flows and with sedimentary rocks of the Santa Fe Formation. After emplacement of the volcanic field, the area underwent broad, regional uplift. The uplift caused downcutting by the Rio Grande and Red River, producing the deep gorges present on both rivers.

The Santa Fe Formation (Oligocene-Pliocene) is the only sedimentary unit exposed in the study area. It consists of poorly sorted alluvial gravels and sandstone that were shed off the rising Sangre de Cristo Mountains westward into the rift valley. The sediments become generally finer to the west. Lake beds are present locally. The total thickness of the Santa Fe is approximately 15,000 feet, but only the top few hundred feet are exposed. (No boreholes are known to have been drilled to the basement rocks beneath the sediments/volcanics in the Guadalupe Mountain area.)

1.4 REGIONAL HYDROGEOLOGY

Ground water in southern Sunshine Valley (north of Guadalupe Mountain) and the Red River/Rio Grande confluence area (hereafter referred to as the confluence) occurs within alluvial sediments, within volcanics that underlie and are interbedded with the sediments, and within the volcanic core and flanks of Guadalupe Mountain. Ground-water flow occurs in the sediments through pore-space permeability and in the volcanics by fracture and bedding-plane permeability and, to a lesser degree, vesicular

permeability. In the eastern half of Sunshine Valley, wells are usually completed in the thick accumulation of alluvial sediments that were derived from the Sangre de Cristo Mountains. In the western portion of Sunshine Valley, wells are completed in both the alluvium and the volcanics. In the confluence area, wells are completed in the volcanics.

Ground water in the study area generally flows in a westerly and then southwesterly direction from the Sangre de Cristo Mountains to the Red River and Rio Grande. Seepage studies have shown that the Rio Grande gains ground water from the regional system for most of its course between Ute Mountain and the confluence (Water Resources Associates, 1984). The Rio Grande is therefore thought to be a baseline regional drain for surface and ground water.

Ground-water flow in the study area is complex. In the Sunshine Valley area to the north, Winograd (1959) indicated the presence of a semi-perched water table in the shallow alluvial aquifer and a deeper regional aquifer in the underlying volcanic rock. To the south, in the confluence area, substantially saturated zones do not appear to be present in the superficial gravels and alluvium overlying the volcanics. In the study area, the aquifer east of the Red River Fault Zone is in the volcanics. There is significant ground-water discharge in this area to both the Rio Grande and Red River. West of the Red River Fault Zone, the volcanics generally lie above the water table. However, a significantly deeper dacite flow extends across this area to the wall of the Rio Grande gorge above Big Arsenic Springs. Other deep volcanic flow may be present. Most of the ground-water discharge west of the Red River Fault Zone appears to be associated with these relatively deep volcanics. Otherwise, ground-water flow west of the Red River Fault Zone appears to be restricted by the relatively low permeability of the alluvium underlying the volcanics. Water-table conditions appear to occur generally in the regional system, but local confining/perching conditions, gradient changes, and effective permeability changes could occur in the volcanics.

2.0 GUADALUPE MOUNTAIN TAILINGS DISPOSAL SITE

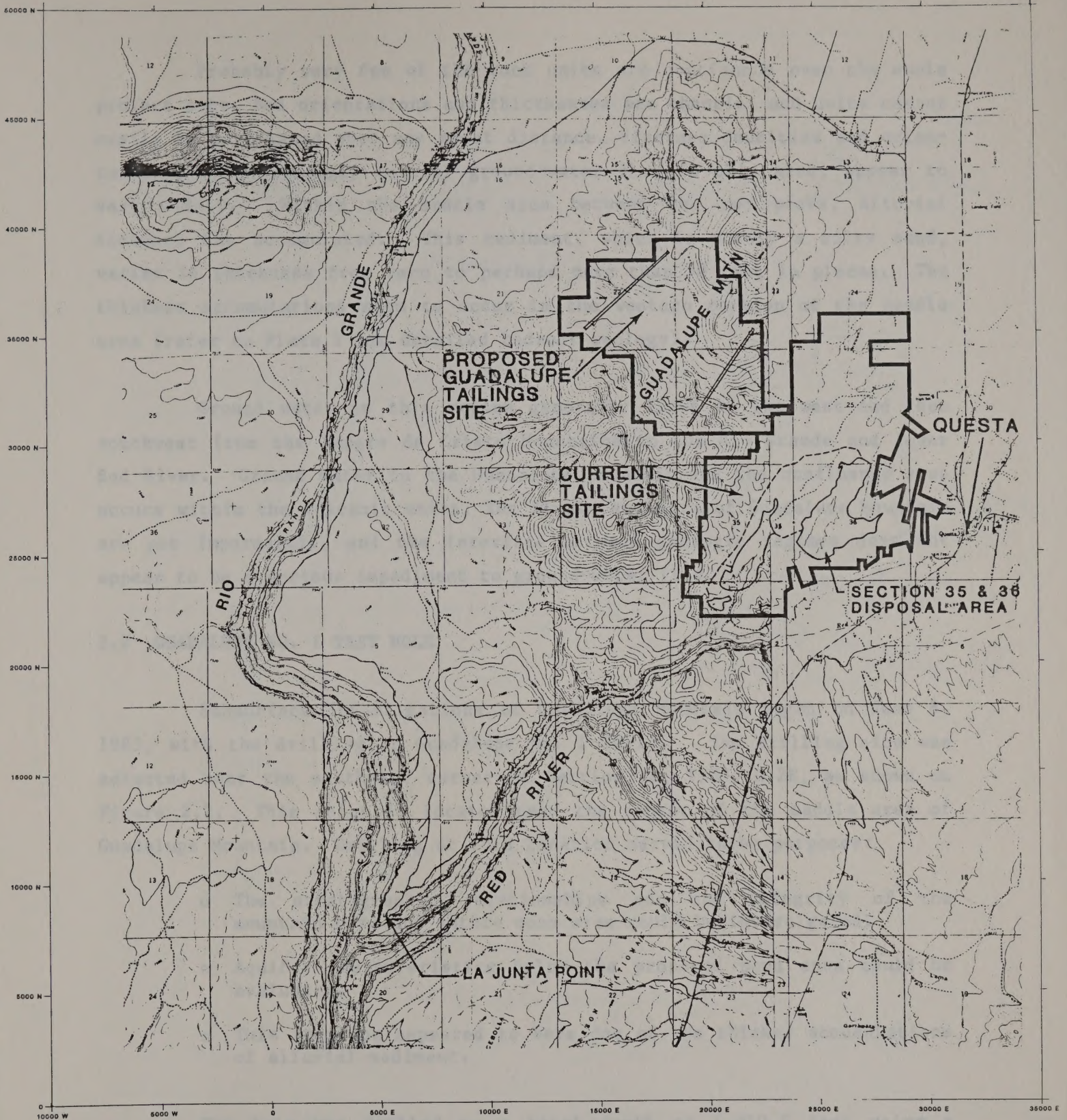
2.1 SITE SELECTION AND GENERAL SITE GEOLOGY

Guadalupe Mountain is located in the confluence area of the Rio Grande and Red River (Figure 2.1). This potential site has several favorable attributes that make it the primary option for MolyCorp's new tailings disposal area: proximity to the current disposal area, great depth to ground water, and favorable site geometry that will facilitate site development. This site, when fully developed, would encompass approximately 500 acres and would have a tailings capacity in excess of 200 million tons.


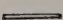
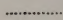
Guadalupe Mountain consists of a pair of volcanic exogenous domes and vent structures that have overlapped and sutured into one another. This activity has emplaced a variety of volcanic lithologic types. The most common types are dacites, colluvial and surge breccias, rhyodacite, and an occasional cinder bed. Chemically, the rocks of Guadalupe Mountain have been defined as rhyodacite by Lipman and Mehnert (1979) and as dacite by Dungan and others (1984). These and other descriptive terms can generally be defined as:

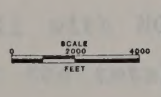
- o dacite - rhyodacite - platy jointing, flattened elongate vesicles, rare orthopyroxene and clino pyroxene.
- o olivine andesite - probably confined to south of the southern peak, below 7,650 feet. Difficult to distinguish in cuttings and core. Olivine grains with definite reaction rims of orthopyroxene. This rock may be present in Guadalupe test holes G-1 and G-3 (see Sections 2.2 and 2.4).
- o basalt - distinctly round, abundant vesicles at flow tops, possibly reddish, abundant glassy olivine, highly crystalline with translucent plagioclase abundant in ground mass.

For the balance of Section 2.0 and in Appendix A, the term "basalt" or "andesite" is generally used to describe fine-grained volcanic rocks that vary from basalt to dacites, rhyodacites, or other volcanics. What is significant is the primary and secondary permeability of the rocks, rather than specific rock or rock-chemistry identification. Most identifications were made in the field, without laboratory aids.



LEGEND

-  CLAIM BOUNDARY
-  DAM
-  ROAD



**MAP OF
GUADALUPE MOUNTAIN
TAILINGS DISPOSAL
SITE**

Figure 2.1

Probably very few of the rock units are continuous over the whole project site. Bed orientations and thicknesses are chaotic, and units cannot easily be correlated over any great distance. Fracture densities and orientations, which strongly control ground-water flow in this area, appear to vary widely. Within the saddle area between the two peaks, alluvial sediment has accumulated. This sediment, which is mostly a silty sand, varies in thickness from zero to perhaps more than 50 feet in places. The thickest accumulations seem to occur in the western portion of the saddle area (refer to Plate 1 for detailed bedrock geology).

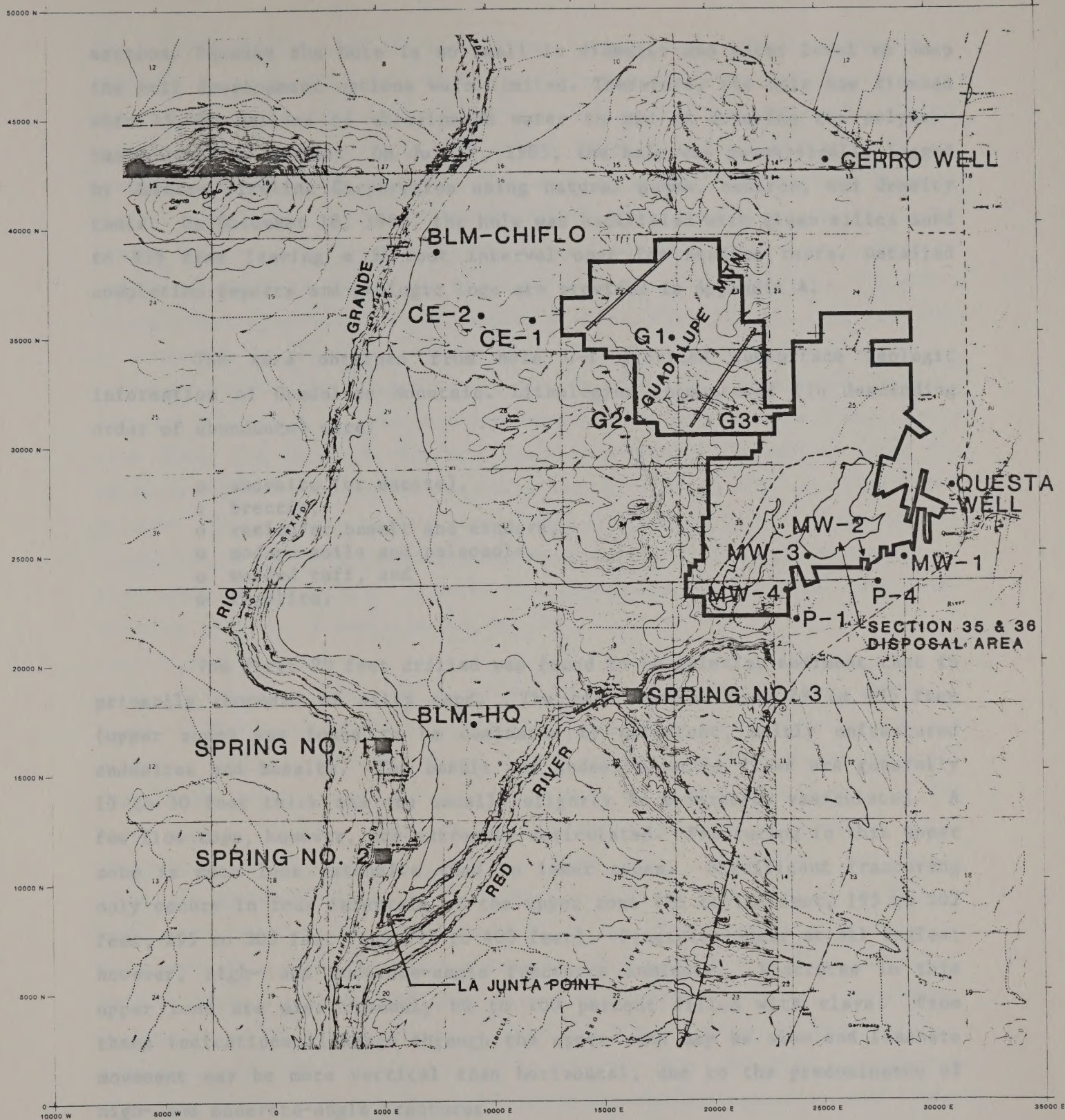
Ground water in this region generally flows to the west and then southwest from the Sangre de Cristo Mountains to the Rio Grande and lower Red River. Ground water in the Guadalupe Mountain and the confluence area occurs within the volcanic units. The flanks and core of Guadalupe Mountain are not impermeable, and the interface between geologic regimes does not appear to be a serious impediment to ground-water flow.

2.2 GUADALUPE NO. 1 TEST HOLE

Subsurface investigations of Guadalupe Mountain began on June 8, 1985, with the drilling of Guadalupe No. 1 (G-1). The drilling site was selected near the southeast corner of Section 22, T30N, R12E, as shown on Figure 2.2. This point is located near the center of the saddle area of Guadalupe Mountain. Drilling at this location served three purposes:

- o The stratigraphic relationships and the integrity of the mountain core and suture zone area could be investigated.
- o Aquifer characteristics below the proposed pond area could be evaluated.
- o This location appeared to have one of the thicker accumulations of alluvial sediment.

The hole was drilled to a total depth of 1,010.5 feet using a Longyear 44 diamond drill with HQ core rods (3.5 inches O.D.; core = 2.5 inches diameter). After the total depth had been reached on July 3, 1985, the drill rods were pulled back to 780 feet to provide an aquifer test



LEGEND

- CLAIM BOUNDARY
- DAM
- ROAD
- MONITORING WELL

MAP OF GUADALUPE MOUNTAIN MONITORING LOCATIONS

Figure 2.2

section. Because the hole is so small in diameter and water level so deep the well development options were limited. Therefore, the hole was flushed with 15,000 gallons of chlorinated water to aid in diluting the polymer-based drilling fluids. On July 7, 1985, the hole was geophysically logged by Western Wireline Corporation using natural gamma, neutron, and density tools. On December 18, 1985, the hole was backfilled with clean silica sand to 838 feet leaving a 58-foot interval open for aquifer tests. Detailed completion reports and geologic logs are provided in Appendix A.

The core obtained from hole G-1 provided subsurface geologic information of Guadalupe Mountain. Lithologies encountered (in descending order of abundance) were:

- o andesite (or dacite),
- o breccia,
- o vesicular basalt and cinders,
- o modern soils and paleosols,
- o welded tuff, and
- o rhyolite.

The first 29 feet drilled was found to be alluvial sediment that is primarily composed of silty sand. The core section from 29 to 435 feet (upper zone) was found to be dominated by competent, mainly unfractured andesites and basalts. The basalt and andesite/dacite flows are generally 15 to 30 feet thick and are usually slightly to moderately vesiculated. A few flow tops, however, are extremely vesiculated. Fracturing in this upper zone is much less extensive than in lower zones. Significant fracturing only occurs in four intervals of the upper zone (95 to 125 feet, 195 to 202 feet, 295 to 305 feet, and 395 to 405 feet). Fractures occur at all angles; however, high- and moderate-angle fractures dominate. Fractures in this upper zone are also commonly 60 to 100 percent filled with clays. From these indications, leakage through the upper zone may be slow and leachate movement may be more vertical than horizontal, due to the predominance of high- and moderate-angle fractures.

The middle zone of core section, which occurs from 435 to 644 feet, is dominated by alternating beds of andesite/basalt and breccia. Flows in this zone are generally thinner, with thicknesses ranging from 5 to 30 feet.

The breccia beds vary in thickness from 10 to 50 feet. Flows are generally slightly to moderately vesiculated and are considerably more fractured at all angles, as compared to the upper zone. Clay infilling and weathering of fractures are more pronounced than in the upper zone. The breccia units are all very similar to one another. They generally consist of angular volcanic gravel and cobbles in a semi-consolidated gray sandy clay matrix. The coarse fraction material (gravel and larger) commonly appears to be matrix-supported, which is indicative of debris flow or surge deposits. The soft, fine-grained, semi-consolidated nature of the matrix and the complete lack of fractures in the core suggests that fractures in these breccias may be self-healing and that the breccias may have a low permeability in-situ. Although the flows in this zone are considerably more fractured than those from above, the degree of fracture weathering/closure and the nature of the breccias suggest that probable leachate leakage through this zone would also be slow. The breccias in this middle zone also appear to have potential for adsorption of adverse leachate components due to their high percentage of fine fraction material. A more detailed discussion of this adsorption capacity is found in Sections 5.0 and 7.0.

The lower zone, which occurs from 644 feet to at least the total depth (1010.5 feet) of the hole, is characterized by scoriaceous basalts and cinders. Other rock types found in the upper and middle zones are still present but are thinner, and more mafic rock types appear to dominate. The only highly silicic rocks (a welded tuff bed and a rhyolite flow) encountered in the core also occur in this zone. Cinder beds and basalt flows are generally 20 to 30 feet thick. Andesite flows are 10 to 20 feet thick, and breccias are only a few feet thick. The uppermost cinder bed in this zone occurs in the interval between 644 to 677 feet. The geophysical natural gamma log indicated this bed as slightly radioactive. (A further discussion of this unit appears in Section 4.0.) Flows in this zone are generally very highly fractured and have little clay infilling and fracture closure. Cinder beds are generally unconsolidated and appear to have a high effective porosity and permeability.

2.3 GUADALUPE NO. 2 TEST HOLE

Subsurface investigations continued on Guadalupe Mountain with the drilling of Guadalupe No. 2 (G-2) on October 10, 1985. The drilling site was selected on the ridge southwest of the saddle area, near the middle of Section 27, T30N, R12E (Figure 2.2). Drilling at this location served three purposes:

- o This location could provide the most complete stratigraphic section southwest of the proposed tailings disposal site.
- o Aquifer characteristics southwest of the proposed site could be evaluated.
- o A monitoring location could be established on the southwest corner of the claim boundary.

Initially the planned final depth of the hole had been approximately 1500 feet. However, due to exceptionally poor drilling conditions, the hole was only drilled to 869 feet, which was assumed to be approximately 500 feet short of the water table. The hole was first drilled to a depth of 460 feet with HQ (3.5-inch) rods, at which point it was necessary to switch to NQ (2.75-inch) rods. When the NQ rods became stuck at 869 feet, it was decided that further reductions would render the hole useless. The drill rods were pulled and the hole was allowed to cave. Geophysical logging was not performed on this hole.

Nevertheless, the core obtained from the hole to 869 feet did provide useful information on the stratigraphy southwest of Guadalupe Mountain. In addition to soils at 0 to 40 feet, rock types encountered (in descending order of abundance) were:

- o breccia,
- o andesite/dacite, and
- o basalt.

The occurrence of these rock types was of a somewhat cyclic nature. Breccia tended to alternate with andesite and basalt. The andesites encountered in this hole are lithologically very similar to those that occur

at hole G-1. The difference between the two holes is in the bed thicknesses and apparent lack of clear flow boundaries in thick beds. Andesite and basalt beds exposed in G-2 core vary from 18 to 140 feet in thickness. The flows are consistently well-fractured at all angles, and infilling with clay and carbonates is minor to moderate.

The breccias are quite different from those found in G-1 core: G-2 breccias are generally loose and very porous conglomerations of cinders and broken rock and have little fine-grained matrix material. Most of these breccias were found in the upper portions of the hole. The breccias in the lower portion of the hole are somewhat more weathered and, therefore, most likely have lower permeabilities than those from above. Neither of these breccia types compare to the tight clay matrix breccias found in G-1 core.

In general, core from the lower portion of the hole also appears to have an increasing percentage of andesite, which could be relatively correlated to the intermediate rock types found in the upper zones of hole G-1. (The elevation of lower G-2 is equivalent to upper G-1.) Rock types that occur at the water table or at depths that could be correlated to the lower zones of hole G-1 are not known.

2.4 GUADALUPE NO. 3 TEST HOLE

Subsurface stratigraphic investigations were concluded on Guadalupe Mountain with the drilling of Guadalupe No. 3 (G-3) on December 21, 1985. The drilling site was selected in the southern portion of Section 26, T30N, R12E (Figure 2.2). This location is situated southeast of the proposed east dam of the proposed tailings disposal site. Drilling at this location served three purposes:

- o The stratigraphic inter-relationships between the volcanics could be evaluated.
- o Aquifer characteristics on the southeast side of the mountain could be evaluated.
- o A monitoring location could be established on the southeast corner of the claim boundary.

The hole was drilled to a total depth of 496 feet using HQ (3.5-inch) core rods. After the total depth had been reached on January 6, 1986, the drill rods were pulled back to 440 feet, and a chlorinated water solution was circulated into the hole to decrease the viscosity of the polymer-based drilling fluid. On January 15, 1986, hole G-3 was geophysically logged using natural gamma, neutron, and density tools. Detailed geologic logs are provided in Appendix A.

The core obtained from hole G-3 provided information regarding volcanics of Guadalupe Mountain. In addition to soils, rock types encountered (in descending order of abundance) were:

- o basalt,
- o andesite/dacite, and
- o breccia.

These rock types again occurred, as in hole G-2, in a somewhat cyclic pattern. The section can be broken into two zones. The upper zone (11 to 335 feet) is characterized by a cyclic interbedding of basalt and intermediate rock types, which is indicative of near-simultaneous volcanism on the plateau and on Guadalupe Mountain. Most of the beds in the upper zone range from 10 to 40 feet in thickness; however, some are much thicker. Most of the beds are also very highly fractured at moderate and high angles and have abundant clay infilling of fractures and whole rock weathering and decay. Breccias are uncommon.

In the lower zone, basalts are absent, and andesite and breccia dominate. These rock types are indicative of dome volcanics and pre-date the plateau basalts. Average bed thickness ranges from 10 to 30 feet, but some may be as much as 80 feet thick. The breccias found in the lower zone are tight, clast-supported and have a sandy matrix somewhat similar to those found in the lower zone of hole G-2. However, the breccias are highly weathered and, in some intervals, refractured. The andesites are similar to those in the upper zone in lithology, fracturing and degree of fracture closure. The andesite that contains the top of the water table has numerous open fractures and may have high effective permeability. The overlying units appear to have generally poor permeabilities.

2.5 EXISTING WELLS

Despite the relatively undeveloped nature of Guadalupe Mountain, a number of existing wells and test holes are located in the study area (Figure 2.2). These include Cerro, Questa and Bureau of Land Management (BLM) production wells, and the U.S. Army Corps of Engineers and Molycorp test holes. For a few of the holes or wells, limited water-quality, geologic, and construction data are available; for most, incomplete or few details are available. However, all of these wells provide valuable water sampling and water-level measuring points.

2.5.1 BLM Wells

Located directly to the west of Guadalupe Mountain is the BLM Rio Grande Gorge Wild and Scenic River Area. The BLM has developed several campgrounds along the rim and at river level as well as a visitors center and headquarters facility. The water supply for these facilities is obtained from two production wells--one located at the headquarters facility and one near the Chiflo Campground (Figure 2.2). These wells are completed in the regional volcanic aquifer. The BLM Headquarters well is approximately down-gradient, with respect to ground-water flow, of the proposed Guadalupe disposal site. The Chiflo well is not down-gradient. Known completion details are presented in Appendix A. These wells produce approximately 30 gallons/minute, are equipped with flow meters, and operate on a pressure-demand basis.

Since the BLM Headquarters (BLM-HQ) well is the only active water supply well down-gradient of the proposed Guadalupe disposal site, a monitoring program was begun to establish the ambient water quality and water levels. Inorganic water-quality data have been collected periodically since 1983 and sporadically prior to 1983, as described in Section 6.0. Water-level sounding tubes were installed by Dames & Moore in November 1985, and monitoring was started. This periodic monitoring could detect seasonal water-level changes or changes due to heavy agricultural pumping in Sunshine Valley. (See Section 3.0 for water-level readings taken to date.)

2.5.2 U.S. Army Corp of Engineers Chiflo Dam Test Holes

During the mid-1940's, the U.S. Army Corps of Engineers drilled at least six stratigraphic and geotechnical core holes for the then proposed Chiflo Dam site on the east side of the Rio Grande gorge and west of Guadalupe Mountain. The Corps of Engineers issued their report on this effort in 1946. All known original drilling logs of that report have been destroyed. The only remaining logs are found in Winograd (1959). According to Winograd, two (and possibly more) of these holes, CE-1 and CE-2 (Figure 2.2), penetrated the regional aquifer. Winograd's stated static water levels (SWL) were: 701 feet at CE-1 and 430 feet at CE-2 (approximately 7150 feet above sea level).

Five of these holes were located by Dames & Moore staff in July 1985, and the known construction details of those test holes penetrating the water table can be found in Appendix A. Three of these test holes (CE-3, CE-4 and CE-5) were dry. Upon inspection, CE-2 was found to be plugged at the surface with rocks. CE-1 was sounded out at 665 feet without encountering water in July, but in December 1985, CE-1 was re-entered and the obstruction was cleared. The current SWL in CE-1 is 696.5 feet (7159 feet above sea level). Due to its location on the west/northwest flank of Guadalupe Mountain, hole CE-1 can be used as a western monitor well.

2.5.3 Questa and Cerro Municipal Production Wells

The Questa and Cerro municipal wells are high-capacity production wells serving the drinking water needs of their respective towns (Figure 2.2). These wells are both located up-gradient with respect to regional ground-water flow from the proposed Guadalupe Mountain site. At this time, construction details and water-level data for these wells are not available. The State of New Mexico has occasionally sampled these wells and some water quality data are available. Neither of these wells has been included in Molycorp's water-level and water quality monitoring program at this time.

3.0 GROUND-WATER OCCURRENCE, MOVEMENT, AND DISCHARGE, GUADALUPE MOUNTAIN REGION

This section describes the ground-water flow regime in the area under and down-gradient of the proposed mine tailings disposal facility in the Guadalupe Mountain region of Northern Taos County. As described in previous studies relating to the proposed mine tailings disposal, and as will be used here, "down-gradient" denotes the area that lies approximately between due south and due west of the Guadalupe Mountain saddle. This study area was established based in part on the following information:

1. In the Red River Canyon, the river level upstream of approximately the Fish Hatchery is above the regional water table at the proposed tailings site; therefore, ground water flowing under the proposed tailings pond would not discharge to the Red River upstream of the Fish Hatchery area; and
2. The elevation of the Rio Grande upstream of approximately Cerro Chiflo is above the regional water table at the proposed tailings site, and ground water flowing under the proposed tailings pond would not discharge to the Rio Grande upstream of Cerro Chiflo.

Thus, this investigation of ground-water flow emphasizes that quadrant that lies between the Fish Hatchery, downstream along Red River to the confluence, and upstream along the Rio Grande to the Cerro Chiflo crossing (see Plate 1).

3.1 GENERAL OCCURRENCE OF GROUND WATER

Winograd (1959) describes the general characteristics of ground-water occurrence in the region. The primary emphasis of the Winograd report was on ground-water occurrence within the Sunshine Valley area, north of Guadalupe Mountain. At the time of Winograd's work, both geologic and hydrogeologic data for the region southwest of Guadalupe Mountain were sparse. His observations are supplemented primarily by studies commissioned by Molycorp, Inc. More recent studies on geology and hydrogeology of the area have been conducted by:

- o Dames & Moore;
- o Water Resources Associates (1984)

- o Vail Engineering, Inc. (especially a report by Dr. Scott G. Vail, March 1987: "Geological Evaluation of the Guadalupe Mountain Area");
- o C. M. Menges, June 1984: "Geologic Investigation In Questa Area for EID"; and
- o Molycorp geologists.

The Sangre de Cristo Mountains and other upland areas over 8,000 feet in elevation are the principal areas of ground-water recharge. Recharge results both from direct percolation of precipitation and from infiltration from several streams. Precipitation in the region varies from an annual average of 14 inches or less below 8,000 feet of elevation to over 30 inches in higher elevations. A significant percentage of precipitation eventually reaches the water table. Also streams, upon leaving their mountain courses and entering the plateau area, lose much of their flow to permeable alluvial sediments or to bedrock (except for Red River and Cabresto Creek).

Ground water occurs primarily within the volcanic rocks in the region of study east of the Red River Fault Zone. Flow within the volcanic units is primarily via fracture permeability, flow-boundary permeability, and to a lesser extent by vesicular permeability. Flow in the region is from areas of recharge to natural discharge points in and adjacent to the Red River and Rio Grande. Discharge via wells is only from the BLM headquarters well and the BLM - Chiflo well (Figure 2.2).

3.2 CONTROLS TO GROUND-WATER MOVEMENT

Ground-water flow down-gradient from Guadalupe Mountain is controlled primarily by hydraulic properties of volcanics (dacite and olvine andesite flows form the Guadalupe Mountain complex) and by the sedimentary Santa Fe Formation. A series of northwest- to southeast-trending faults (referred to here as the Red River Fault Zone; see Plate 1) bisects the area along the southwestern toe of the Guadalupe Mountain complex. West of the fault zone, the Santa Fe Formation has been uplifted, the result of which is that the water table is below the volcanics and in the Santa Fe Formation (see Plates 2 and 3). An exception to this condition can be found in the

Big Arsenic Springs area (see Plates 2 and 4) where a lobate dacite flow followed and filled a paleo valley (possibly an ancestral Red River Valley) at a depth that is now a few hundred feet below the top of the Santa Fe alluvium).

East of the Red River Fault Zone, the rock units are down-dropped several hundred feet relative to that west of the zone. As a result, the volcanics provide an aquifer of high conductivity in this area.

The Santa Fe alluvium underlying the volcanics, in general, has a relatively low permeability and acts as an aquitard restricting ground-water flow from volcanic aquifers east of the fault zone to the Rio Grande and to the lower 2 miles of Red River. An exception is the dacite-filled paleo valley within the Santa Fe Formation that crops out at the Big Arsenic Springs. The dacite has a relatively high permeability and appears to be an avenue of higher flow through the Santa Fe Formation. This condition explains the presence of the approximately 18 cfs of ground-water discharge in the Big Arsenic Springs complex. These springs are discussed in more detail later in this section.

The Servilleta Basalts extend from near the ground surface to a depth of a few hundred feet over much of the plateau area west of Guadalupe Mountain and along the Rio Grande and Red River gorges. The Servilleta Basalts generally lie above the water table west of the Red River Fault Zone and, therefore, have little or no influence on the ground-water flow in this area. East of the Red River Fault Zone, the Servilleta Basalts probably interfinger with the andesite from Guadalupe Mountain and are part of the aquifer. East of the Red River Fault Zone, the volcanic formations of Guadalupe Mountain rest on the Santa Fe alluvial deposits. The elevation of the top of the Santa Fe sediments beneath Guadalupe Mountain has not been ascertained; however, it probably is a few hundred feet below the water table. The volcanics of Guadalupe Mountain generally predate the Servilleta Basalt flows in the area, and therefore, the Servilleta Basalts probably do not extend beneath the mountain.

3.3 DIRECTIONS AND GRADIENTS OF GROUND-WATER FLOW

Ground-water flow via fracture or vesicular permeability in volcanic units is complex on a small scale due to variations in bed thickness and degree of fracturing and weathering. On a larger or regional scale, the ground-water system becomes somewhat more predictable. In general, ground-water recharge occurs mainly on the western slopes of the Sangre de Cristo Mountains. The ground water travels west then southwest where it eventually discharges into the Rio Grande and Red River.

Ground-water flow gradients vary widely. Near the mountains, the gradient is quite steep (Winograd, 1959), but it flattens across the plateau and may steepen again near the rivers. Local anomalies in the flow direction, gradient, and velocity are to be expected due to the unpredictable fractured nature of the aquifer and the frequent changes of lithology.

Indications of high volcanic rock permeability have been observed in the vicinity of Guadalupe Mountain. For example, such conditions were observed during examination of cores and of geophysical logs of test holes drilled by MolyCorp plus the log of the Corps of Engineers test hole CE-1 (see Figure 2.2). Each of these logs indicate that ground water could be readily conducted from the alluvial aquifers northeast of Guadalupe Mountain, under the mountain complex, and then toward the Red River Fault Zone. A water-level monitoring network on Guadalupe Mountain has been established. Five wells in the Guadalupe Mountain and the confluence area can be regularly measured and sampled. These wells are G-1, G-3, CE-1, and the BLM wells (HQ, Chiflo) (Figure 2.2).

Table 3.1, which gives representative water-level measurements taken on the wells, can be used to show that the ground-water system in the Guadalupe Mountain area appears to be in relative equilibrium and exhibits no major noticeable pumping effects or perhaps even seasonal declines. In fact, the historical data show that water levels have remained relatively stable or may have risen a few feet. From the water-level data (Table 3.1), a series of three-point problems were solved to evaluate direction(s) and gradient(s) of ground-water flow. The graphical solutions to these problems

are presented in Appendix B. Figure 3.1 presents a rose diagram summary of the various graphical solutions. Although these solutions are based on a limited number of data points, they indicate that ground water generally flows from Guadalupe Mountain in a south-southwesterly direction at least as far as the Red River Fault Zone.

TABLE 3.1
WATER-LEVEL MEASUREMENTS, GUADALUPE MOUNTAIN AREA

Well and Elevation of Measuring Point (feet above MSL)	Depth to Water (in feet)					
	Historical	7/10/85	8/15/85	10/24/85	11/21/85	1/17/86
G-1 (7939.87)		788.4	787.2	785.9	785.5	786.4
G-3 (7626.57)						475.0
CE-1 (7855.95)	701 (1959)					696.5
BLM - HQ (7569.52)	487 (8/72)			485.0	484.7	485.4
BLM - Chiflo (7492.71)	344 (9/72)			342.0	342.0	343.3

As seen in the graphical solutions, ground-water flow direction and gradient vary significantly. The solutions that use Guadalupe Mountain wells as data points all generally show a south by southwesterly flow direction and a shallow gradient of 0.0036 feet/foot (ft/ft) or approximately 19 feet/mile (ft/mi). Solutions that use confluence area wells and springs show a significant variation in flow direction and gradient. Flow directions vary from nearly due south to due west. However, an overall sense of southwesterly flow is still observed. Flow gradients also appear to increase significantly in the confluence area, as compared to the Guadalupe Mountain area. Gradient values range from 19 ft/mi (0.0036 ft/ft) east of the Red River Fault Zone to over 300 ft/mi (0.06 ft/ft) through the Santa Fe alluvium west of the fault zone.

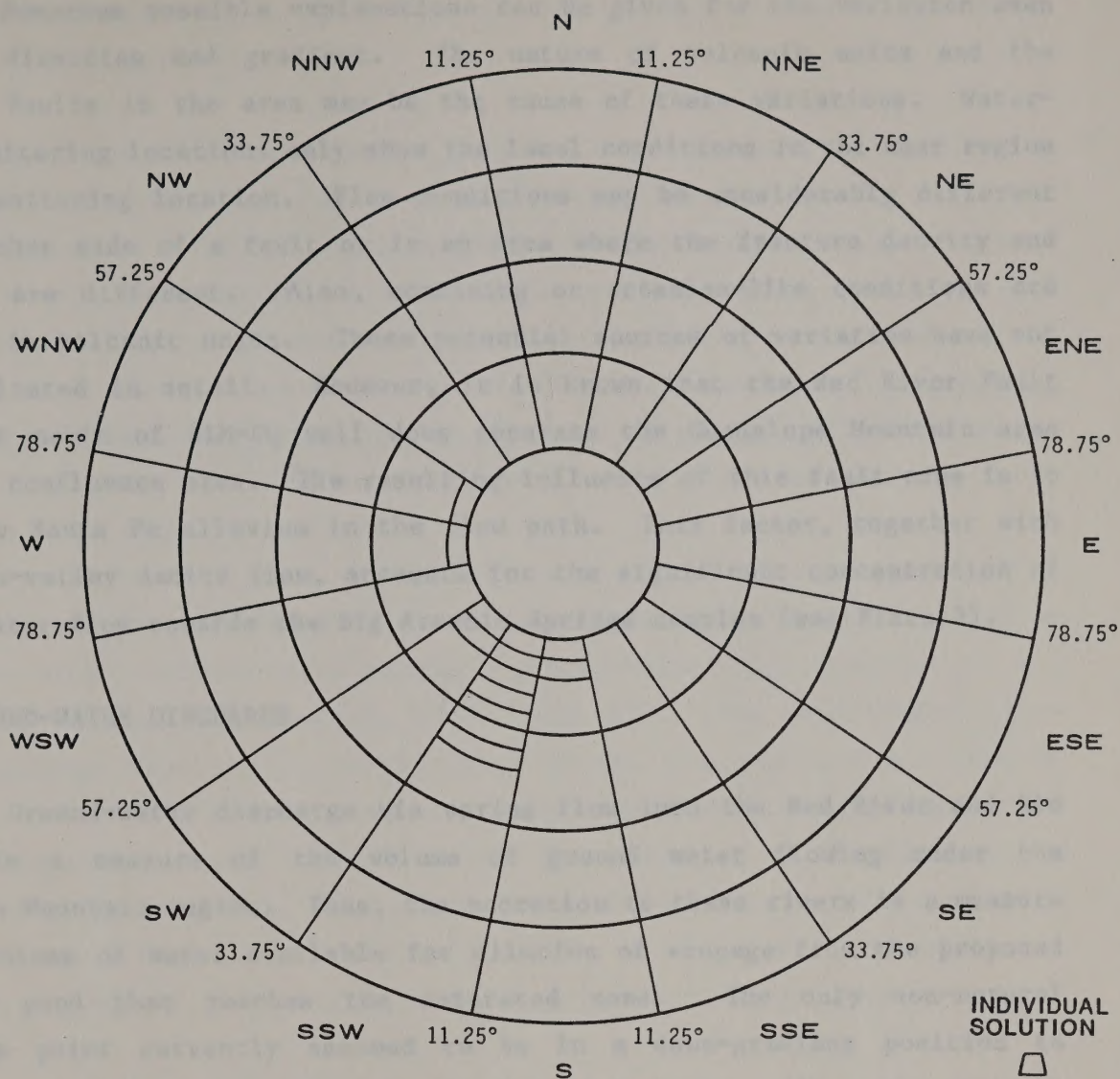


FIGURE NO. (APPENDIX B)	SOLUTION POINTS	FLOW DIRECTION	GRADIENT
B-1	BLM-CHIFLO,G-3,BLM-HQ	S30°W	0.0037
B-2	BLM-CHIFLO,G-1,BLM-HQ	S26°W	0.0035
B-3	G-1,G-3,BLM-HQ	S34°W	0.0035
B-4	CE-1,G-1,BLM-HQ	S4°E	0.0042
B-5	G-1,G-3,SPRING NO.1	S32°W	0.016
B-6	G-1,BLM-CHIFLO,SPRING NO.1	S21°W	0.017
B-7	G-1,BLM-HQ,SPRING NO.1	N64°W	0.093
B-8	G-1,G-3,SPRING NO.2	S38°W	0.014
B-9	BLM-HQ,SPRING NO.1,SPRING NO.2	S87°W	0.072
B-10	SPRING NO.2,BLM-HQ,SPRING NO.3	S7°E	0.068
B-11	BLM-CHIFLO,G-1,SPRING NO. 3	S26°W	0.0034
B-12	G-1,G-3,SPRING NO.3	S24°W	0.0037
B-13	G-1,BLM-HQ,SPRING NO.3	S30°W	0.0035

ROSE DIAGRAM OF GROUND-WATER FLOW DIRECTION SOLUTIONS

GUADALUPE MOUNTAIN AND
CONFLUENCE AREA

Figure 3.1

Numerous possible explanations can be given for the variation seen in flow direction and gradient. The nature of volcanic units and the numerous faults in the area may be the cause of these variations. Water-level monitoring locations only show the local conditions in the near region of the monitoring location. Flow conditions may be considerably different on the other side of a fault or in an area where the fracture density and patterns are different. Also, confining or artesian-like conditions are possible in volcanic units. These potential sources of variation have not been evaluated in detail. However, it is known that the Red River Fault Zone just north of BLM-HQ well does separate the Guadalupe Mountain area from the confluence area. The resulting influence of this fault zone is to place the Santa Fe alluvium in the flow path. This factor, together with the paleo-valley dacite flow, accounts for the significant concentration of ground-water flow towards the Big Arsenic Springs complex (see Plate 5).

3.4 GROUND-WATER DISCHARGE

Ground-water discharge via spring flow into the Red River and Rio Grande is a measure of the volume of ground water flowing under the Guadalupe Mountain region. Thus, the accretion to these rivers is a measure of the volume of water available for dilution of seepage from the proposed tailings pond that reaches the saturated zone. The only non-natural discharge point currently assumed to be in a down-gradient position to potential tailings-pond seepage is the BLM Headquarters well, approximately 3 miles southwest of the proposed pond.

3.4.1 Accretion Measurements

Seepage-run measurements have been made on several occasions by U.S. Geological Survey (USGS) personnel. Winograd (1959) noted that, in 1928, the USGS made a seepage run along Red River from the head of the canyon to its mouth, a stretch of 7 miles. These measurements showed a gain of about 31 cfs out of a total flow at the Red River mouth of 84 cfs. Winograd (1959) also deduced that the accretion to the Rio Grande from the Chiflo Campground gaging station to above the confluence with the Red River was on the order of 40 cfs. Subsequent measurements by the USGS, in 1963

and 1965, indicate that the accretion in this stretch of the Rio Grande is probably in excess of 45 cfs.

Based on these measurement data and on discussions below (Section 3.4.2 and 3.4.3), the total ground-water flow southwest to the Red River and Rio Grande, across a line from Cerro Chiflo to the head of Red River Canyon (about a 5-mile straight-line distance), is at least 50 cfs (see Table 3.2 for summary). This is ground water discharging from the north bank of the Red River and the east bank of the Rio Grande. Therefore, the average ground-water flow across this line is at least 10 cfs per mile, within the upper-most ground-water flow system. It is this flow system that is of concern in this study.

Currently available data indicate that Guadalupe Mountain serves as an infiltration gallery for regional ground-water flow similar to Ute Mountain (described by Winograd, 1959, page 33). The ground-water flow under Guadalupe Mountain in the vicinity of the proposed tailings pond is presumed to be approximately equal to the average flow cross the region (10 cfs per linear mile), and possibly more. The footprint of seepage from the proposed pond on the water table is predicted to be at least 7,000 feet wide (1 1/3 miles). Thus, between 14 cfs and 15 cfs of ground water should be available for dilution of seepage from the proposed tailings pond.

3.4.2 Accretion to the Red River

As stated previously, seepage measurements by the USGS along the Red River were made in 1928, showing a gain of 31 cfs over a 7-mile reach upstream of the confluence with the Rio Grande. Winograd (1959) also stated that, from 1950 to 1956, the records of the USGS indicated a gain of 33 cfs from below Questa to the mouth of Red River during the winter months when evaporation and diversions are at a minimum. In November 1965, a seepage investigation by the USGS indicated an accretion of 36.2 cfs between and head of the Red River Canyon and the mouth of the Red River. Review of subsequent stream-flow records confirm that seepage and spring flow accretion to the Red River from below Questa to the mouth of the Red River

TABLE 3.2

**SUMMARY OF ACCRETION TO
RED RIVER AND RIO GRANDE**

	<u>Total Gain to the River</u>	<u>Gain From Guadalupe Mountain Area</u>
<u>Rio Grande</u>		
o Cerro Chiflo to Red River Fault Zone	22 cfs	11 cfs from east
o Red River Fault Zone to Confluence	23 cfs	18 cfs from Big Arsenic Springs complex; 2 cfs from east
<u>Red River</u>		
o Questa to Fish Hatchery	18 cfs	12 cfs from north
o Fish Hatchery to Red River Fault Zone	10 cfs	7 cfs from north
o Red River Fault Zone to Confluence	5 cfs	2 cfs from north
		52 (rounded to 50 for purposes of conservatism)

is still from 32 to 34 cfs (exclusive of seepage and surface return flows from Molycorp's existing tailings ponds).

Based on an analysis of the drainage areas and observations of spring flow, it is estimated that at least 65 percent (21 cfs) of the 33 cfs of accretion in the lower several miles of the Red River is from the north and northeast. A more detailed discussion of accretion to the Red River follows.

Questa To Fish Hatchery

Downstream from Questa, over 50 percent of the ground-water and spring-flow accretion to Red River occurs along the 2-mile reach above the Fish Hatchery. A large portion of the flow emanates from an olivine andesite formation that originated from a volcano south of and predating the present Guadalupe Mountain. Since the elevation of Red River over much of this segment is above the water table beneath the tailings site, it will not be affected by seepage from the proposed ponds. A significant portion of the seepage from the present ponds is, however, probably being discharged with the spring flow in this area. The spring flow and ground-water seepage accretion to Red River from below Questa to the confluence is on the order of 21 cfs (see Table 3.2). Of this amount, approximately 12 cfs occurs upstream of the Fish Hatchery, as indicated by stream flow data.

Questa Springs, which is located on the north bank of Red River several hundred yards upstream from the entrance to the Red River Canyon, has an estimated flow in excess of 5 cfs. Questa Springs apparently discharges flow directly from the alluvial formation east of Guadalupe Mountain as evidenced by its water temperature, which is several degrees lower than that of the springs farther downstream and along the Rio Grande.

The other springs upstream of the Fish Hatchery appear to emanate from an olivine andesite formation found on both sides of Red River. Extensive talus slopes along this reach hide the specific discharge points of these springs. The springs from the volcanic formations upstream of the Fish Hatchery appear to flow about equally from both sides of the river.

Thus, for springs located upstream of the Fish Hatchery, including Questa Springs, approximately 12 cfs of accretion to Red River occurs from the north. A significant portion of this spring flow is collected before it reaches Red River and is piped to the Fish Hatchery. This accretion, therefore, is not reflected in the stream-flow measurements at the natural spring discharge points.

Fish Hatchery to Confluence Area

A significant ground-water discharge area down-gradient from the tailings pond site is along the reach of Red River, from approximately the Fish Hatchery area downstream to the westerly reach of the Red River Fault Zone (Plate 1). Lobate dacite volcanic flows are the principal conduits for the water emanating as springs along this reach of the river. The conductivity of the volcanics in this area is probably enhanced by fault-induced fractures.

The channel along the lower part of the Red River is generally steep and lined with large boulders making accurate flow measurement difficult. Based on the few gauging measurements available and other considerations, over 7 cfs of accretion has been estimated to occur between the Fish Hatchery and the western limits of the Red River Fault Zone and less than 2 cfs of accretion to occur downstream of the fault zone. In this area, larger and more numerous springs were observed along the north side of Red River.

Downstream of the fault zone, seepage to Red River from both sides of the river is diffused through the Santa Fe alluvium and no evidence of a significant concentration of spring flow was found. The geography of this area indicates that the greater part of the accretion along this reach is from the southeast. Accretion from the north is estimated to be on the order of 2 cfs along this reach of the river.

3.4.3 Accretion to the Rio Grande

The total ground-water accretion to the Rio Grande (from the Chiflo Campground gaging station to the confluence area) is on the order of 45 cfs (see Table 3.2). This accretion is from ground-water flow from both the east and west. From the Colorado border to the confluence of the Rio Grande and Red River, the drainage basin on the west has an overall area of approximately 630 square miles, while the area on the east is approximately 520 square miles. However, in the drainage area to the east, approximately 260 square miles are above 9,000 feet in elevation and over 200 square miles are above 10,000 feet. To the west, approximately 130 square miles are above 9,000 feet, and only about 25 square miles are above 10,000 feet. The NOAS precipitation charts indicate a significantly higher average rainfall over the east drainage area. Based on the higher terrain and amount of precipitation and on review of other topographic features, the major portion of the accretion to the Rio Grande in this area is from the east.

Subtraction of an estimated 18 cfs of Big Arsenic Springs complex discharge from the total 45 cfs of accretion in this reach leaves a balance of 27 cfs. Reconnaissance of the Rio Grande from La Junta Point to Cerro Chiflo by MolyCorp personnel and consultants indicated that no major spring complexes occur along the west side of the river and that exclusive of Big Arsenic, the spring and seepage flow from the east was probably equal to or greater than that from the west. It is probable, therefore, that at least 13 cfs of seepage flow to the river is from the east in addition to the 18 cfs from the Big Arsenic Springs complex.

Cerro Chiflo to Fault Zone

Along the Rio Grande, north of the Red River Fault Zone to Cerro Chiflo, the flow of ground water is primarily in and controlled by massive volcanic dacite flows that erupted from Guadalupe Mountain and possibly in some areas from Cerro Chiflo. Minor springs were noted at fairly frequent intervals along this reach and particularly in the area at the base of the trail from the Chiflo Campground. An even greater amount of accretion along this reach probably occurs from beneath the river. Although no significant

springs were noted in the area, it is likely that a substantial amount of accretion is occurring in the vicinity of the fault zone. The USGS seepage surveys in 1963 and 1964 indicate that on the order of 25 cfs of accretion occurs from Cerro Chiflo to below the fault zone. Accretion in this area is limited by the fairly low hydraulic gradient of the water table. In addition, the hydraulic conductivity of the massive volcanic flows generally is significantly less than that of the more lobate flows above Big Arsenic Springs and below the Fish Hatchery. The fairly low conductivity of the massive volcanic flows in this area was evidenced by the artesian conditions that were observed in the U.S. Army Corps of Engineers test hole No. 3 when the drilling penetrated a permeable zone approximately 148 feet below the river level. The brief pump test of the BLM Chiflo well drilled in this area also indicated a conductivity substantially less than that at the BLM Headquarters well.

The elevation of the Rio Grande upstream of Cerro Chiflo is above the water table levels beneath Guadalupe Mountain and, therefore, will not be affected by seepage from the tailings ponds. Upstream from Cerro Chiflo, it appears that the Servilleta Basalts extend to the river levels and control the ground-water flow along this reach in the classic manner described in the Winograd (1959) report.

From the Red River Fault Zone north to Cerro Chiflo, a distance of approximately 2 miles, over 35 seeps and small springs were inventoried along the east shoreline of the Rio Grande. The largest of these had an estimated flow of 15 gpm. The total estimated flow of all of these springs is less than 100 gpm. Springs along this reach were more numerous in the vicinities of Cerro Chiflo and the fault zone. Along this reach, the river banks were often saturated, and phreatic plant growth was fairly prevalent in many areas. A few small springs discharging from below the river water line were also noted.

North of where the Red River Fault Zone crosses the Rio Grande, ground water moves through fairly massive flows of andesites. Ground-water movement in such rocks is generally concentrated along flow boundaries and in open fracture zones. This situation results in the concentration of

ground water at localized points of discharge and results in the numerous noticeable seeps and springs along this reach. Although the combined flow of the observed springs and seeps in this area was less than 100 gpm, the stream flow indicates that the accretion along this reach averages approximately 10 cfs per mile. The log of U.S. Army Corps of Engineers test hole No. 3 indicates that a significant upward vertical gradient occurs in or near the Rio Grande in the Cerro Chiflo area (Winograd, 1959). Thus, much of the accretion along this reach may be occurring along the stream bottom. In particular, a significantly greater amount of inflow to the Rio Grande probably is occurring in the area of the Red River Fault Zone than was noticeable along the river shore line.

Fault Zone to Confluence

The east bank of the Rio Grande was geologically examined over nearly its full reach from the confluence to the Red River Fault Zone. Except for Little Arsenic Springs and the Big Arsenic Springs complex, no springs or minor seeps were found along this reach. At some locations, reedy grass, willows, and/or other water-thriving brush were noted up to a level of approximately 15 feet above the river level, indicating the possibility of phreatic seepage.

Of an estimated 31 cfs accretion to the Rio Grande from the east, approximately 60 percent (18 cfs) occurs at the Big Arsenic Springs complex. Little Arsenic Springs, which is located approximately one mile to the south, has a flow of about 0.25 cfs.

The sediments of the Santa Fe Formation along the reach from the confluence to the fault zone have some permeability and are discharging some ground water to the Rio Grande from the relatively high water table to the east. Based on an analysis of probable permeability of the Santa Fe alluvium in this area, the maximum estimate for this flow is approximately 2 cfs per mile. In the Santa Fe alluvium in this area, ground-water flow and discharge is highly diffused. Theoretically, a large part of the seepage should be discharged beneath the river level. Accretion of 1 cfs per mile is equivalent to 0.085 gpm per foot. Even if 75 percent of this amount

of this amount occurred below the river level, the seepage along and above the shore line would be approximately 1 gpm per 50 feet. It is probable that seepage in excess of this amount would be observable in many locations.

3.4.4 Age of Ground Water Discharging to Springs

From available data on spring discharge (see Table 3.3), some trends are apparent. The springs along the Rio Grande appear to have a relatively constant flow. A slight seasonal decline in flow may occur in late summer, but the amount of data is insufficient to evaluate precisely this occurrence. These springs discharge from a regional aquifer. Some of the springs along the Red River appear to decline in late summer and fall, suggesting that these springs may be at least partially interconnected with the Red River surface-water system via stream bed alluvium. The flow at the main Red River spring complex, although dispersed, appear to remain relatively constant. This constant flow indicates that these springs are not influenced by surface-water flow but are tied to the ground-water flow through the northwest-trending fault zone that occurs at these springs.

One method for evaluating the source of spring water is to analyze the spring waters for short-lived radioisotopes such as tritium and radium 228. In theory, older ground water would lack these isotopes, whereas recent waters, which have been recharged since the start of atmospheric nuclear weapons testing in 1954, would have more elevated levels. Five springs were tested for tritium and gross alpha and beta activity. The data obtained from these analyses are presented in Table 3.4.

These results indicate a very low radioactivity level for the springs along the Rio Grande, which supports a supposition that these springs are not discharging recently infiltrated water. Springs along the Red River also have low radioactivity levels, again an indication that most of the discharged water has not been recently infiltrated. The elevated beta activity in Red River 9 and Fish Hatchery 2 is comparable with ambient levels found in municipal production wells sampled by the State in the area. However, these results may indicate a minor contribution from surface-water sources.

TABLE 3.3

SPRING FLOW DATA

Spring Name and Number	Date of Measurement						
	6/20/85	7/2/85	7/18/85	8/14/85	9/24/85	11/18/85	1/18/86
Big Arsenic (staff gauge, feet)	1.5	1.45	1.45	1.46	1.45	1.5	1.5
Little Arsenic (visual, gpm)	10-15			10-15		10-15	
Cerro - 3 seeps (visual, gpm)	1-3			1-3		1-2	
Red River 1 & 2 (visual, gpm)	< 1			dry		dry	
Red River 10 (visual, gpm)	1			1		1	
Fish Hatchery 1 & 2 (visual, gpm)	3-5			2-4		2-4	

TABLE 3.4

ANALYSES OF TRITIUM AND OF GROSS ALPHA
AND BETA ACTIVITY FOR SPRING WATERS

	<u>Tritium</u>	<u>Gross Alpha</u>	<u>Gross Beta</u>
Big Arsenic	<500	<2	<3
Little Arsenic	<500	<2	<3
Cerro Chiflo	<500	<2	<3
Fish Hatchery 2	<500	<2	6+/-3
Red River 9	<500	<2	4+/-3

Units are in pico Curies/liter.
< indicates below detection limit.

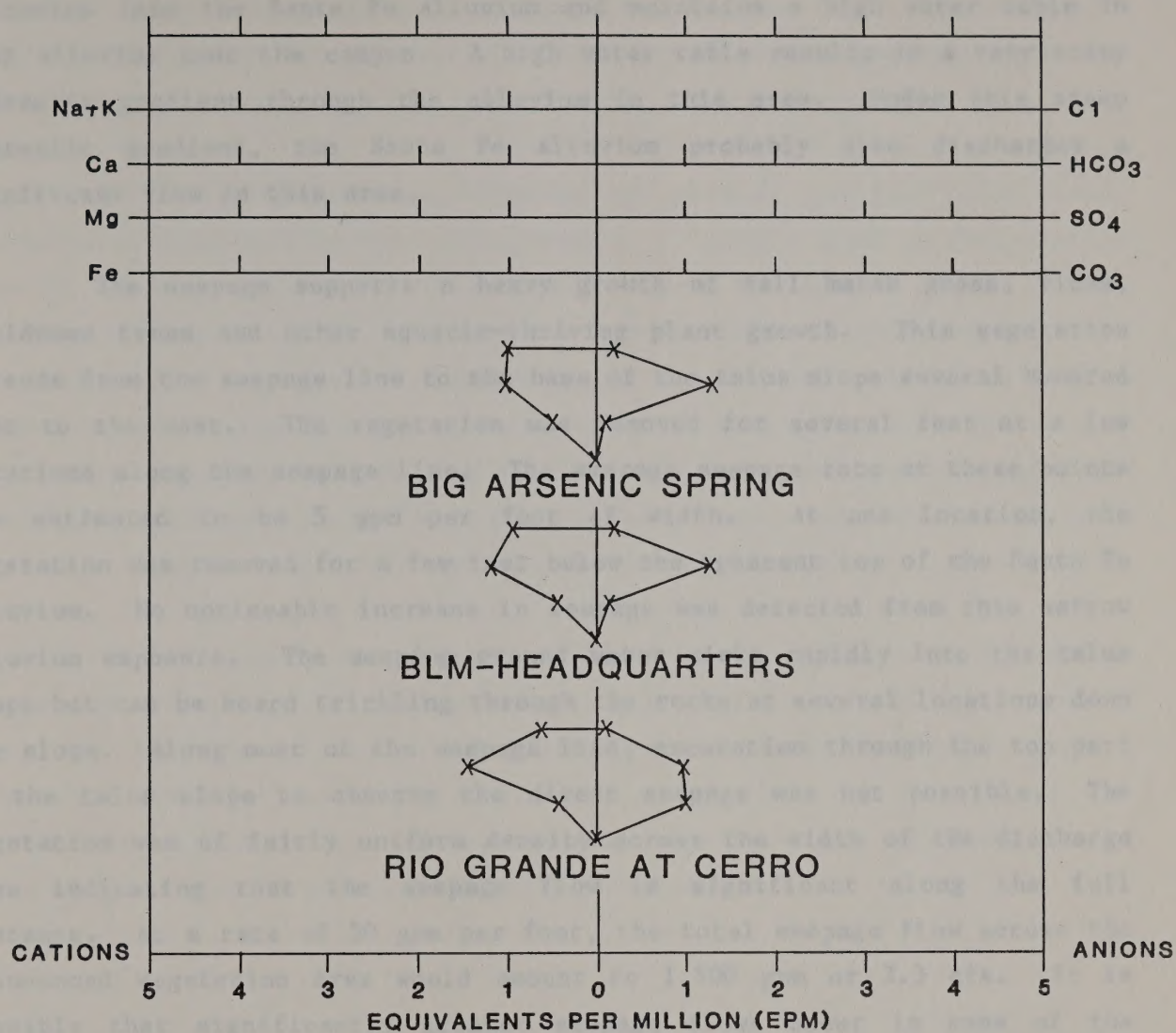
Water qualities can be compared from various sampling locations for chemical signatures that would identify the water's provenance. Figure 3.2 shows a Stiff diagram comparison of water quality samples from Big Arsenic Spring, Rio Grande surface water, and the BLM-HQ well. As can be seen, the spring and well water chemistries compare closely, indicating that the springs are discharging regional ground water.

3.5 BIG ARSENIC SPRINGS COMPLEX AS A SPECIAL CASE OF GROUND-WATER DISCHARGE

References to Big Arsenic Springs have generally pertained to the notable large and relatively isolated specific spring flow to the Rio Grande at the base of the trail from the Big Arsenic Springs campground. This spring is part of and closely related to a series of springs referred to in this report as the Big Arsenic Springs complex. Big Arsenic Springs is located near the southern edge of the complex and has an estimated total flow of 4 to 5 cfs. The complex extends to the north for a distance of some 2,000 feet and has a total estimated flow of at least 18 cfs.

The existence of Big Arsenic Springs complex is primarily due to the lobate dacite flow exposed in the canyon wall several hundred feet above the spring area. This volcanic flow from the vent area of Guadalupe Mountain appears to have followed a westerly trending paleo valley through the older Santa Fe alluvium. The dacite flow underlies the Servilleta Basalts which are above the water table in this area. The dacite formation extends along the canyon wall for a distance of approximately 3,000 feet. The base of the dacite formation at its lowest point of exposure is at elevation 7033 feet MSL, which is some 270 feet above the river level and 490 feet below the rim of the gorge. The top of the dacite flow along the exposure is at an elevation of approximately 7,200 feet. Ground water discharges directly from the lower part of the dacite formation and the underlying volcanic rubble for a distance of approximately 300 feet along the canyon wall above the Big Arsenic Springs complex.

The dacite flow provides a hydraulic conduit for transporting ground water from the Red River Fault Zone to the Red River gorge. Only a



**STIFF DIAGRAM OF
BIG ARSENIC SPRING,
RIO GRANDE, AND
BLM-HEADQUARTERS
WATER QUALITY**

Figure 3.2

part of the ground water is transported the full distance through the volcanics to the canyon. A percentage of the ground water seeps from the volcanics into the Santa Fe alluvium and maintains a high water table in that alluvium near the canyon. A high water table results in a very steep hydraulic gradient through the alluvium in this area. Under this steep hydraulic gradient, the Santa Fe alluvium probably also discharges a significant flow in this area.

The seepage supports a heavy growth of tall marsh grass, vines, deciduous trees and other aquatic-thriving plant growth. This vegetation extends from the seepage line to the base of the talus slope several hundred feet to the west. The vegetation was removed for several feet at a few locations along the seepage line. The average seepage rate at these points was estimated to be 5 gpm per foot of width. At one location, the vegetation was removed for a few feet below the apparent top of the Santa Fe alluvium. No noticeable increase in seepage was detected from this narrow alluvium exposure. The seeping ground water sinks rapidly into the talus slope but can be heard trickling through the rocks at several locations down the slope. Along most of the seepage line, excavation through the top part of the talus slope to observe the direct seepage was not possible. The vegetation was of fairly uniform density across the width of the discharge area indicating that the seepage flow is significant along the full distance. At a rate of 50 gpm per foot, the total seepage flow across the pronounced vegetation area would amount to 1,500 gpm or 3.3 cfs. It is possible that significantly greater seepage flows occur in some of the obscured areas.

3.6 DISCUSSION ON GROUND-WATER UNDERFLOW AND DISCHARGE

Published information on gains in stream flow are used to measure accretion due to ground-water discharge. This measurement was done to supplement information presented in Section 7.0 so that dilution of effluent (especially total dissolved solids and sulfates) could be demonstrated. It was calculated that approximately 11 cfs of ground water per linear mile of cross section flows toward discharge in the Red River or Rio Grande in the quadrant southwest of the proposed tailings pond. This amount of underflow

within the uppermost ground-water flow system is sufficient to dilute expected concentrations of total dissolved solids and sulfates that will reach the water table from pond seepage (see Section 7.0). The amount of underflow discussed in Section 3.0 is significantly greater than the conservative value of underflow used in model studies (Section 7.0).

In the project area, because of complex geologic conditions, ground-water flow must be viewed regionally. A single drop of ground water takes a tortuous path as it moves down-gradient through the region. That same drop of ground water, however, must adhere to basic governing controls -- it moves from an area of recharge to an area of discharge as part of a larger volume of underflow. Thus, in the study area of concern, the ground water moves generally southwest as it flows under the proposed seepage pond. When that underflow reaches the Red River Fault Zone, that underflow diverts (at least in part) toward the Big Arsenic Springs complex.

In addition to dilution of effluent in the vadose zone and within the saturated zone to the claim boundary, mixing will occur through time and over the distance between the claim boundary and discharge points. Dispersion and dilution should continually occur along the flow route. By the time of discharge in a spring complex, or use at the BLM Headquarters well, effluent should have been mixed and diluted.

4.0 CINDER LEACH TEST

Drilling at the Guadalupe No. 1 test hole revealed a cinder bed from 644 to 677 feet below the surface. Down-hole natural gamma log surveying indicated that the cinder bed was slightly radioactive (Appendix A). A gamma spectral analysis of representative samples of the cinder bed and of the overlying bedrock showed comparable levels of gamma emitters. Table 4.1 shows the results of that testing.

TABLE 4.1

**RESULTS OF GAMMA SPECTRAL ANALYSIS OF CINDERS
AND BEDROCK, GUADALUPE NO. 1**

<u>Isotope</u>	<u>Bedrock</u>	<u>Cinders</u>
Radium 226	0.74+/-0.02	0.46+/-0.02
Lead 212	0.49+/-0.02	0.34+/-0.02
Lead 214	0.61+/-0.02	0.68+/-0.03
Actinium 228	1.06+/-0.04	0.68+/-0.03
Thallium 208	0.28+/-0.01	0.19+/-0.01
Bismuth 214	1.46+/-0.07	1.02+/-0.06
Total Uranium	0.55	0.17

Units = pico Curies/gram.

The cinders and bedrock may be in contact with leachate from the proposed tailings pond seepage. Due to the tendency of metals to complex with numerous other ions or ligands in solution (Stumm and Morgan, 1981), the radioisotopes were first thought to be susceptible to preferential solubility in the tailings leachate. An experiment was devised to assess if slurry or current tailings pond outfall solutions would leach the radioisotopes from the cinders or bedrock.

Three solutions (slurry, outfall, and distilled deionized water) and the two rock materials were prepared for initial gross alpha, gross beta, total uranium, and gamma spectral analyses. The three solutions were then mixed with representative samples of bedrock and cinders. A rock to solution ratio of 1:20 was selected based on the following considerations:

- o good contact and mixing would be achieved between the solid and solution,
- o adequate fluid quantities for analysis would be obtainable, and
- o general leaching test procedures (such as EP TOX) were reviewed.

The batch containers were tumbled for a one-week time period. The clear liquid was filtered to remove suspended solids and the larger colloids. Identical radio-analyses were performed on the resulting filtrate. Appendix C provides the test procedure and the analytical data derived from the tests.

Significant increases in a radioactive component in the filtrate over the initial contacting solution concentration would indicate leachability of that component by the contacting solution. In contrast, a decrease in a radioactive component during the contact period would be indicative of adsorption of the component onto the rock material or the formation of filterable colloidal suspensions.

The results of the cinder leach test were analyzed by several statistical comparison methods. The first method assesses if the post-treatment concentrations represent the same concentrations as the pre-treatment concentrations. By making use of the 95 percent confidence level, the concentration ranges of the pre- and post-analyses are compared. If the post-treatment concentration range is greater than the pre-treatment concentration range, leaching can be postulated as the cause of the concentration increase. In the second statistical test, observations were combined by rock type for the outfall treatment. This method assesses, by means of a paired t-test ($\alpha = 0.05$), if leaching occurred when an adjustment was

made for rock type. The result is an overall conclusion as to the significance of the leachability of the radioisotopes.

Table 4.2 summarizes the results of the statistical analysis. For the outfall solution, the number of leached radionuclides is greater for the cinders and mixture of bedrock and cinders than for bedrock alone. Nuclides appear to be more soluble from the cinders than from the bedrock. This condition may be due to variation in particle sizes or tortuosity within the bedrock that would limit the movement of the radionuclide to a rock or soil surface for solubilization.

The degrees of leaching observed for the cinder test and of the mixture of the bedrock and cinder test in the outfall solution were similar. These results suggest that passage through the bedrock will not change any character of the tailings pond seepage that may induce the leaching potential of the solution.

TABLE 4.2

CINDERS LEACHING TEST RESULTS

<u>Radionuclide</u>	<u>Outfall</u>			<u>Slurry/ Cinders</u>	<u>Dist. Water Cinders</u>	<u>Outfall</u>
	<u>Cinders</u>	<u>Bedrock</u>	<u>Cinders and Bedrock</u>			<u>Combined Cinders and Rock</u>
Radium 226	+	-	+	-	+	-
Lead 212	-	-	-	-	+	-
Lead 214	+	-	+	+	+	-
Actinium 228	+	+	+	+	+	+
Thallium 208	+	+	+	+	+	+
Bismuth 214	+	+	+	+	+	+

+ = Increase in concentration with treatment

- = No apparent increase in concentration with treatment

Leaching of cinders in distilled water shows whether or not the solubilization of the radionuclides into the outfall or slurry solutions is

preferential. All six radionuclides were brought into solution by distilled water (in which they were initially undetected). The magnitudes of the average change between before- and after-treatment concentration levels were similar to the changes observed for the outfall and slurry solutions, except for lead 212 and bismuth 214.

Although leaching of some radioisotopes was observed in many of the test scenarios, the levels of radioactivity observed in the pre- and post-treatment solutions were below radioactivity standards set by the State of New Mexico. In fact, the radioactivity levels observed fall within the range of values reported for ambient ground water sampled from municipal wells in the area. It should be noted though that the analysis method used for the Cinder Leaching Experiments was gamma spectral analysis, rather than radium detection by the emanation method. The emanation method is more commonly used for drinking-water tests. However, because of the overall low levels detected in the conservative rock to solution ratios used, the outfall or slurry does not appear to have a chemical quality that preferentially brings radionuclides of concern into solution from the bedrock or cinder strata. In short, the radionuclide leaching potential of the tailings pond seepage may be less than or equivalent to that of pure water.

5.0 ADSORPTION EXPERIMENTS

Review of leachate chemistry revealed several parameters that may require attenuation to meet New Mexico State Drinking Water Quality criteria. One physical chemical mitigation process is adsorption. Adsorption is analogous to condensation: a constituent dissolved in a liquid is deposited onto a solid until an equilibrium is attained between the two phases that are in contact. Even in the unsaturated zone where many of the pore spaces contain gases, a film of water surrounds the rock particle because water is a wetting fluid (air is non-wetting). The water film in contact with the rock particle would develop an equilibrium with the particle. Various natural and synthetic absorbents are possible. Clays, which have large surface areas, are often cited as an example of a naturally occurring adsorbent. The Guadalupe No. 1 test hole revealed several sandy clay, matrix-supported breccias that may possess adsorption potential.

Adsorption tests can be conducted in two different manners: column and batch tests. Column adsorption tests attempt to simulate selected flow conditions. The influent solution may not contact all solid material due to preferential flow paths. Thus, it would be difficult to assess the mass of adsorbent that was involved in the observed decrease of the solute. Results of column adsorption tests are difficult to replicate due to variability between core sections. In contrast, batch adsorption tests are easily and quickly performed and show positive adsorption if adsorption potential is significant. Batch tests may over-estimate adsorption by the physical mixing process exposing more particles to the solution (i.e., more mass may be participating in the adsorption process). Batch adsorption tests are often used to assess the attenuation potential of geologic materials. Batch adsorption tests are the subject of an EPA Technical Resource Document to provide guidance to the evaluation of adsorption potential of soils for solutes in waste leachates (Roy and others, 1985). Thus, batch adsorption tests were selected because:

- o significant adsorption potential can be rapidly evaluated;
- o the mass of material contacted is known;

- o in the unsaturated zone, a film of water would exist that would be in equilibrium with the solid material. Thus, at the rock-to-solution ratios used, batch tests are conservative; and
- o batch adsorption tests have been used by others (Roy and others, 1985) for evaluating adsorption potential of geologic materials.

On occasion, batch tests do not result in observable adsorption because of the large solution volumes. In such cases, column adsorption tests are utilized. However, the generally accepted assumption is that significant adsorption will be observed in batch tests.

Adsorption is observed as the decrease in initial solute concentration following solution/solid contact. The relationship between the resulting solid and solution concentrations can be explained in terms of a constant. The Freundlich adsorption equation is:

$$X/M = K_f C^{1/n}$$

Where X = the amount of solution,

M = the mass of adsorbent,

C = the equilibrium solute concentration, and

K_f and n are adsorbent-specific constants.

Where n is equal to 1 (the isotherm is linear), K_f becomes equal to K_d , the overall distribution coefficient between the phases. Data from adsorption tests are used to construct adsorption isotherms that are reviewed for linearity. Then K_d is calculated.

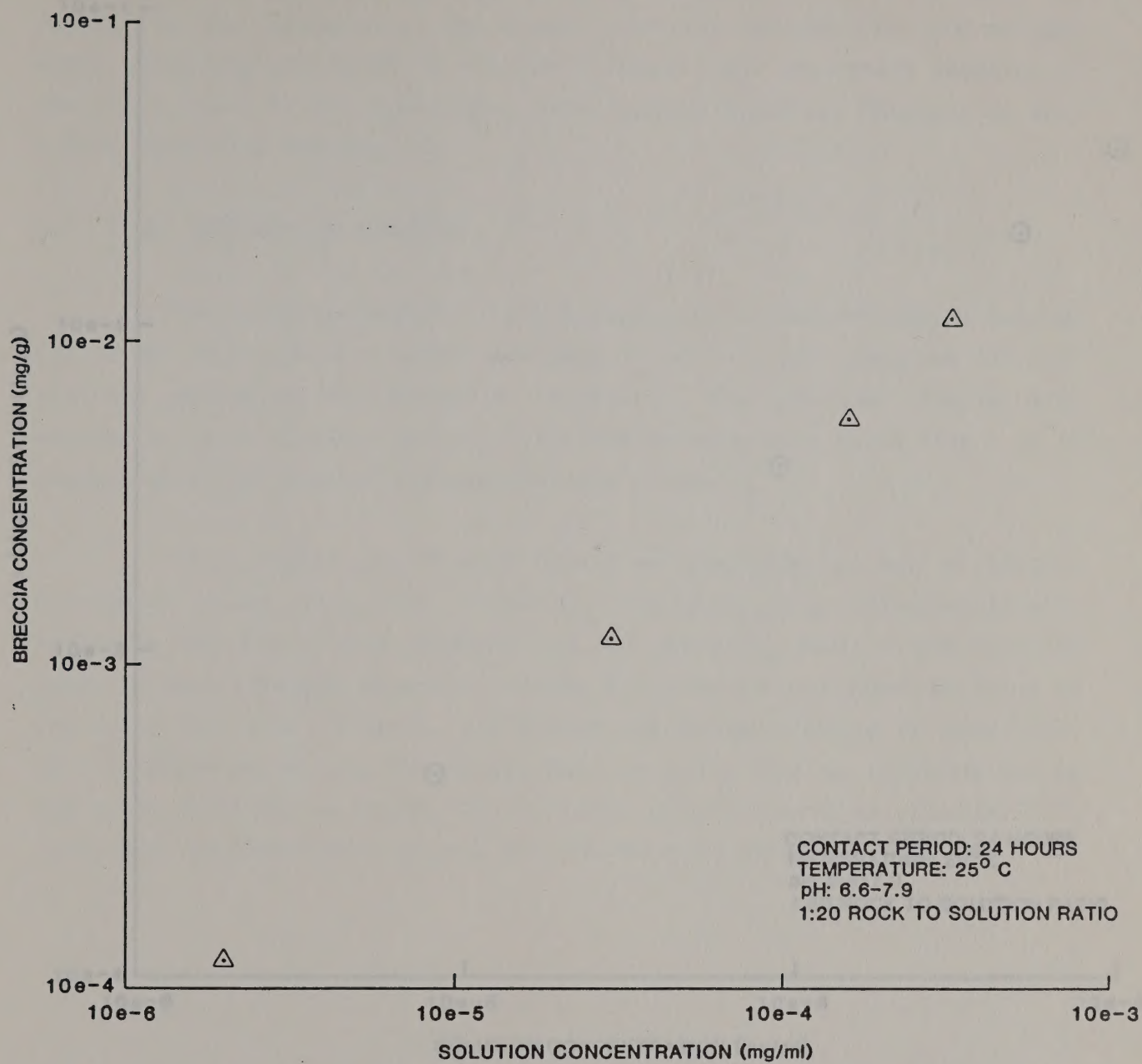
Batch adsorption tests were conducted to evaluate the adsorptive capability of a representative sample of the breccias and the bedrock (broken to gravel size, but not screened). Batch adsorption tests (Roy and others, 1985) were run, covering a wide range of rock-to-solution ratios, to detect the occurrence of adsorption and the best rock-to-solution ratio at which to observe the phenomenon. Appendix D presents the procedure and data derived from the experiments. If adsorption were observed, as indicated by a loss from the solution of greater than 10 percent, the data would be used to develop an adsorption isotherm.

5.1 TEST RESULTS

Test results indicated that anions and cations behaved differently in the batch adsorption system. Fluoride, sulfate and total dissolved solids increased in the leachate at all rock-to-solution ratios, indicating some solubility of these parameters from the rock materials. The cation lead did not show appreciable adsorption except at the higher rock-to-solution ratio of 1:20 that more closely approximates in-situ conditions (Appendix D). Molybdenum adsorption was observed at all rock-to-solution ratios tested.

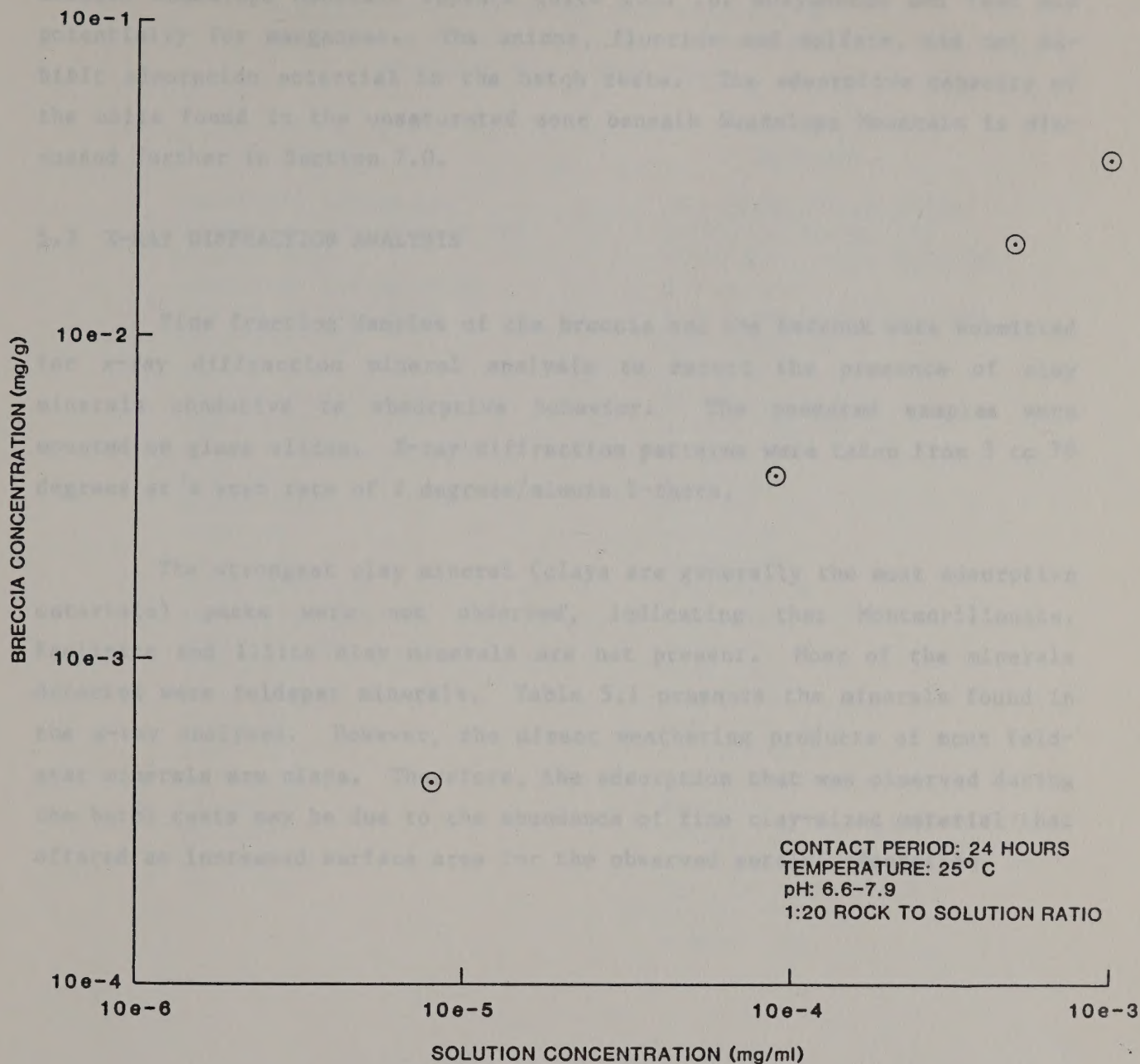
The adsorption isotherms presented in Figures 5.1 and 5.2 represent the relationship between the concentrations of the breccia and solution after a 24-hour contact period. The 1:20 rock-to-solution data are presented for consistency. The correlation coefficient of these isotherms is greater than 0.99, indicating a linear relationship for the concentration ranges studied and that $n=1$. The breccia K_d is estimated to be about 37 ml/mg for both lead and molybdenum. A similar review of the data shows that bedrock has similar adsorption potential.

Although lead and molybdenum were shown to adsorb to the test adsorbents, the adsorption mechanisms may be different. Adsorption mechanisms may account for adsorption of molybdenum being observed at all rock-to-solution ratios, while lead adsorption was observed at the highest rock-to-solution ratio of 1:20. Molybdenum is generally adsorbed by ligand exchange with a surface OH group. Molybdenum adsorption may be pH-dependent given this mechanism. Lead and manganese (which exceed New Mexico State Drinking Water Quality Standards) exist in solution as divalent cations that have water molecules arranged about the ion. Adsorption for lead and manganese involves the diffuse double layer at the particle surface. The adsorption of lead and manganese may also be influenced by pH when high pHs deprotonate surface hydroxyls. Both lead and manganese may compete for available adsorption sites, but this competition would be accounted for by the use of leachate solution in the adsorption experiments. No experiments were conducted to assess if the observed adsorption were reversible.



LEAD ADSORPTION
ISOTHERM:
BRECCIA AND SOLUTION
CONCENTRATIONS

Figure 5.1



**MOLYBDENUM ADSORPTION
ISOTHERM:
BRECCIA AND SOLUTION
CONCENTRATIONS**

Figure 5.2

In summary, the leachate mitigation potential by the rock materials beneath Guadalupe Mountain appears quite good for molybdenum and lead and potentially for manganese. The anions, fluoride and sulfate, did not exhibit adsorption potential in the batch tests. The adsorptive capacity of the units found in the unsaturated zone beneath Guadalupe Mountain is discussed further in Section 7.0.

5.2 X-RAY DIFFRACTION ANALYSIS

Fine fraction samples of the breccia and the bedrock were submitted for x-ray diffraction mineral analysis to detect the presence of clay minerals conducive to absorptive behavior. The powdered samples were mounted on glass slides. X-ray diffraction patterns were taken from 3 to 70 degrees at a scan rate of 2 degrees/minute 2-theta.

The strongest clay mineral (clays are generally the most adsorptive materials) peaks were not observed, indicating that Montmorillonite, Kaolinite and Illite clay minerals are not present. Most of the minerals detected were feldspar minerals. Table 5.1 presents the minerals found in the x-ray analyses. However, the direct weathering products of most feldspar minerals are clays. Therefore, the adsorption that was observed during the batch tests may be due to the abundance of fine clay-sized material that offered an increased surface area for the observed metals' adsorption.

TABLE 5.1

MINERALS DETECTED IN THE FINE FRACTION OF
BEDROCK AND BRECCIA VIA X-RAY DIFFRACTION,
GUADALUPE NO. 1 TEST HOLE

<u>Breccia</u>	<u>Bedrock</u>
ANORTHITE SODIAN LOW	ANORTHITE SODIAN INTER
ANORTHITE SODIAN HIGH SYN	ANORTHITE SODIAN LOW
ALBITE HIGH	ANORTHITE SODIAN HIGH SYN
ANORTHITE SODIAN INTER	ALBITE HIGH
ALBITE CALCIAN HIGH	ALBITE CALCIAN HIGH SYN
ANORTHITE LOW	ANORTHITE LOW
ALBITE LOW	GRAPHITE 2H
ALBITE CALCIAN LOW	GRAPHITE 2H SYN
BAYLDONITE	ALBITE CALCIAN LOW
ALBITE CALCIAN HIGH SYN	PUCHERITE
BEUSITE	MIERSITE
SCHREYERITE	BARATOV
BERRYITE	FENAKSITE
WALLISITE	GISMONDINE
SEARLESITE SYN	SCHIRMERITE
TRIPHYLITE SYN	BERZELIANITE
MONETITE SYN	DIOPSIDE
GUSTAVITE	NAMBULITE
FAIRFIELDITE	WALLISITE
DIOPSIDE	ANGLESITE SYN
MORINITE	CL TYRETSKITE
LAUTARITE SYN	HYDROHETAEROLITE
USSINGITE	KRUTAITE
BARATOV	QUARTZ LOW
GETCHELLITE	FAIRFIELDITE
SCAWTITE	TESCHEMACHERITE SYN
	TRIPHYLITE SYN
	CUPRITE SYN

6.0 WATER QUALITY

In an effort to assess the fate of tailings pond seepage, the quality of ground water and surface water in the vicinity of the present tailings pond was reviewed. The tailings pond outfalls are the best representation of tailings pond seepage, and characterization will better identify those parameters for which mitigation by dilution or adsorption should be investigated. Ground-water and surface-water quality may lend clues concerning the relationships between ground water and surface water in the confluence area and the movement or attenuation of constituents of interest in the ground water. Laboratory analyses of inorganic parameters conducted by the Molycorp laboratory during 1983 and 1985 provided the basis for the review. A brief description of the sampling locations; classification as to ambient ground water, leachate, or surface water; and the abbreviated location name are provided in Appendix E.

An effort was made to characterize the water sampling locations into three classifications: ambient ground water, surface water, and current leachate. A representative water quality status for each classification was developed from the mean of the laboratory results for the two years that data were available. A comparison was made between individual observations of water quality and the New Mexico State Ground-Water Standards. A gross comparison between ambient ground water, surface water and leachate is presented in Table 6.1 and shown visually in Figure 6.1.

6.1 AMBIENT GROUND-WATER QUALITY

Ten springs and two wells were selected to represent ambient ground-water quality. Three Rio Grande springs and seven Red River springs were sampled for water quality analyses in 1983 and 1985. The two BLM wells in the confluence area were also sampled at two locations. The first sample from each well was taken at the well head, and the second was taken at a point approximately 0.5 mile distant from the well. Thus, the Chiflo Campground well was also sampled at the Sheep Crossing Campground, and the Headquarters well was also sampled at the Big Arsenic Campground. The

TABLE 6.1

MEAN WATER QUALITY OF AMBIENT GROUND WATER,
SURFACE WATER, AND LEACHATE*

Parameter	New Mexico Ground- Water Standards	Ambient Ground- Water Quality ^(a)	Leachate Chemistry ^(b)	Surface- Water Quality ^(c)
pH	9	8.04	7.64	7.56
COD	—	ND	7.44	...
TSS	—	31.00	7.88	28.91
TDS	1000	198.22	1332.27	185.01
CN	0.2	ND	0.002	...
F	1.6	0.99	1.31	0.57
Cd	0.01	0.002	0.009	0.003
Fe	1.0	0.60	0.31	1.36
Mn	0.2	0.18	0.55	0.54
Mo	1.0	0.06	1.07	ND
Zn	10.0	0.19	0.17	0.34
Pb	0.05	0.02	0.059	0.02
Cu	1.0	0.018	0.02	0.04
As	0.1	ND	0.009	...
Hg	0.002	0.0001	ND	...
SO ₄	600	38.92	850.24	59.18
Ba	1.0	ND
Cr	0.05	0.01
Ni	0.2	0.03
Ca	—	22.21
Ag	0.05	ND
Cl	250	8.90
Al	5	ND
Mg	—	6.72

ND Below Detection Limit

... Not analyzed

— No Standard

* Values in parts per million.

(a) Rio Grande and Red River Springs and 2 wells (10 locations)

(b) Approximate sampling locations to present tailings pond (11 locations)

(c) Red River, Columbine & Cabresto Creeks (5 locations)

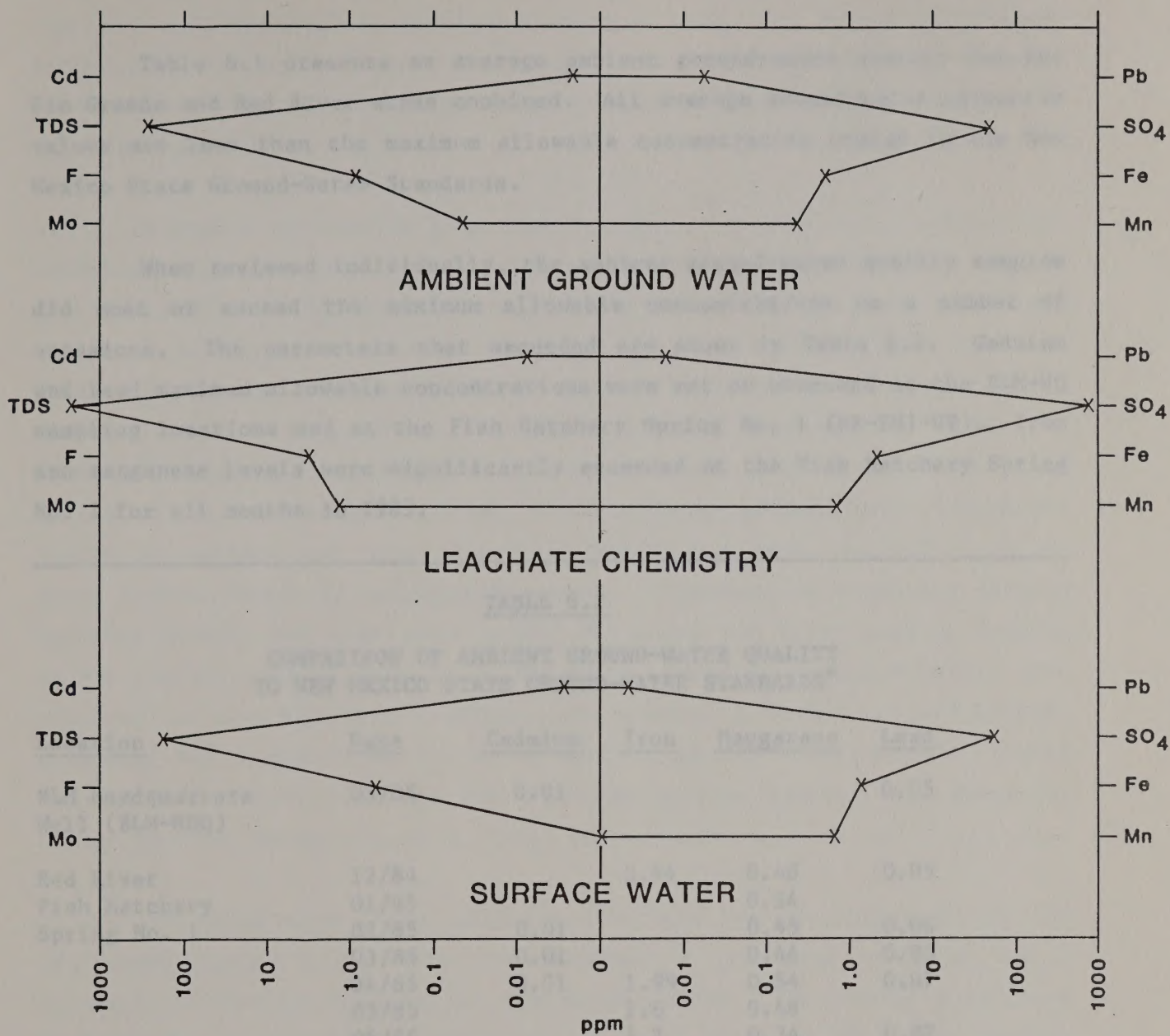


DIAGRAM OF AVERAGE WATER QUALITY PARAMETERS

Figure 6.1

analyses made of the samples taken from the campground and wellhead locations have been included in the review of ambient ground-water quality.

Table 6.1 presents an average ambient ground-water quality for the Rio Grande and Red River areas combined. All average ground-water parameter values are less than the maximum allowable concentration stated in the New Mexico State Ground-Water Standards.

When reviewed individually, the ambient ground-water quality samples did meet or exceed the maximum allowable concentrations on a number of occasions. The parameters that exceeded are shown in Table 6.2. Cadmium and lead maximum allowable concentrations were met or exceeded at the BLM-HQ sampling locations and at the Fish Hatchery Spring No. 1 (RR-FH1-SP). Iron and manganese levels were significantly exceeded at the Fish Hatchery Spring No. 1 for all months in 1985.

TABLE 6.2

COMPARISON OF AMBIENT GROUND-WATER QUALITY
TO NEW MEXICO STATE GROUND-WATER STANDARDS*

<u>Location</u>	<u>Date</u>	<u>Cadmium</u>	<u>Iron</u>	<u>Manganese</u>	<u>Lead</u>
BLM Headquarters Well (BLM-HDQ)	05/85	0.01			0.05
Red River	12/84		2.94	0.48	0.05
Fish Hatchery	01/85			0.34	
Spring No. 1	02/85	0.01		0.45	0.06
	03/85	0.01		0.46	0.05
	04/85	0.01	1.99	0.54	0.07
	05/85		2.6	0.48	
	06/85		4.2	0.34	0.07
	07/85	0.01	2.9	0.25	
	08/85			0.24	
	09/85	0.01	2.4	0.7	
	10/85	0.01	4.03	0.66	
<hr/>					
New Mexico State Drinking Water Quality Standards		0.01	1.0	0.2	0.05

* Monthly means of values exceeding or equivalent to New Mexico State Ground-Water Standards. Concentrations in parts per million.

5.2 Average water quality between the confluence area wells and the Red River springs was compared. This comparison was made to evaluate the possibility of a hydraulic connection through a fault zone trending northwest between the two major rivers. Past comparisons (Water Resources Associates, 1984) showed that waters may be related based on relationships between the major inorganic ions.

A number of samples from the Red River springs were analyzed for sulfate, calcium, magnesium, chloride and total dissolved solids. Samples from the BLM well (BLM-HDQ-W) were analyzed for total dissolved solids and sulfate. A comparison of mean 1983 and 1985 data indicates that the confluence ground water is comparable to that of the Red River springs complex (RR-1-SP through RR-10-SP). The Fish Hatchery springs (RR-FH1-SP and RR-FH2-SP) samples have higher sulfate, chloride, calcium and total dissolved solids concentrations than the confluence ground water. Elevated levels of sulfate and total dissolved solids are more indicative of Red River surface water or tailings leachate. A comparison of metals concentrations between the confluence ground water and Red River springs samples do not correlate as closely as do the salts. Confluence ground water, when compared to the Red River springs, was generally higher in molybdenum, manganese and copper. The Red River springs samples were generally higher in zinc and mercury, and the Fish Hatchery springs samples were generally higher in iron, manganese, zinc, lead, and mercury.

The results of these comparisons between Red River springs and the confluence ground water were inconclusive in providing evidence for a hydraulic connection between the two major rivers. To provide additional evidence for a hydraulic connection, a consistent set of water quality parameters will need to be evaluated, and Rio Grande sampling locations will need to be added to the water quality program. However, it does appear from a review of the water quality data that springs along the lower Red River are discharging some regional ground water.

6.2 SURFACE-WATER QUALITY

Five locations in the study area were sampled to evaluate surface-water quality. Three locations are on the Red River; the other locations are on Cabresto Creek and Columbine Creek. All surface-water sampling locations are upstream of the present tailings pond. Table 6.1 shows an average of the surface-water quality for all locations sampled in 1983 and 1985. Overall surface-water quality is generally within New Mexico State Ground-Water Standards, although the average concentrations of iron and manganese exceed State drinking water standards.

Data from individual sampling locations show that maximum allowable concentrations are frequently equaled or exceeded, as outlined on Table 6.3. Cadmium levels were quantified at all locations. Cadmium levels are normally below State standards but a cyclical period of levels meeting State standards is noted for all locations for 1985. Cadmium concentrations which meet the maximum allowable concentrations occurred in February-March, June-July, and September-October 1985. The maximum allowable concentrations for zinc were significantly exceeded in April 1985 on the Red River at the Questa Bridge and Ranger Station sampling stations. Iron concentration levels were moderately to significantly exceeded at all surface-water sampling locations; Cabresto Creek (1983) and Red River at the Mill Plant Bridge (October 1985) exhibited the peak iron concentrations. Manganese concentrations were often high in Cabresto Creek and the Red River. The maximum allowable concentrations for lead were met or exceeded on occasion at all locations in the Red River and Cabresto Creek. Columbine Creek appears to have the best water quality based on the available records. Cadmium concentration levels for Columbine Creek did meet the maximum allowable concentration on occasion, and iron concentrations were above allowable levels on only one occasion.

The periodic deterioration of surface-water quality is apparently influenced by the mineralization of the Red River basin. Seasonal precipitation events are providing runoff that has traveled over highly mineralized rocks and imparts a short-lived but significant impact to the quality of Red River surface water (MolyCorp, personal communication).

TABLE 6.3

COMPARISON OF SURFACE-WATER QUALITY
TO NEW MEXICO STATE GROUND-WATER STANDARDS*

<u>Location</u>	<u>Date</u>	<u>Cadmium</u>	<u>Iron</u>	<u>Manganese</u>	<u>Zinc</u>	<u>Lead</u>
Cabresto Creek	03/83	0.01				
	04/83		2.65			
	05/83		11.0	0.4		
	09/83			0.46		
	02/85			0.22		
	04/85			0.25		
	05/85	0.01				
	06/85			0.32		
	07/85					0.06
Columbine Creek	03/83	0.01				
	05/83		1.22			
	02/85	0.01				
	05/85	0.01				
	06/85	0.01				
Red River at the Mill Plant Bridge	12/84			0.23		0.05
	01/85			0.25		
	02/85			0.33		
	03/85	0.01				
	04/85	0.01		0.25		0.05
	05/85		1.19			
	06/85	0.01	2.17			
	07/85	0.01				
	09/85	0.01	1.37	0.61		0.08
	10/85	0.01	40.7	0.35		0.15
Red River at Questa Bridge	12/84		2.2	0.78		
	01/85			0.78		
	02/85	0.01	1.91	0.98		
	03/85	0.01	1.77			0.05
	04/85		2.99	0.86	18.0	
	05/85		1.75	0.53		
	06/85	0.01	2.86	0.37		
	07/85	0.01	2.87	0.4		
	08/85			0.35		
	09/85	0.01	1.51	0.6		0.055
	10/85	0.01	4.57	0.91		0.05

(Continued on Next Page)

New Mexico State	0.01	1.0	0.2	10.0	0.05
Ground-Water Standards					

* Monthly means of values exceeding or equivalent to New Mexico State Ground-Water Standards. Concentration in parts per million.

TABLE 6.3 (Continued)

<u>Location</u>	<u>Date</u>	<u>Cadmium</u>	<u>Iron</u>	<u>Manganese</u>	<u>Zinc</u>	<u>Lead</u>
Red River	12/84		1.66	1.23		
Ranger	01/85		1.44	1.61		
Station	02/85	0.01	2.26			
	03/85	0.01	2.07			
	04/85		1.85	0.99	14.0	0.06
	05/85	0.01	2.56	0.68		
	06/85		2.04	0.45		
	07/85	0.01	3.6	0.38		
	08/85			0.47		0.05
	09/85	0.01	3.7	1.15		0.07
	10/85	0.01	3.01	1.01		
<hr/>						
New Mexico State		0.01	1.0	0.2	10.0	0.05
Ground-Water Standards						

* Monthly means of values exceeding or equivalent to New Mexico State Ground-Water Standards. Concentration in parts per million.

6.3 LEACHATE CHEMISTRY

To characterize tailings pond leachate, 11 sampling locations were selected on the basis of proximity to the present tailings pond. The two Outfall sampling locations, in which Outfall 002 collects leachate through a french drain system and Outfall 001 collects surface discharge, and the West Ditch (W-ditch) samples (decant from the present tailings pond) are assumed to be the most representative of the leachate due to their proximate locations to the current tailings facility. Leachate may change through time in quality due to changes in the chemical composition of slurry, slurry discharge rates, and pond seepage rates. It is difficult to anticipate such changes. However, the data from the 11 sampling locations are the best approximation to "mature" leachate available.

The average of all water-quality data for the locations (shown in Table 6.1) indicates that parameters that exceed the maximum allowable concentrations are total dissolved solids, manganese, molybdenum, lead and sulfate. Comparisons of water quality from individual sampling locations (Table 6.4) with the New Mexico State Ground-Water Standards show that the

TABLE 6.4 (Page 1 of 2)

COMPARISON OF LEACHATE/TAILING AREA WATER QUALITY TO
NEW MEXICO STATE GROUND-WATER STANDARDS*

<u>Location</u>	<u>Date</u>	<u>TDS</u>	<u>Fluoride</u>	<u>Cadmium</u>	<u>Iron</u>	<u>Manganese</u>	<u>Molybdenum</u>	<u>Lead</u>	<u>Sulfate</u>
Outfall 001	05/84		1.6				1.86		
	01/85	1318	2.1		1.11				797
	02/85	1285	1.9	0.02	1.34			0.07	830
	03/85	1144	1.9	0.02	1.26			0.07	861
	04/85		2.0	0.01		0.4		0.05	836
	10/85	1161	2.3	0.01				0.07	850
Outfall 002	05/83					1.22	2.90		
	09/83					1.41	2.86		
	05/84	1700	2.2			1.27	2.51		
	01/85	1545	2.1			1.38	2.66		966
	02/85	1500	2.1	0.01		1.19	2.31	0.07	939
	03/85	1439	2.1	0.01		1.44	2.51	0.08	1078
	04/85	1439	2.0	0.01		1.39	2.43	0.06	1077
	05/85	1562	2.0	0.01		1.35	2.39	0.06	940
	06/85	1459	2.2	0.01		1.65	2.55		885
	07/85	1476	2.3	0.02		1.76	2.74	0.11	816
	08/85	1430	2.1	0.01		1.61	2.76	0.07	863
	09/85	1400	2.1	0.01		1.53	2.67	0.09	885
	10/85	1296	2.0	0.02		1.56	2.11	0.11	862
Tail Dry Well	09/83				5.0				
	01/85			0.01	1.37				
	02/85				1.17				
	04/85			0.01	1.13				
	07/85							0.09	
<hr/>									
New Mexico State		1000	1.6	0.01	1.0	0.2	1.0	0.05	600
Ground-Water Standards									

* Monthly means of values exceeding or equivalent to New Mexico State Standards. Concentrations in parts per million.

(Continued)

TABLE 6.4 (Page 2 of 2)

<u>Location</u>	<u>Date</u>	<u>TDS</u>	<u>Fluoride</u>	<u>Cadmium</u>	<u>Iron</u>	<u>Manganese</u>	<u>Molybdenum</u>	<u>Lead</u>	<u>Sulfate</u>
West Ditch	01/85	1081	2.1			0.36	1.5	0.08	748
	02/85	1150	1.8	0.01		0.49	1.39	0.08	755
	03/85	1057	1.8	0.01		0.49	1.10	0.07	821
	04/85	1048	1.7	0.01		0.51	1.3		693
	05/85	1029	1.9	0.01			1.09		737
	06/85	1154	1.7	0.01			1.24		672
	07/85	1148	2.0	0.02			1.58	0.07	792
	08/85		2.4				2.01		998
	10/85	1138	1.8						
New Mexico State Ground-Water Standards	1000	1.6	0.01	1.0	0.2	1.0	0.05	600	

* Monthly means of values exceeding or equivalent to New Mexico State Standards. Concentrations in parts per million.

samples from the Outfalls and West Ditch also meet or exceed maximum allowable concentrations of fluoride, cadmium, and iron, as well as those already mentioned.

7.1 INTRODUCTION

Evaluation of the probable leachate seepage from the Guadalupe site, when compared to the current site, will assist in evaluating the impact of tailings pond seepage on the ground water in the Guadalupe Mountain area. The mitigation of leachate components in the ambient ground water is addressed in Section 7.0.

This chapter discusses the results of mathematical modeling to estimate the transport of dissolved constituents from the Guadalupe site to the West Ditch. The model was developed using the MODFLOW computer program, which is a finite difference method for simulating groundwater flow and solute transport. The model was calibrated using data from the current site, and the results were used to estimate the potential leachate seepage from the Guadalupe site. The model results show that the potential leachate seepage from the Guadalupe site is significantly higher than the current site, and this could have a significant impact on the ground water in the Guadalupe Mountain area.

Potential leachate seepage rates from the Guadalupe site are discussed in Section 7.0. In that report, which is based on an analysis of the current site, the potential leachate seepage rate was estimated to be 0.1 to 0.2 gallons per day (gpd) per foot of tailings. This rate is based on a comparison of the current site to the Guadalupe site, which has a higher potential leachate seepage rate. The potential leachate seepage rate from the Guadalupe site is estimated to be 0.3 to 0.5 gpd per foot of tailings. This rate is based on a comparison of the current site to the Guadalupe site, which has a higher potential leachate seepage rate. The potential leachate seepage rate from the Guadalupe site is estimated to be 0.3 to 0.5 gpd per foot of tailings. This rate is based on a comparison of the current site to the Guadalupe site, which has a higher potential leachate seepage rate.

7.0 SIMULATION OF CONTAMINANT TRANSPORT BENEATH THE PROPOSED GUADALUPE MOUNTAIN TAILINGS DISPOSAL SITE

7.1 INTRODUCTION

Seepage from the tailings pond is expected to contain concentrations of metals and other dissolved constituents in excess of the New Mexico State Ground-Water Standards for ground water (New Mexico Water Quality Control Commission, 1986). This chapter summarizes the results of mathematical modeling to simulate the transport of dissolved constituents (metals and anions) through the unsaturated zone, and their mixing in the saturated zone beneath the pond. Predictions were made of: (1) the rate of solute migration to the water table, and (2) the concentration of solute at the water table directly beneath the pond and at the claim boundary down-gradient of the pond. The expected amount of time that mill tailings will be slurried to the proposed Guadalupe Mountain site is about 30 years. Predictions of contaminant transport beneath the proposed tailings pond were made for 27 years after the start of disposal and for 50 years after pond closure.

Potential seepage rates from the Guadalupe site are discussed in Geocon (1983). In that report, which is based on an analysis of the current disposal site, an expected seepage rate from the Guadalupe site might be 0.3 cfs from a 200-acre wetted pond bottom. This rate is qualified by a "worst-case" seepage rate of 1.0 to 1.5 cfs from the Guadalupe site in order to cover uncertainties in their analysis. Seepage values ranging from 0.5 to 1.5 cfs were used in this analysis. The actual seepage rate from the pond may vary due to variations in fracture density of bedrock beneath the pond and due to pond design features. For example, special tailings spigoting techniques may be used whereby the pond bottom is sealed with tailings slimes. Also the various pond channels could be lined to prevent seepage. Design features such as these can significantly reduce the seepage rate from the pond.

7.2 TECHNICAL APPROACH

A variable-saturated, integrated finite-difference model, known as TARGET (see Appendix F for details of the mathematical background of this model), was selected to simulate the vertical transport of solute beneath the proposed tailings pond. A two-dimensional model was selected because migration of dissolved constituents through the unsaturated zone and subsequent migration in the saturated zone are primary concerns. In the unsaturated zone, flow is expected to be primarily vertical. Concern for potential development of a water-table mound, for contaminant mixing below the water table, and for travel time to the claim boundary precluded the use of a one-dimensional model. A three-dimensional model was not considered to be necessary since conditions in the third dimension are not expected to be variable.

The TARGET model is capable of solving complex flow and transport ground-water problems in variably saturated and/or saturated soil and rock. The model has been applied extensively to contamination problems, particularly in the western United States and has been verified and validated through comparison of predicted results with laboratory, analytical and other model simulation results. In addition, validation of model predictions is available from a number of projects. For example, seepage and contaminant transport through the unsaturated zone due to evaporation pond leakage at a site in New Mexico was simulated. Geophysical data later established that the mixing depth predicted by the model was accurate. Furthermore, peer reviews of this model have been conducted in connection with other projects (Appendix G).

The unsaturated zone beneath the proposed tailings pond is basically comprised of basalt and andesite flows exhibiting varying degrees of fracturing. A common approach to analyzing contaminant migration in fractured rock is to treat the problem in the same manner as for porous media that has corresponding hydraulic properties. Measurements of bulk hydraulic conductivity in fractured rock are based on Darcian flow assumptions. It is generally agreed (Snow, 1969; Streltsova, 1976; Freeze and Cherry, 1979) that flow velocities in fractures obey Darcy's Law if the

fracture spacing is close enough for the rock to behave similarly to a porous medium. In modeling terms, if the model calculation cells contain a number of fractures, then the behavior of the aggregate is similar to flow in granular soil. Within the volcanic terrain of this study, fracturing predominantly occurred as the result of brecciation processes (flow breccias and explosion breccias) and tectonic movements. In a brecciated unit, fracture densities are high and statistically isotropic. In the present application, the cell sizes are large enough (typically 20 feet by 200 feet) to encompass many fractures so that the assumption of equivalent porous media flow in this fractured rock situation is applicable.

Contaminant transport may be influenced by the presence of fractures rather than inter-granular flow paths. What this implies is: (1) diffusion into the rock matrix may retard the transport of even non-reactive contaminants (Grisak and Pickens, 1980); (2) adsorption may be more appropriately described on the basis of adsorption per unit surface area of fracture (Freeze and Cherry, 1979; Burkholder, 1976); and (3) molecular diffusion may overwhelm mechanical dispersion in fracture flow due to low flow velocities. In the present modeling effort, the following assumptions were made:

- o diffusion into the rock matrix is conservatively neglected;
- o adsorption distribution coefficients measured in the laboratory were used as the starting point for a sensitivity analysis in an attempt to simulate in-situ conditions; and
- o the dispersion term in the model incorporates both molecular diffusion and mechanical dispersion so that dispersion for a range of flow velocities may be represented.

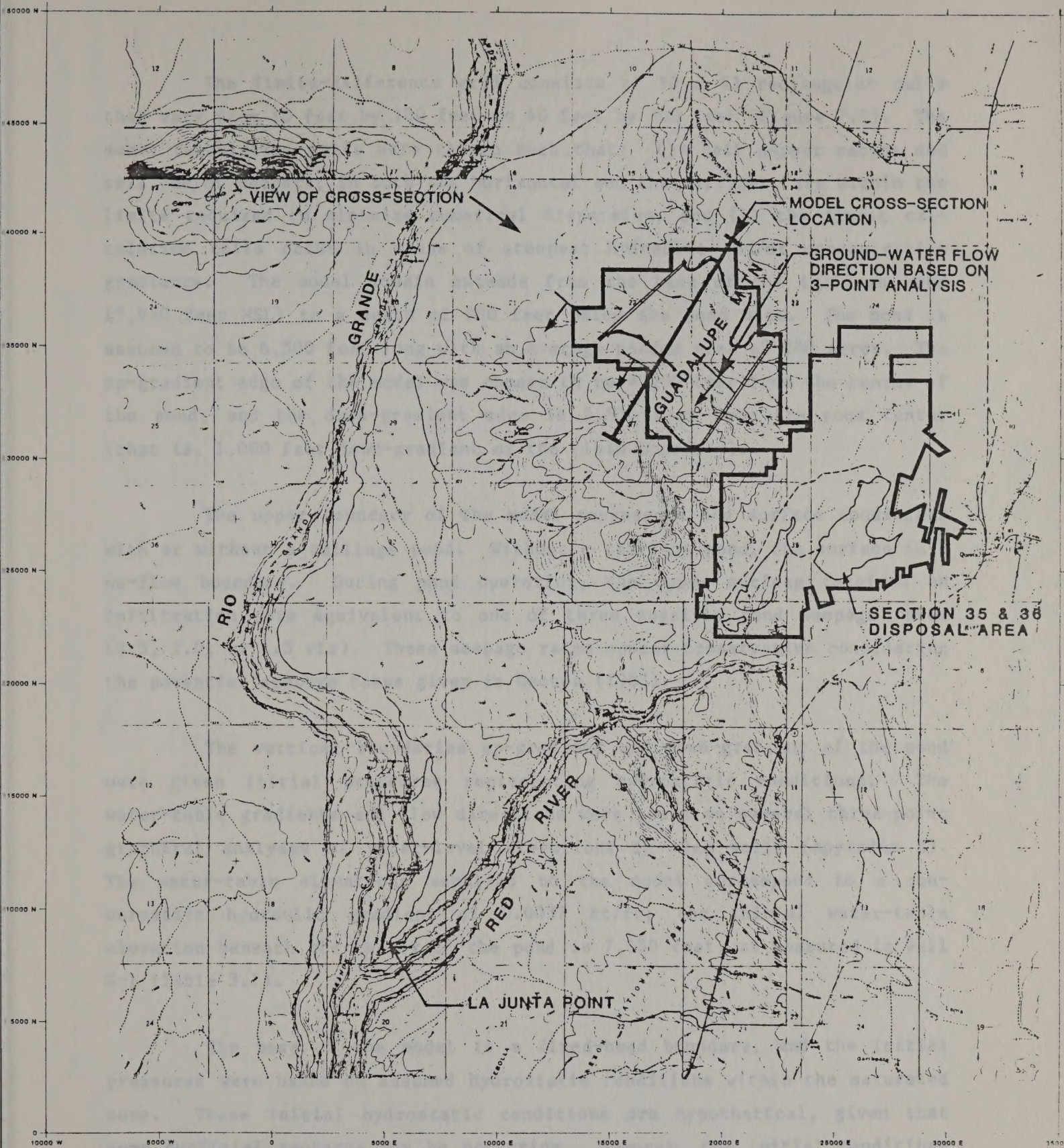
While advection and dispersion of contaminants in fractured rock may be represented by analogy with a porous medium having anisotropic properties and low porosity, the representation of contaminant adsorption in fractures is more problematic. Processes governing solute adsorption in fractures include:

- o solute diffusion into the rock matrix,
- o fracture aperture size,
- o ground-water velocity,
- o matrix porosity,
- o adsorption distribution coefficient (K_d), and
- o degree of saturation.

Solute diffusion into the rock matrix will result in solute storage (this is conservatively neglected in the model). Larger fracture apertures and/or ground-water velocities will reduce the likelihood of matrix diffusion or adsorption. Larger matrix porosity will enhance the possibility of matrix storage. Larger K_d 's imply a greater probability of solute immobilization through ion-exchange, hydrolysis, and other methods. The greater the degree of saturation, the greater the surface area available for potential reaction.

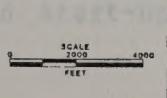
In the present instance, batch adsorption experiments were conducted on rock fragments from boring G-1 in order to measure the upper-limit K_d 's for the fractured rock at this site. In the modeling analyses, conservative assumptions were made to neglect matrix diffusion and fracture storage. Since contaminated ground water is the wetting fluid, it was assumed that reactions may occur even in partially saturated fractures. As ground-water flow velocities in the partially saturated fractures are expected to be low, it is assumed that sufficient time is available for equilibrium conditions to prevail in rock/solution interactions. However, it was not assumed that the K_d 's measured in the batch tests were representative of in-situ reaction conditions. Since the latter two assumptions may not be conservative, K_d 's were examined in a sensitivity analysis (see Section 7.4.2) and K_d 's substantially lower than those measured in the batch tests were used in the modeling analyses.

The orientation and lateral extent of the calculation domain are shown on Figure 7.1. Water well locations are shown in Figure 2.2. The direction of ground-water flow in the vicinity of Guadalupe Mountain is identified on Figure 7.1.



LEGEND

- CLAIM BOUNDARY
- DAM
- ROAD



GROUND-WATER MODEL LOCATION MAP

Figure 7.1

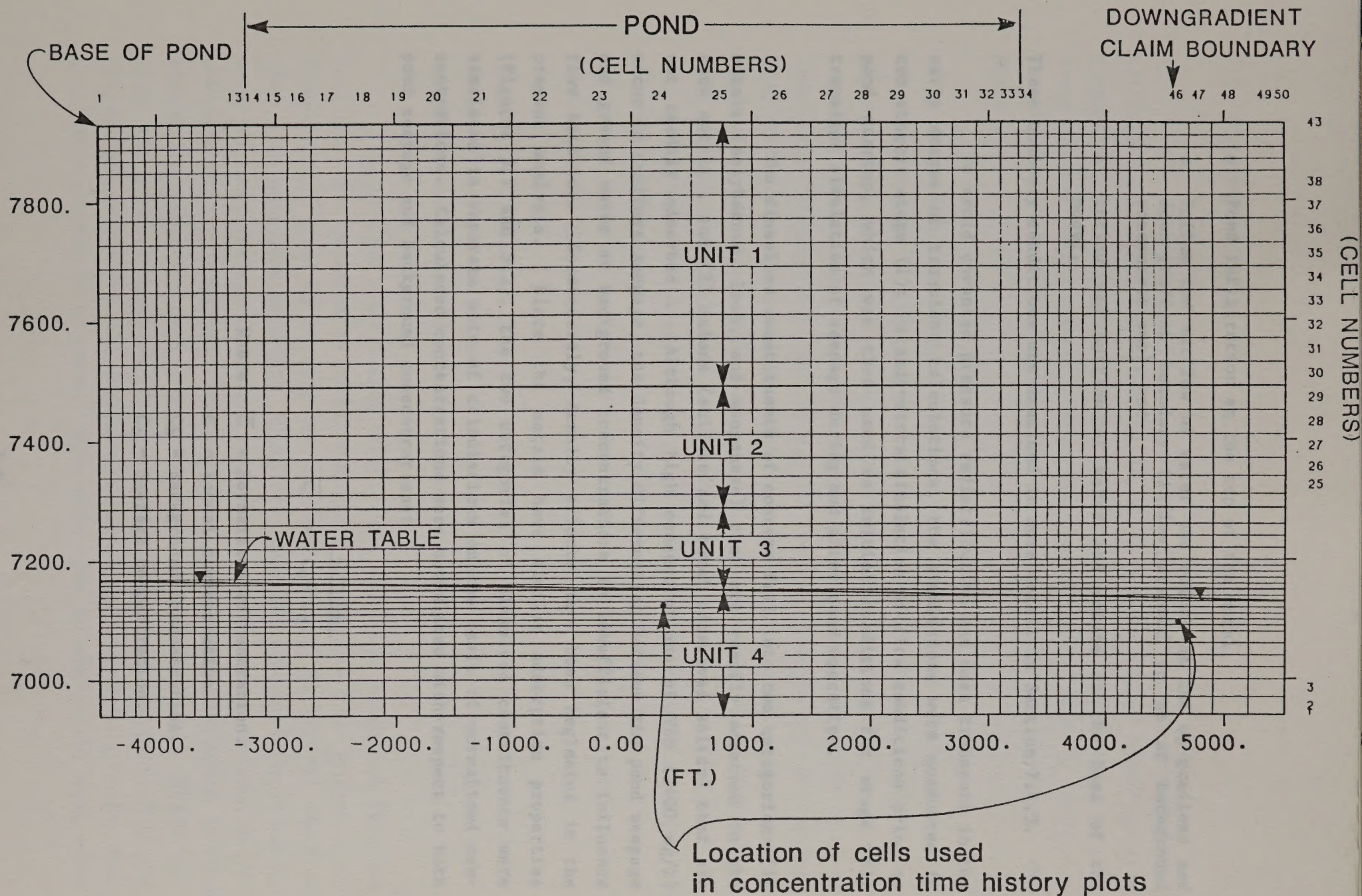
The finite-difference grid consists of 50 x 43 rectangular cells that vary from 10 feet by 100 feet to 40 feet by 500 feet (Figure 7.2). The model calculation cells were chosen such that: (1) cell aspect ratios and cell Peclet numbers, in both the horizontal and the vertical, are within the limits required to minimize numerical dispersion; and (2) the finest calculation cells occur in areas of steepest hydraulic and/or concentration gradients. The model domain extends from the base of the tailings pond (7,930 feet MSL) to a depth of 990 feet below the pond base. The pond is assumed to be 6,500 feet long with an average ponded area of 200 acres. The up-gradient edge of the model was chosen to be 4,500 feet from the center of the pond, and the down-gradient edge is 5,500 feet from the pond center (that is, 1,000 feet down-gradient of the claim boundary).

The upper boundary of the model represents the surface conditions with or without a tailings pond. Without a tailings pond, the surface is a no-flow boundary. During pond operation, the upper surface received an infiltration rate equivalent to one of three possible pond seepage rates (0.5, 1.0, or 1.5 cfs). These seepage rates appear conservative considering the potential seepage rates given in Geocon (1983).

The vertical boundaries up-gradient and down-gradient of the pond were given initial pressures representing hydrostatic conditions. The water-table gradients and flow directions were based on several three-point graphical analyses of water-level elevations in area wells (Appendix B). The water-table elevations supplied to the model correspond to a conservative hydraulic gradient of 0.0037 ft/ft; the initial water-table elevation beneath the center of the pond is 7,150 feet, as measured in Well G-1 (Table 3.1).

The base of the model is a fixed-head boundary, and the initial pressures were based on assumed hydrostatic conditions within the saturated zone. These initial hydrostatic conditions are hypothetical, given that some surficial recharge may be occurring. However, the initial conditions are superseded when pond start-up is simulated. The boundary conditions supplied provide for:

(FT. AMSL)



FINITE DIFFERENCE MESH
USED IN CASES 2 THRU 16

- o Pond infiltration at the top of the model,
- o Inflow and outflow of water and solute at the up-gradient and down-gradient boundary (inflow assumed to be at background concentrations), and
- o Inflow and outflow of water and solute at the base of the model.

These boundary conditions are examined in more detail in Section 7.4.3.

To avoid unwanted pressure redistribution and mass transport in the early stages of transient calculations, the simulations were conducted in two stages: stage (1): steady-state simulation of flow conditions prior to pond startup, which was then used as initial conditions for stage (2): transient simulation of seepage during and after pond operation.

The dissolved constituents of concern fall into two categories: (1) metals (molybdenum, lead, and manganese) that are readily adsorbed in the rock matrix, and (2) anions (sulfate and total dissolved solids) that are not readily adsorbed. Although high concentrations of TDS (1400 mg/l) occur in tailings seepage, the density differential between the pond seepage and ground water at background concentrations is insufficient to influence flow behavior. Consequently, density effects have been neglected in the present analysis. Since the metals have similar adsorption properties (Figures 5.1 and 5.2), the two categories of dissolved constituents were simulated in separate sets of calculations on the basis of normalized concentrations. Calculated concentrations were normalized with respect to both pond seepage and background concentrations:

$$\bar{C} = \frac{C - C_b}{C_o - C_b}$$

Where: \bar{C} = Normalized concentration.

C = Actual concentration.

C_b = Background concentration.

C_o = Seepage concentration.

7.3 SITE-SPECIFIC DATA

The subsurface geologic conditions used in the model were based on drilling information developed by Dames & Moore. Three hydrologically distinct units occur beneath Guadalupe Mountain (Unit 3 is subdivided into saturated and unsaturated to provide four units for the model). Table 7.1 provides a summary of geologic and hydrogeologic data pertinent to the model.

In addition, dispersivity (or empirical measure of the tortuosity and heterogeneity of the medium) must be defined. Anderson (1979) summarized regional dispersivities established in modeling studies for similar settings. The ranges quoted for fractured basalt are: 90 to 280 feet for longitudinal dispersivity, and 55 to 400 feet for transverse dispersivity. Since the extent of the model domain in this study is smaller than some of the studies referenced above, dispersivities on the lower end of the ranges were selected. In this way, mechanical mixing and hence dilutions of the solutes would not be overestimated. Generally, longitudinal to transverse dispersivity ratios of 3 to 10 are expected and a value of 10 was used in this study. Values of 100 feet for longitudinal dispersivity and 10 feet for transverse dispersivity were used in the model.

The hydraulic material properties for the bedrock units underlying the pond have been estimated. A range of values have been used in the model investigations because of the uncertainty associated with these data.

Adsorption distribution coefficients (K_d s) for molybdenum (Mo) and lead (Pb) were measured in batch laboratory experiments (see Section 5 and Appendix D). A K_d of 37 ml/g was measured for both Mo and Pb, based on adsorption onto rock material. Since the finer-grained particles typically found in fractures and as breccia matrix are believed to be responsible for the bulk of the adsorption measured, two methods for estimating in-situ adsorption properties were used. In the first method, Unit 2 (which contains the greatest fraction of finer-grained material, see Table 7.2) was assumed to account for all adsorption, having a K_d of 37 ml/g. The other units were assumed to be inert. This assumption is used in the model cases

TABLE 7.1

Geologic and Hydrogeologic Data For
Units Beneath Guadalupe Mountain

Unit	Depth (feet)	Thickness (feet)	Porosity (%)	Specific Yield (%)	Adsorption Distribution Coefficient (ml/gm) ^(a) Medium Kd	Average Hydraulic Conductivity (cm/s)	Description
1	0 to 440	440	1.5	10	0.13	X 2.5×10^{-3} Z 2.5×10^{-4}	Basalt and andesite flows, 20 to 30 feet thick, competent, weakly fractured.
2	440 to 643	203	30	20	4.07	X 5.1×10^{-3} Z 5.1×10^{-4}	Alternating beds of andesite/ basalt and breccia, 5 to 30 feet thick with breccia beds 10 to 50 feet thick, clay common in fractures and breccia matrix.
3	643 to 800	157	10(1)	15	0.14	X $2.5 \times 10^{-2(b)}$ Z 2.5×10^{-3}	Scoriaceous basalt and cinder beds, 10 to 30 feet thick, highly fractured with minor clay in fractures.
4	800 to 1000	200	5	15	0	X $1.0 \times 10^{-2(b)}$ Z 1.0×10^{-3}	Scoriaceous basalt as above, saturated (below water table).

(a) See discussion in text.

(b) Water Resources Associates, June 1984. Hydrologic and hydrogeologic analysis for the Guadalupe Mountain ground-water discharge plan: Report to MolyCorp, Inc.

NOTE: Values for porosity, specific yield, and hydraulic conductivity are estimated unless referenced to Water Resources Associates, 1984.

TABLE 7.2

Derivation of Adsorption Distribution Coefficients For Medium Kd Case

Unit ^(a)	Cubic Feet Of Rock In 2.5 Inch Diameter Core A	Porosity, B (%)	Fracture & Pore Space Volume, C ^(b) (ft ³)	Estimated Fraction of Adsorptive Material, D (%)	Volume Adsorptive Material, E ^(c) (ft ³)	Estimated Density Of Rock, F (lbs/ft ³)	Total Weight of Core, G ^(d) (lbs)	Weight Of Adsorptive Material, H ^(e) (lbs)	Weight Fraction Of Adsorptive Material, I ^(f) (%)	Adsorption Distribution Coefficient, J ^(g) (ml/gm)
1	14.2	1.5	0.21	39	0.08	160	2,272	8	0.35	0.13
2	7.1	30	2.13	42	0.89	110	781	89	11.0	4.07
3	5.5	10	0.55	5	0.027	130	715	2.7	0.38	0.14

- Assumptions:
1. Unit 4 is non-adsorptive.
 2. The bulk density of soil and adsorptive material is 100 lbs/ft³.
 3. The bulk density of solid andesite is 170 lbs/ft³.

NOTES: In the "high Kd" case, Unit 2 was assumed to contain 100 percent of the adsorptive material. The measured Kd of 37 ml/gm was, therefore, applied to Unit 2 only.

(a) Refer to Table 7.1 for description

(b) $C = A \times B$

(c) $E = C \times D$

(d) $G = A \times F$

(e) $H = E \times F$

(f) $I = H/G$

(g) $J = \text{Measured Kd (37 ml/g)} \times I$

referred to as "high Kd" cases. In the second method, it was assumed that greater adsorption potential was measured in the laboratory than would occur in-situ because the laboratory sample was broken exposing more surfaces to solution than occurs naturally. Therefore, the adsorption properties of each unit were distributed using the estimated weight fraction of finer-grained material in each unit. The resulting, more conservative, values for Kd are summarized in Table 7.2. This assumption is used in the model cases referred to as "medium Kd" cases. In all cases, manganese (Mn) was assumed to have the same adsorptive properties as Mo and Pb due to chemical similarities (see Section 5 and Appendix D).

No adsorption was assumed to occur in the case of sulfate (SO_4^{-2}) and total dissolved solids (TDS). This assumption is conservative in that weak bonding may be expected to occur for these (Corey, 1981; Dames & Moore, 1980).

The unsaturated properties of fractured bedrock needed to complete the description of the unsaturated zone include the degree of saturation and the unsaturated zone hydraulic conductivity. However, the degree of saturation and hydraulic conductivity as a function of negative pressure heads in fractured rock are not readily available for the Guadalupe Mountain site. A similar modeling study was completed by Stephenson and Freeze (1974). Their investigations consisted of modeling unsaturated/saturated flow through altered and fractured volcanic rock, similar to conditions in the subsurface at Guadalupe Mountain.

An important input parameter to the model is the unsaturated hydraulic conductivity curve. Since no field measurements are available to derive this curve, nor are any reliable ones likely to be obtained, the alternative to use a data set previously tested in a similar field and modeling situation was adopted. Stephenson and Freeze developed curves realistically representing the behavior of volcanic formations. The moisture content/pressure head curves used by Stephenson and Freeze were obtained from field measurements. The relative hydraulic conductivity/pressure head curves were determined by Stephenson and Freeze from the moisture content/pressure head relationships using the modified Burdine

theory (Burdine, 1953; Jeppson, 1970). Following a series of sensitivity runs, Stephenson and Freeze found that the system was far more sensitive to the relative saturated conductivity values than to the nature of the unsaturated hydraulic conductivity/pressure head curve.

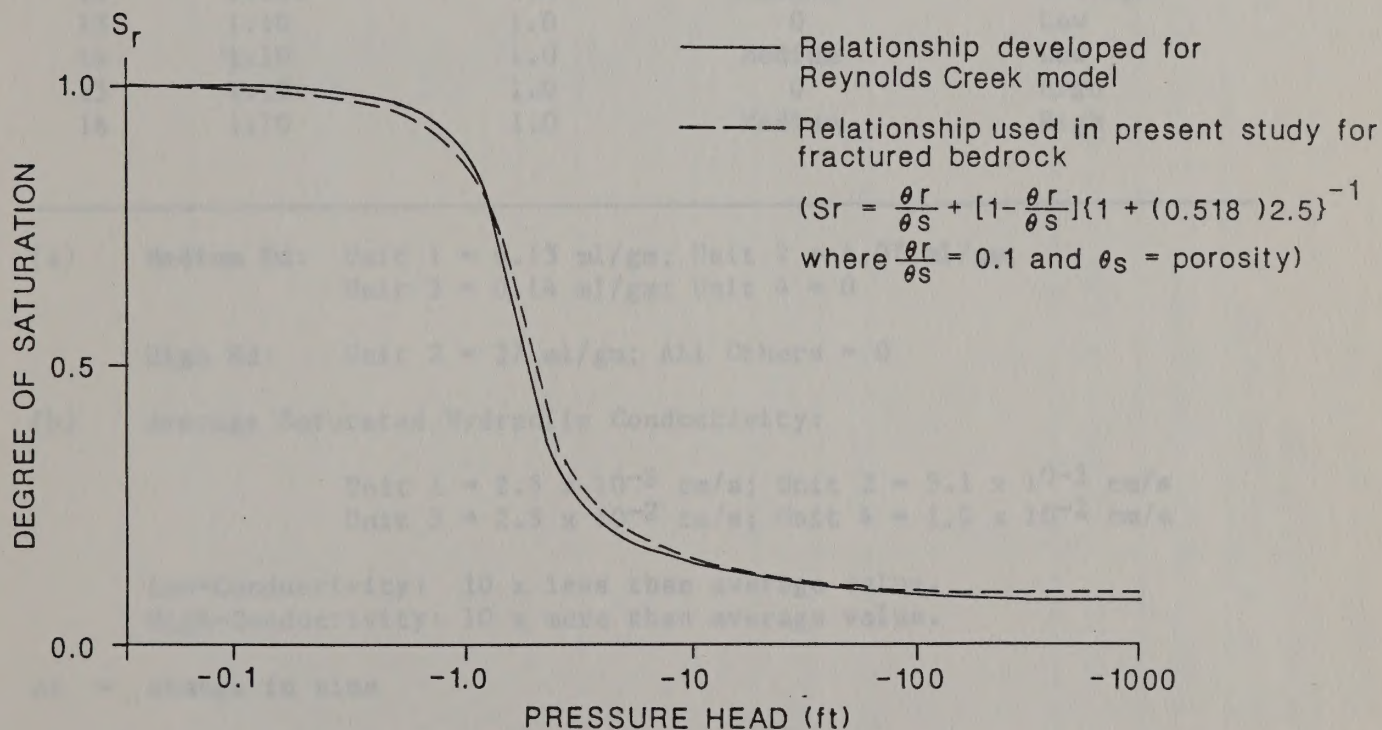
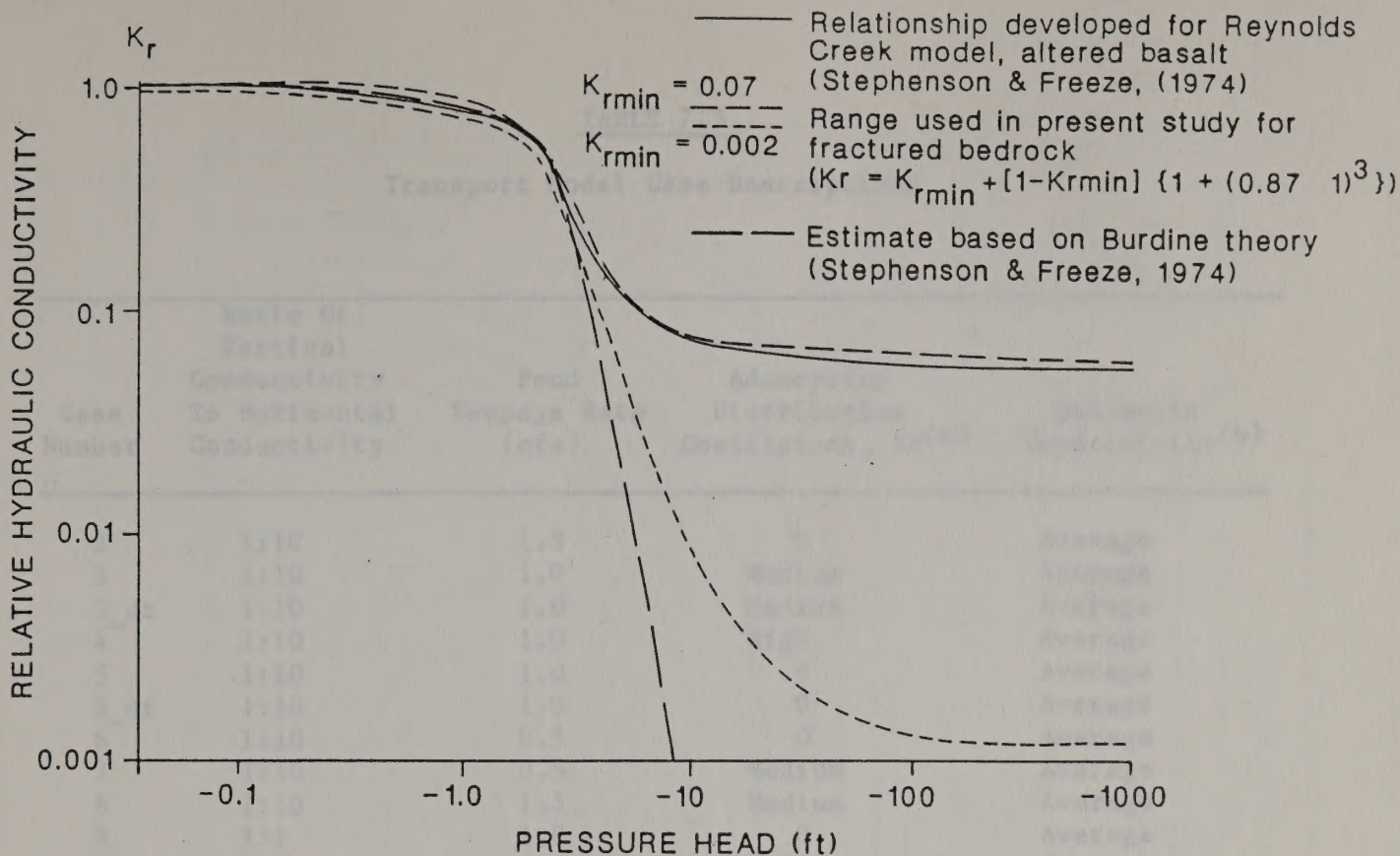
Because of the thorough evaluation of the unsaturated conductivity curve relationships under similar conditions by Stephenson and Freeze, the bedrock geologic characteristics supplied to the model tested by them were utilized in the present study. Their unsaturated rock properties were fitted to standard equations and used as the starting point for the Molycorp model (Figure 7.3).

7.4 PREDICTED RESULTS

7.4.1 Summary of Simulations

The purposes of the model simulations are: (1) to characterize the solute transport under average, assumed conditions; (2) to analyze the sensitivity of the model predictions to uncertainties in site conditions; and (3) to assess the model sensitivity to numerical parameters (such as size of timestep; see Appendix F). To accomplish this, a series of 3 steady-state and 17 transient model runs were undertaken (Table 7.3). The results of these calculations are presented in terms of normalized concentration plume plots (Appendix H), and concentration time histories (Figures 7.5 through 7.12). The concentration plumes are illustrations, in the vertical plane, of predicted normalized concentrations 3 years before pond shutdown (27 years after pond startup), and 50 years after pond shutdown. The concentration time histories are illustrations of predicted normalized concentrations just below the water table beneath the center of the pond and at the down-gradient claim boundary (locations shown on Figure 7.2).

Each of the transient simulations was preceded by a steady-state calculation of flow conditions prior to pond startup. During pond operation, flow in the unsaturated zone beneath the pond is primarily vertical while flow beneath the water table remains horizontal (Figure 7.4). Only a few feet of mounding at the water table during pond operation is



ESTIMATED UNSATURATED PROPERTIES
OF FRACTURED BEDROCK

Figure 7.3

TABLE 7.3

Transport Model Case Descriptions

Case Number	Ratio Of Vertical Conductivity To Horizontal Conductivity	Pond Seepage Rate (cfs)	Adsorption Distribution Coefficient, K _d (a)	Hydraulic Conductivity(b)
2	1:10	1.5	0	Average
3	1:10	1.0	Medium	Average
3 _{dt}	1:10	1.0	Medium	Average
4	1:10	1.0	High	Average
5	1:10	1.0	0	Average
5 _{dt}	1:10	1.0	0	Average
6	1:10	0.5	0	Average
7	1:10	0.5	Medium	Average
8	1:10	1.5	Medium	Average
9	1:1	1.0	0	Average
10	1:1	1.0	Medium	Average
11	1:100	1.0	0	Average
12	1:100	1.0	Medium	Average
13	1:10	1.0	0	Low
14	1:10	1.0	Medium	Low
15	1:10	1.0	0	High
16	1:10	1.0	Medium	High

(a) Medium K_d: Unit 1 = 0.13 ml/gm; Unit 2 = 4.07 ml/gm;
Unit 3 = 0.14 ml/gm; Unit 4 = 0

High K_d: Unit 2 = 37 ml/gm; All Others = 0

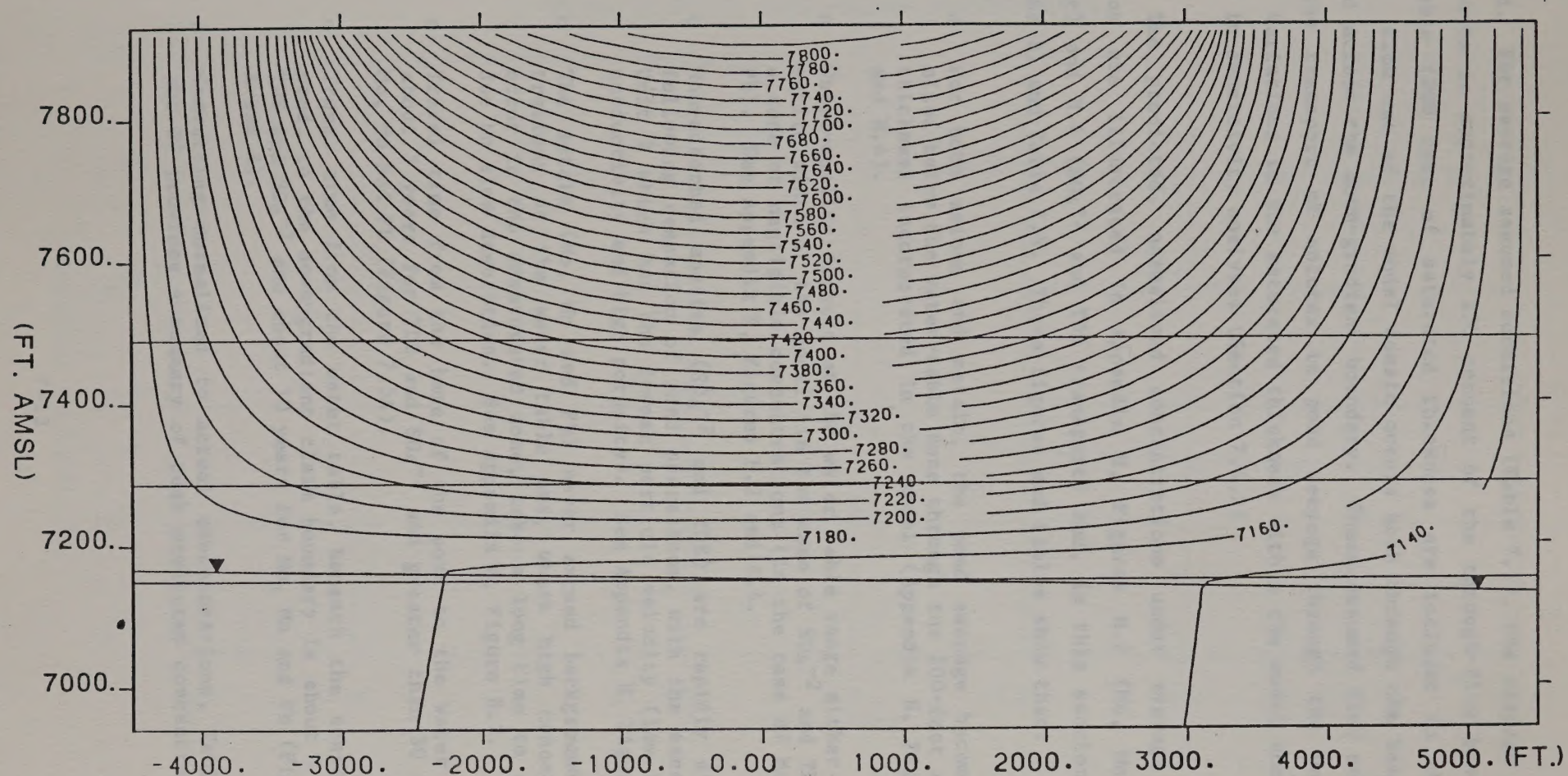
(b) Average Saturated Hydraulic Conductivity:

Unit 1 = 2.5×10^{-3} cm/s; Unit 2 = 5.1×10^{-3} cm/s
Unit 3 = 2.5×10^{-2} cm/s; Unit 4 = 1.0×10^{-2} cm/s

Low-Conductivity: 10 x less than average value.

High-Conductivity: 10 x more than average value.

dt = change in time



MOLYCORP: METAL TRANSPORT: 1.5 CFS SEEP RATE, $KH:KV=10:1$, ZERO KD CASE

CONTOURS OF HYDRAULIC HEAD
DURING POND OPERATION

TIME = 27 YEARS

CONTOUR INTERVAL = 20.0 FEET

Figure 7.4

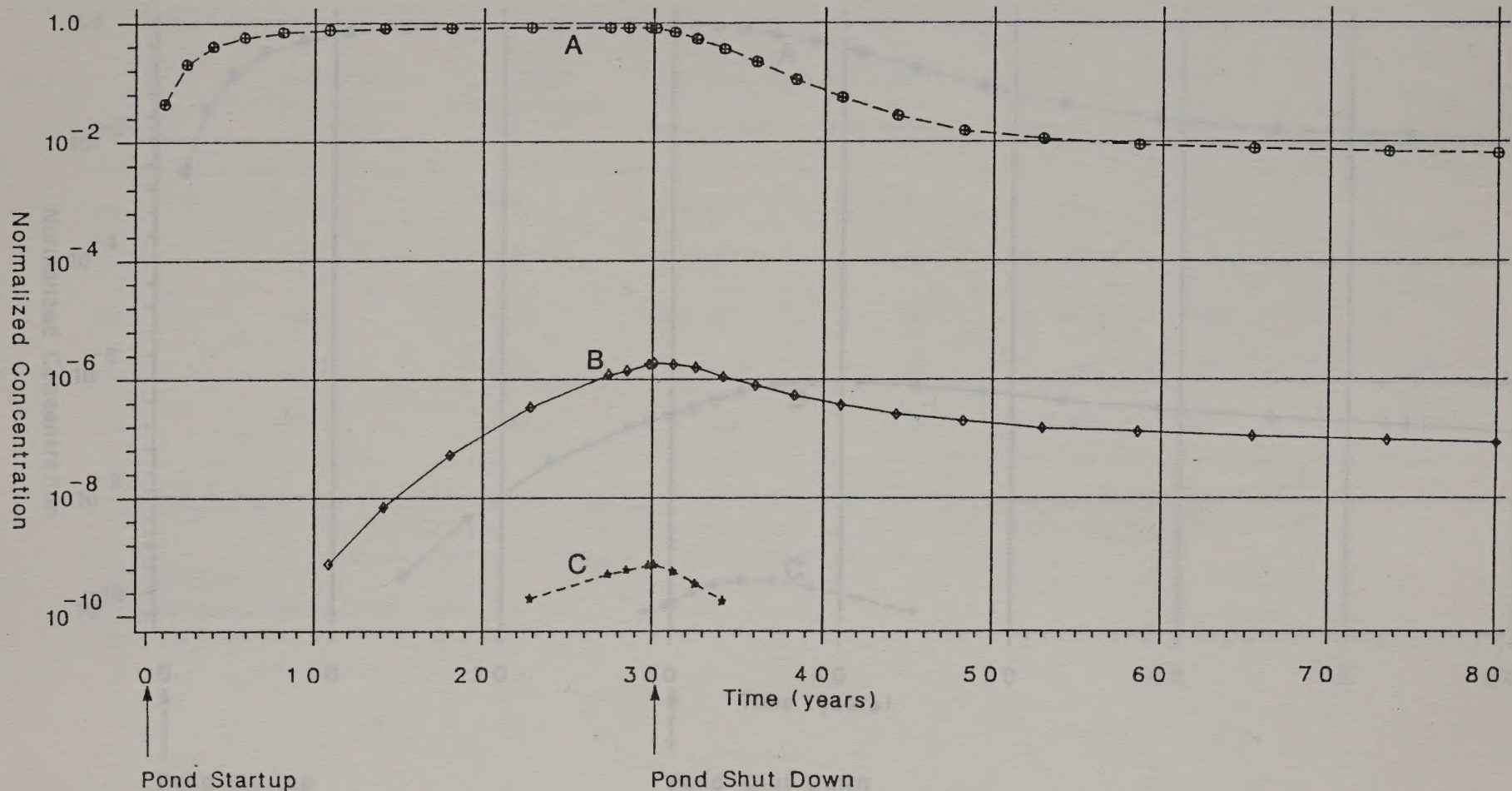
predicted. For average assumed conditions (Table 7.1), the seepage from the pond amounts to approximately 250 percent of the through-flow beneath the water table (200 feet of saturated thickness are included in the model domain). Flow out of the model domain occurs both through the base of the model and across the down-gradient boundary. These assumed flow conditions govern the transport of solutes in pond seepage through the underlying layers. Variations in the saturated thickness within the model domain were examined in sensitivity analyses (Section 7.4.2)

The predicted, normalized concentrations under average assumed conditions are illustrated in Appendix H, Figures H.2 (Mo, Mn and Pb transport) and H.4 (SO_4^{-2} and TDS transport) and, in this section, Figure 7.5 (A and B) and Table 7.4. These figures and tables show that:

- o For both anions and metals, the pond seepage becomes fully mixed below the water-table zone through the 200-foot saturated thickness incorporated in the model (Appendix H, Figures H.2 and H.4).
- o Water-quality impacts at the water table range either over the entire width of the model (in the case of SO_4^{-2} and TDS) or to a zone of negligible concentrations (in the case of Mo, Mn and Pb). See Appendix H, Figures H.2 and H.4.
- o Non-adsorbed species (SO_4^{-2} and TDS) are rapidly dissipated following cessation of pond operations, with the exception of Unit 2 which has the lowest particle velocity (low hydraulic conductivity and high porosity). See Appendix H, Figure H.4.
- o The metals (Mo, Mn and Pb) never exceed background concentrations at the water table and, where high concentrations occur in the unsaturated zone, take a long time to dissipate due to slow desorption. See Appendix H, Figure H.2.
- o Travel time from the base of the pond to the water table is about 5 years for TDS and SO_4^{-2} and greater than 30 years for Mo, Mn and Pb (Figure 7.5A).
- o Travel time from the water table, beneath the center of the pond, to the down-gradient claim boundary is about 1 year for TDS and SO_4^{-2} and about 10 years for Mo, Mn and Pb (Figures 7.5 A and B).
- o Converting normalized to actual concentrations, Table 7.4 (A and B) provides a summary of peak predicted concentrations for

TIME HISTORY OF CONCENTRATION AS A FUNCTION OF ADSORPTION DISTRIBUTION COEFFICIENT

MOLYCORP, INC: GUADALUPE MTN PROPOSED TAILINGS AREA
BENEATH POND, JUST BELOW WATER TABLE



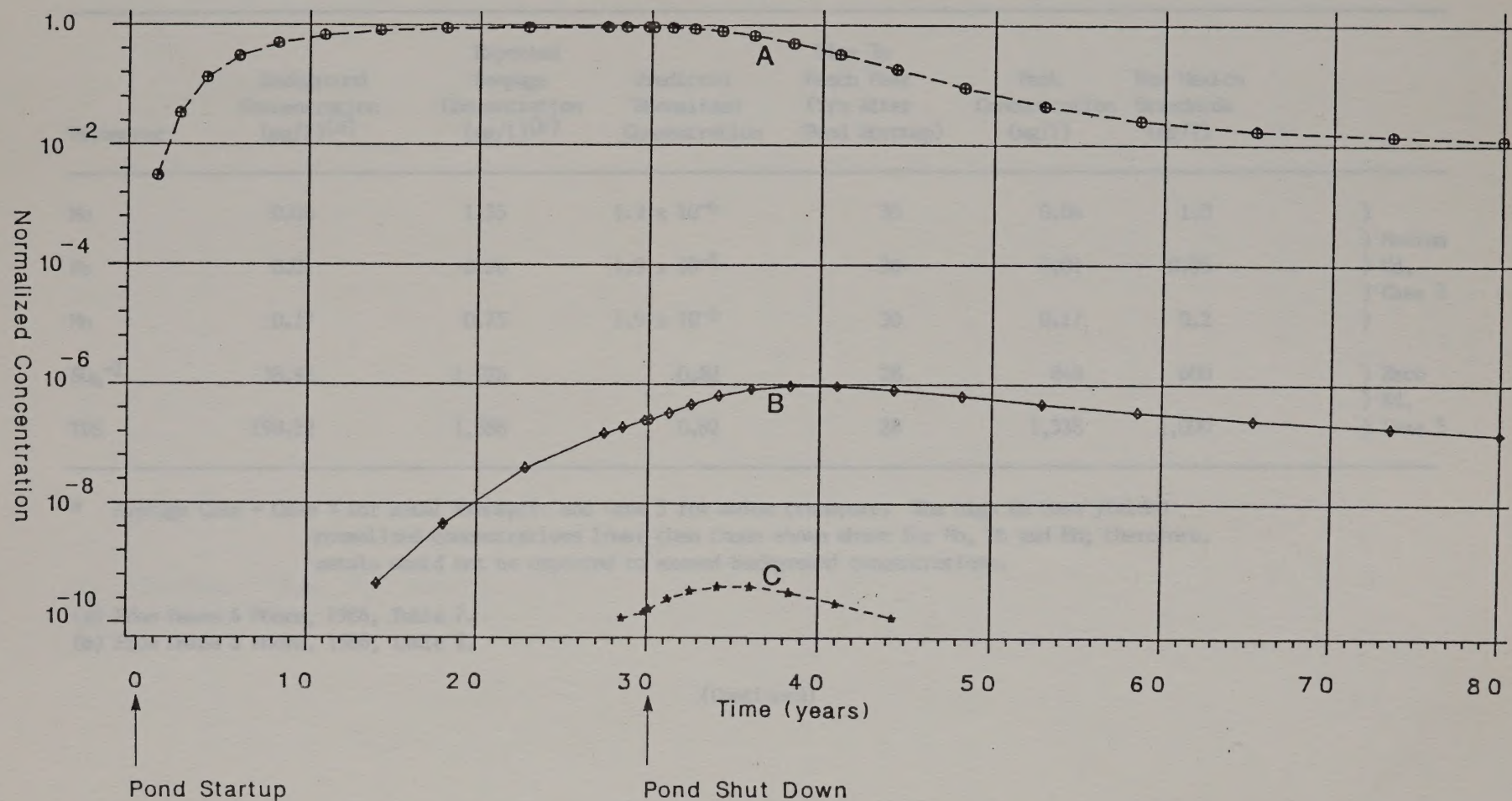
- A = Case 5; Zero adsorption case; pond seepage rate = 1.0 cfs; $K_v:K_h = 1:10$
 B = Case 3; Medium adsorption case; pond seepage rate = 1.0 cfs; $K_v:K_h = 1:10$
 C = Case 4; High adsorption case; pond seepage rate = 1.0 cfs; $K_v:K_h = 1:10$

$$\text{Normalized Concentration} = \frac{\text{Actual Concentration} - \text{Background Concentration}}{\text{Seepage Concentration} - \text{Background Concentration}}$$

Figure 7.5A

TIME HISTORY OF CONCENTRATIONS AS A FUNCTION OF ADSORPTION DISTRIBUTION COEFFICIENT

MOLYCORP, INC: GUADALUPE MTN PROPOSED TAILINGS AREA
AT DOWN-GRADIENT CLAIM BOUNDARY



- A = Case 5: Zero adsorption case; $K_v:K_h = 1:10$; pond seepage rate = 1.0 cfs
 B = Case 3: Medium adsorption case; $K_v:K_h = 1:10$; pond seepage rate = 1.0 cfs
 C = Case 4: High adsorption case; $K_v:K_h = 1:10$; pond seepage rate = 1.0 cfs
- Normalized Concentration = $\frac{\text{Actual Concentration} - \text{Background Concentration}}{\text{Seepage Concentration} - \text{Background Concentration}}$

Figure 7.5B

TABLE 7.4 (A)

Predicted Concentrations For Average Case*:
At Water Table Beneath Pond

Parameter	Background Concentration (mg/l)(a)	Expected Seepage Concentration (mg/l)(b)	Predicted Normalized Concentration	Time To Reach Peak (Yrs After Pond Startup)	Peak Concentration (mg/l)	New Mexico Standards (mg/l)	
Mo	0.06	1.35	1.9×10^{-6}	30	0.06	1.0)
Pb	0.01	0.06	1.9×10^{-6}	30	0.01	0.05) Medium) Kd,) Case 3
Mn	0.17	0.75	1.9×10^{-6}	30	0.17	0.2)
SO ₄ ⁻²	38.92	1,026	0.82	28	848	600) Zero) Kd,
TDS	198.22	1,588	0.82	28	1,338	1,000) Case 5

* Average Case = Case 3 for metal transport and Case 5 for anion transport. The high Kd case yielded normalized concentrations lower than those shown above for Mo, Pb and Mn; therefore, metals would not be expected to exceed background concentrations.

(a) From Dames & Moore, 1986, Table 7.

(b) From Dames & Moore, 1986, Table 2.

(Continued)

TABLE 7.4 (B)

Predicted Concentrations for Average Case*:
At Down-gradient Claim Boundary

Parameter	Background Concentration (mg/l)(a)	Expected Seepage Concentration (mg/l)(b)	Predicted Normalized Concentration	Time To Reach Peak (Yrs After Pond Startup)	Peak Concentration (mg/l)	New Mexico Standards (mg/l)	
Mo	0.06	1.35	9.4×10^{-7}	38	0.06	1.0)
Pb	0.01	0.06	9.4×10^{-7}	38	0.01	0.05) Medium
Mn	0.17	0.75	9.4×10^{-7}	38	0.17	0.2) Kd, Case 3
SO ₄ ⁻²	38.92	1,026	0.92	30	947	600)
TDS	198.22	1,588	0.92	30	1,477	1,000) Zero Kd, Case 5

* Average Case = Case 3 for metal transport and Case 5 for anion transport. The high Kd case yielded normalized concentrations lower than those shown above for Mo, Pb and Mn; therefore, metals would not be expected to exceed background concentrations.

(a) From Dames & Moore, 1986, Table 7.

(b) From Dames & Moore, 1986, Table 2.

each species. It can be seen that: (1) predicted peak concentrations for Mo, Mn and Pb are at background levels in the saturated zone; (2) predicted peak concentrations for SO_4^{-2} and TDS are above New Mexico standards since little dilution of these species occur; and (3) even if one assumed zero adsorption for Mo, natural dilution alone would be sufficient to drop concentrations below the standards.

7.4.2 Physical Sensitivity Analyses

Because some of the hydraulic properties of the units below the proposed pond were estimated rather than measured, a sensitivity analysis in which key parameters were varied was undertaken.

Adsorption Distribution Coefficient, Kd

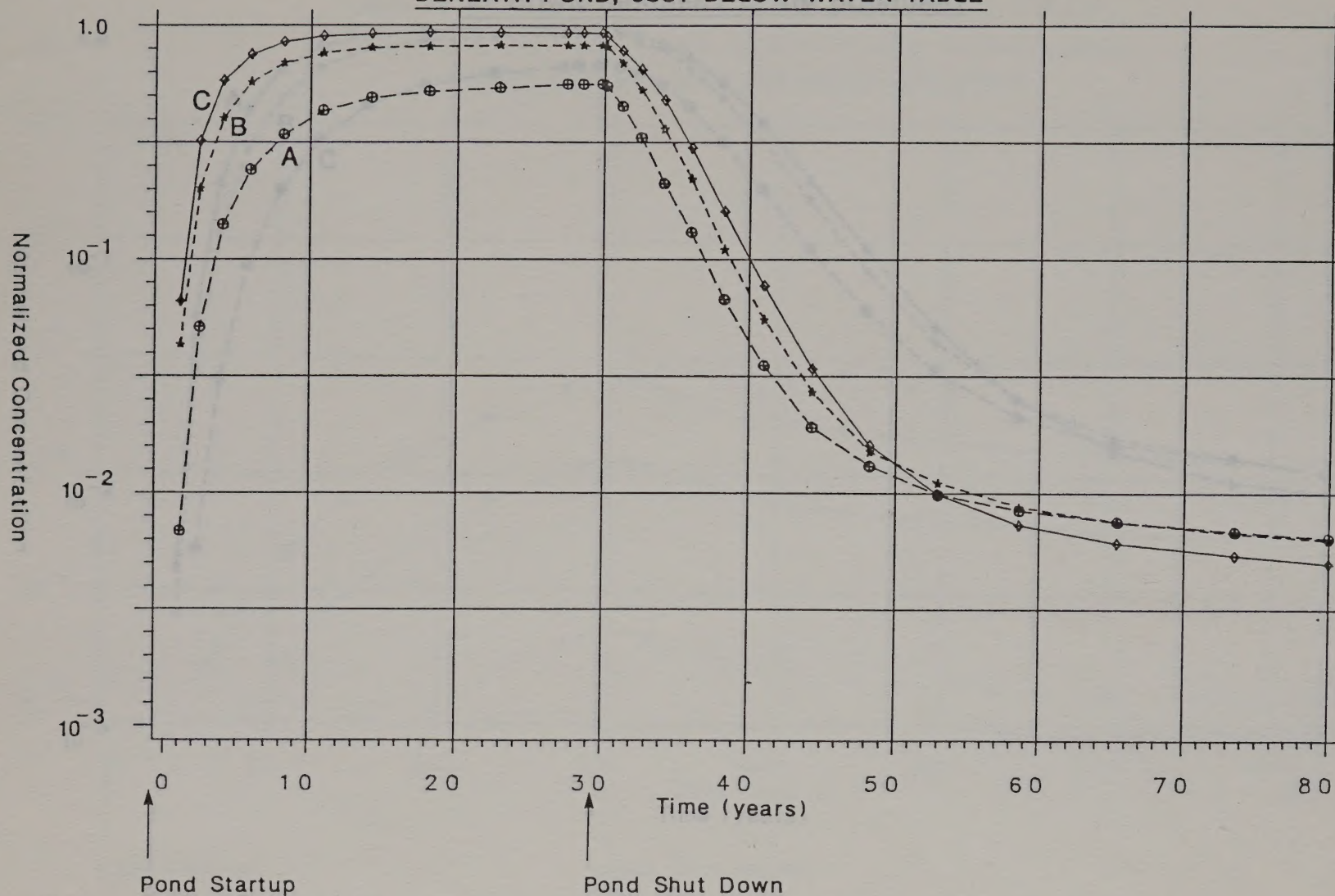
Three different assumptions for adsorption distribution coefficient were analyzed: (1) zero adsorption in all units (Case 5); (2) small values of Kd distributed according to the weight fraction of adsorbing material in each unit, in Units 1, 2 and 3 (Case 3); and (3) laboratory-measured Kd, assumed concentrated in the layer containing the greatest fraction of adsorptive material, Unit 2 (Case 4). These are also known as the "zero, medium and high" Kd cases, respectively. The results of these analyses are shown in Figure 7.5 (A and B), and in Appendix H, Figures H.2 through H.4. These figures indicate that both the travel time and the predicted concentrations are sensitive to the assumed Kds. Both the time of travel to the water table and the time for plume dissipation increases as Kd increases. The predicted peak concentrations decrease as Kd increases. Because of the sensitivity of the predictions to Kd, conservative assumptions were made for Kd values supplied to the model in the average case.

Pond Seepage Rate

Pond seepage rates of 0.5, 1.0 and 1.5 cfs were assumed in Cases 2, 5, 6, 7 and 8 (Figures 7.6 A and B, 7.7 A and B, H.2 and H.4 through H.7). These seepage rates were estimated on the basis of flow mass balance calculations for neighboring ponds (Geocon, 1983). These figures show that travel time to the water table increases and the peak predicted concentrations decrease as the pond seepage rate decreases. The influence of

TIME HISTORY OF ANION CONCENTRATIONS AS A FUNCTION OF POND SEEPAGE RATE

MOLYCORP, INC: GUADALUPE MTN PROPOSED TAILINGS AREA
BENEATH POND, JUST BELOW WATER TABLE

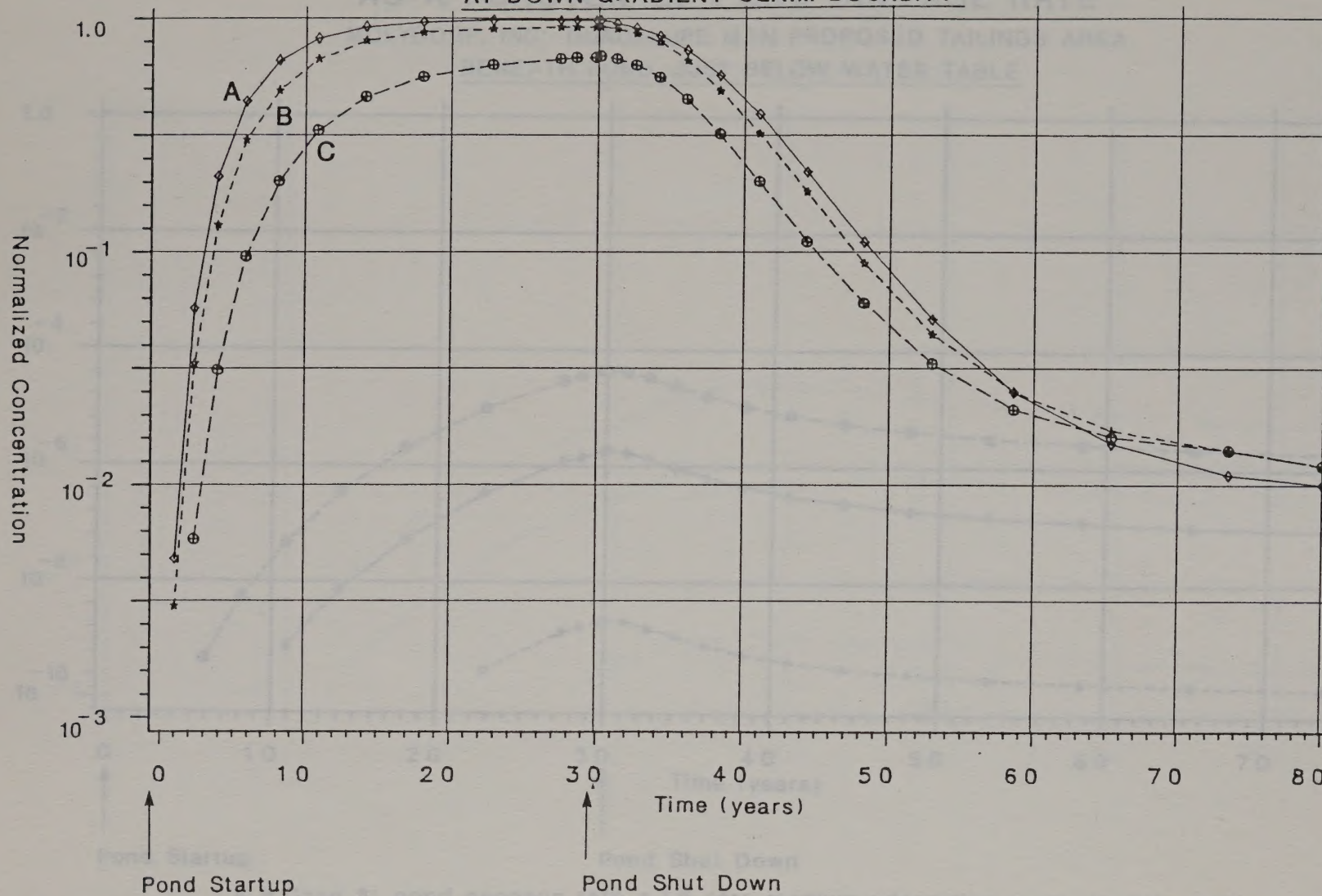


- A = Case 6: pond seepage rate = 0.5 cfs; zero adsorption case; $K_v:K_h = 1:10$
- B = Case 5: pond seepage rate = 1.0 cfs; zero adsorption case; $K_v:K_h = 1:10$
- C = Case 2: Pond seepage rate = 1.5 cfs; zero adsorption case; $K_v:K_h = 1:10$

$$\text{Normalized Concentration} = \frac{\text{Actual Concentration} - \text{Background Concentration}}{\text{Seepage Concentration} - \text{Background Concentration}}$$

TIME HISTORY OF ANION CONCENTRATIONS AS A FUNCTION OF POND SEEPAGE RATE

MOLYCORP, INC: GUADALUPE MTN PROPOSED TAILINGS AREA
AT DOWN-GRADIENT CLAIM BOUNDARY



A = Case 2: pond seepage rate = 1.5 cfs; zero adsorption case; $K_v:K_h = 1:10$

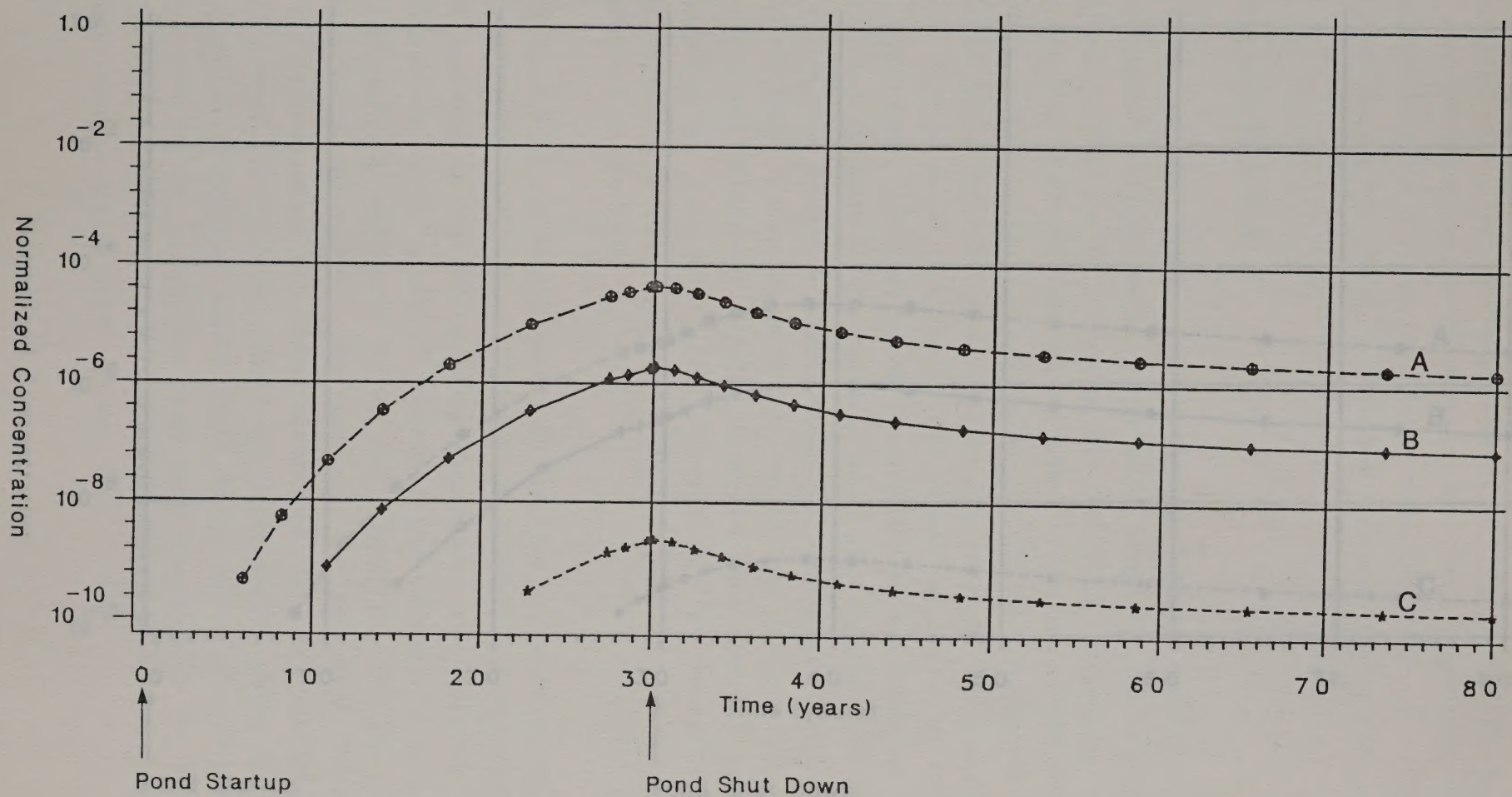
B = Case 5: pond seepage rate = 1.0 cfs; zero adsorption case; $K_v:K_h = 1:10$

C = Case 6: pond seepage rate = 0.5 cfs; zero adsorption case; $K_v:K_h = 1:10$

$$\text{Normalized Concentration} = \frac{\text{Actual Concentration} - \text{Background Concentration}}{\text{Seepage Concentration} - \text{Background Concentration}}$$

TIME HISTORY OF METAL CONCENTRATIONS AS A FUNCTION OF POND SEEPAGE RATE

MOLYCORP, INC: GUADALUPE MTN PROPOSED TAILINGS AREA
BENEATH POND, JUST BELOW WATER TABLE



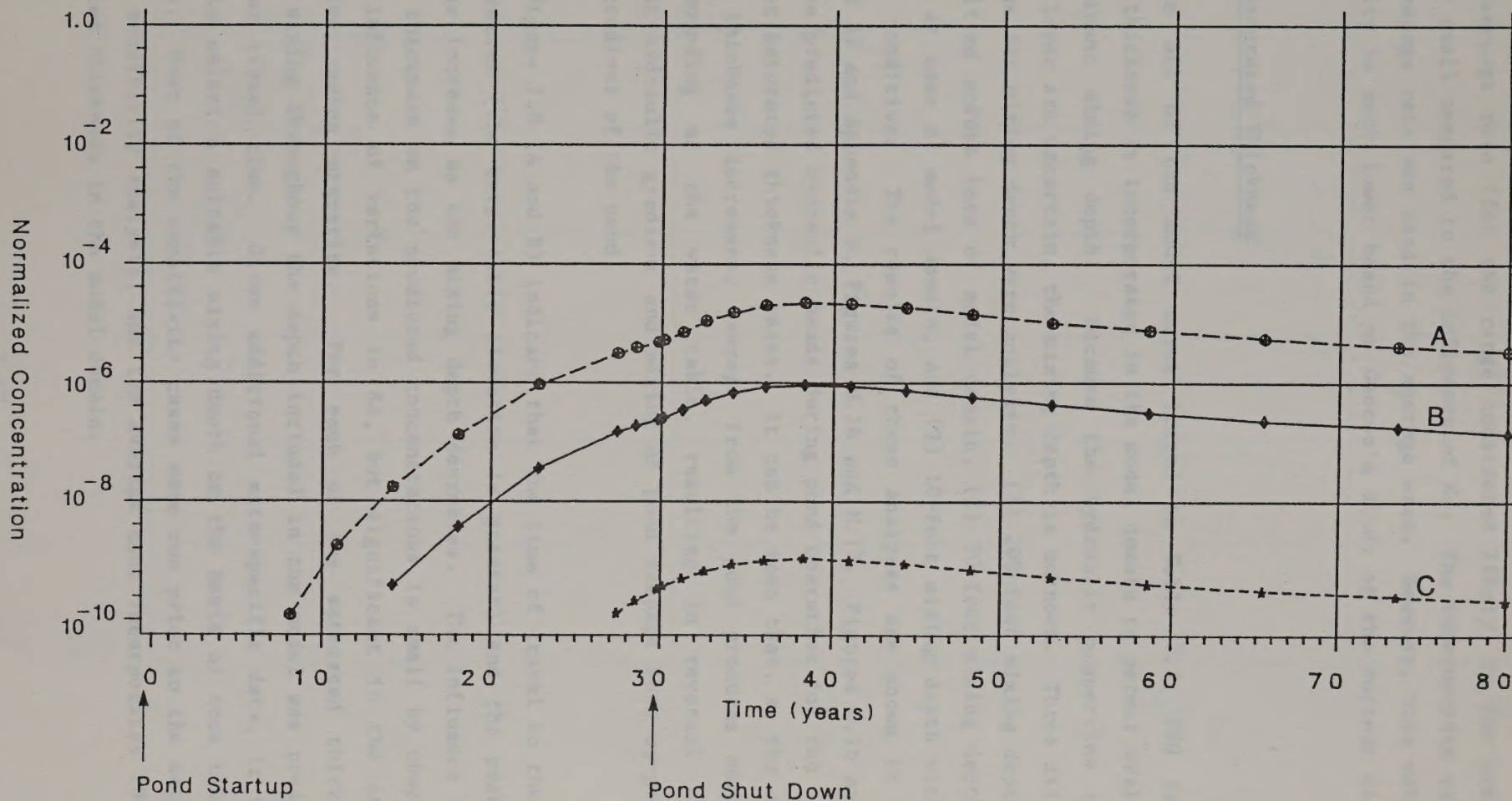
- A = Case 8: pond seepage rate = 1.5 cfs; medium adsorption case; $K_v:K_h = 1:10$
 B = Case 3: pond seepage rate = 1.0 cfs; medium adsorption case; $K_v:K_h = 1:10$
 C = Case 7: pond seepage rate = 0.5 cfs; medium adsorption case; $K_v:K_h = 1:10$

$$\text{Normalized Concentration} = \frac{\text{Actual Concentration} - \text{Background Concentration}}{\text{Seepage Concentration} - \text{Background Concentration}}$$

Figure 7.7A

TIME HISTORY OF METAL CONCENTRATIONS AS A FUNCTION OF POND SEEPAGE RATE

MOLYCORP, INC: GUADALUPE MTN PROPOSED TAILINGS AREA
AT DOWNGRADIENT CLAIM BOUNDARY



A = Case 8: Pond seepage rate = 1.5 cfs; medium adsorption case; $K_v:K_h = 1:10$

B = Case 3: pond seepage rate = 1.0 cfs; medium adsorption case; $K_v:K_h = 1:10$

C = Case 7: pond seepage rate = 0.5 cfs; medium adsorption case; $K_v:K_h = 1:10$

$$\text{Normalized Concentration} = \frac{\text{Actual Concentration} - \text{Background Concentration}}{\text{Seepage Concentration} - \text{Background Concentration}}$$

Figure 7.7B

the pond seepage rate (for the range considered likely) on the predicted results is small compared to the influence of K_d . The intermediate value of 1.0 cfs seepage rate was used in the average case. However, this value may in actuality be much lower based on Geocon's study of the current disposal facility.

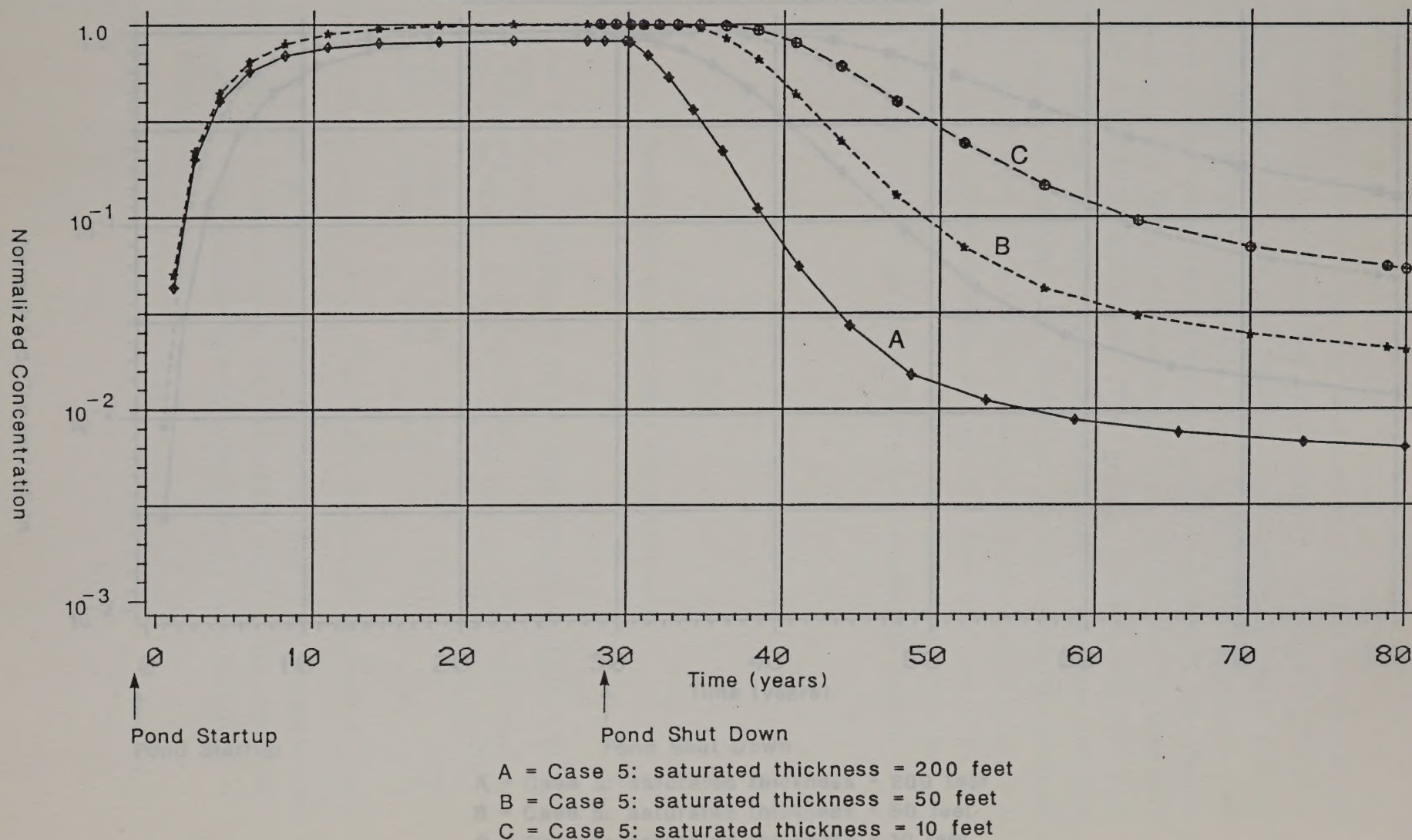
Saturated Thickness

In all of the model cases listed in Table 7.3, 200 feet of saturated thickness is incorporated in the model domain to permit evaluation of contaminant mixing depth. Because the hydraulic properties of the saturated layer are uncertain, the mixing depth is unknown. Three different assumptions for mixing depth were analyzed: (1) 200-foot mixing depth with flow permitted across base of model domain, (2) 50-foot mixing depth with zero flow at base of model domain, and (3) 10-foot mixing depth with zero flow base condition. The results of these analyses are shown in Figure 7.8 (A and B) and Appendix H, Figures H.16 and H.17. Figures H.16 and H.17 present the predicted hydraulic heads during pond operation for the 10-foot and 50-foot saturated thickness cases. It can be seen that, as the assumed saturated thickness decreases, seepage from the pond produces more pronounced mounding at the water table, resulting in reversal of the up-gradient hydraulic gradient and mixing of pond seepage both up-gradient and down-gradient of the pond.

Figure 7.8 (A and B) indicate that the time of travel to the water table decreases (the water-table elevation is greater) and the peak concentrations increase as the mixing depth decreases. The influence of the saturated thickness on the predicted concentrations is small by comparison with the influence of variations in K_d , but significant in the case of non-reactive, anion migration. For each of the saturated thicknesses examined, mixing throughout the depth included in the model was predicted, for 80-year travel time. Given additional site-specific data, it may be feasible to select a suitable mixing depth on the basis of rock hydraulic properties. Most of the sensitivity cases were run prior to the saturated thickness sensitivity analysis, and the average case incorporates 200 feet of saturated thickness in the model domain.

TIME HISTORY OF ANION CONCENTRATIONS AS A FUNCTION OF SATURATED THICKNESS

MOLYCORP, INC: GUADALUPE MTN PROPOSED TAILINGS AREA
BENEATH POND, JUST BELOW WATER TABLE

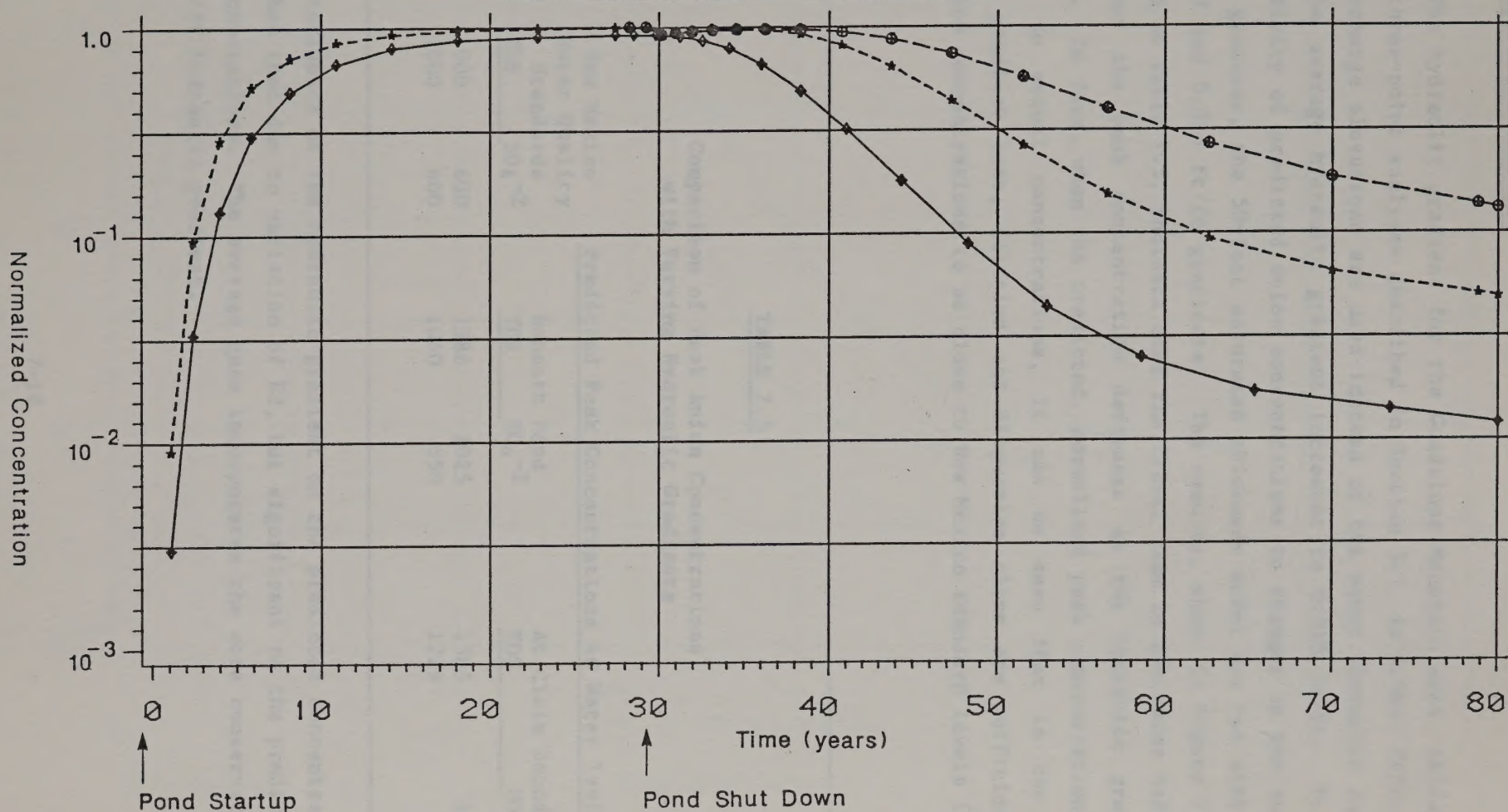


$$\text{Normalized Concentration} = \frac{\text{Actual Concentration} - \text{Background Concentration}}{\text{Seepage Concentration} - \text{Background Concentration}}$$

Figure 7.8A

TIME HISTORY OF ANION CONCENTRATIONS AS A FUNCTION OF SATURATED THICKNESS

MOLYCORP, INC: GUADALUPE MTN PROPOSED TAILINGS AREA
AT DOWN-GRADIENT CLAIM BOUNDARY



$$\text{Normalized Concentration} = \frac{\text{Actual Concentration} - \text{Background Concentration}}{\text{Seepage Concentration} - \text{Background Concentration}}$$

Figure 7.8B

Hydraulic Gradient

The hydraulic gradient for the Guadalupe Mountain area, calculated from the three-point analyses described in Section 3.1, is 0.0037 ft/ft. If spring discharge elevations are used instead of the water elevation in Well BLM-HQ, the average hydraulic gradient increases to 0.015 ft/ft. To test the sensitivity of predicted anion concentrations to changes in the assumed hydraulic gradient, the 50-foot saturated thickness model was run with both the 0.0037 and 0.015 ft/ft gradients. The results, shown in Figure 7.9 (A and B) and on Table 7.5, indicate that the travel time to the water table is similar but the peak concentration decreases as the hydraulic gradient increases. In fact, when the predicted, normalized peak concentrations are converted to actual concentrations, it can be seen that in the high hydraulic gradient case, dilution and dispersion alone are sufficient to reduce anion concentrations to be close to New Mexico standard levels (Table 7.5).

TABLE 7.5

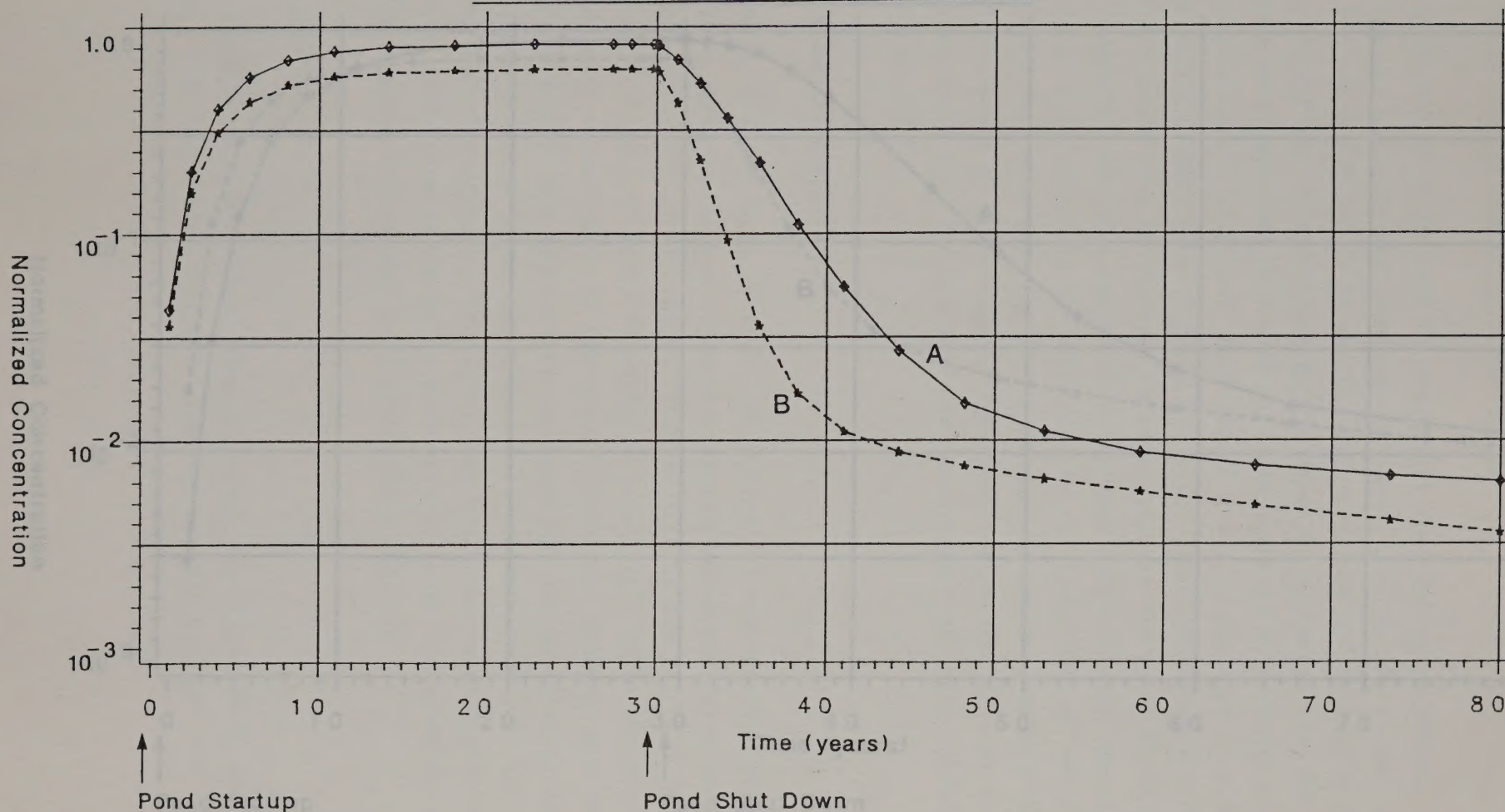
Comparison of Peak Anion Concentrations
with Varying Hydraulic Gradients

Hydraulic Gradient (ft/ft)	New Mexico Water Quality Standards		Predicted Peak Concentrations At Water Table (mg/l)			
	TDS	SO ₄ ⁻²	Beneath Pond		At Claim Boundary	
			TDS	SO ₄ ⁻²	TDS	SO ₄ ⁻²
0.0037	1000	600	1586	1025	1585	1024
0.015	1000	600	1060	650	1229	771

The influence of the hydraulic gradient on the predicted concentrations is less than that due to variation of K_d , but significant to the predicted anion concentrations. The average case incorporates the more conservative 0.0037 ft/ft hydraulic gradient.

TIME HISTORY OF ANION CONCENTRATIONS AS A FUNCTION OF HYDRAULIC GRADIENT

MOLYCORP, INC: GUADALUPE MTN PROPOSED TAILINGS AREA
BENEATH POND, JUST BELOW WATER TABLE



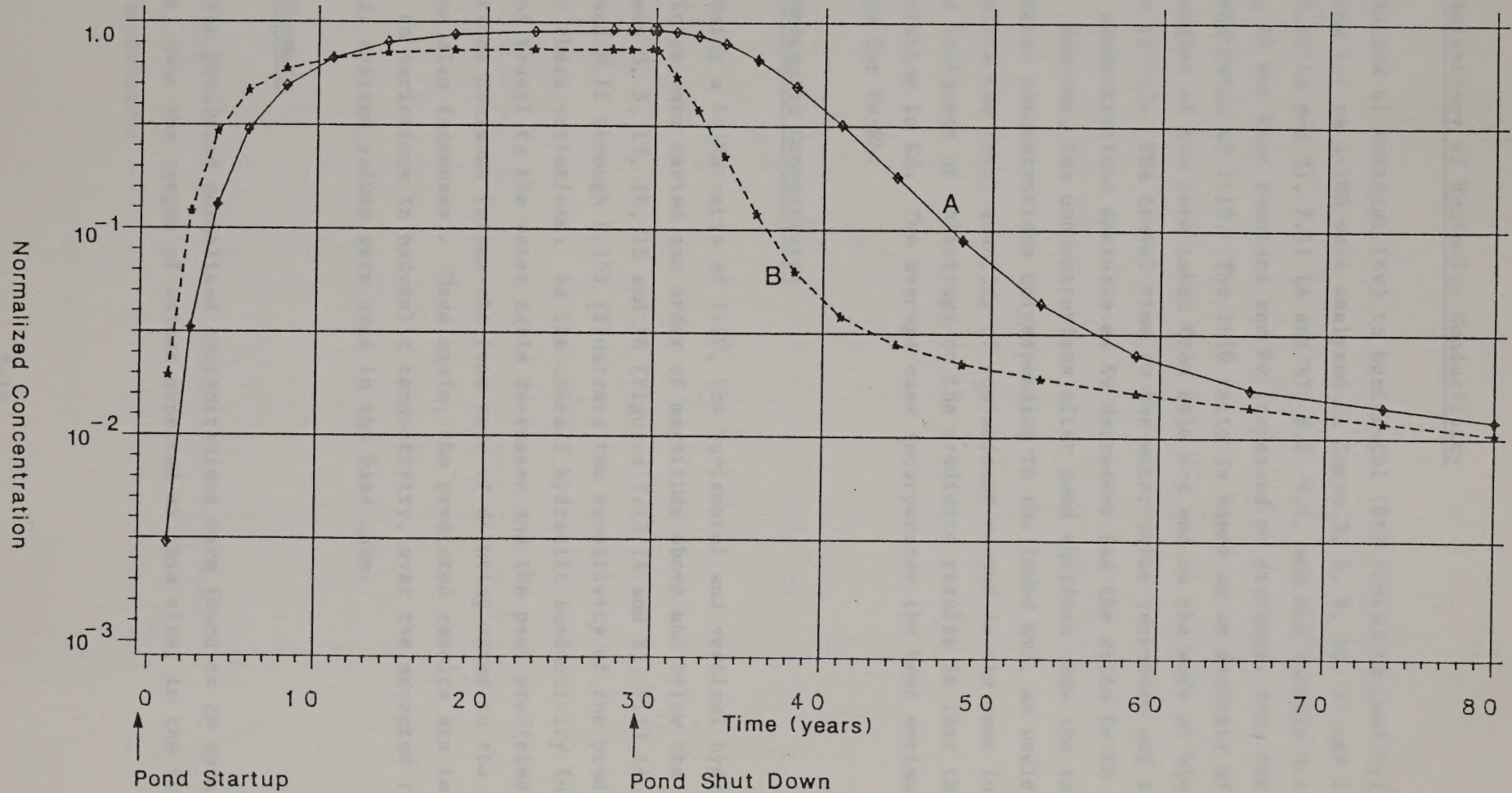
A = Case 5: hydraulic gradient = 0.0037 ft/ft; saturated thickness = 200 feet

B = Case 5: hydraulic gradient = 0.015 ft/ft; saturated thickness = 50 feet

$$\text{Normalized Concentration} = \frac{\text{Actual Concentration} - \text{Background Concentration}}{\text{Seepage Concentration} - \text{Background Concentration}}$$

TIME HISTORY OF ANION CONCENTRATIONS AS A FUNCTION OF HYDRAULIC GRADIENT

MOLYCORP, INC: GUADALUPE MTN PROPOSED TAILINGS AREA
AT DOWN-GRADIENT CLAIM BOUNDARY



A = Case 5: hydraulic gradient = 0.0037 ft/ft; saturated thickness = 200 feet

B = Case 5: hydraulic gradient = 0.015 ft/ft; saturated thickness = 50 feet

$$\text{Normalized Concentration} = \frac{\text{Actual Concentration} - \text{Background Concentration}}{\text{Seepage Concentration} - \text{Background Concentration}}$$

Figure 7.9B

Anisotropy of Hydraulic Conductivity

Ratios of vertical (K_v) to horizontal (K_h) hydraulic conductivity ranging from 1:1 to 1:100 were analyzed in Cases 3, 5, 9, 10, 11 and 12 (Figures 7.10 (A and B), 7.11 (A and B), H.2, H.4, and H.8 through H.10). In each case, K_h was kept constant and K_v increased or decreased from the base or average case ratio of 1:10. The 1:10 ratio is based on an analysis of fracture angles of the core taken from hole G-1 and on the work of Stephenson and Freeze (1974). The travel time to the water table increases and the peak predicted concentrations decrease as K_v decreases (as the ratio $K_v:K_h$ increases). However, the concentrations after pond shutdown show the reverse trend (greater concentrations corresponding to the lower K_v), as would be expected since the total quantity of contaminant seeped is the same in each case. The influence of anisotropy on the predicted results is less than that due to variation in K_d . The average case incorporates the best estimate, or 1:10, ratio for $K_v:K_h$.

Hydraulic Conductivity

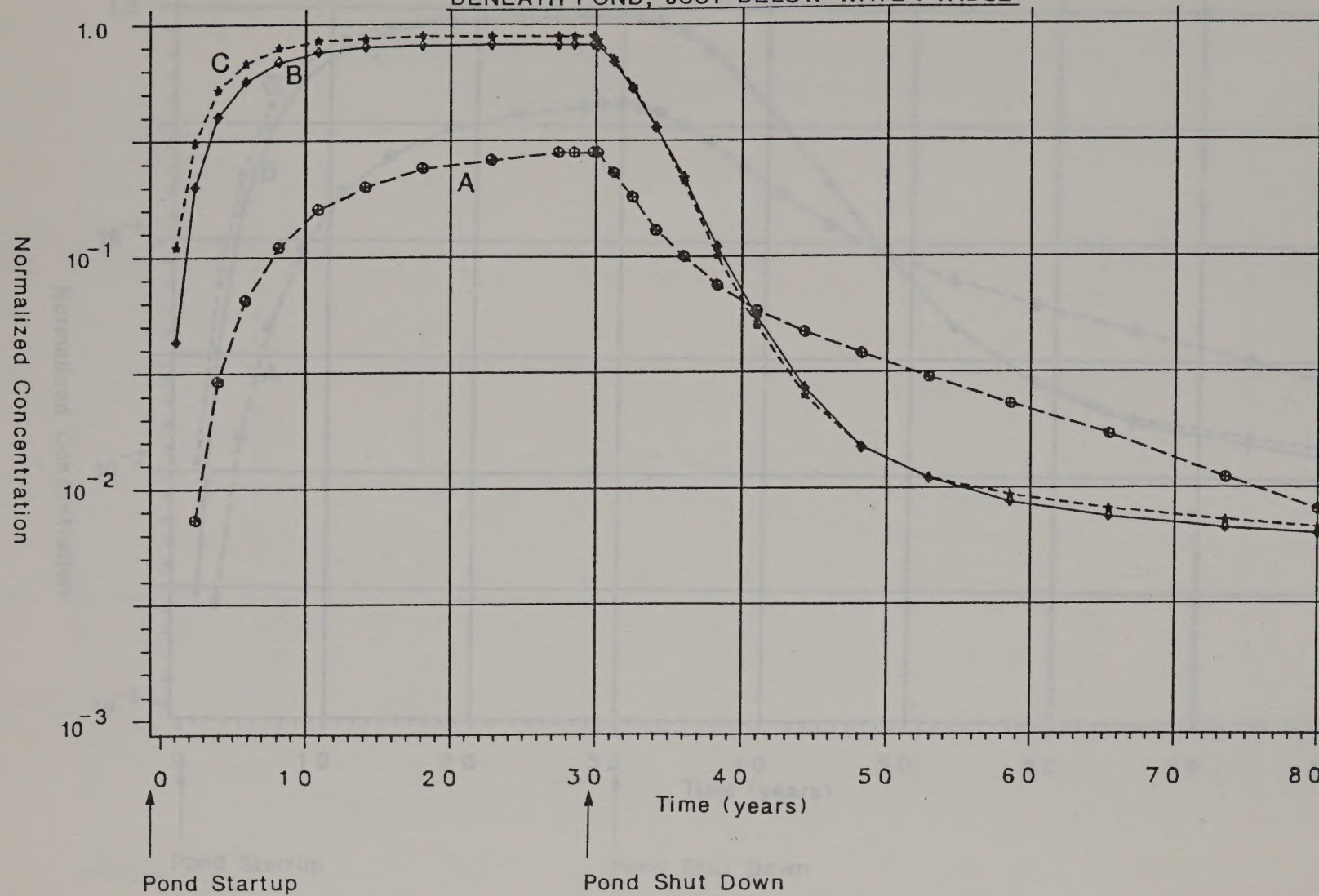
Using a $K_v:K_h$ ratio of 1:10, the horizontal and vertical hydraulic conductivities were varied one order of magnitude above and below the average case. Cases 3, 5, 13, 14, 15 and 16 (Figures 7.12 (A and B), 7.13 (A and B), H.2, H.4 and H.12 through H.15) illustrate the sensitivity of the predicted results to these variations. As the overall hydraulic conductivity increases, the time of travel to the water table decreases and the peak predicted concentrations decrease (since the flow rate of diluting water in the saturated zone also increases). Once again, the predicted results are less sensitive to variations in hydraulic conductivity, over the expected range, than to K_d ; average values were used in the base case.

Summary

The predicted normalized concentrations were found to be sensitive to variations, over the ranges of values expected at this site, in the following order of importance:

TIME HISTORY OF ANION CONCENTRATIONS AS A FUNCTION OF HYDRAULIC CONDUCTIVITY ANISOTROPY

MOLYCORP, INC: GUADALUPE MTN PROPOSED TAILINGS AREA
BENEATH POND, JUST BELOW WATER TABLE

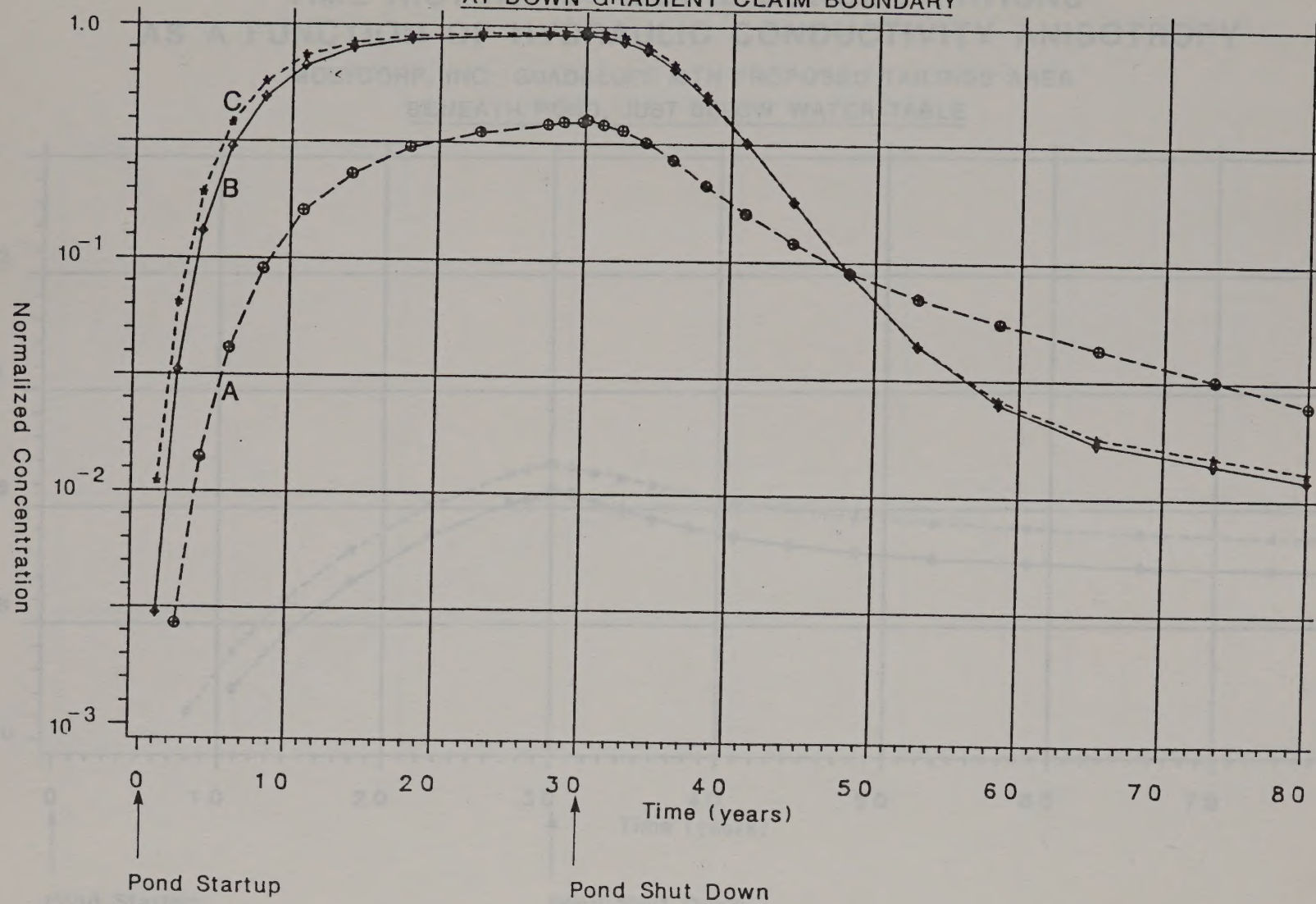


- A = Case 11: ratio vertical to horizontal hydraulic conductivity = 1:100; zero adsorption; seepage = 1.0 cfs
 B = Case 5: ratio vertical to horizontal hydraulic conductivity = 1:10; zero adsorption; seepage = 1.0 cfs
 C = Case 9: ratio vertical to horizontal hydraulic conductivity = 1:1; zero adsorption; seepage = 1.0 cfs

$$\text{Normalized Concentration} = \frac{\text{Actual Concentration} - \text{Background Concentration}}{\text{Seepage Concentration} - \text{Background Concentration}}$$

TIME HISTORY OF ANION CONCENTRATIONS AS A FUNCTION OF HYDRAULIC CONDUCTIVITY ANISOTROPY

MOLYCORP, INC: GUADALUPE MTN PROPOSED TAILINGS AREA
AT DOWN-GRADIENT CLAIM BOUNDARY



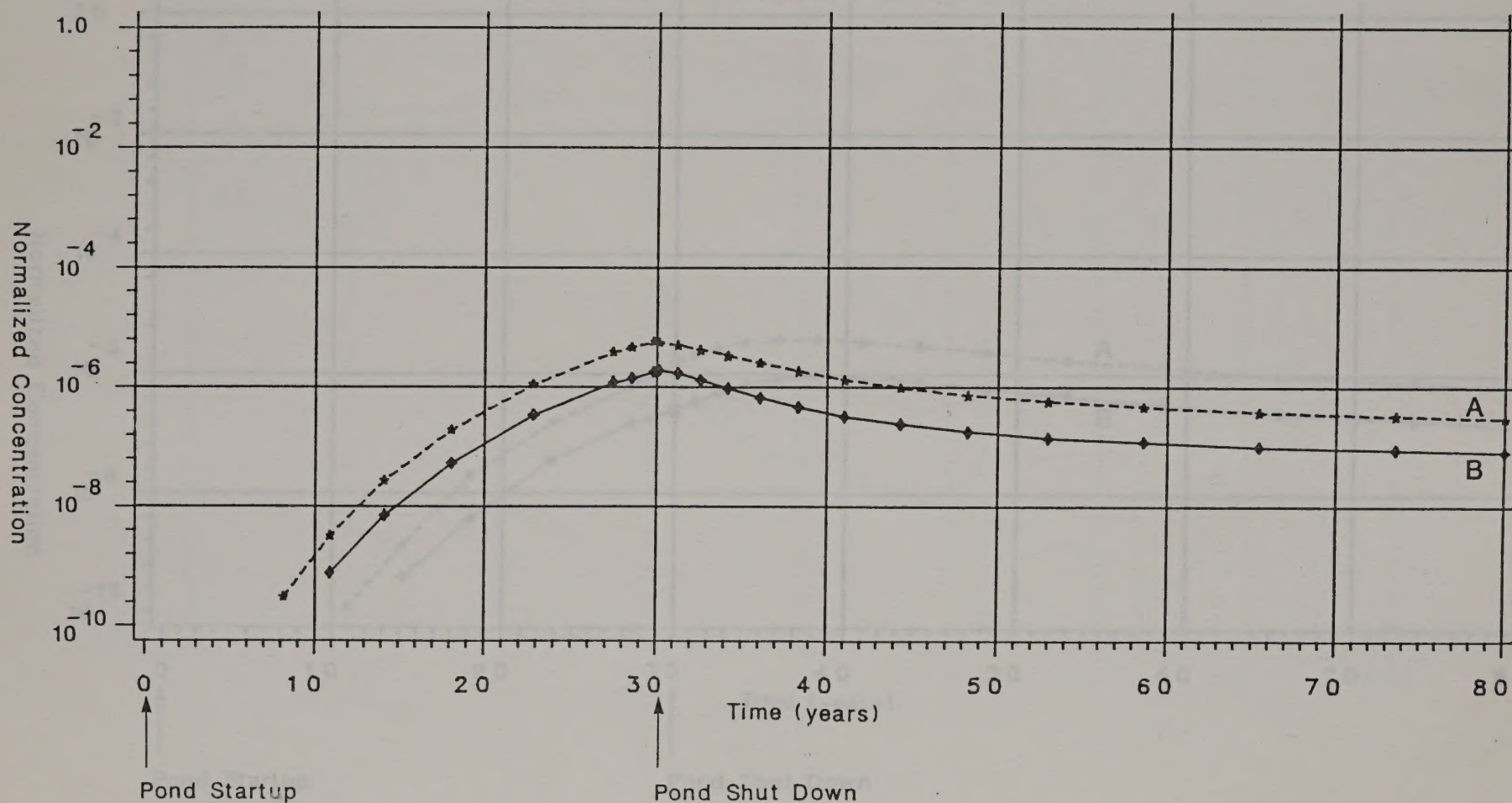
- A = Case 11: Ratio vertical to horizontal hydraulic conductivity = 1:100; zero adsorption; seepage = 1.0 cfs
- B = Case 15: Ratio vertical to horizontal hydraulic conductivity = 1:10; zero adsorption; seepage = 1.0 cfs
- C = Case 9: Ratio vertical to horizontal hydraulic conductivity = 1:1; zero adsorption; seepage = 1.0 cfs

$$\text{Normalized Concentration} = \frac{\text{Actual Concentration} - \text{Background Concentration}}{\text{Seepage Concentration} - \text{Background Concentration}}$$

Figure 7.10B

TIME HISTORY OF METAL CONCENTRATIONS AS A FUNCTION OF HYDRAULIC CONDUCTIVITY ANISOTROPY

MOLYCORP, INC: GUADALUPE MTN PROPOSED TAILINGS AREA
BENEATH POND, JUST BELOW WATER TABLE



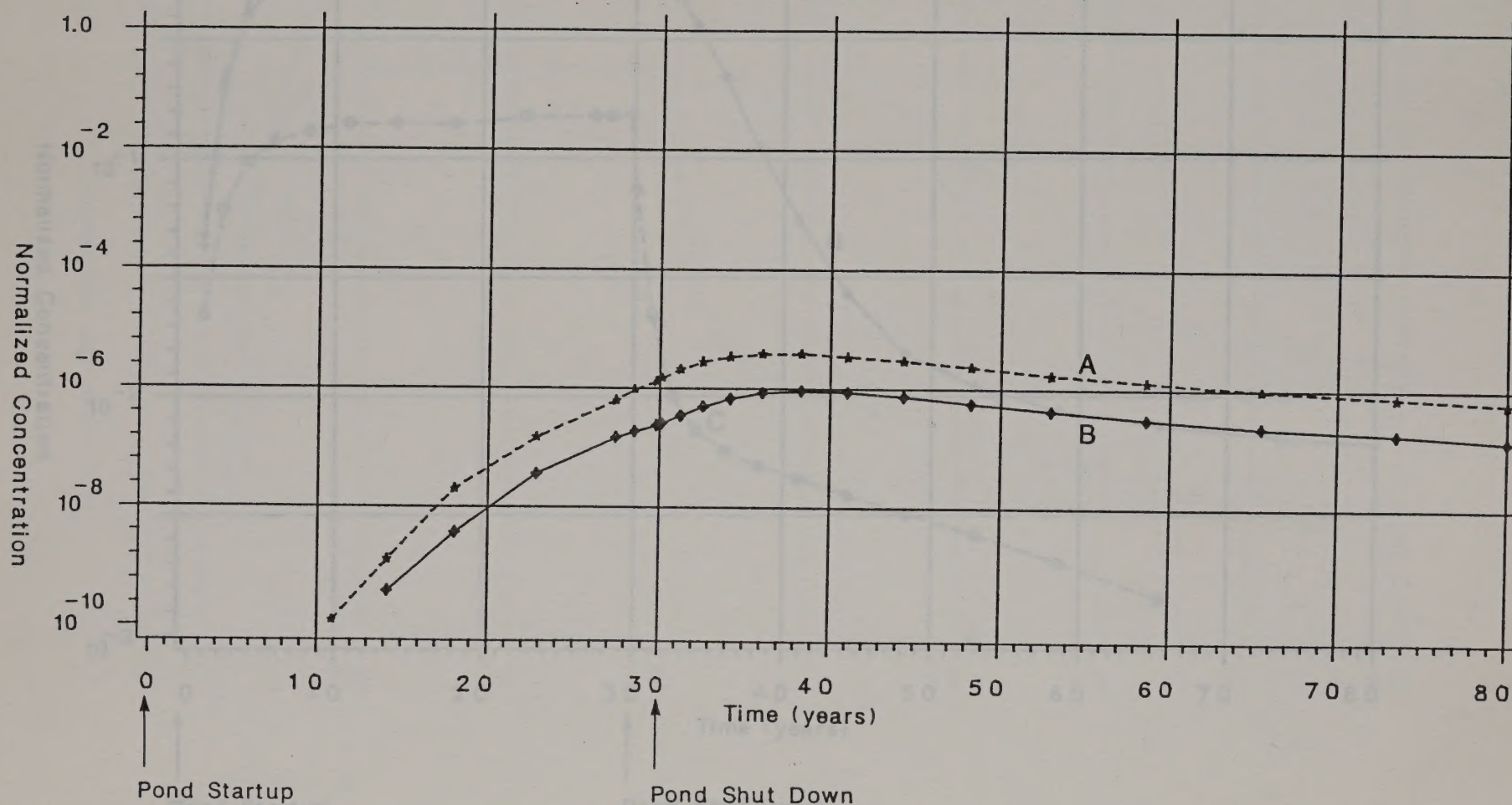
A = Case 10: ratio of vertical to horizontal hydraulic conductivity = 1:1; seepage rate = 1.0 cfs; Kd = medium case
 B = Case 3: ratio of vertical to horizontal hydraulic conductivity = 1:1; seepage rate = 1.0 cfs; Kd = medium case
 Note: Predicted Normalized Concentrations for $K_v:K_h = 1:100$ (Case 12) are less than 10^{-10}

$$\text{Normalized Concentration} = \frac{\text{Actual Concentration} - \text{Background Concentration}}{\text{Seepage Concentration} - \text{Background Concentration}}$$

Figure 7.11A

TIME HISTORY OF METAL CONCENTRATIONS AS A FUNCTION OF HYDRAULIC CONDUCTIVITY ANISOTROPY

MOLYCORP, INC: GUADALUPE MTN PROPOSED TAILINGS AREA
AT DOWN-GRADENT CLAIM BOUNDARY



A = Case 10: ratio of vertical to horizontal hydraulic conductivity = 1:1; seepage rate = 1.0 cfs; K_d = medium case

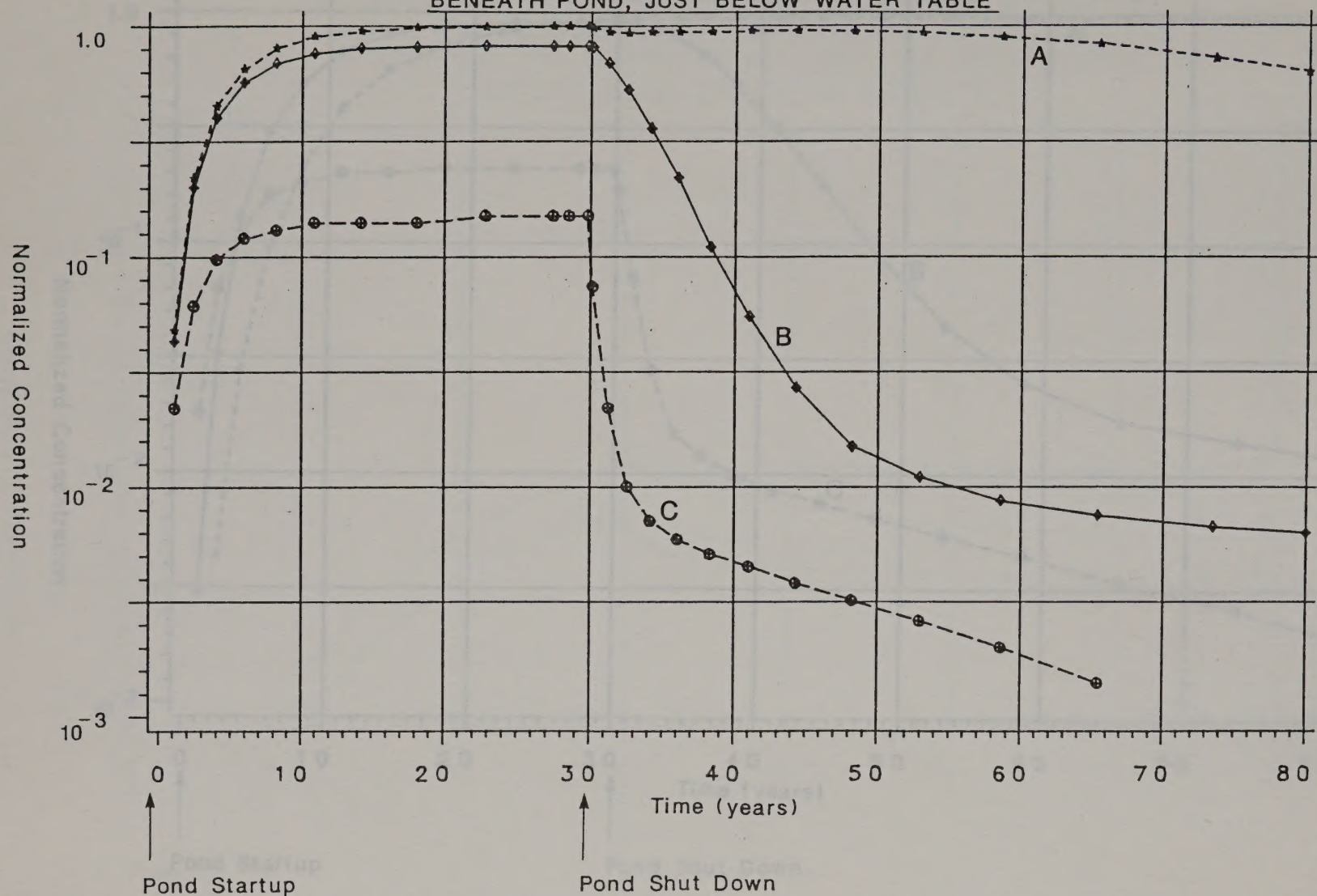
B = Case 3: ratio of vertical to horizontal hydraulic conductivity = 1:10; seepage rate = 1.0 cfs; K_d = medium case

Note: Predicted Normalized concentrations for K_v:K_h = 1:100 (Case 12) are less than 10⁻¹⁰

$$\text{Normalized Concentration} = \frac{\text{Actual Concentration} - \text{Background Concentration}}{\text{Seepage Concentration} - \text{Background Concentration}}$$

TIME HISTORY OF ANION CONCENTRATIONS AS A FUNCTION OF HYDRAULIC CONDUCTIVITY

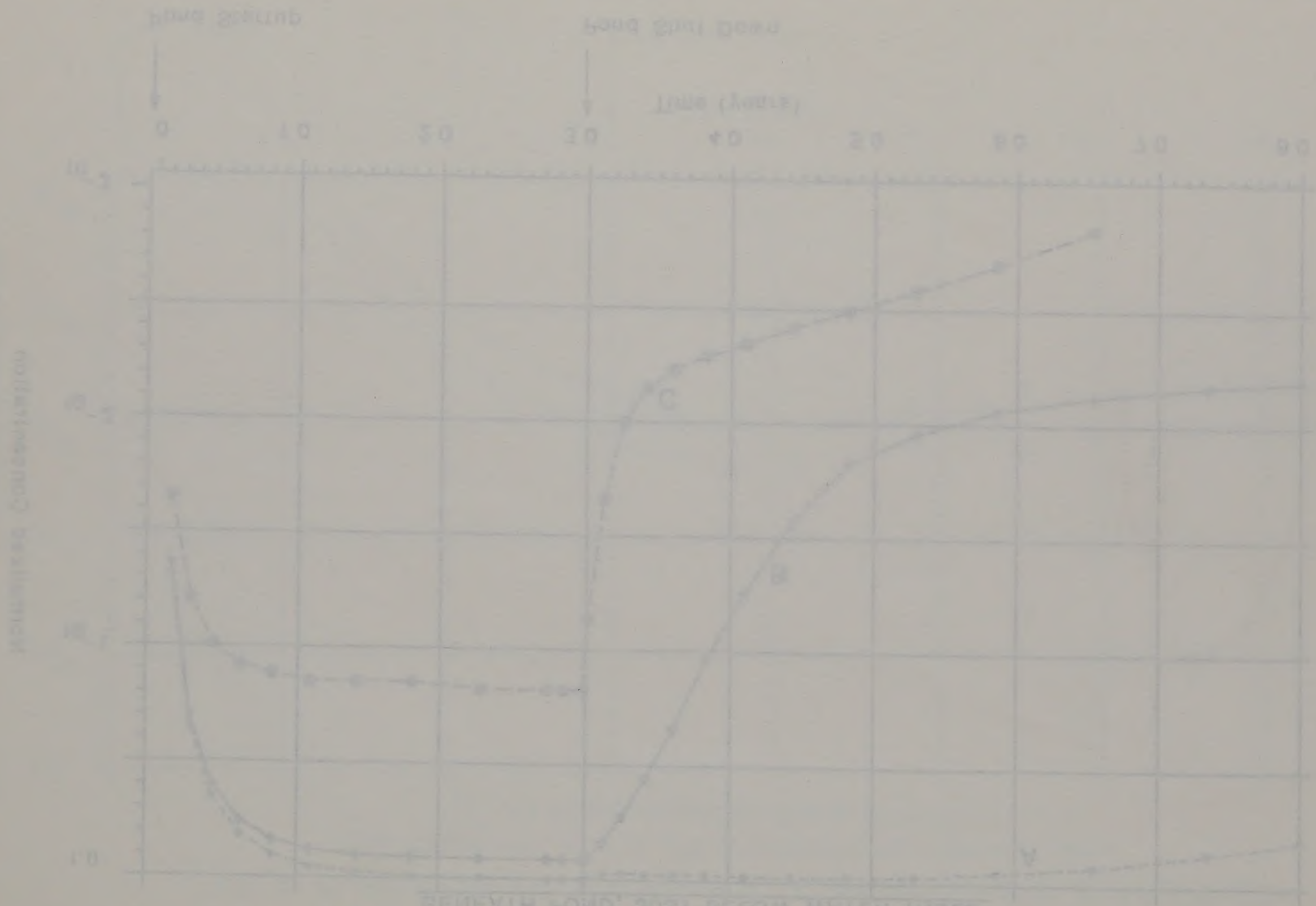
MOLYCORP, INC: GUADALUPE MTN PROPOSED TAILINGS AREA
BENEATH POND, JUST BELOW WATER TABLE



- A = Case 13: low hydraulic conductivity; zero adsorption; pond seepage rate = 1.0 cfs
- B = Case 5: average hydraulic conductivity; zero adsorption; pond seepage rate = 1.0 cfs
- C = Case 15: high hydraulic conductivity; zero adsorption; pond seepage rate = 1.0 cfs

$$\text{Normalized Concentration} = \frac{\text{Actual Concentration} - \text{Background Concentration}}{\text{Seepage Concentration} - \text{Background Concentration}}$$

concentration - porewater concentration
 initial concentration - porewater concentration
 C = 0.15 g/l; initial concentration; porewater concentration
 B = 0.15 g/l; initial concentration; porewater concentration
 A = 0.15 g/l; initial concentration; porewater concentration

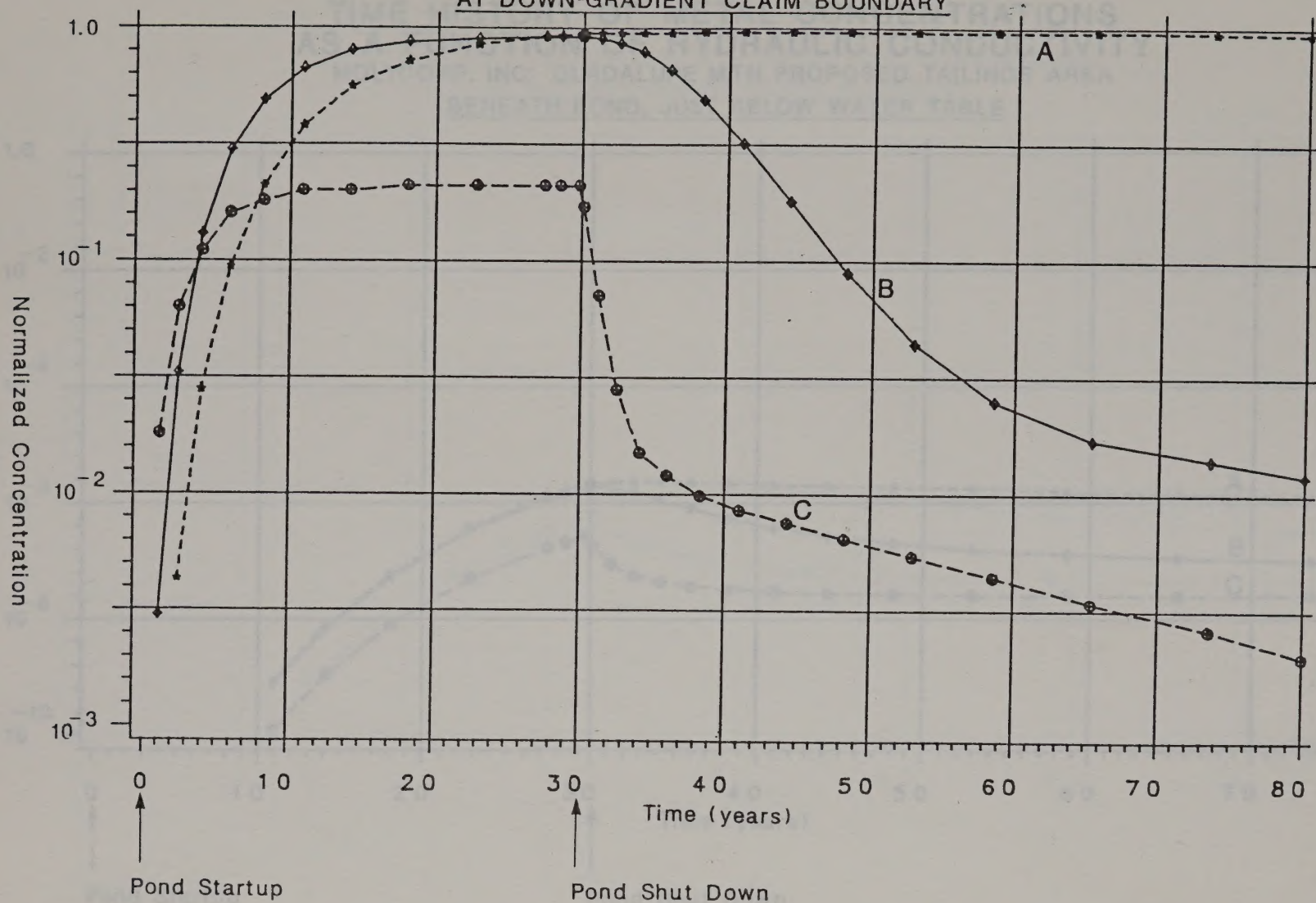


AS A FUNCTION OF HYDRAULIC CONDUCTIVITY
 TIME HISTORY OF ANION CONCENTRATIONS
 BENEATH SAND, FIRST BELOW WATER TABLE
 MOGASONE, INC. STUDYING WITH PROPOSED TUNNELS AREA

TIME HISTORY OF ANION CONCENTRATIONS AS A FUNCTION OF HYDRAULIC CONDUCTIVITY

MOLYCORP, INC: GUADALUPE MTN PROPOSED TAILINGS AREA

AT DOWN-GRADIENT CLAIM BOUNDARY



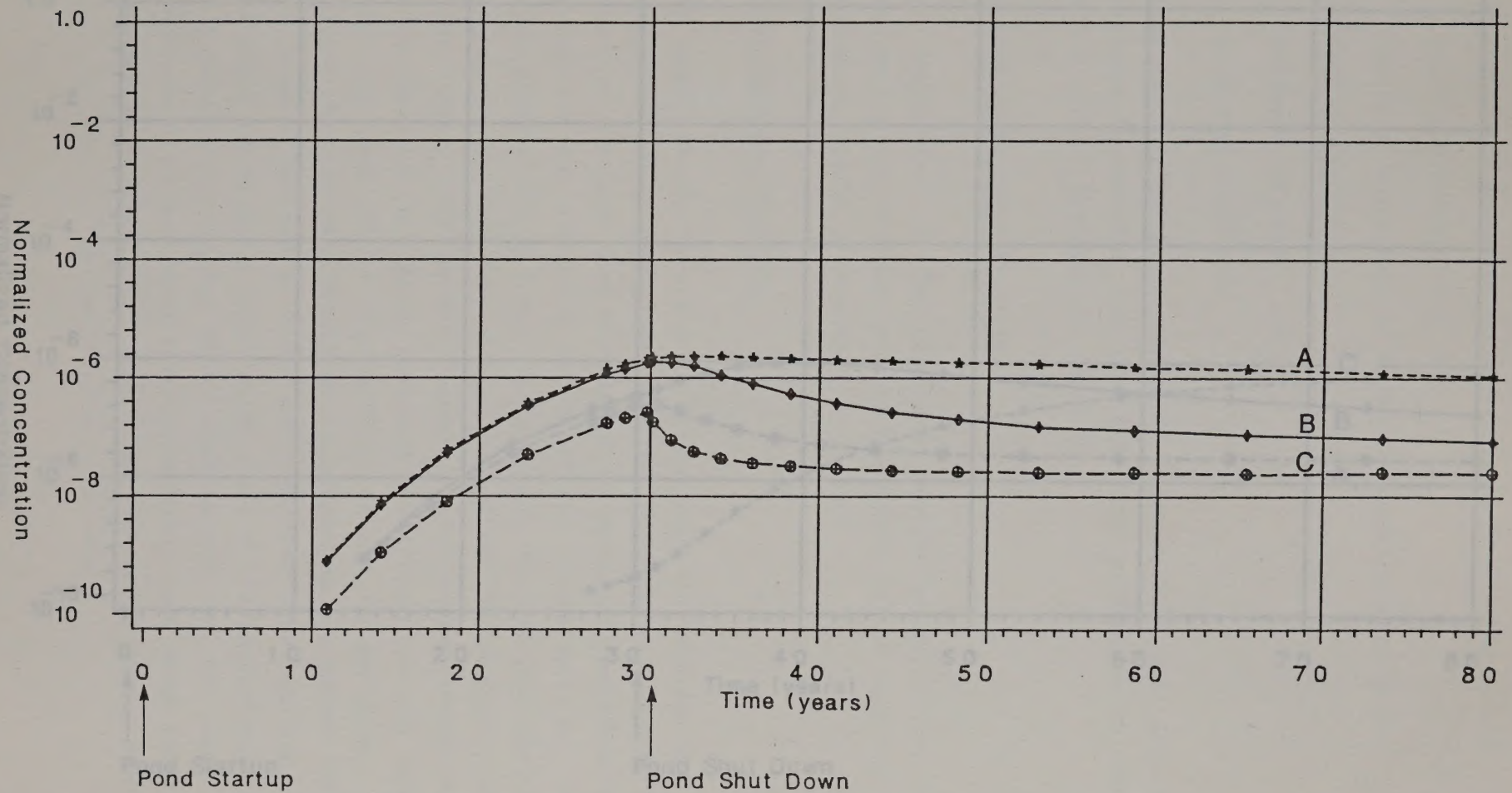
- A = Case 13: low hydraulic conductivity; zero adsorption; pond seepage rate = 1.0 cfs
- B = Case 5: average hydraulic conductivity; zero adsorption; pond seepage rate = 1.0 cfs
- C = Case 15: high hydraulic conductivity; zero adsorption; pond seepage rate = 1.0 cfs

$$\text{Normalized Concentration} = \frac{\text{Actual Concentration} - \text{Background Concentration}}{\text{Seepage Concentration} - \text{Background Concentration}}$$

TIME HISTORY OF METAL CONCENTRATIONS AS A FUNCTION OF HYDRAULIC CONDUCTIVITY

MOLYCORP, INC: GUADALUPE MTN PROPOSED TAILINGS AREA

BENEATH POND, JUST BELOW WATER TABLE



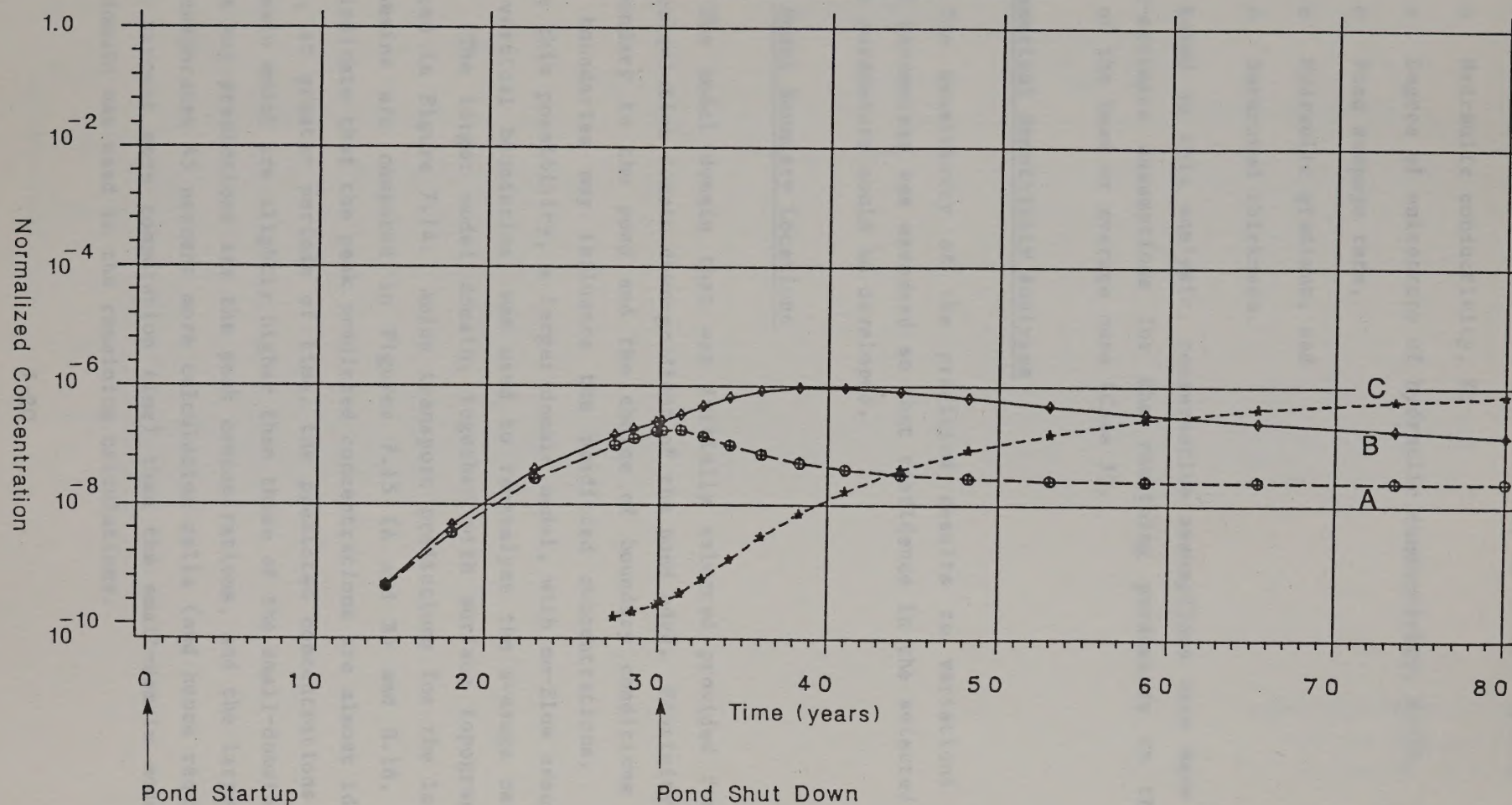
- A = Case 14: low hydraulic conductivity; medium adsorption case; pond seepage rate = 1.0 cfs; $K_v:K_h = 1:10$
 B = Case 3: average hydraulic conductivity; medium adsorption case; pond seepage rate = 1.0 cfs; $K_v:K_h = 1:10$
 C = Case 16: high hydraulic conductivity; medium adsorption case; pond seepage rate = 1.0 cfs; $K_v:K_h = 1:10$

$$\text{Normalized Concentration} = \frac{\text{Actual Concentration} - \text{Background Concentration}}{\text{Seepage Concentration} - \text{Background Concentration}}$$

Figure 7.13A

TIME HISTORY OF METAL CONCENTRATIONS AS A FUNCTION OF HYDRAULIC CONDUCTIVITY

MOLYCORP, INC: GUADALUPE MTN PROPOSED TAILINGS AREA
AT DOWN-GRADIENT CLAIM BOUNDARY



- A = Case 16; High hydraulic conductivity; medium adsorption case; pond seepage = 1.0 cfs
- B = Case 3; Medium hydraulic conductivity; medium adsorption case; pond seepage = 1.0 cfs
- C = Case 14; Low hydraulic conductivity; Medium adsorption case; pond seepage = 1.0 cfs

$$\text{Normalized Concentration} = \frac{\text{Actual Concentration} - \text{Background Concentration}}{\text{Seepage Concentration} - \text{Background Concentration}}$$

- o Adsorption distribution coefficient, K_d (metals only),
- o Hydraulic conductivity, K ,
- o Degree of anisotropy of hydraulic conductivity, $K_v:K_h$,
- o Pond seepage rate,
- o Hydraulic gradient, and
- o Saturated thickness.

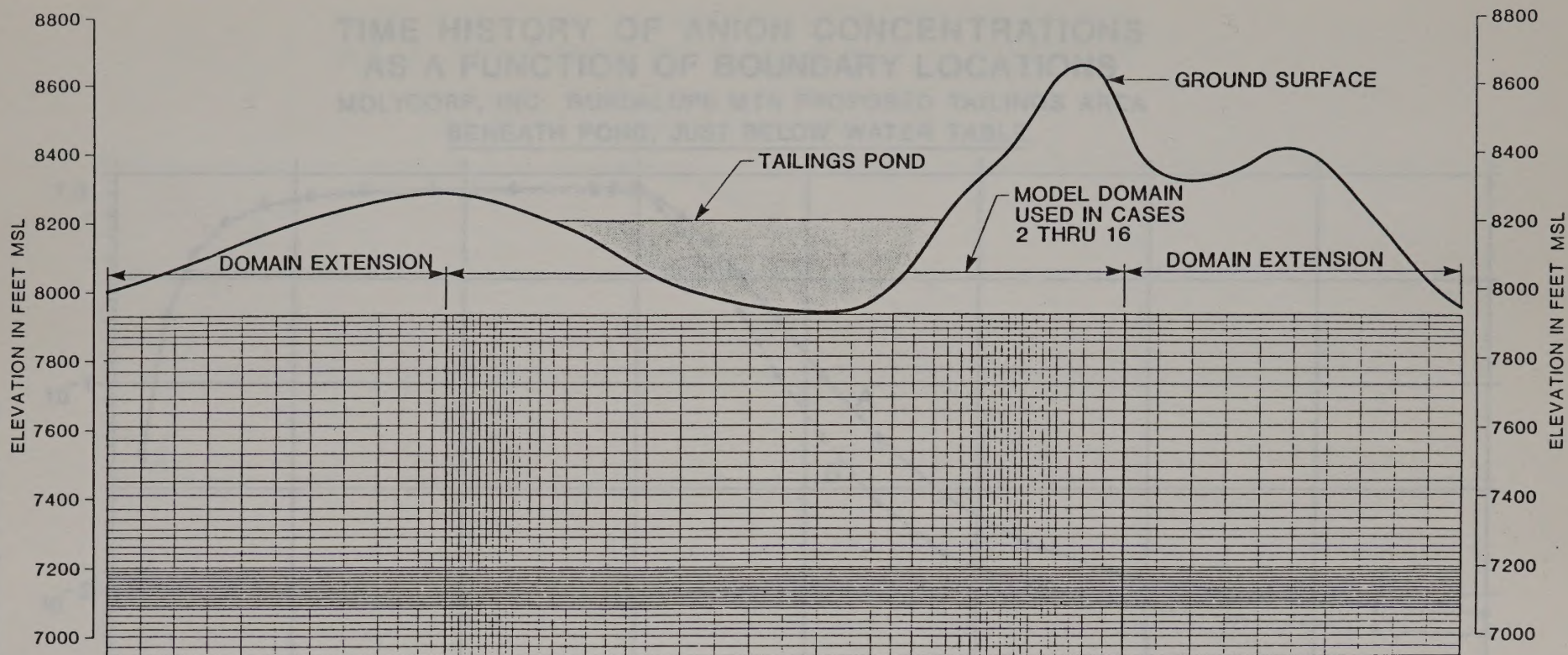
Based on this analysis, conservative assumptions were made for K_d and best-estimate assumptions for the remaining parameters in the formulation of the base or average case (Case 3).

7.4.3 Numerical Sensitivity Analyses

The sensitivity of the predicted results to variations in key numerical parameters was assessed so that confidence in the selected values for these parameters could be developed.

Model Boundary Locations

The model domain that was initially selected provided for 1,500 feet of calculation domain down-gradient of the pond edge. Proximity of the model boundary to the pond and the choice of boundary conditions at the vertical boundaries may influence the predicted concentrations. To investigate this possibility, a larger domain model, with no-flow assumptions for the vertical boundaries, was used to re-analyze the average case conditions. The larger model domain, together with surface topography, is illustrated in Figure 7.14. Anion transport predictions for the large and small domains are compared in Figures 7.15 (A and B) and H.18. These figures indicate that the peak predicted concentrations are almost identical and that, at greater periods of time, the predicted concentrations in the large-domain model are slightly higher than those of the small-domain model. Since the key predictions are the peak concentrations, and the large-domain model incorporates 45 percent more calculation cells (and hence requires at least 45 percent more computation time) than the small-domain model, the smaller domain was used in the remaining calculations.



FINITE DIFFERENCE MESH USED
TO TEST SENSITIVITY TO
BOUNDARY LOCATIONS

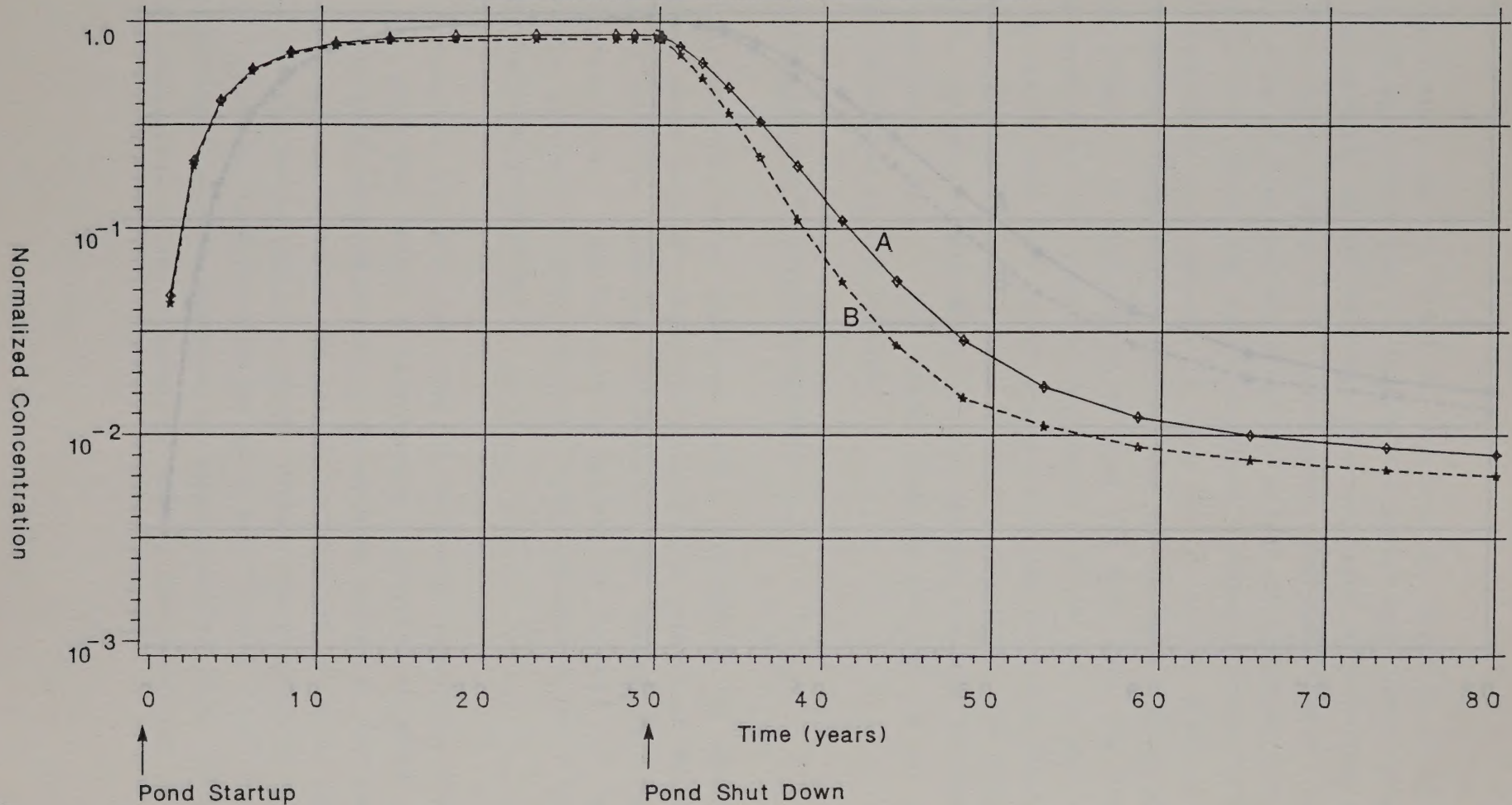
Figure 7.14

A - Case 3 - expanded model domain (72 x 43 cells)
B - Case 3 - original model domain (50 x 43 cells)

Normalized Concentration = $\frac{\text{Actual Concentration} - \text{Background Concentration}}{\text{Sewage Concentration} - \text{Background Concentration}}$

TIME HISTORY OF ANION CONCENTRATIONS AS A FUNCTION OF BOUNDARY LOCATIONS

MOLYCORP, INC: GUADALUPE MTN PROPOSED TAILINGS AREA
BENEATH POND, JUST BELOW WATER TABLE



A = Case 5: expanded model domain (72 x 43 cells)

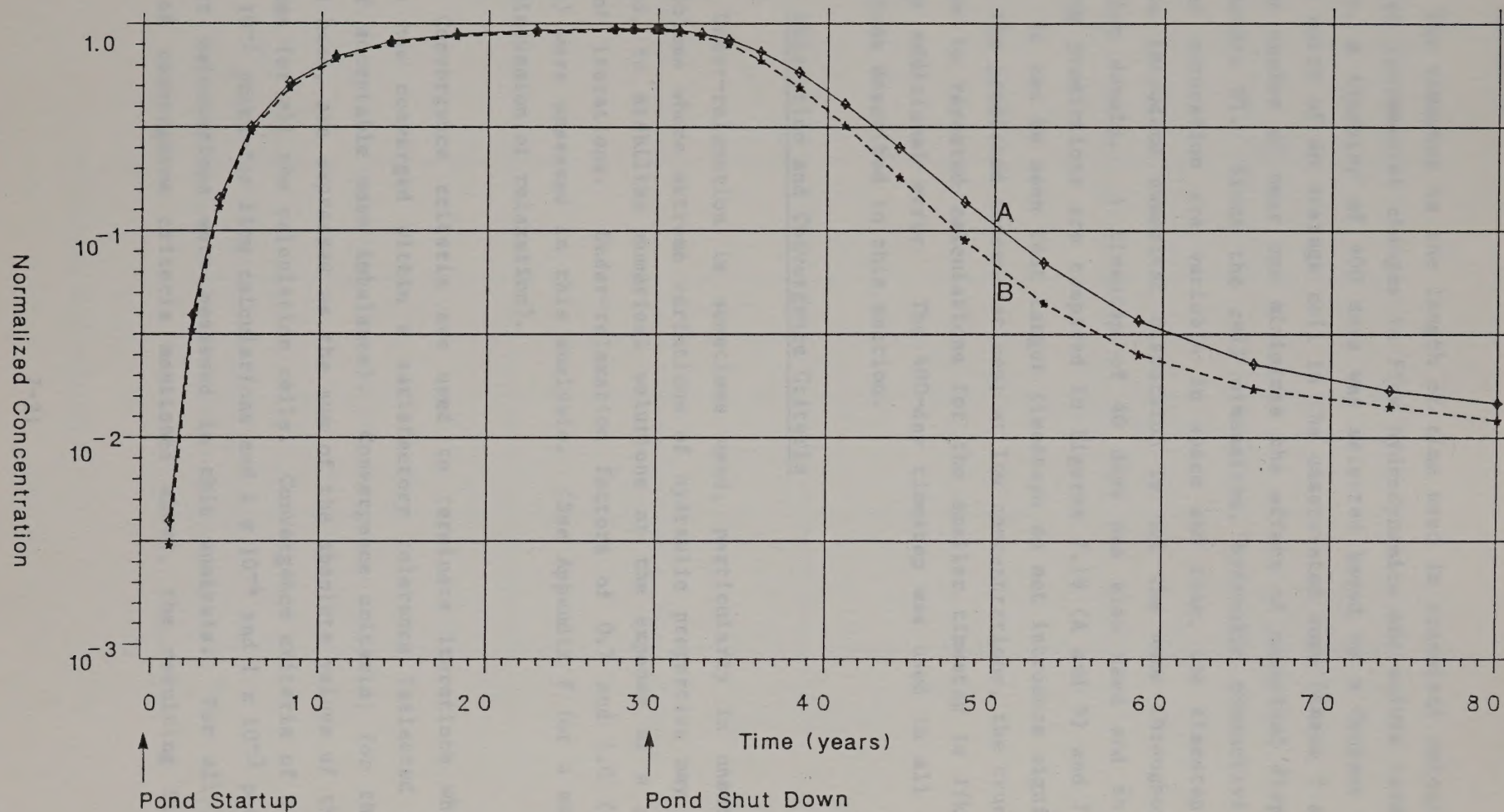
B = Case 5: original model domain (50 x 43 cells)

$$\text{Normalized Concentration} = \frac{\text{Actual Concentration} - \text{Background Concentration}}{\text{Seepage Concentration} - \text{Background Concentration}}$$

Figure 7.15A

TIME HISTORY OF ANION CONCENTRATIONS AS A FUNCTION OF BOUNDARY LOCATIONS

MOLYCORP, INC: GUADALUPE MTN PROPOSED TAILINGS AREA
AT DOWN-GRADIENT CLAIM BOUNDARY



A = Case 5: expanded model domain (72 x 43 cells)

B = Case 5: original model domain (50 x 43 cells)

$$\text{Normalized Concentration} = \frac{\text{Actual Concentration} - \text{Background Concentration}}{\text{Seepage Concentration} - \text{Background Concentration}}$$

Figure 7.15B

Timestep

The timestep is the length of time used in transient calculations to predict incremental changes in flow hydrodynamics and solute transport. Initially, a timestep of 400 days was selected based on a Courant number close to unity of an average cell in the unsaturated zone (Cases 3 and 5). A Courant number of near one minimizes the effect of numerical dispersion (see Appendix F). Since the cell dimensions, hydraulic conductivity and degree of saturation are variable in space and time, the timestep least likely to introduce numerical dispersion is not the same throughout the calculation domain. A timestep of 40 days was also used and the corresponding predictions are compared in Figures 7.16 (A and B) and 7.17 (A and B). It can be seen that larger timesteps do not introduce significant error to the predicted concentrations; at low concentrations, the truncation error due to repeated calculations for the smaller timestep is likely to introduce additional error. The 400-day timestep was used in all of the calculations described in this section.

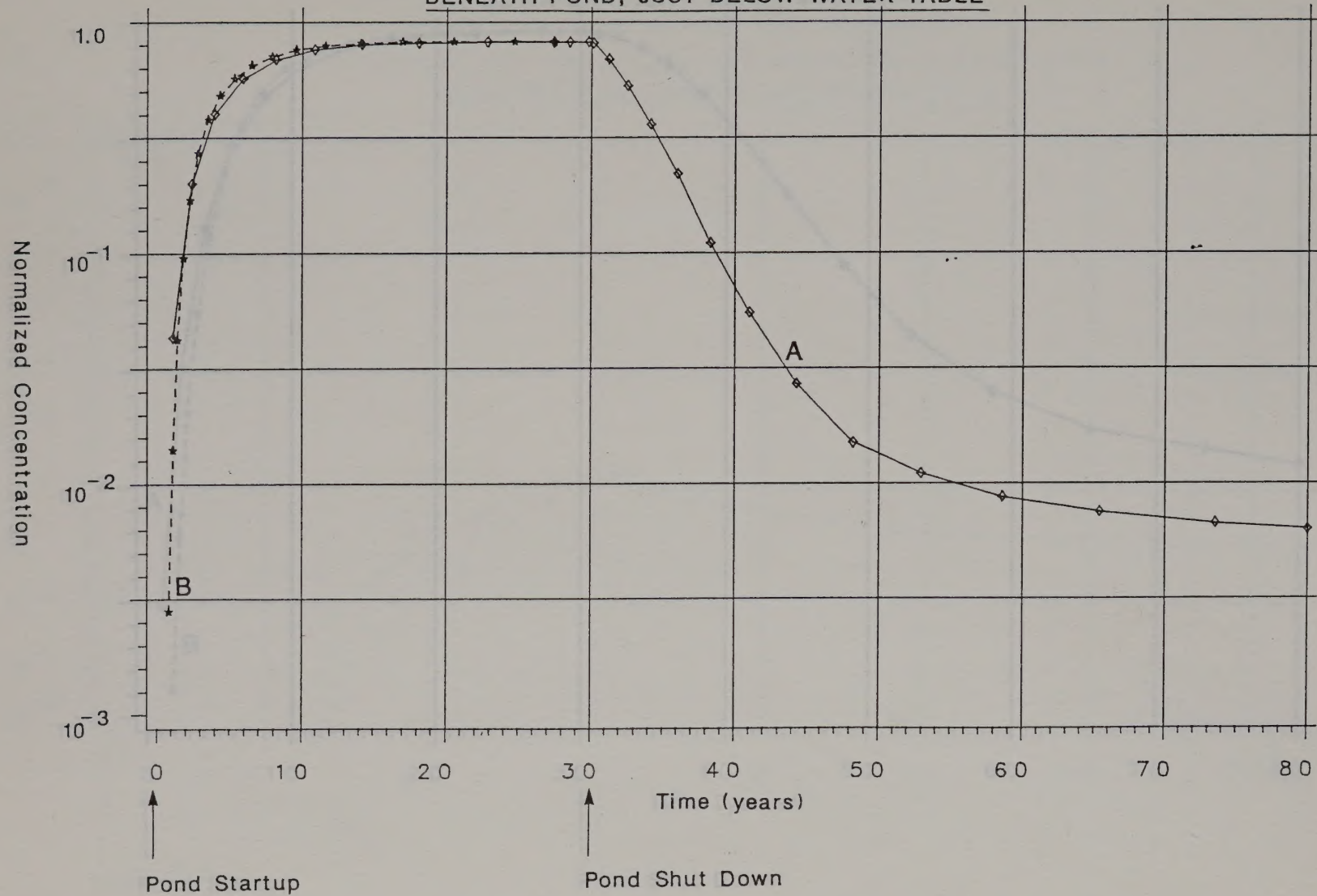
Relaxation and Convergence Criteria

Under-relaxation is sometimes used, particularly in unsaturated flow problems where extreme variations of hydraulic properties may be encountered, to stabilize numerical solutions at the expense of a greater number of iterations. Under-relaxation factors of 0.7 and 1.0 (no relaxation) were assessed in this analysis. (See Appendix F for a more detailed discussion of relaxation).

Convergence criteria are used to terminate iterations when the solution has converged within a satisfactory tolerance (selected on the basis of acceptable mass imbalance). Convergence criteria, for the code employed here, are expressed as the sum of the absolute values of the mass imbalances for all the calculation cells. Convergence criteria of 1×10^{-2} and 1×10^{-1} pound for flow calculations and 1×10^{-4} and 1×10^{-3} pound for transport calculations were assessed in this analysis. For all of the values of convergence criteria mentioned above, the resulting flow and

TIME HISTORY OF ANION CONCENTRATIONS AS A FUNCTION OF TIMESTEP

MOLYCORP, INC: GUADALUPE MTN PROPOSED TAILINGS AREA
BENEATH POND, JUST BELOW WATER TABLE



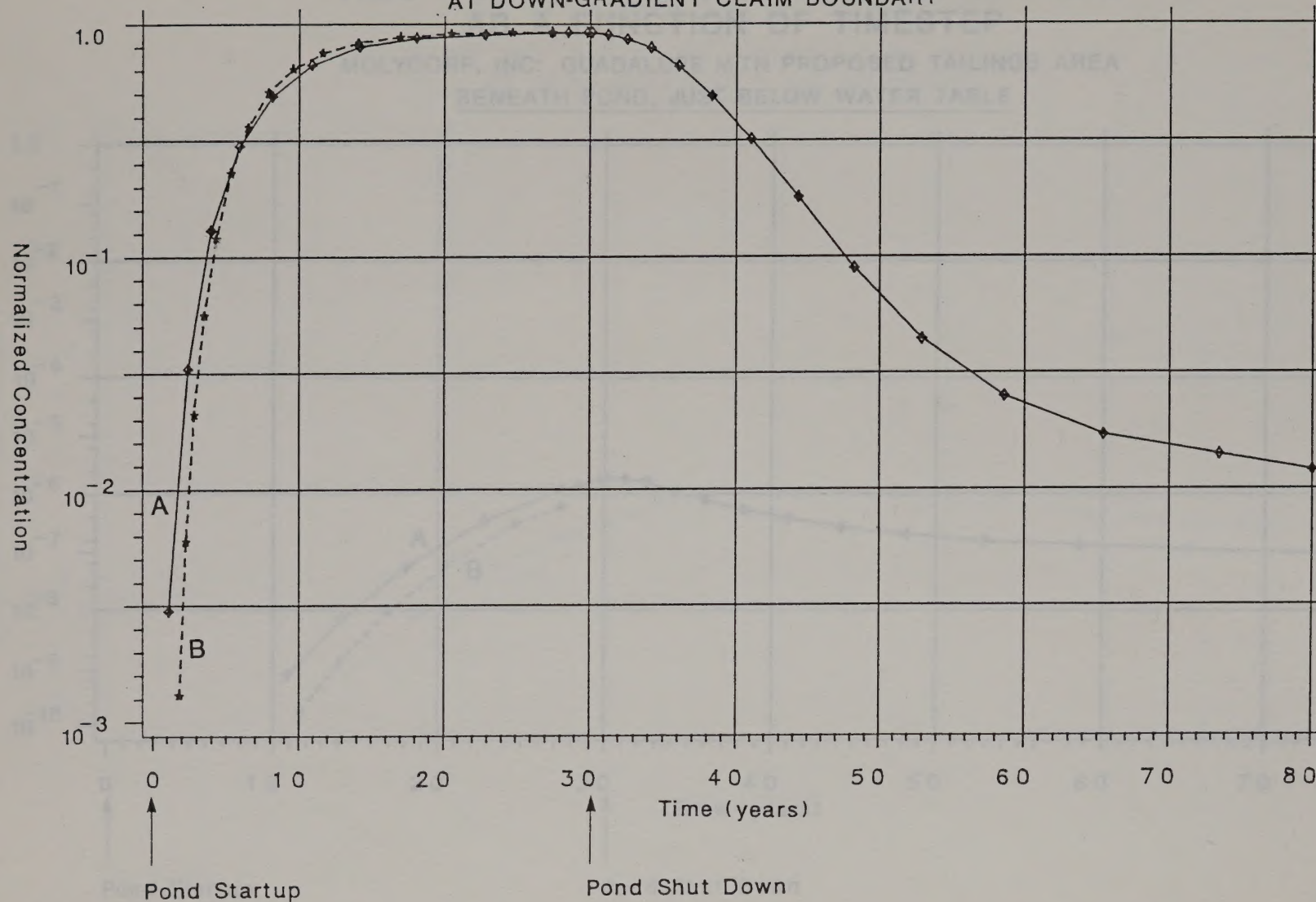
- A = Case 5: 400 day initial time step; zero adsorption case; pond seepage rate = 1.0 cfs
- B = Case 5: 40 day initial time step; zero adsorption case; pond seepage rate = 1.0 cfs

$$\text{Normalized Concentration} = \frac{\text{Actual Concentration} - \text{Background Concentration}}{\text{Seepage Concentration} - \text{Background Concentration}}$$

Figure 7.16A

TIME HISTORY OF ANION CONCENTRATIONS AS A FUNCTION OF TIMESTEP

MOLYCORP, INC: GUADALUPE MTN PROPOSED TAILINGS AREA
AT DOWN-GRADIENT CLAIM BOUNDARY



A = Case 5: 400 day initial time step; zero adsorption case; pond seepage rate = 1.0 cfs

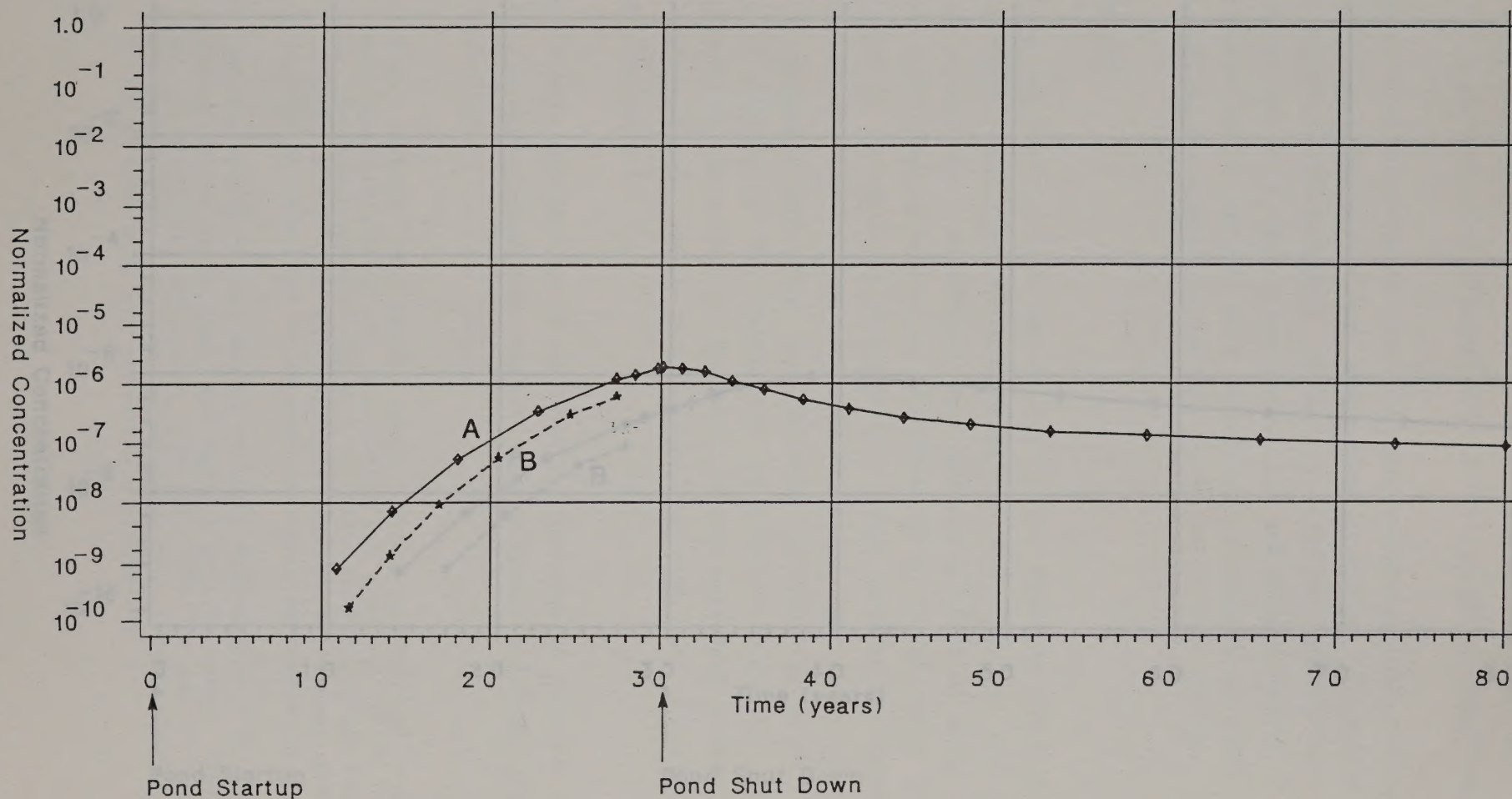
B = Case 5: 40 day initial time step; zero adsorption case; pond seepage rate = 1.0 cfs

$$\text{Normalized Concentration} = \frac{\text{Actual Concentration} - \text{Background Concentration}}{\text{Seepage Concentration} - \text{Background Concentration}}$$

Figure 7.16B

TIME HISTORY OF METAL CONCENTRATIONS AS A FUNCTION OF TIMESTEP

MOLYCORP, INC: GUADALUPE MTN PROPOSED TAILINGS AREA
BENEATH POND, JUST BELOW WATER TABLE



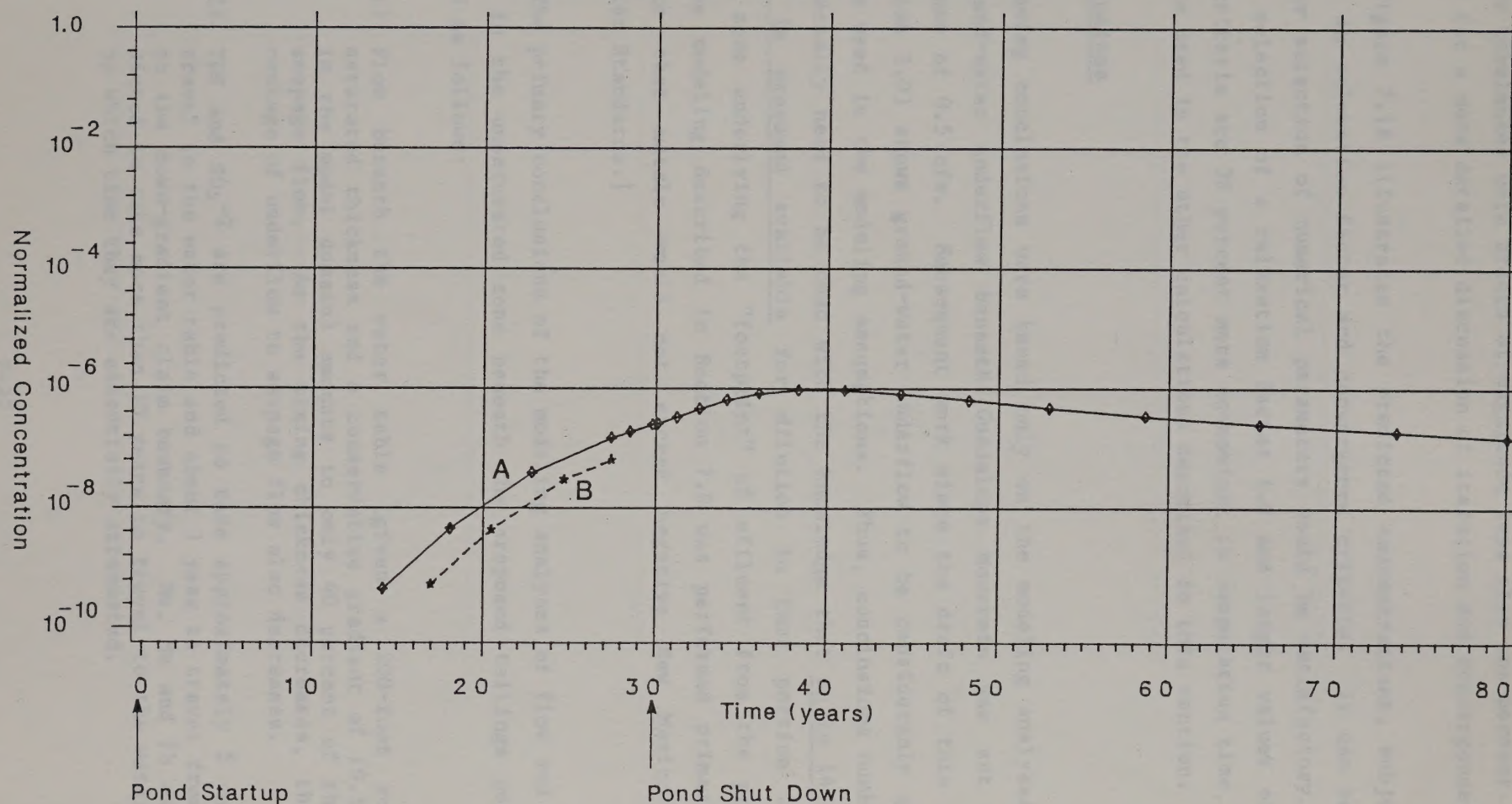
A = Case 3: 400 day initial time step; medium case adsorption; pond seepage rate = 1.0 cfs

B = Case 3: 40 day initial time step; medium case adsorption; pond seepage rate = 1.0 cfs

$$\text{Normalized Concentration} = \frac{\text{Actual Concentration} - \text{Background Concentration}}{\text{Seepage Concentration} - \text{Background Concentration}}$$

TIME HISTORY OF METAL CONCENTRATIONS AS A FUNCTION OF TIMESTEP

MOLYCORP, INC: GUADALUPE MTN PROPOSED TAILINGS AREA
AT DOWN-GRADIENT CLAIM BOUNDARY



A = Case 3; 400 day initial time step; medium case adsorption; pond seepage rate = 1.0 cfs

B = Case 3; 40 day initial time step; medium case adsorption; pond seepage rate = 1.0 cfs

$$\text{Normalized Concentration} = \frac{\text{Actual Concentration} - \text{Background Concentration}}{\text{Seepage Concentration} - \text{Background Concentration}}$$

solute mass imbalances were orders of magnitude less than one percent. (See Appendix F for a more detailed discussion of iteration and convergence).

Figure 7.18 illustrates the predicted concentrations, subject to variations in relaxation factor and convergence criteria. It can be seen that either selection of numerical parameters would be satisfactory. Because the selection of a relaxation factor 1.0 and larger values of convergence criteria are 30 percent more economical in computation time, these values were used in the other calculations described in this section.

7.5 Conclusions

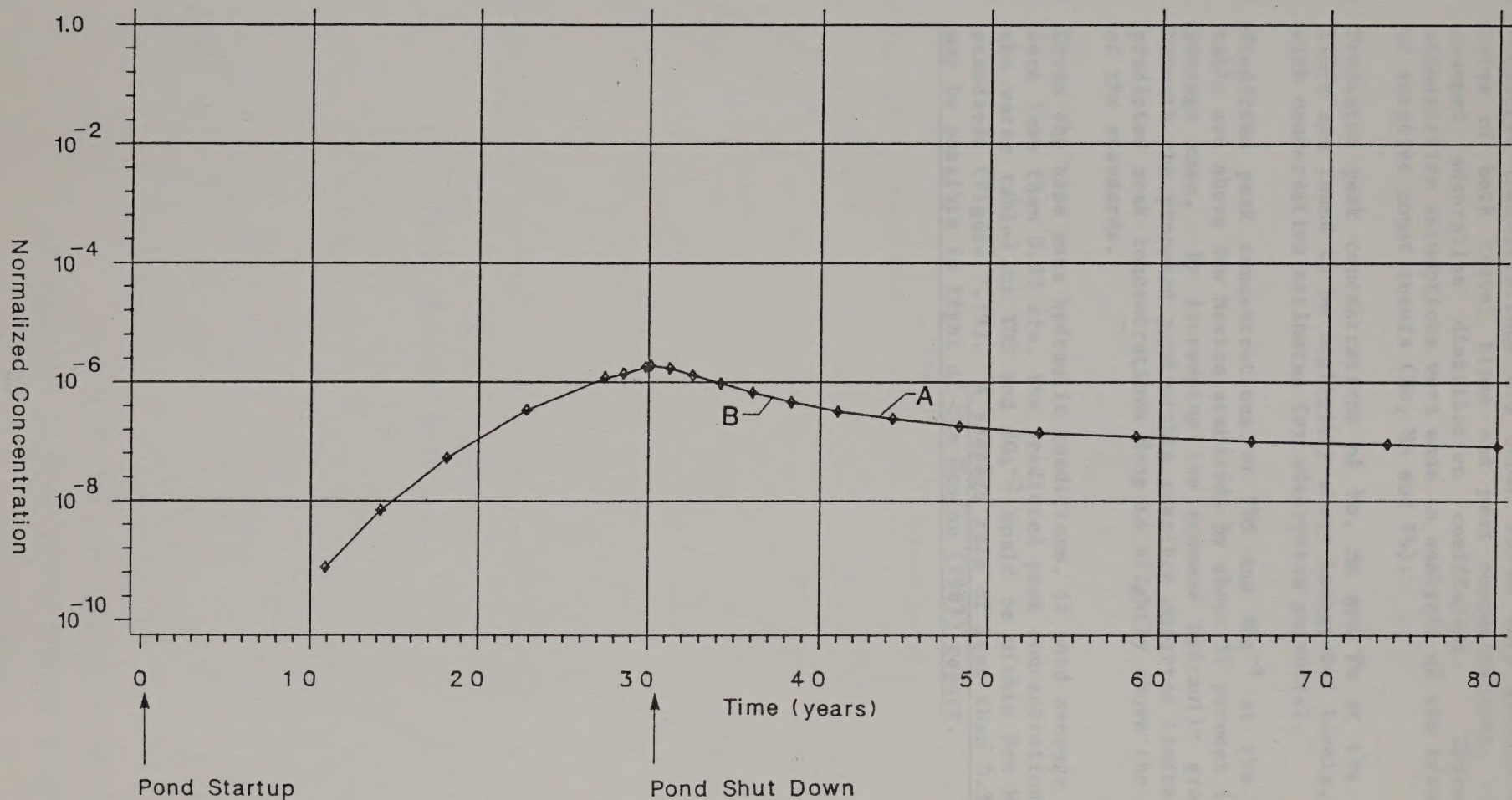
[The following conclusions were based only on the modeling analyses. As such, ground-water underflow beneath Guadalupe Mountain was set at an average case of 0.5 cfs. Subsequent work since the draft of this report (see Section 3.0) shows ground-water underflow to be considerably greater than those used in the modeling assumptions. Thus, conclusions numbered 1 and 5 especially need to be read with the knowledge that up to 14 cfs of underflow is presumed available for dilution in that portion of the saturated zone underlying the "footprint" of effluent from the proposed pond. The modeling described in Section 7.0 was performed primarily to demonstrate that metals would not exceed negative New Mexico State Ground-Water Standards.]

The primary conclusions of the modeling analyses of flow and solute transport in the unsaturated zone beneath the proposed tailings pond are summarized as follows:

- 1) Flow beneath the water table (given a 200-foot zone of saturated thickness and a conservative gradient of 19.5 ft/mi in the model domain) amounts to only 40 percent of the pond seepage flow. As the mixing thickness decreases, the percentage of underflow to seepage flow also decreases.
- 2) TDS and SO_4^{-2} are predicted to take approximately 5 years to travel to the water table and about 1 year to travel from there to the down-gradient claim boundary. Mo, Mn and Pb are predicted to take more than 30 years to travel to the water table by which time they are essentially attenuated.

TIME HISTORY OF METAL CONCENTRATIONS AS A FUNCTION OF RELAXATION FACTOR AND CONVERGENCE CRITERIA

MOLYCORP, INC: GUADALUPE MTN PROPOSED TAILINGS AREA
BENEATH POND, JUST BELOW WATER TABLE



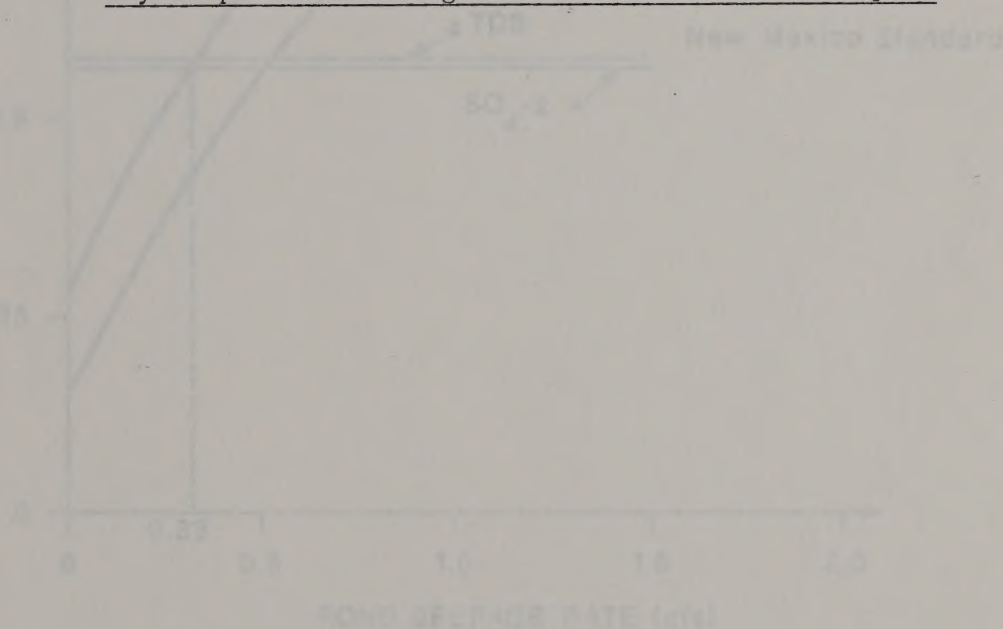
A = Relaxation factor of 0.7, convergence criteria = 1×10^{-2} (flow) and 1×10^{-4} (solute)

B = Relaxation factor of 0.7, convergence criteria = 1×10^{-2} (flow) and 1×10^{-4} (solute)

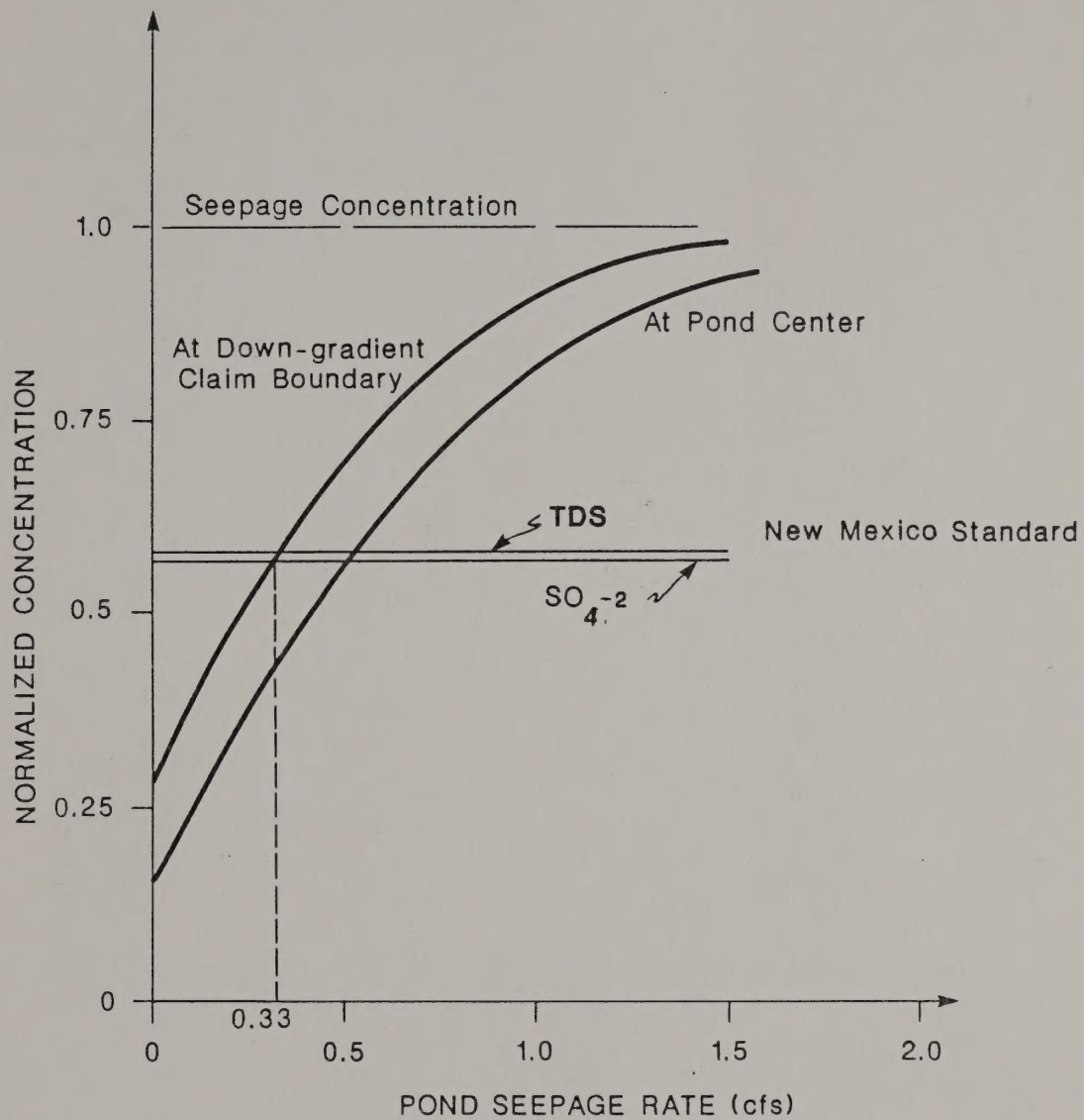
$$\text{Normalized Concentration} = \frac{\text{Actual Concentration} - \text{Background Concentration}}{\text{Seepage Concentration} - \text{Background Concentration}}$$

Figure 7.18

- 3) Predicted concentrations are shown to be very sensitive, in terms of both travel times and peak concentrations, to the assumed adsorption distribution coefficient. Therefore, conservative assumptions were made in analysis of the transport of sorptive constituents (Mo, Mn and Pb).
- 4) Predicted peak concentrations of Mo, Mn and Pb at the water table are found to be negligibly above background levels, even with conservative estimates for adsorption potential.
- 5) Predicted peak concentrations of TDS and SO_4^{-2} at the water table are above New Mexico standards by about 50 percent in the average case. By increasing the assumed hydraulic gradient beneath the proposed pond within possible observed limits, the predicted peak concentrations drop to slightly above the level of the standards.
- 6) Given the base case hydraulic conditions, if pond seepage rates were less than 0.33 cfs, the predicted peak concentrations (at the water table) of TDS and SO_4^{-2} would be within New Mexico standards (Figure 7.19). A seepage rate of less than 0.33 cfs may be possible in light of the Geocon (1983) report.



VARIAION OF CONCENTRATION
AT WATER TABLE WITH POND SEEPAGE RATE



VARIATION OF CONCENTRATION
AT WATER TABLE WITH POND SEEPAGE RATE

Figure 7.19

References

Appendix

8.0 REFERENCES

- Anderson, M.P., 1979, Using models to simulate the movement of contaminants through ground-water flow systems. Critical Reviews in Environmental Control, Volume 9, Issue 2.
- Burdine, N.T., 1953, Relative permeability calculations from pore-size distribution data: Transactions, AIME, v. 198, pp. 71-77.
- Burkholder, H. C., 1976, Methods and data for predicting nuclide migration in geologic media. International Symposium on Management of Waste from the LWR Fuel Cycle, Denver, Colorado.
- Cordell, L., 1978, Regional Geophysical Setting of the Rio Grande rift in Southern New Mexico. Geological Society of America Bulletin, v. 89, pp. 1073-1089.
- Corey, R. B., 1981, Chemical reactions in soils and underlying materials. short course in modeling pollutant movement: in Ground Water, University of Wisconsin - Extension.
- Dames & Moore, 1980, Detailed seepage investigation of mill waste disposal alternatives, West Gas Hills, Wyoming. Report to Federal American Partners.
- Dungan, M.A., Muehlberger, W.R., Leininger, L., Peterson, C., McMillan, N.J., Gunn, G., Lindstrom, M., and Haskin, L., 1984, Volcanic and sedimentary stratigraphy of the Rio Grande Gorge and the Late Cenozoic geologic evolution of the southern San Luis Valley: in Rio Grande Rift, Northern New Mexico. New Mexico Geological Society Guidebook, 35th Field Conference, October 11-13, 1984, pp. 157-170.
- Freeze, R. A. and Cherry, J. A., 1979, Ground Water: Published by Prentice-Hall, New Jersey.
- Geocon, 1983, Study of potential seepage, proposed Guadalupe Mountain tailing area: Report to Molycorp Inc.
- Grisak, G.E. and Pickens, J. F., 1980, Solute transport through fractured media 1. The effect of matrix diffusion: Water Resources Research, Vol. 16, No. 4, pp. 719-730.
- Jeppson, R.W., 1970, Solution to transient vertical moisture movement based upon saturation-capillary pressure data and a modified Burdine theory: Utah Water Research Laboratory, Utah State University, Logan, Reprint No. PRWG-59c-5, 46 p.
- Lipman, P.W. and Mehnert, H.H., 1979, The Taos Plateau volcanic field, northern Rio Grande Rift, New Mexico: in Riecker, R.E., ed., Rio Grande Rift: Tectonics and Magmatism, American Geophysical Union, Washington, D.C., pp. 289-311.

- Menges, C.M., 1984, Geologic investigations in Questa area for EIB. Final Report to J.F. Callender, April 13, 1984, 10 pages and 3 figures.
- New Mexico Water Quality Control Commission, 1986, Water Quality Regulations as amended through March 3, 1986.
- Ralph E. Vail Consulting Engineers, April 1982, Feasibility Study; Long range disposal, Guadalupe Mountain area: Report to Molycorp Inc.
- Roy, W.R., and others, 1985, Development of standardized batch adsorption procedures -- Experimental considerations: in Land Disposal of Hazardous Waste, Proceedings of the Eleventh Annual Research Symposium, EPA/600/9-85/013, pp. 169-177.
- Snow, D.T., 1969, Anisotropic permeability of fractured media: Water Resources Research, Vol. 5, pp. 1273-1289.
- Stephenson, G. R., and Freeze, R.A., 1974, Mathematical simulation of subsurface flow contributions to snowmelt runoff, Reynolds Creek, Idaho: Water Resources Research, Vol. 10, No. 2, April.
- Streltsova, T.D., 1976, Hydrodynamics of groundwater flow in a fractured formation: Water Resources Research, Vol. 12, No. 3, pp. 405-414.
- Stumm, W. and Morgan, J.J., 1981, Aquatic Chemistry: John Wiley & Sons, New York, pp. 324-325.
- Summers, W.K., and Hargis, L.L., 1984, Hydrogeologic cross-section through Sunshine Valley, Taos County, New Mexico: New Mexico Geological Society Guidebook, 35th Field Conference, Rio Grande Rift, Northern New Mexico, pp. 245-248.
- Vail, S.G., 1987, Geologic evaluation of the Guadalupe Mountain area, Taos County, New Mexico: Report to Molycorp, Inc., Questa Division, March 16, 1987, 9 pages.
- Water Resources Associates, June 1984, Hydrologic and hydrogeologic analysis for the Guadalupe Mountain ground-water discharge plan: Report to Molycorp Inc.
- Winograd, I.J., 1959, Ground-water conditions and geology of Sunshine Valley and western Taos County, New Mexico: State of New Mexico, State Engineer Office, Technical Report No. 12.
- Winograd, I.J., 1985, Commentary on "Hydrogeologic Cross-Section through Sunshine Valley, Taos County, New Mexico" by W.K. Summers and L.L. Hargis: New Mexico Geology, vol. 7, no. 3. pp. 54-56.

APPENDIX A

GEOLOGIC AND COMPLETION LOGS
GUADALUPE MOUNTAIN
AREA WELLS

APPENDIX A

TABLE OF CONTENTS

	<u>Page</u>
A.1 Well Completion Diagram - Guadalupe No. 1	A-1
Core Log - Guadalupe No. 1 Test Hole	A-2
Core Log - Guadalupe No. 2 Test Hole (Abandoned)	A-6
A.2 Well Completion Diagram - Guadalupe No. 3	A-8
Core Log - Guadalupe No. 3 Test Hole	A-9
A.3 Guadalupe Mountain Area Well Data	A-11

Client MolyCorp

Job No. 14300-002-33

A.1 WELL COMPLETION DIAGRAM

Well Number Guadalupe #1 (G#1)

Geologist Michael Matheson

Project Guadalupe Mtn. Tailings Site

Driller Longyear - Phoenix

Aquifer Basalt/Andesite

Date of Installation 6-85

Static Water Level 786 feet

Hole Depth 1011.5

Stickup 0

Depth

Protective Casing to Total

Well Casing 0 to 780' Total 780'

Top Seal

 from to

 from to

Hole Diameter 3.7 inch

Casing Diameter 3.5 inch O.D.

Well Casing Depth 780 feet - HQ rods

Screen Diameter N/A

Screen Depth N/A

Centralizers N/A

Pump Type None

Pump Capacity N/A

Average Pumping N/A

Remarks Hole is open below 780 feet.

Hole has been back filled with clean

silica sand to 838 feet. Fifty foot

aquifer test section left open.

clean silica sand
to 838'

HQ core rods
@ 780'

T.D. 1011.5'

<u>FEET</u>	<u>DESCRIPTION</u>
0-29	SILTY SAND, Lt. Brown, some clay, very little to no gravel, minor caliche from 19' - 29'.
29-60	ANDESITE, Lt. Grey, slightly to moderately vesicular, most fractures lo angle (0-30°), a few high angle fractures (60°-90°), fractures partially filled with clay, good RQD*, some flow drag folds at base.
60-86	ANDESITE, Lt. Grey, slightly vesicular, mostly moderate angle fractures (30°-60°), a few high angle fractures, fractures partially filled with clay, good to fair RQD, poor RQD 68'-70'.
86-99	ANDESITE, Lt. Grey, very slightly vesicular, highly fractured, lo and high angle, mostly lo angle, fractures partially filled with clay, poor RQD.
99-100	SANDY CLAY, Lt. Brown, interbed-paleosol, minor amounts of volcanic gravel, moderate consolidation.
100-137	BASALT, Dk. Grey to Black, slightly to moderate vesicular, weak-highly fractured, mostly moderate and high angle fractures, some fractures clay filled, some lo angle fractures, fair to poor RQD.
137-148	ANDESITE, Lt. Gry, dense, lo to high angle fractures, a little clay filling in fractures, some fractures filled with calcite, good RQD.
148-158	ANDESITE, similar to above with some vesicles.
158-192	ANDESITE, Lt. Grey, dense, very few vesicles, a few high angle fractures-healed with calcite, a few moderate angle fractures with minor clay infilling, very good RQD.
192-202	BASALT, Red/Brown, weathered, vesicular, weak-highly fractured, some clay pervasive, poor RQD.
202-208	BASALT, Grey/Black, un-weathered portion of overlying unit, moderately vesicular, moderate angle fractures with some clay infilling, good RQD.
208-264	ANDESITE/BASALT, Grey, vesicular (large vesicles), many high angle fractures, rubble zone (217'-218') heavily clay infilled, fair to good RQD, improving RQD from 218' on, extremely vesicular from 244' to 254' with more moderate angle fracturing.
264-298	ANDESITE, Lt. Grey, moderately vesicular, dense, a few moderate and high angle fractures with moderate clay infilling, very good RQD.

*RQD - Rock Quality Determinate

FEETDESCRIPTION

298-301	BASALT, Red/Brown, vesicular, weathered, highly fractured with some clay infilling, mostly moderate and high angle fractures.
301-336	ANDESITE, Grey, moderately to highly vesicular, dense, mostly lo and moderate angle fractures, a few high angle fractures, minor clay infilling, drag folds at base, good RQD, somewhat more fractured from 328'-332'.
336-353	ANDESITE, Lt. Grey, very vesicular at top to much less so at base, dense, moderate angle fractures, moderate clay infilling, very good RQD.
353-359	BASALT, Red/Black, very weathered, highly fractured at all angles, 90% to 100% infilling of fractures with clay.
359-369	BASALT, Black, un-weathered base of above, vesicular, some high and moderate angle fractures, 90% to 100% infilling of fractures with clay, 367'-369' highly fractured with very heavy clay infill.
369-405	ANDESITE, Lt. Grey, moderately vesicular, large elongate vesicles, dense, mostly moderate and high angle fractures, moderate clay infill, 393'-400' somewhat more fractured and clay infilled, moderate to good RQD.
405-413	BASALT, Red/Brown, highly fractured at all angles, very weathered, moderate to minor clay infill, minor mineralization (siderite?), somewhat less fractured and weathered at base.
413-435	ANDESITE, Grey, minor to no vesicles, mostly lo and high angle fractures, moderate clay infilling, more vesicles and fractures at base, good RQD. Base of relatively good quality rock (upper zone).
435-437	BASALT, Black, moderately weathered, moderately to highly fractured, mostly moderate angle fractures, moderate to heavy clay infilling.
437-439	SILTY CLAY, Lt. Orange, interbed-plaeosol, moderate amounts of volcanic gravel, moderately consolidated, overlain by 6" of silicic tuff, dense/soft.
439-467	BASALT/ANDESITE, Grey, slightly to moderately vesicular, highly fractured at all angles, minor clay infilling, moderate to very poor RQD.
467-489	ANDESITE, Lt. Grey, minor to no vesicles, highly fractured, mostly moderate to high angle fractures, moderate to heavy clay infilling, some fractures 100% filled.
489-500	BRECCIA, angular volcanics in Lt. Grey clay matrix, clast to matrix supported, clasts range from .25" to 1.0", probably tight in-situ.

<u>FEET</u>	<u>DESCRIPTION</u>
500-507	ANDESITE, Dk. Grey, dense, some healed moderate angle fractures, a few only partially filled with clay, 502'-503' highly fractured and clay filled, good RQD in general.
507-532	BRECCIA, angular to sub-angular volcanics in grey to brown clay matrix, clast to matrix supported, clasts range from .25" to 3.0".
532-540	BASALT, Dk. Grey, slightly vesicular, moderately fractured, mostly lo and high angle fractures, moderate to heavy clay infilling, 534'-536' highly fractured and clay infilled.
540-567	BRECCIA, very similar to previous, clasts range from .25" to 2.0", larger clasts appear to dominate, some large clasts refractured with heavy clay infilling.
567-587	ANDESITE, Lt. Grey, moderately vesicular, large vesicles in middle portion, moderately fractured, mostly moderate and high angle fractures, 90% of fractures 100% healed with clay or orthoclase (567'-570'), good RQD in general.
587-644	BRECCIA, similar to previous, clasts range from .25" to 3.0", moderate size clasts dominate, angular to sub-rounded, some open vugs filled with laminated clays, some large clasts refractured and clay filled.
	Base of middle zone
644-677	CINDERS, Black, loose to semi-consolidated, bedded at 30-50, gamma log shows as radioactive.
677-708	BASALT, Black, scoriaceous to very vesicular, very highly fractured, little to no clay infilling, mostly high angle splinter fractures, scoria towards top-vesicular towards base, fair RQD in mid-portion (695'-702').
708-713	BRECCIA, similar to previous, highly weathered good Po and K, clasts range <.25"-.75", clay-volcanic sand matrix.
713-722	ANDESITE/BASALT, Dk. Grey, slightly vesicular, moderately fractured, mostly moderate angle fractures, fractures healed with calcite or open.
722-725	BRECCIA, similar to previous, clasts range from <.25" - 3.0", clay/sand matrix.
725-775	SCORIACIOUS BASALT and CINDERS, interbedded, highly to moderately fractured, moderately to highly weathered, mostly moderate and high angle fractures, minor clay infilling, RQD is generally poor, more cinders towards base.

FEETDESCRIPTION

775-794	ANDESITE/BASALT, Dk. Grey, highly to moderately fractured, moderate to some heavy weathering, mostly moderate and high angle fractures, minimal clay infilling, middle portion very vesicular to scoriaceous.
794-813	BASALT, Black, very vesicular to scoriaceous, highly fractured, mostly moderate angle fractures, some high and low angle, slight to moderate clay infilling, fair RQD in places.
813-825	CINDERS, Black, fair to good consolidation.
825-832	ANDESITE, Grey, moderately fractured, some clay infilling, mostly moderate and high angle fractures, dense-no vesicles, 70% of fractures 100% healed with clay or calcite, fair RQD.
832-837	BRECCIA, similar to previous, clasts range from .25"-6", matrix supported, sandy clay matrix.
837-855	RHYOLITE, Pinkish, slightly to non-vesicular, moderately fractured, mostly moderate and high angle fractures, minor to moderate clay infilling, more vesicular towards base, fair RQD.
855-858	CLAYEY SAND, Tan, well consolidated, paleosol (?), moderately weathered, some volcanic gravel, perhaps a weathered tuff.
858-866	TUFF, Tan, highly weathered, moderately fractured, moderate to heavy clay infilling, dense.
866-890	ANDESITE, Lt. Grey, slightly to moderately vesicular, highly to moderately fractured, mostly moderate and high angle fractures, a few fractures healed with clay infill, mostly minor clay infilling.
890-956	BASALT, Black, highly vesicular to scoriaceous, large vesicles, highly to moderately fractured, mostly low and high angle fractures, minor clay infilling, moderately weathered towards top, very broken and weathered from 908'-915' and 921'-940'.
956-960	ANDESITE, Lt. Grey, dense, very slightly vesicular, a few moderate and high angle fractures with minor clay infilling, good RQD.
960-994	BASALT, Black, highly vesicular to scoriaceous, moderately weathered, more scoria and weathering towards top, moderately to highly fractured, minor clay infilling, fair RQD in middle portions.
994-1011 TD	ANDESITE, Lt. Grey, slightly vesicular, moderately fractured, mostly moderate angle fractures with minor to moderate clay infilling, a few large vesicles, fair to moderate RQD.

<u>FEET</u>	<u>DESCRIPTION</u>
0-40	CONGLOMERATIC SILTY SAND, Lt. Brown, 15%-20% weathered gravel, subangular to angular, 30% silt with clay, 50% fine to coarse sand, poorly sorted, very minor induration, increasing sand and gravel content with depth, no apparent bedding.
40-134	BRECCIA, Dark Red to Brown, 30%-40% gravel, subangular to angular, 60%-70% fine to coarse sand, all material is mafic volcanic, moderate to poor sorting, mostly matrix supported, poorly to well indurated, fryable when shocked, mostly moderately indurated, apparent flow bedding, surge breccia (?), probably few open fractures in-situ.
134-215	ANDESITE, Lt. Grey, xenolithic (vesicular basalt), slightly vesicular, moderately well-fractured at mostly high and moderate angles, minor to moderate infilling of fractures with carbonate, fractures decrease with depth to 180' then increase sharply to 215'.
215-394	BRECCIA, Red Brown to Brown, 30%-50% fine to coarse gravel, subangular to angular, 70%-50% fine to coarse sand, material is mafic volcanic, moderate to poor sorting, mostly matrix-supported, poorly to well indurated, mostly moderately indurated, minor flow bedding, colluvial to some surge breccia (?), probably few open fractures in-situ, little variation through the interval.
394-440	ANDESITE, Lt. Grey, slightly to non-vesiculated, highly fractured at all angles, mostly low and moderate angles, 70% of fractures filled with clay weathering products and carbonate, fracturing relatively constant over the interval.
440-454	BRECCIA, Grey, 70% fine to coarse gravel, angular, 30% silty sand (matrix); material is andesitic, moderately well indurated, fryable when shocked, mostly clast-supported, fracture breccia (?), probably few open fractures in-situ.
454-594	ANDESITE, Lt. Grey, slightly to non-vesiculated, moderately to highly fractured at mostly moderate and high angles, some minor infilling of fractures with clay weathering product and carbonate; most fractures are open; fracturing and lithology are constant over the interval; no obvious flow breaks.
594-600	BRECCIA, Grey, 80% fine to coarse gravel, angular, 20% silty sand (matrix); material is andesite, poorly indurated, fryable when shocked, clast-supported, fracture breccia (?), a few open fractures.
600-618	ANDESITE, Lt. Grey, slightly vesiculated, moderately to highly fractured at all angles, mostly moderate and high angles, minor infilling of fractures with clay weathering products; most fractures are open; fracturing and lithology are constant over the interval.

CORE LOG - GUADALUPE No. 2 TEST HOLE (ABANDONED)

<u>FEET</u>	<u>DESCRIPTION</u>
618-625	BASALT, Dark Red, non-vesicular, very highly fractured at all angles, some infilling of fractures with carbonate, (90%-100% closure), very weak and friable, upper portion of flow.
625-637	BASALT, Dark Red, slightly vesicular, moderately to highly fractured at mostly moderate and high angles, fractures decrease with depth, very minor infilling of fractures, lower portion of flow.
637-653	ANDESITE, Grey, slightly vesicular, highly fractured at mostly high angles, minor infilling of fractures and vesicles with carbonate.
653-660	BRECCIA, Red-Grey, 70% fine to coarse gravel, angular, 30% fine to coarse sand (matrix); material is andesite, moderately indurated, friable when shocked, clast-supported, fracture breccia (?), carbonate cement and infilling in fractures.
660-796	ANDESITE, Lt. Grey, moderately vesicular, moderately to slightly fractured, 90% at high angles, minor to moderate infilling of fractures and vesicles with carbonate; most fractures are open; fracturing and lithology are constant over the interval, no obvious flow breaks.
796-869 TD	BASALT, Red Brown, non-vesicular, slightly weathered, moderately fractured at mostly low and moderate angles, moderate to heavy infilling of fractures with clay weathering products and carbonate, (70%-90% closure); fracturing and lithology are generally constant over the interval; flow breaks at 796', 812', and 839'.

Well Logging Sheet No. 1001, 201 1001

Screen Diameter 8 1/2

Screen Depth 8 1/2

Control Valve 8 1/2

Pump Type None

Pump Capacity 8 1/2

Average Pumping 8 1/2

Remarks Hole is open below 800'

Hole has caved to 400'. Test hole

gulfed test section left open.

Client Molycorp

Job No. 14300-002-33

A.2 WELL COMPLETION DIAGRAM

Well Number Guadalupe #3 (G#3)

Geologist Michael Matheson

Project Guadalupe Mtn. Tailings Site

Driller Longyear - Phoenix

Aquifer Basalt/Andesite

Date of Installation 1/86

Static Water Level 475 feet

Hole Depth 496.0 feet

Stickup 0

Depth

Protective Casing to Total

Well Casing 0 to 440 Total 440

Top Seal

 from to

 from to

Hole Diameter 3.7 inch

Casing Diameter 3.5 inch O. D.

Well Casing Depth 440 feet, HQ rods

Screen Diameter N/A

Screen Depth N/A

Centralizers N/A

Pump Type None

Pump Capacity N/A

Average Pumping N/A

Remarks Hole is open below 440'.

Hole has caved to 486'. Fortysix foot
aquifer test section left open.

HQ core rods

@ 440'

T.D. 496'

<u>FEET</u>	<u>DESCRIPTION</u>
0-11	SANDY SILT, Dark Brown, 65% silt, 30%-25% fine sand, 5%-10% fine gravel, subrounded, poorly indurated, carbonate cement, moderately sorted, increasing coarse fraction with depth.
11-18	ANDESITE, Grey, slightly vesicular, moderately fractured at low and moderate angles, heavy infilling of fractures with silt and clay (80%-100% closure).
18-35	BASALT, Dark Grey/Black, slightly vesicular, very heavily weathered and fractured at all angles, heavy infilling of fractures with weathering product clays (90%-100% closure), upper portion is somewhat brecciated, fractures decrease with depth, upper portion of flow.
35-61	BASALT, Dark Grey/Black, slightly vesicular, moderately to heavily fractured at mostly high angles, minor infilling of fractures with clays (10%-20% closure), fractures decrease with depth, lower portion of flow.
61-79	BASALT, Black, moderately vesicular, highly fractured at mostly moderate angles, moderately weathered, friable, minor clay infilling, fracture and lithology constant over the interval.
79-90	BASALT, Red Brown, slightly to non-vesicular, moderately fractured at mostly low angles, heavily weathered, particularly 83'-86', heavy infilling of fractures with clays, extensive rock decay (soft).
90-120	ANDESITE, Lt. Grey, non-vesicular, highly fractured at a consistent 50-degree angle throughout the interval, very minor infilling of fractures with clay; fracturing and lithology are constant over the interval.
120-158	BASALT, Dark Grey/Black, moderately vesicular, highly fractured at all angles, heavy weathering and rock decay (soft) throughout interval, very heavy infilling of fractures with clay from 145'-151', minor infilling for the rest of the interval.
158-190	BASALT, Dark Grey/Black, moderately vesicular, highly fractured at mostly low and moderate angles, minor infilling of fractures with clays, heavily weathered and decayed from 179'-190'.
190-200	ANDESITE, Lt. Grey, moderately vesicular, moderately fractured at mostly high angles, very minor infilling of fractures; middle of interval is more fractured than the top and bottom.
200-235	BASALT, Black, moderately well vesiculated, highly fractured at mostly high angles, moderate infilling of fractures with clays (50% closure), moderately weathered and decayed from 221'-223'.

<u>FEET</u>	<u>DESCRIPTION</u>
235-335	BASALT, Black, very well vesiculated (some interconnected), moderately fractured at mostly moderate and high angles, very heavy infilling of fractures with clays (90%-100% closure), fracturing, infilling and lithology fairly constant throughout the interval, some minor brecciation from 315'-322'.
335-358	BRECCIA, Dark Grey/Black, 70% fine to coarse gravel, angular, 30% silty sand (matrix); all material is basalt, clast-supported, poorly sorted, moderately well indurated; fractures are closed with weathering product clays.
358-371	ANDESITE, Lt. Grey, slightly vesicular, highly fractured at all angles, mostly moderate and high angles, very minor infilling of fractures with clays; fracturing and lithology are fairly constant throughout the interval.
371-378	BRECCIA, Dark Brown/Black, 60% fine to coarse gravel, angular 40% fine to coarse sand (matrix); material is basalt/andesite, clast-supported, poorly sorted, moderately to poorly indurated.
378-386	ANDESITE, Dark Grey, very slightly vesicular, highly fractured at all angles, very minor clay infilling of fractures.
386-415	BRECCIA, Brown/Grey, 80% fine to coarse gravel and cobbles, angular, 20% silty sand (matrix); clasts are basalt/andesite, clast-supported, very poorly sorted, poor to fair induration; secondary fractures are weathering product clay-filled; clast size increases with depth.
415-496 TD	ANDESITE, Lt. Grey, very slightly vesicular, moderately fractured at mostly high and moderate angles, minor infilling of fractures with clay (<10% closure); fracturing and lithology are fairly constant throughout the interval.

A.3 Guadalupe Mountain Area
Well Data

Location	Owner	Depth	Diam.	Elev.	Perf. Interval	Water Level		Use	Remarks
						Static	Date		
BLM - Headquarters	BLM	546 ft.	6 in.	7965.5	513- 536 ft.	7084.1	1/17/86	Potable Water	30 GPM rated, sound- ing tube installed
BLM - Chiflo Campground	BLM	415 ft.	6 in.	7492.7	391- 410 ft.	7149.4	1/17/86	Potable Water	30 GPM rated, sound- ing tube installed
CE - 1	Corp of Engineers	735 ft.	2 in.	7855.9	UNK	7159.4	1/17/86	Test Hole	
G - 1	Molycorp	1011 ft.	3.5 in.	7939.9	780- 838 ft. (open hole)	7154.4	1/17/86	Test Hole	
G - 3	Molycorp	496 ft.	3.5 in.	7626.5	440- 496 ft. (open hole)	7151.5	1/17/86	Test Hole	

APPENDIX B

GRAPHIC SOLUTIONS OF
GROUND-WATER FLOW
DIRECTION AND GRADIENT

APPENDIX B

GRAPHS OF ATTITUDE OF WATER TABLE
AND
DIRECTION OF FLOW

GUADALUPE MOUNTAIN AREA

Figure B-1 Flow Direction S 30° W, Gradient 0.0037
Figure B-2 Flow Direction S 26° W, Gradient 0.0035
Figure B-3 Flow Direction S 34° W, Gradient 0.0035
Figure B-4 Flow Direction S 4° E, Gradient 0.0042
Figure B-5 Flow Direction S 32° W, Gradient 0.016
Figure B-6 Flow Direction S 21° W, Gradient 0.017
Figure B-7 Flow Direction N 64° W, Gradient 0.093
Figure B-8 Flow Direction S 38° W, Gradient 0.014

* - - - - -

Figure B-11 Flow Direction S 26° W, Gradient 0.0034
Figure B-12 Flow Direction S 24° W, Gradient 0.0037
Figure B-13 Flow Direction S 30° W, Gradient 0.0035

CONFLUENCE AREA

*Figure B-9 Flow Direction S 87° W, Gradient 0.072
Figure B-10 Flow Direction S 7° E, Gradient 0.068

BLM-CHIFLO
7149.4 FEET

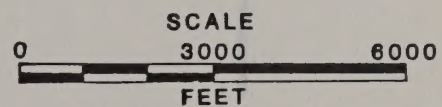
GUADALUPE NO. 3
7151.5 FEET

BLM-HQ
7084.1 FEET

NOTE: ELEVATIONS ARE THAT OF THE WATER
TABLE ABOVE SEA LEVEL TAKEN 1/17/86

GRAPH OF
ATTITUDE OF WATER TABLE
AND DIRECTION OF FLOW
(FLOW DIRECTION S30°W
GRADIENT 0.0037)
GUADALUPE MOUNTAIN AREA

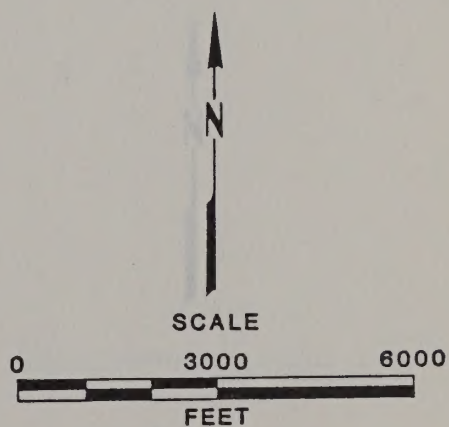
Figure B-1



BLM-CHIFLO
7149.4 FEET

GUADALUPE NO.1
7153.5 FEET

BLM-HQ
7084.1 FEET



GRAPH OF ATTITUDE OF WATER TABLE AND DIRECTION OF FLOW

(FLOW DIRECTION S26°W
GRADIENT 0.0035)

GUADALUPE MOUNTAIN AREA

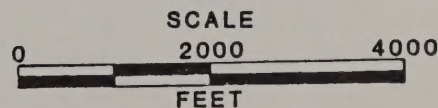
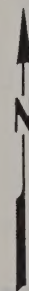
Figure B-2

NOTE: ELEVATIONS ARE THAT OF THE WATER
TABLE ABOVE SEA LEVEL TAKEN 1/17/86

GUADALUPE NO. 1
7153.5 FEET

GUADALUPE NO. 3
7151.5 FEET

BLM-HQ
7084.1 FEET



NOTE: ELEVATIONS ARE THAT OF THE WATER
TABLE ABOVE SEA LEVEL TAKEN 1/17/86

GRAPH OF
ATTITUDE OF WATER TABLE
AND DIRECTION OF FLOW
(FLOW DIRECTION S34°W
GRADIENT 0.0035)
GUADALUPE MOUNTAIN AREA

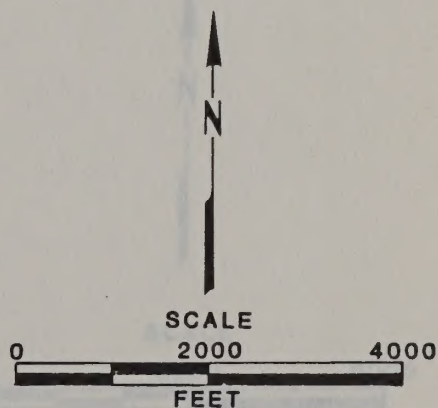
Figure B-3

CE-1
7159.4 FEET

GUADALUPE NO. 1
7153.5 FEET

GUADALUPE NO. 2
7151.6 FEET

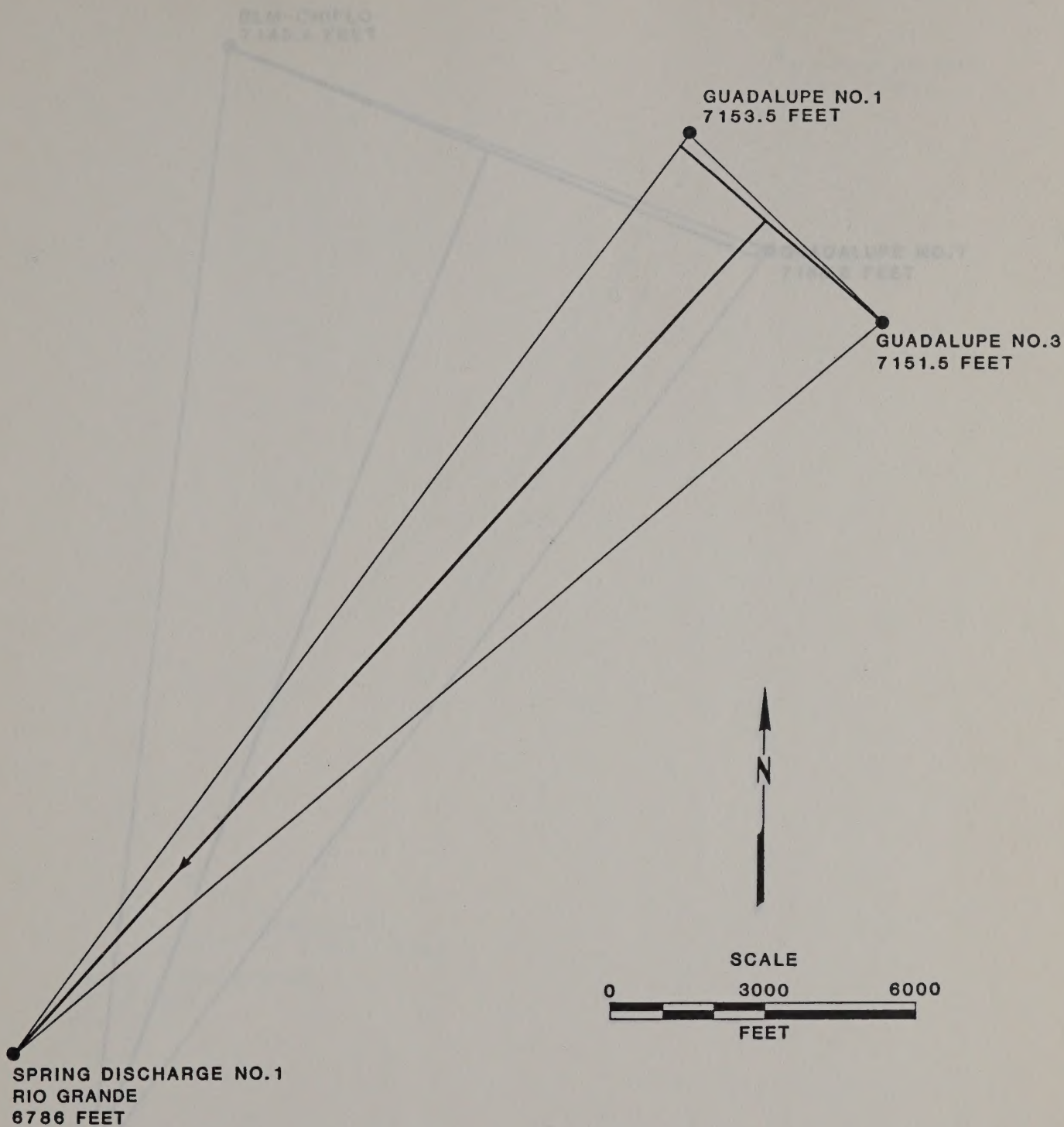
BLM-HQ
7084.1 FEET



GRAPH OF
ATTITUDE OF WATER TABLE
AND DIRECTION OF FLOW
(FLOW DIRECTION S4°E
GRADIENT 0.0042)
GUADALUPE MOUNTAIN AREA

NOTE: ELEVATIONS ARE THAT OF THE WATER
TABLE ABOVE SEA LEVEL TAKEN 1/17/86

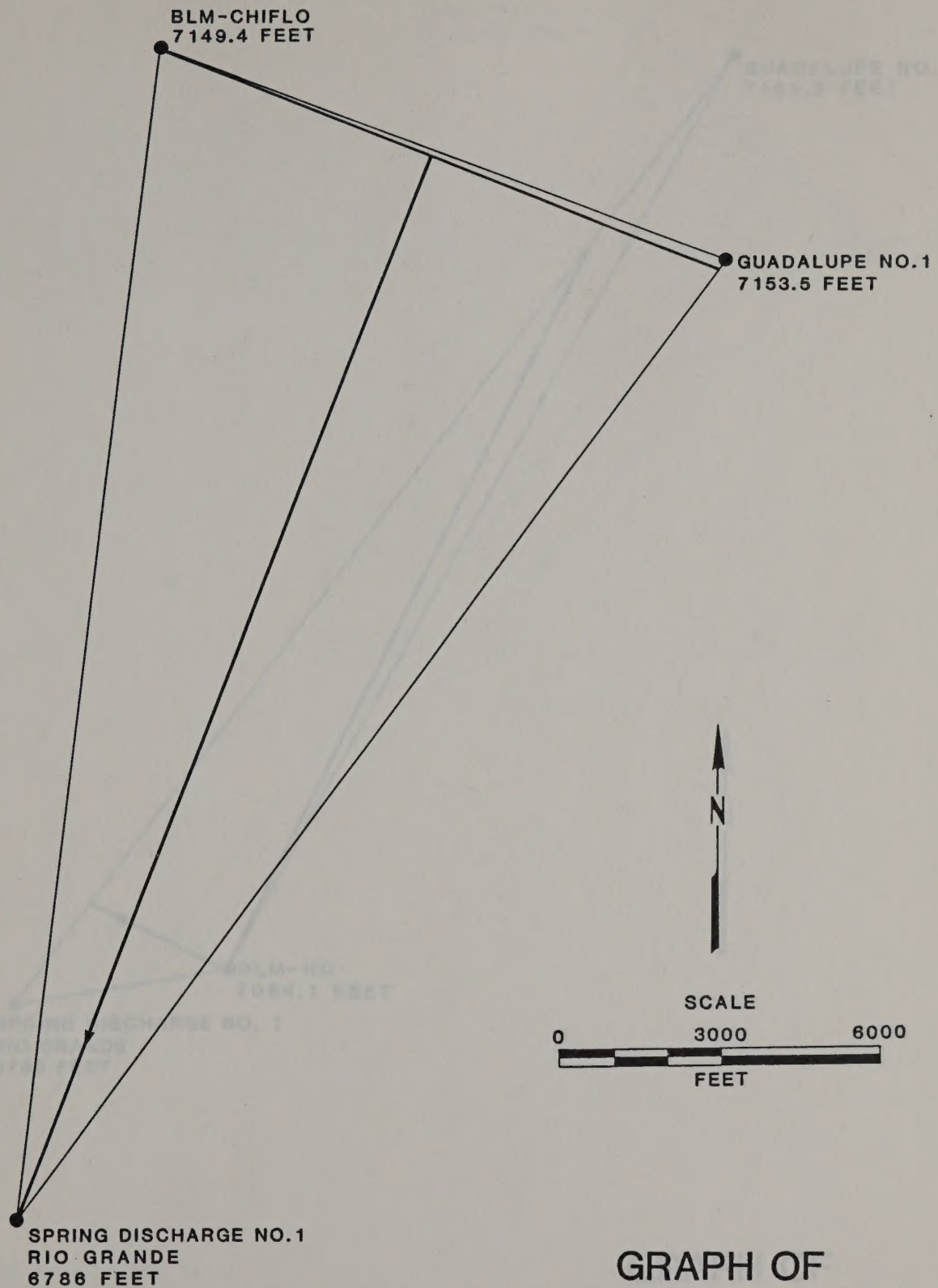
Figure B-4



GRAPH OF
ATTITUDE OF WATER TABLE
AND DIRECTION OF FLOW
(FLOW DIRECTION S32°W
GRADIENT 0.016)
GUADALUPE MOUNTAIN AREA

Figure B-5

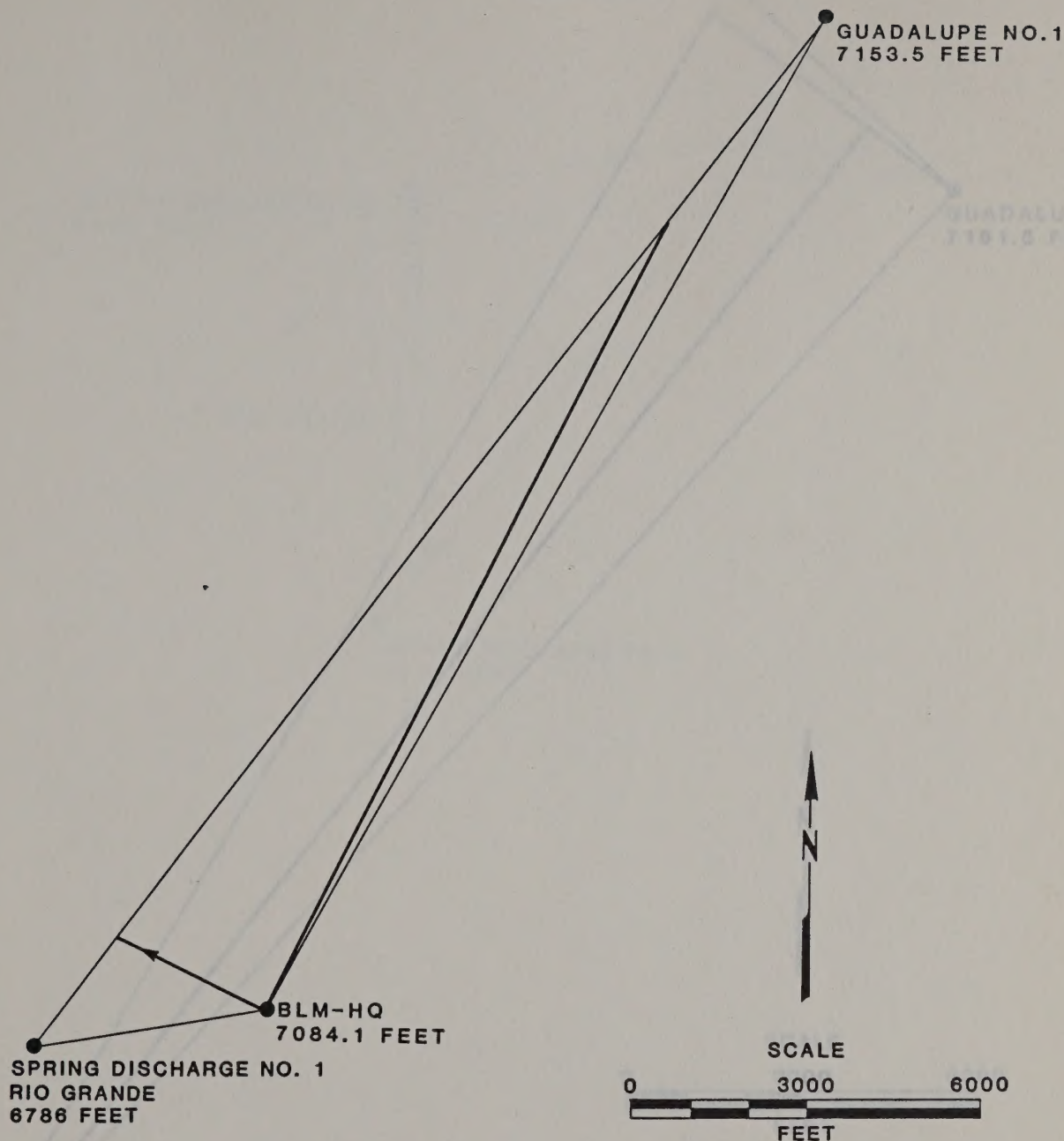
NOTE: ELEVATIONS ARE THAT OF THE WATER
TABLE ABOVE SEA LEVEL TAKEN 1/17/86



GRAPH OF
ATTITUDE OF WATER TABLE
AND DIRECTION OF FLOW
(FLOW DIRECTION S21°W
GRADIENT 0.017)
GUADALUPE MOUNTAIN AREA

Figure B-6

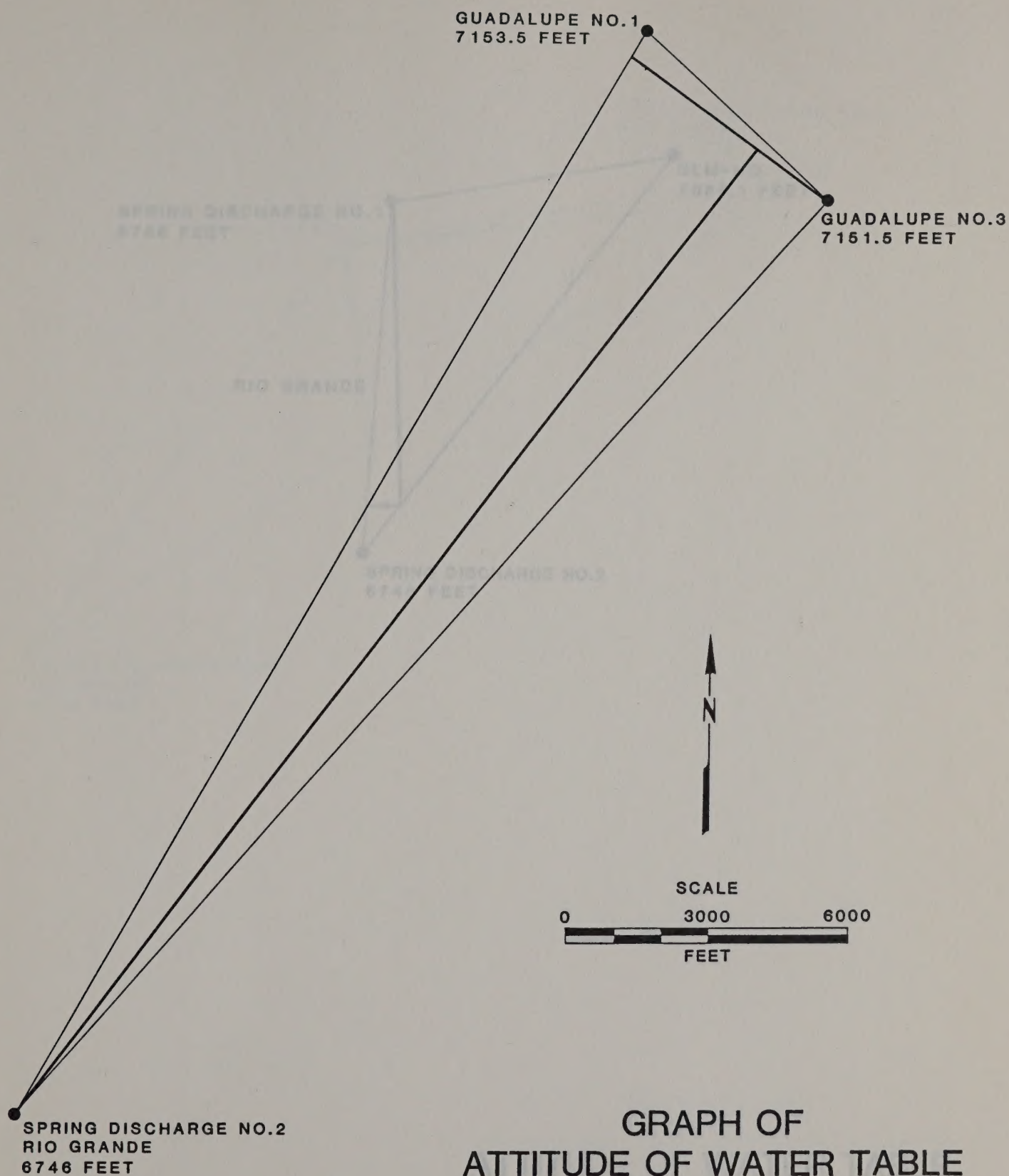
NOTE: ELEVATIONS ARE THAT OF THE WATER
TABLE ABOVE SEA LEVEL TAKEN 1/17/86



GRAPH OF
ATTITUDE OF WATER TABLE
AND DIRECTION OF FLOW
(FLOW DIRECTION $N64^{\circ}W$
GRADIENT 0.093)
GUADALUPE MOUNTAIN AREA

Figure B-7

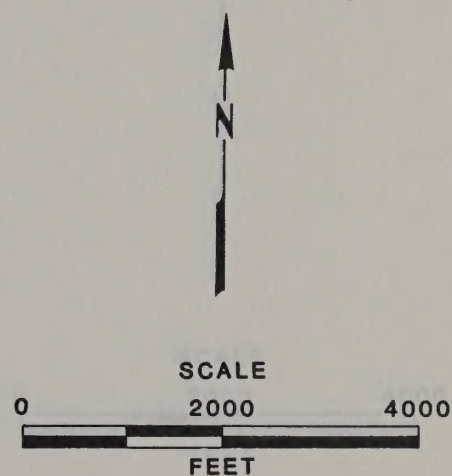
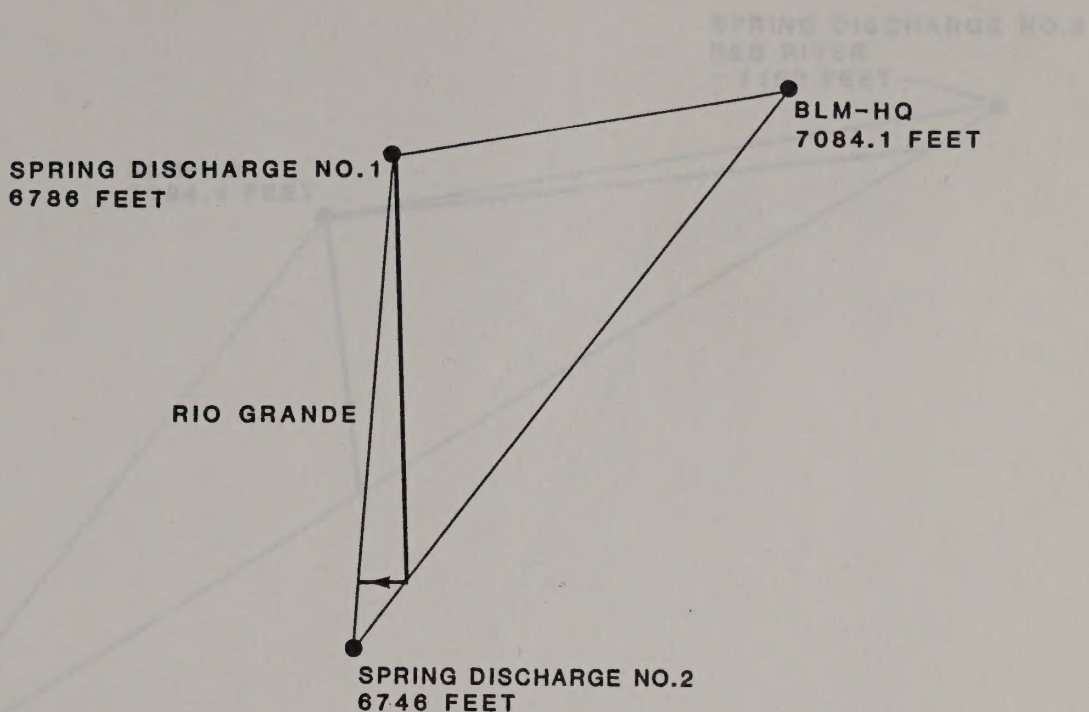
NOTE: ELEVATIONS ARE THAT OF THE WATER
TABLE ABOVE SEA LEVEL TAKEN 1/17/86



GRAPH OF
ATTITUDE OF WATER TABLE
AND DIRECTION OF FLOW
(FLOW DIRECTION S38°W
GRADIENT 0.014)
GUADALUPE MOUNTAIN AREA

Figure B-8

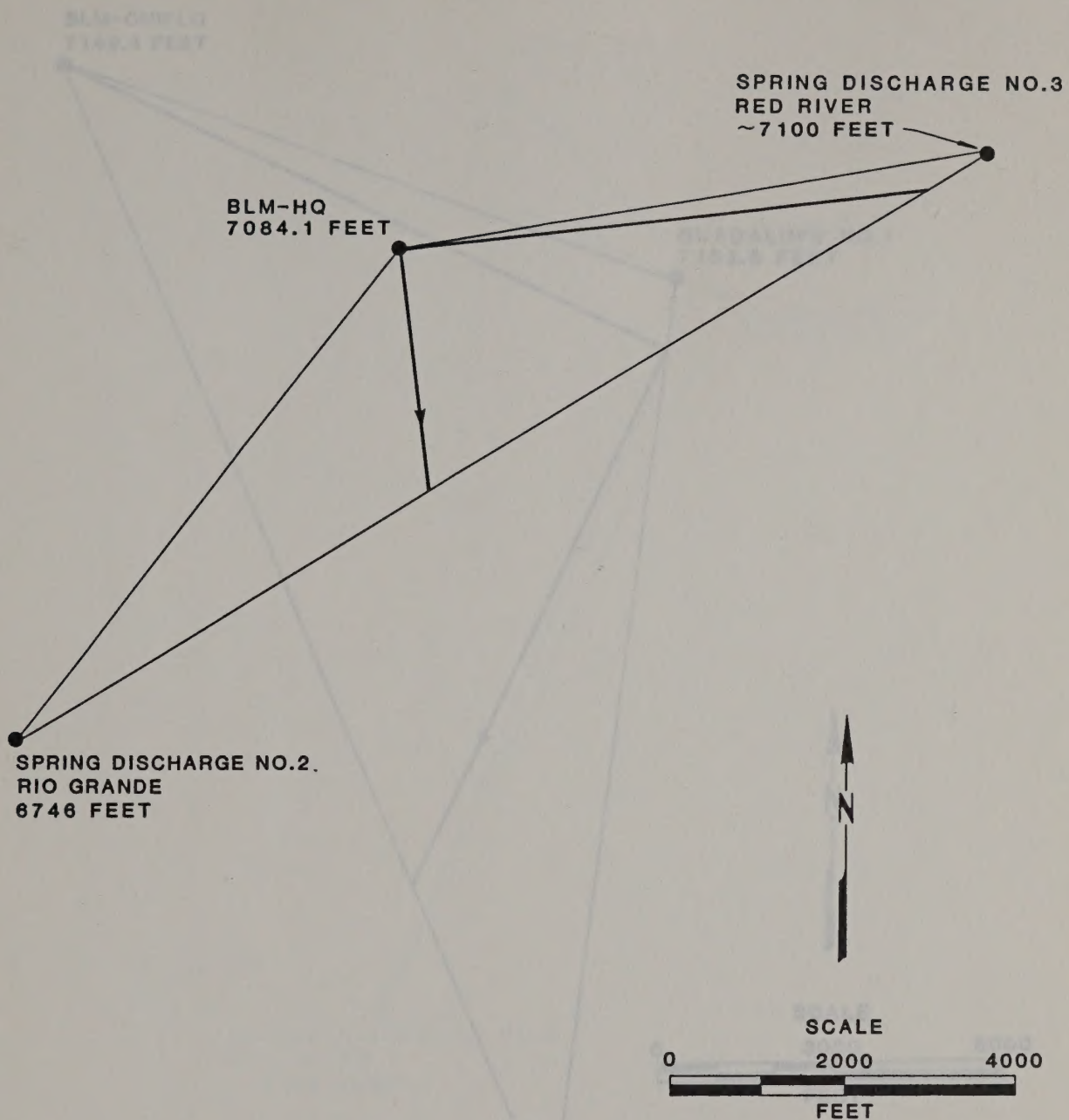
NOTE: ELEVATIONS ARE THAT OF THE WATER
TABLE ABOVE SEA LEVEL TAKEN 1/17/86



GRAPH OF
ATTITUDE OF WATER TABLE
AND DIRECTION OF FLOW
(FLOW DIRECTION S87°W
GRADIENT 0.072)
CONFLUENCE AREA

NOTE: ELEVATIONS ARE THAT OF THE WATER
TABLE ABOVE SEA LEVEL TAKEN 1/17/86

Figure B-9



**GRAPH OF
ATTITUDE OF WATER TABLE
AND DIRECTION OF FLOW
(FLOW DIRECTION S7° E
GRADIENT 0.068)
CONFLUENCE AREA**

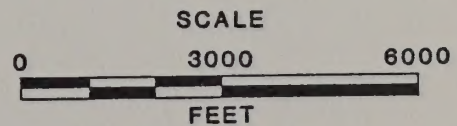
Figure B-10

NOTE: ELEVATIONS ARE THAT OF THE WATER
TABLE ABOVE SEA LEVEL TAKEN 1/17/86

BLM-CHIFLO
7149.4 FEET

GUADALUPE NO.1
7153.5 FEET

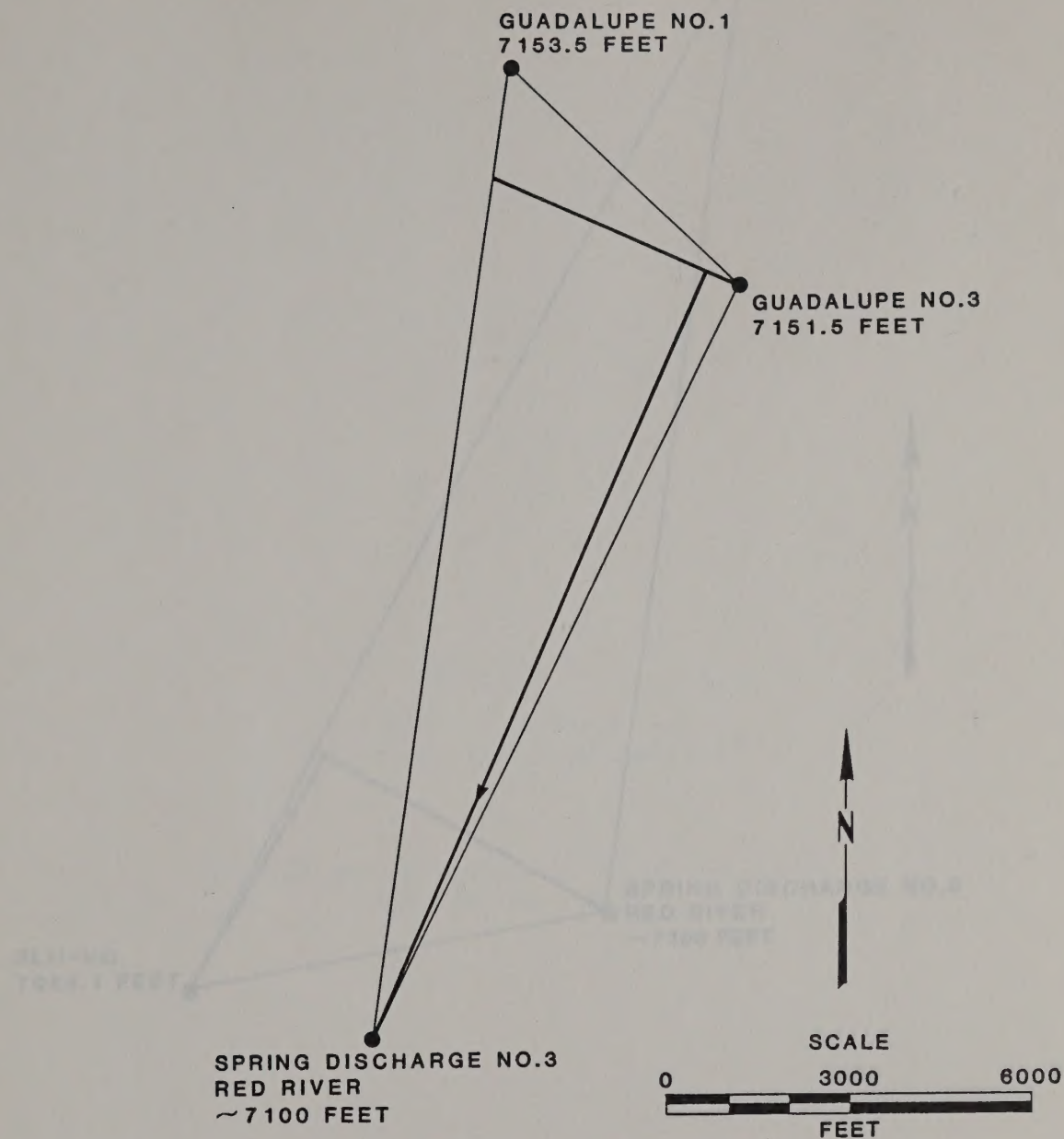
SPRING DISCHARGE NO.3
RED RIVER
~ 7100 FEET



GRAPH OF
ATTITUDE OF WATER TABLE
AND DIRECTION OF FLOW
(FLOW DIRECTION S26°W
GRADIENT 0.0034)
GUADALUPE MOUNTAIN AREA

Figure B-11

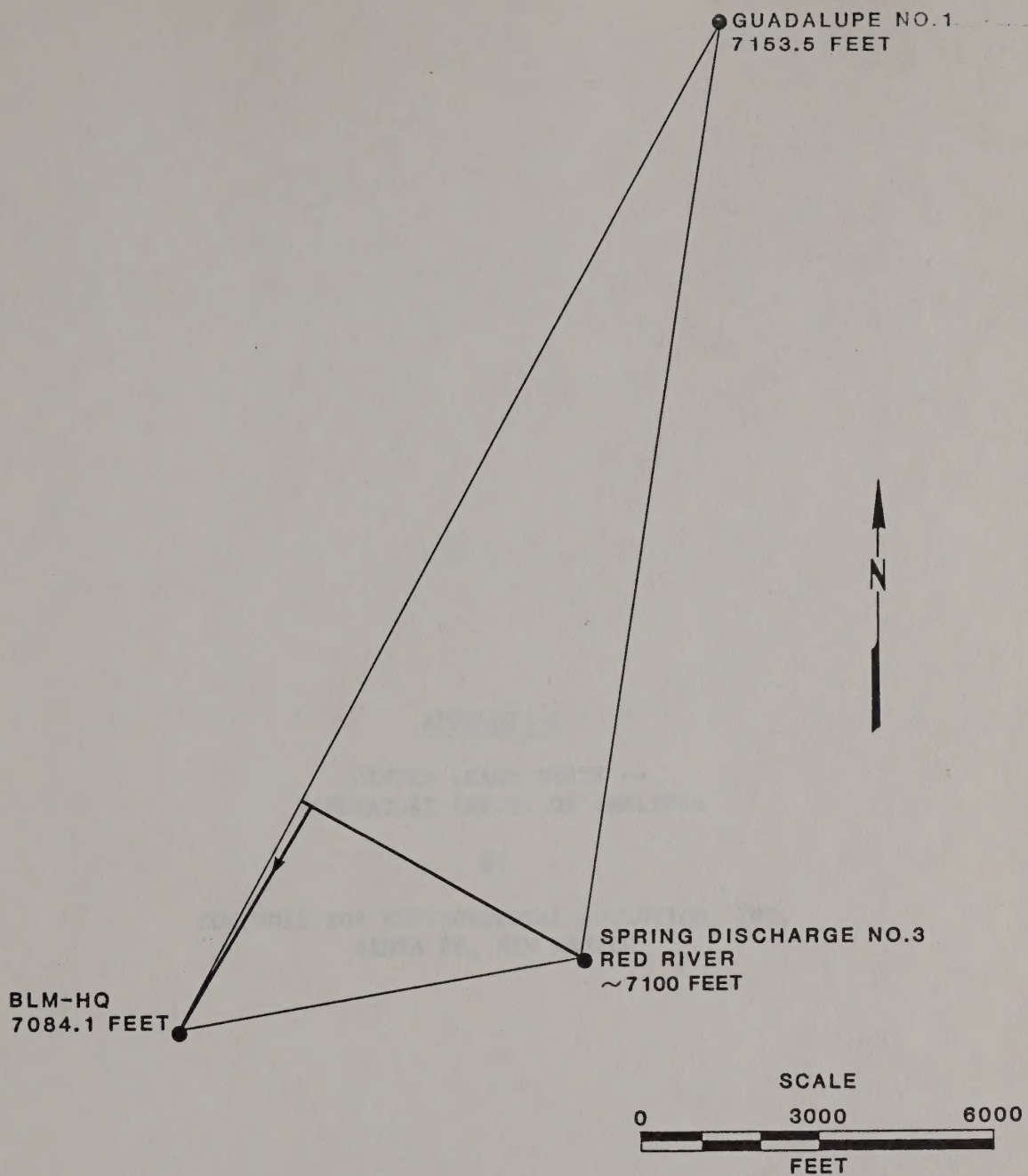
NOTE: ELEVATIONS ARE THAT OF THE WATER
TABLE ABOVE SEA LEVEL TAKEN 1/17/86



GRAPH OF
ATTITUDE OF WATER TABLE
AND DIRECTION OF FLOW
(FLOW DIRECTION S24°W
GRADIENT 0.0037)
GUADALUPE MOUNTAIN AREA

NOTE: ELEVATIONS ARE THAT OF THE WATER
TABLE ABOVE SEA LEVEL TAKEN 1/17/86

Figure B-12



GRAPH OF
ATTITUDE OF WATER TABLE
AND DIRECTION OF FLOW
(FLOW DIRECTION $S30^{\circ}W$
GRADIENT 0.0035)
GUADALUPE MOUNTAIN AREA

NOTE: ELEVATIONS ARE THAT OF THE WATER
TABLE ABOVE SEA LEVEL TAKEN 1/17/86

Figure B-13

APPENDIX C

CINDER LEACH TESTS --
LABORATORY REPORT OF ANALYSES

BY

CONTROLS FOR ENVIRONMENTAL POLLUTION, INC.
SANTA FE, NEW MEXICO

APPENDIX C

TABLE OF CONTENTS

	<u>Page</u>
C.1 LEACHING PROCEDURE	C-1
C.2 SCHEDULE OF TREATMENTS	C-1
REPORTS OF ANALYSES	(6 pages)

The liquid will be mixed with the solid sample to obtain a solution: solid ratio of 20:1. The charged mixing bottom reactor, such as polyethylene, or glass will be tumbled for a one week period. The rpm of the mixing bottles will be noted and recorded as data. A daily temperature in the mixing area should be recorded. The solution pH at beginning and end of leaching process should be recorded.

Following the mixing period, the mixture will be allowed to settle. The supernatant will be prefiltered and then filtered with a 0.45 μ m filter membrane. The filtrate is then subjected to analysis.

C.2 Schedule of Treatments

- 1) Cinders leached with distilled deionized water; filtered to 0.45 μ m with filter membrane; filtrate to counter.
- 2) Cinders leached with slurry liquor; filtered with 0.45 μ m membrane; filtrate to counter.
- 3) Cinders leached with pond leachate; filtered with 0.45 μ m membrane; filtrate to counter.
- 4) Bedrock leached with pond leachate; filtered with 0.45 μ m membrane; leach liquor with the filtrate; filter again; extract filtrate to counter.

APPENDIX C

CINDER LEACH TESTS

C.1 Leaching Procedure

Liquids: slurry liquor
Leachate
distilled deionized water

Solids: bedrocks, sand sized
cinders, sand sized

The liquid will be mixed with the solid sample to obtain a solution: solid ratio of 20:1. The capped mixing bottles (plastic, such as polyethylene, or glass) will be tumbled for a one week period. The rpm of the mixing bottles will be noted and recorded as data. A daily temperature in the mixing area should be recorded. The solution ph at beginning and end of leaching process should be recorded.

Following the mixing period, the mixture will be allowed to settle. The supernatant will be prefiltered and then filtered with a 0.45 um filter membrane. The filtrate is then subjected to radioassay.

C.2 Schedule of Treatments

- 1) Cinders leached with distilled deionized water; filtered to 0.45 um with filter membrane; filtrate to counter.
- 2) Cinders leached with slurry liquor; filtered with 0.45 um membrane; filtrate to counter.
- 3) Cinders leached with pond leachate; filtered with 0.45 um membrane, filtrate to counter.
- 4) Bedrock leached with pond leachate; filtered with 0.45 um membrane; leach cinders with the filtrate; filter again; second filtrate to counter.

REPORT OF ANALYSIS

CUSTOMER Dames & Moore
 ADDRESS 3737 North 7th Street - Suite 211
 CITY Phoenix, AZ 85014
 ATTENTION Rebecca Parker
 INVOICE NO. 510308

SAMPLES RECEIVED 10/04/85

CUSTOMER ORDER NUMBER

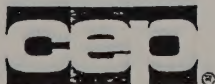
TYPE OF ANALYSIS

Slurry Solution Before Treatment (Filtered through 0.45 micron filter)

Parameter	pCi/l
Gross Alpha	< 2
Gross Beta	7 ± 6
Total Uranium	0.008 mg/l

Sample Type: Condensate before treatment

Parameter	pCi/l
Gross Alpha	0.2
Gross Beta	9.3 ± 0.1
Gross Spectral Analysis	
Radium-226	0.403 ± 0.030
Lead-213	0.349 ± 0.020
Lead-214	0.397 ± 0.018
Actinium-228	0.473 ± 0.011
Thallium-208	1.514 ± 0.014
Bismuth-214	1.020 ± 0.009
Total Uranium	0.17



APPROVED BY

10/30/85 James J. Mueller, President
 PAGE 1 OF 1 PAGE

Controls for Environmental Pollution, Inc.

P.O. Box 5351 • 1925 Rosina • Santa Fe, New Mexico 87502

Telephone 505/982-9841

REPORT OF ANALYSIS

CUSTOMER Dames & Moore
ADDRESS 3737 N. 7th Street, Suite 211
CITY Phoenix, AZ 85014
ATTENTION D.A. Stephenson
INVOICE NO. 509175

SAMPLES RECEIVED

CUSTOMER ORDER NUMBER

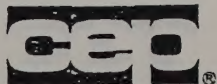
TYPE OF ANALYSIS

Sample Type: Outfall (before treatment)

Parameter	pCi/l
Gross Alpha	4 \pm 2
Gross Beta	6 \pm 1
Gamma Spectral Analysis	
Radium-226	4.09 \pm 0.17
Lead-212	1.86 \pm 0.15
Lead-214	2.73 \pm 0.16
Actinium-228	5.23 \pm 0.29
Thallium-208	1.33 \pm 0.09
pH	6.6 units
	X = 6.6

Sample Type: Cinders (before treatment)

Parameter	pCi/g
Gross Alpha	0.3
Gross Beta	0.3 \pm 0.1
Gamma Spectral Analysis	
Radium-226	0.463 \pm 0.020
Lead-212	0.344 \pm 0.020
Lead-214	0.397 \pm 0.018
Actinium-228	0.678 \pm 0.035
Thallium-208	1.020 \pm 0.064
Bismuth-214	1.020 \pm 0.064
Total Uranium	0.17



APPROVED BY

James J. Mueller, President

9/19/85

PAGE 1 OF 5 PAGE

Controls for Environmental Pollution, Inc.

P.O. Box 5351 • 1925 Rosina • Santa Fe, New Mexico 87502

Telephone 505/982-9841

REPORT OF ANALYSIS

CUSTOMER Dames & Moore
ADDRESS 3737 N. 7th Street, Suite 211
CITY Phoenix, AZ 85014
ATTENTION D.A. Stephenson
INVOICE NO. 509175

SAMPLES RECEIVED

CUSTOMER ORDER NUMBER

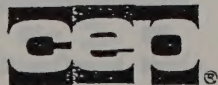
TYPE OF ANALYSIS

Sample Type: Bedrock (before treatment)

Parameter	pCi/g
Gross Alpha	0.9 ± 0.2
Gross Beta	1.2 ± 0.1
Gamma Spectral Analysis	
Radium-226	0.739 ± 0.024
Lead-212	0.491 ± 0.021
Lead-214	0.606 ± 0.022
Actinium-228	1.060 ± 0.040
Thallium-208	0.279 ± 0.013
Bismuth-214	1.460 ± 0.070
Total Uranium	0.55

Sample Type: Slurry (before treatment)

Parameter	pCi/l
Gross Alpha	$1,553 \pm 413$
Gross Beta	$13,982 \pm 337$
Gamma Spectral Analysis	
Radium-226	$1,010 \pm 25$
Lead-212	$1,300 \pm 24$
Lead-214	$1,070 \pm 23$
Actinium-228	$1,490 \pm 41$
Thallium-208	464 ± 13
Bismuth-214	$1,630 \pm 79$
pH	6.6 units



APPROVED BY

James J. Mueller, President

9/19/85

PAGE 2 OF 5 PAGE

Controls for Environmental Pollution, Inc.

P.O. Box 5351 • 1925 Rosina • Santa Fe, New Mexico 87502

Telephone 505/982-9841

REPORT OF ANALYSIS

CUSTOMER Dames & Moore
ADDRESS 3737 N. 7th Street, Suite 211
CITY Phoenix, AZ 85014
ATTENTION D.A. Stephenson
INVOICE NO. 509175

SAMPLES RECEIVED

CUSTOMER ORDER NUMBER

TYPE OF ANALYSIS

Sample Type: Outfall (after treatment with cinders)

Parameter	pCi/l (dissolved)
Gross Alpha	20 ± 1
Gross Beta	6 ± 3
Gamma Spectral Analysis	
Radium-226	4.67 ± 0.19
Lead-212	1.86 ± 0.10
Lead-214	3.07 ± 0.11
Actinium-228	5.88 ± 0.21
Thallium-208	1.53 ± 0.80
Bismuth-214	11.80 ± 0.42
pH	7.7 units
Temperature	24°

Sample Type: Outfall (after treatment with bedrock)

Parameter	pCi/l (dissolved)
Gross Alpha	7 ± 9
Gross Beta	6 ± 3
Gamma Spectral Analysis	
Radium-226	4.19 ± 0.10
Lead-212	1.79 ± 0.08
Lead-214	2.86 ± 0.09
Actinium-228	5.72 ± 0.17
Thallium-208	1.49 ± 0.05
Bismuth-214	10.90 ± 0.34
pH	7.9 units
Temperature	24°



APPROVED BY

James J. Mueller, President

9/19/85 PAGE 3 OF 5 PAGE

Controls for Environmental Pollution, Inc.

P.O. Box 5351 • 1925 Rosina • Santa Fe, New Mexico 87502

Telephone 505/562-3841

REPORT OF ANALYSIS

CUSTOMER Dames & Moore
 ADDRESS 3737 N. 7th Street, Suite 211
 CITY Phoenix, AZ 85014
 ATTENTION D.A. Stephenson
 INVOICE NO. 509175

SAMPLES RECEIVED

CUSTOMER ORDER NUMBER

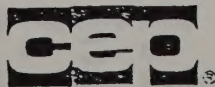
TYPE OF ANALYSIS

Sample Type: Slurry (after treatment with cinders)

Parameter	pCi/l (dissolved)
Gross Alpha	18 ± 11
Gross Beta	39 ± 4
Gamma Spectral Analysis	
Radium-226	2.77 ± 0.11
Lead-212	1.09 ± 0.07
Lead-214	1.85 ± 0.08
Actinium-228	3.69 ± 0.15
Thallium-208	0.89 ± 0.04
Bismuth-214	7.46 ± 0.37
pH	7.3 units
Temperature	25°

Sample Type: Outfall (after treatment with bedrock and cinders)

Parameter	pCi/l
Gross Alpha	18 ± 10
Gross Beta	14 ± 3
Gamma Spectral Analysis	
Radium-226	4.72 ± 0.11
Lead-212	1.99 ± 0.09
Lead-214	3.26 ± 0.10
Actinium-228	6.48 ± 0.20
Thallium-208	1.62 ± 0.06
Bismuth-214	11.80 ± 0.20
pH	8.6 units
Temperature	25°



APPROVED BY

[Signature]
 James J. Mueller, President

9/19/85 PAGE 4 OF 5 PAGE

Controls for Environmental Pollution, Inc.

P.O. Box 5351 • 1925 Rosina • Santa Fe, New Mexico 87502

Telephone 505/982-9841

REPORT OF ANALYSIS

CUSTOMER Dames & Moore
ADDRESS 3737 N. 7th Street, Suite 211
CITY Phoenix, AZ 85014
ATTENTION D.A. Stephenson
INVOICE NO. 509175

SAMPLES RECEIVED

CUSTOMER ORDER NUMBER

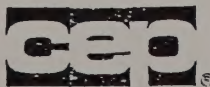
TYPE OF ANALYSIS

Sample Type: Distilled Water (before treatment)

Parameter	pCi/l
Gross Alpha	< 2
Gross Beta	< 3
pH	6.5 units

Sample Type: Distilled Water (after treatment with cinders)

Parameter	pCi/l (dissolved)
Gross Alpha	< 2
Gross Beta	< 3
Gamma Spectral Analysis	
Radium-226	0.472 \pm 0.017
Lead-212	0.198 \pm 0.012
Lead-214	0.337 \pm 0.014
Actinium-228	0.637 \pm 0.027
Thallium-208	0.144 \pm 0.07
Bismuth-214	1.110 \pm 0.52
pH	7.3 units
Temperature	24°



APPROVED BY

James J. Mueller, President

9/19/85 PAGE 5 OF 5 PAGE

Controls for Environmental Pollution, Inc.

P.O. Box 5351 • 1925 Rosina • Santa Fe, New Mexico 87502

Telephone 505/982-9841

APPENDIX D

ADSORPTION CAPACITY TESTS
ON BEDROCK AND BRECCIA SAMPLES:
LABORATORY REPORT OF ANALYSES

BY

CONTROLS FOR ENVIRONMENTAL POLLUTION
SANTA FE, NEW MEXICO

APPENDIX D

Dames & Moore
3737 North 7th Street
Suite 211
Phoenix, Arizona 85014

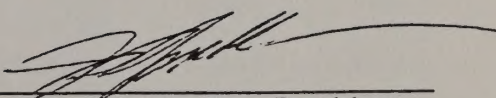
**Adsorption Capacity Tests
On Bedrock And Breccia Samples**

Lab # 86-01-406 and 85-01-407

Invoice # 602131

Performed by
Controls for Environmental Pollution, Inc.
1925 Rosina Street
Santa Fe, New Mexico 87502

Approved by


James J. Mueller, President

Objective

The adsorptive capacity of bedrock and breccia samples will be estimated on the basis of adsorption isotherms. The test constituents analyzed were lead, molybdenum, fluoride, sulfate, and total dissolved solids.

Test Information

Process leachates were obtained by placing 600 mls of the leachate in a plastic bottle and shaking along with the rest of the adsorption test bottles.

The initial leachate was analyzed from one bottle of sample received at CEP. When the adsorption test were performed, solution from all three sample bottles were combined prior to addition to the adsorption test bottles. Therefore any differences in results between the initial leachate solution and the process leachates may be due to slight variations in concentrations between the three sample bottles received at CEP.

The shaker ran at 270 cycles per minute. Throw on shaker was 1.0 cm at 8.0 cm off the axis.

Test Description	mg/l			
	Initial	1:1	1:10	1:100
Initial Leachate - prior to test	2.93	1.41	0.79	0.039
Breccia				
30 grams in 600 mls	0.95	0.69	0.39	0.003
12 grams in 600 mls	1.73	0.34	0.16	0.013
6 grams in 600 mls	2.01	1.01	0.17	0.013
6 grams in 600 mls (process dupl)	2.02	0.99	0.17	0.013
3 grams in 600 mls	2.61	1.23	0.24	0.029
Process Leachate - no breccia	2.54	1.30	0.23	0.029
Bedrock				
30 grams in 600 mls	0.92	0.43	0.25	0.003
12 grams in 600 mls	1.79	0.32	0.16	0.013
6 grams in 600 mls	2.10	0.98	0.19	0.013
6 grams in 600 mls (process dupl)	1.94	0.95	0.18	0.013
3 grams in 600 mls	2.52	1.26	0.21	0.029
Process Leachate - no bedrock	2.54	1.49	0.23	0.029

LEAD

Test Description	ppm			
	Undiluted	1:1	1:10	1:100
Initial Leachate - prior to test*	< 0.01	< 0.01	< 0.01	< 0.01
Breccia				
30 grams in 600 mls	0.33	0.16	0.03	0.002
12 grams in 600 mls	0.94	0.46	0.09	0.008
6 grams in 600 mls	0.94	0.43	0.08	0.008
6 grams in 600 mls (process dup)	0.92	0.45	0.09	0.008
3 grams in 600 mls	0.99	0.50	0.10	0.009
Process Leachate - no breccia	0.92	0.45	0.09	0.008
Bedrock				
30 grams in 600 mls	0.32	0.16	0.03	0.002
12 grams in 600 mls	1.12	0.55	0.12	0.011
6 grams in 600 mls	1.03	0.48	0.10	0.009
6 grams in 600 mls (process dup)	1.01	0.51	0.10	0.009
3 grams in 600 mls	1.08	0.54	0.11	0.010
Process Leachate - no bedrock	0.90	0.45	0.09	0.008

*No lead was determined in the leachate solution.

After initial analysis of the leachate solution, the Dames & Moore procedure required the leachate to be spiked with 1 ppm of lead. Therefore, 1 ppm of lead was added to the solution used in the adsorption test for the breccia and bedrock.

MOLYBDENUM

Test Description	ppm			
	Undiluted	1:1	1:10	1:100
Initial Leachate - prior to test	2.90	1.41	0.29	0.030
Breccia				
30 grams in 600 mls	0.98	0.49	0.09	0.008
12 grams in 600 mls	1.73	0.84	0.16	0.015
6 grams in 600 mls	2.01	1.01	0.19	0.018
6 grams in 600 mls (process dup)	2.02	0.99	0.19	0.018
3 grams in 600 mls	2.61	1.25	0.24	0.024
Process Leachate - no breccia	2.84	1.50	0.28	0.029
Bedrock				
30 grams in 600 mls	0.92	0.45	0.08	0.008
12 grams in 600 mls	1.70	0.82	0.16	0.015
6 grams in 600 mls	2.00	0.98	0.19	0.018
6 grams in 600 mls (process dup)	1.96	0.98	0.18	0.019
3 grams in 600 mls	2.52	1.26	0.24	0.024
Process Leachate - no bedrock	2.83	1.49	0.28	0.029

FLUORIDE

Test Description	ppm			
	Undiluted	1:1	1:10	1:100
Initial Leachate - prior to test	1.40	0.70	0.14	0.015
Breccia				
30 grams in 600 mls*	3.60	2.15	0.51	0.058
12 grams in 600 mls	2.80	1.55	0.34	0.035
6 grams in 600 mls	2.60	1.35	0.29	0.030
6 grams in 600 mls (process dup)	2.60	1.35	0.29	0.029
3 grams in 600 mls	2.50	1.30	0.26	0.026
Process Leachate - no breccia	2.40	1.20	0.25	0.024
Bedrock				
30 grams in 600 mls*	2.90	1.70	0.42	0.050
12 grams in 600 mls	2.70	1.50	0.32	0.034
6 grams in 600 mls	2.50	1.30	0.29	0.030
6 grams in 600 mls (process dup)	2.50	1.30	0.28	0.030
3 grams in 600 mls	2.50	1.25	0.26	0.026
Process Leachate - no bedrock	2.40	1.20	0.24	0.025

*Verified by triplicate analysis

After initial analysis of the leachate solution, the Dames & Moore procedure required the leachate to be spiked with 1 ppm of fluoride. Therefore, 1 ppm of fluoride was added to the solution used in the adsorption test for the breccia and bedrock.

TOTAL DISSOLVED SOLIDS

Test Description	ppm			
	Undiluted	1:1	1:10	1:100
Initial Leachate - prior to test	1873	931	186	17
Breccia				
30 grams in 600 mls	2685	1336	267	28
12 grams in 600 mls	2301	1143	232	27
6 grams in 600 mls	2118	1063	220	20
6 grams in 600 mls (process dup)	2051	1081	200	24
3 grams in 600 mls	1992	1004	210	19
Process Leachate - no breccia	1870	931	189	16
Bedrock				
30 grams in 600 mls	2682	1315	255	23
12 grams in 600 mls	2460	1221	250	22
6 grams in 600 mls	2268	1117	234	20
6 grams in 600 mls (process dup)	2254	1124	217	20
3 grams in 600 mls	2111	1023	193	22
Process Leachate - no bedrock	1899	932	173	17

APPENDIX E

DESCRIPTION OF WATER QUALITY
SAMPLING LOCATIONS

APPENDIX E

DESCRIPTION OF WATER QUALITY SAMPLING LOCATIONS

Within the Guadalupe Mountain/Questa area, water-flow or water-quality were evaluated at several localities. These sampling points include wells, springs, drain systems, and surface waters. The following is a description of locations where water measurements were made. Sampling points are identified by both their full name and abbreviated names, and the sampling location or occurrence and its use in the investigation are discussed.

BIG ARSENIC SPRING (RG BARSP)

This spring is the largest natural spring in the area. It is located on the Rio Grande, about 1.5 miles upstream from the confluence of the Red River and Rio Grande. The actual spring is a single source located approximately 40 feet above river level. A few much smaller seeps occur a few hundred feet upstream. This spring was used for spring flow staff gauging and was sampled for ambient ground-water quality evaluation.

LITTLE ARSENIC SPRING (RG LARSP)

This spring is a single source that has a relatively high discharge. It is located approximately 0.75 mile upstream from the confluence and originates about 30 feet above river level. This spring was used for visual spring flow gauging and was sampled for ambient ground-water quality evaluation.

CERRO SPRING (RG CERSP)

This spring is an area of about a dozen seeps along the Rio Grande, just below Cerro Canyon. The seeps occur at river level and vary in discharge from a very small trickle to a couple gallons per minute. Proceeding north to south, the seeps are labeled A through L. Cerro C, one of the larger seeps, was used for visual spring flow gauging and was sampled for ambient ground-water quality evaluation.

FISH HATCHERY 1 AND 2 (RR-FH1-SP, RR-FH2-SP)

These springs are an area of broad, relatively high discharge seeps. They are located about 0.75 mile upstream of the Red River Fish Hatchery and occur about 5 to 10 feet above river level. These springs were used for visual spring flow gauging and were sampled for ambient ground-water quality evaluation.

RED RIVER 1 AND 2 (RR No. 1 SP, RR No. 2 SP)

These springs are very small seeps located at river level a few hundred feet downstream from El Aujae Campground. During late summer, these springs sometimes go dry. These samples were used for visual spring gauging and were sampled for ambient ground-water quality evaluation.

RED RIVER 3, 4, 5, 6, 7, 8, 9, AND 10 (RR-3-SP - RR-10-SP)

This spring complex is located approximately 0.5 mile downstream from the Red River Fish Hatchery. The springs are located at river level and vary in discharge from small seeps to single sources that have moderate discharges. They were used for visual spring gauging and sampled for ambient ground-water quality evaluation.

BLM CHIFLO CAMPGROUND WELL (BLMCHI W and SHEEPX W)

This well is located approximately 0.5 mile southeast of the Chiflo Campground. The well is 415 feet deep and taps the regional basalt aquifer. Samples from this well were used for ambient ground-water quality evaluation, water-level surveys, and aquifer testing. Water samples from this well are collected at the wellhead and at Sheeps Crossing Campground after being piped for approximately 0.5 mile.

BLM HEADQUARTERS WELL (BLMHDQ W and BARSEN W)

This well is located at the BLM Wild and Scenic River Headquarters facility. The well is 546 feet deep and taps the regional basalt aquifer. Samples from this well were used for ambient ground-water quality evaluation, water-level surveys, and aquifer testing. Water samples from this well were collected at the wellhead and at the Big Arsenic Campground after being piped for approximately 0.5 mile.

OUTFALL 001, 002, 003 (FALLO01, FALLO02, FALLO03)

The Outfalls 001, 002 and 003 are the discharge points for the french tile drain system that underlies the current tailings disposal facility. Outfall 001 rarely flows. Discharges from Outfalls 002 and 003 are combined before the sampling point. Samples from these locations were used for leachate chemistry analyses.

MW-1, 2, 3, 4

These monitor wells are less than 50 feet deep and are positioned along the face of the current tailings dam. Water samples were sporadically taken with a bailer and were used for leachate chemistry analyses.

HERRERA WELL (P-1)

This shallow private well is located 0.25 mile south of the current tailings disposal site. Water samples were collected from the household tap and were used for leachate chemistry evaluation.

RAEL WELL (P-4)

This shallow private well is located 0.5 mile south of the current tailings disposal site. Water samples were collected from the household tap and were used for leachate chemistry evaluation.

TAILINGS DRY WELL (TAILDRY)

This well is located 0.25 mile east of the current tailings disposal site. Water samples were collected at the wellhead. Well specifications are unknown at this time. Samples from this well were used for leachate chemistry evaluation.

WEST DIVERSION DITCH (W DITCH)

This diversion ditch channels decant water from the current tailings disposal site to the Ion Exchange plant by Pope Lake. Water samples were collected at the last wier before Pope Lake. The decant water was used for leachate chemistry evaluation.

RED RIVER AT THE PLANT BRIDGE (RR PBR S)

Surface-water samples were taken from the Red River at the mill plant bridge and were used for ambient surface-water quality evaluation.

RED RIVER AT THE CARSON NATIONAL FOREST RANGER STATION (RR RST S)

Surface-water samples were taken from the Red River at the bridge crossing the river to the ranger station. These samples were used in evaluating ambient surface-water quality.

RED RIVER AT THE QUESTA-HIGHWAY 3 BRIDGE (RR QBR S)

Surface-water samples were taken from the Red River at the New Mexico Highway 3 bridge. These samples were used in evaluating ambient surface-water quality.

RED RIVER AT JUNEBUG CAMPGROUND (RR JNBGS)

Surface-water samples were taken from the Red River at Carson National Forest Junebug Campground. These samples were used in the evaluation of ambient surface-water quality.

CABRESTO CREEK (CB CRK S)

Surface-water samples were taken from Cabresto Creek where it crosses New Mexico Highway 38. These samples were used in evaluating ambient surface-water quality.

COLUMBINE CREEK (CO CRK S)

Surface-water samples were taken from Columbine Creek at its confluence with the Red River. These samples were used in evaluating ambient surface-water quality.

APPENDIX F

SUMMARY OF TARGET
MODELS

(DAMES & MOORE MATHEMATICAL MODEL
OF GROUND-WATER FLOW AND
SOLUTE TRANSPORT:

SUMMARY OF
BACKGROUND TO VARIABLY-
SATURATED AND DENSITY-
COUPLED MODELS)

APPENDIX F

TABLE OF CONTENTS

	<u>Page</u>
LIST OF FIGURES	F-ii
F.1 INTRODUCTION	F-1
F.2 PHYSICAL MECHANISMS AND CHEMICAL PROCESSES	F-3
F.2.1 Ground-Water Flow	F-4
F.2.2 Solute Transport	F-5
F.3 MATHEMATICAL FORMULATION	F-11
F.3.1 Governing Equations	F-11
F.3.2 guess and Correct Algorithm	F-16
F.3.3 Initial Conditions	F-17
F.3.4 Boundary Conditions	F-18
F.3.5 Internal Sources and Sinks	F-18
F.4 NUMERICAL METHODS	F-19
F.5 SOLUTION TECHNIQUES	F-21
F.5.1 Iterative Method	F-21
F.5.2 Matrix Solution Algorithm	F-23
F.5.3 Relaxation	F-24
F.6 VALIDATION CASES	F-25
F.7 REFERENCES	F-51

APPENDIX F

LIST OF FIGURES

	<u>Page</u>
Figure F.1 - Relationship Between Relative Permeability and Pressure Head for Various Soils	F-6
Figure F.2 - Relationship Between Degree of Saturation and Pressure Head for Various Soils	F-7
Figure F.3 - Iteration Scheme	F-22

F.1 INTRODUCTION

This appendix summarizes the physical and chemical hypotheses, mathematical formulation, and numerical framework of a numerical model of ground-water flow and chemical-species transport in variably saturated porous media. The numerical model, developed by Dames & Moore over the past 5 years, is known as TARGET (Transient Analyzer of Reacting Ground Water and Effluent Transport). The purpose of this document is to provide a general description of the methodology and assumptions employed in the model.

Documents covering details of the mathematical formulation, model input data structure and definitions, and validation cases covering the range of model applicability are available separately. Due to similarity in approach, this appendix relates to three of the series of five models in the TARGET family; namely TARGET_2DU (two-dimensional, vertical cross-section, variably saturated), TARGET_3DU (three-dimensional, variably saturated), and TARGET_3DS (three-dimensional, fully saturated).

The state-of-the-art of mathematical models for predicting fluid dynamics and associated mass transport in variably-saturated porous media has advanced considerably within the past few years. The literature describing these advances is vast; it has been reviewed by several authors including Narasimhan and Witherspoon (1977), Lappala (1980), and Heijde et al. (1985). Comprehensive reviews of ground-water numerical modeling techniques are provided by Remson et al. (1971), Pinder and Gray (1977), and

Mercer and Faust (1981). The model presented in the following pages falls into the category of integrated finite-difference procedures that solve the density-coupled flow and reactive mass transport equations in variably saturated porous media by employing a sophisticated hybrid differencing scheme. Details of the mathematical formulation of the model are presented in Dames & Moore (1985a and b). Applications of the model have been reported by Highland et al. (1983) and Sharma et al. (1983) among others.

The TARGET model capabilities accommodate the following site features:

- o Physical mechanisms that influence hydrodynamics:

- Regional or local recharge or discharge,
- Hydraulic-induced and density-induced pressure gradients, and
- Compressibility of the matrix and water;

- o Variable saturation;

- o Material property variations;

- o Boundary conditions of all types:

- Specified head boundaries,
- Specified flux boundaries, and
- Mixed boundary conditions;

- o Man-made features:

- Injection or extraction wells,
- Waste disposal facilities, and
- Pollution-abatement measures;

and

o Mass transport mechanisms:

- Advection,
- Dispersion,
- Density effects,
- Viscosity effects, and
- Sorption and chemical reactions.

Models of the TARGET family have been applied in more than 80 projects to a range of water management and contaminant control problems including: dewatering of multiple aquifers during operation of an Australian strip mine, simulation of alternate remedial measures of five Superfund sites, and prediction of containment and extraction of light hydrocarbons and dense mine wastes. During the course of these applications, the model approach and predictions have been reviewed and approved by many regulatory agencies including the U.S. Geological Survey and U.S. Environmental Protection Agency. In addition, a satisfactory peer review of the model formulation was given by Professor Allan Freeze, who was solicited by Dames & Moore. These review opinions, as well as publications and model validation cases, provide the basis for background substantiation of model predictions.

F.2 PHYSICAL MECHANISMS AND CHEMICAL PROCESSES

The purpose of this section is to summarize the major assumptions used in developing the physical and chemical hypotheses embedded in the model.

F.2.1 Ground-Water Flow

The flow mechanisms incorporated in the model are unsaturated pore-pressure gradients, saturated pressure head gradients, gravity-induced and density-induced pressure gradients, as well as changes in storage due both to compressibility of the ground water and the matrix and to water-table fluctuations. Assumptions made in the development of the hydrodynamic equations for saturated unsaturated flow presented in Section F.3 are:

- o The porous medium is deformable, but not consolidating.
- o Ground water is compressible, but density changes due to compression are neglected.
- o In unsaturated regions, pressure gradients in the air are negligible and air pressure is equal to atmospheric pressure.
- o An empirical expression (Darcy's law) can be used to relate macroscopic ground-water velocity to the gradient of pore-fluid pressure.
- o Changes in storage due to changes in pressure result both from the elastic properties of the aquifer and ground water, and from drainage from pores.
- o The principal directions of the hydraulic conductivity tensor are aligned with the cartesian coordinate system adopted in the model.
- o Evaporation from the water table may be neglected.

In order to completely describe the physical processes occurring in variably-saturated soils, auxiliary relationships that describe the variation of hydraulic conductivity, $K_r(\psi)$, and degree of saturation, $S_r(\psi)$, with negative pore pressures must be defined. In general, the relationships may only be realistically obtained through laboratory measurements of the soil types of interest. However, an S-shaped curve may

be expected for most soil types (see Figures F.1 and F.2) and several authors have developed derivations for $K_r(\psi)$ based on the corresponding $S_r(\psi)$ relationship (e.g., Jackson et al., 1965) and Mualem, 1976). The following forms of relationships fit most data sets and are used in the model:

$$S_r = \frac{\theta_r}{\theta_s} + (1 - \frac{\theta_r}{\theta_s}) \left\{ 1 + (a_{0s} |\psi|)^{a_{1s}} \right\}^{a_{2s}} ; -\infty < \psi < 0$$

$$S_r = 1 ; \psi > 0 \quad (2-1)$$

$$K_r = K_{r_{\min}} + (1 - K_{r_{\min}}) \left\{ 1 + (a_{0k} |\psi|)^{a_{1k}} \right\}^{a_{2k}} ; -\infty < \psi < 0$$

$$K_r = 1 ; \psi > 0 \quad (2-2)$$

a_{0s}, a_{1s}, a_{2s} = coefficients in S_r relationship
 a_{0k}, a_{1k}, a_{2k} = coefficients in K_r relationship
 K_r = relative hydraulic conductivity [-]
 $K_{r_{\min}}$ = minimum relative hydraulic conductivity for dry conditions
 ψ = pressure head [L]
 θ_r = residual moisture content [-]
 θ_s = saturated moisture content [-]
 S_r = degree of saturation [-].

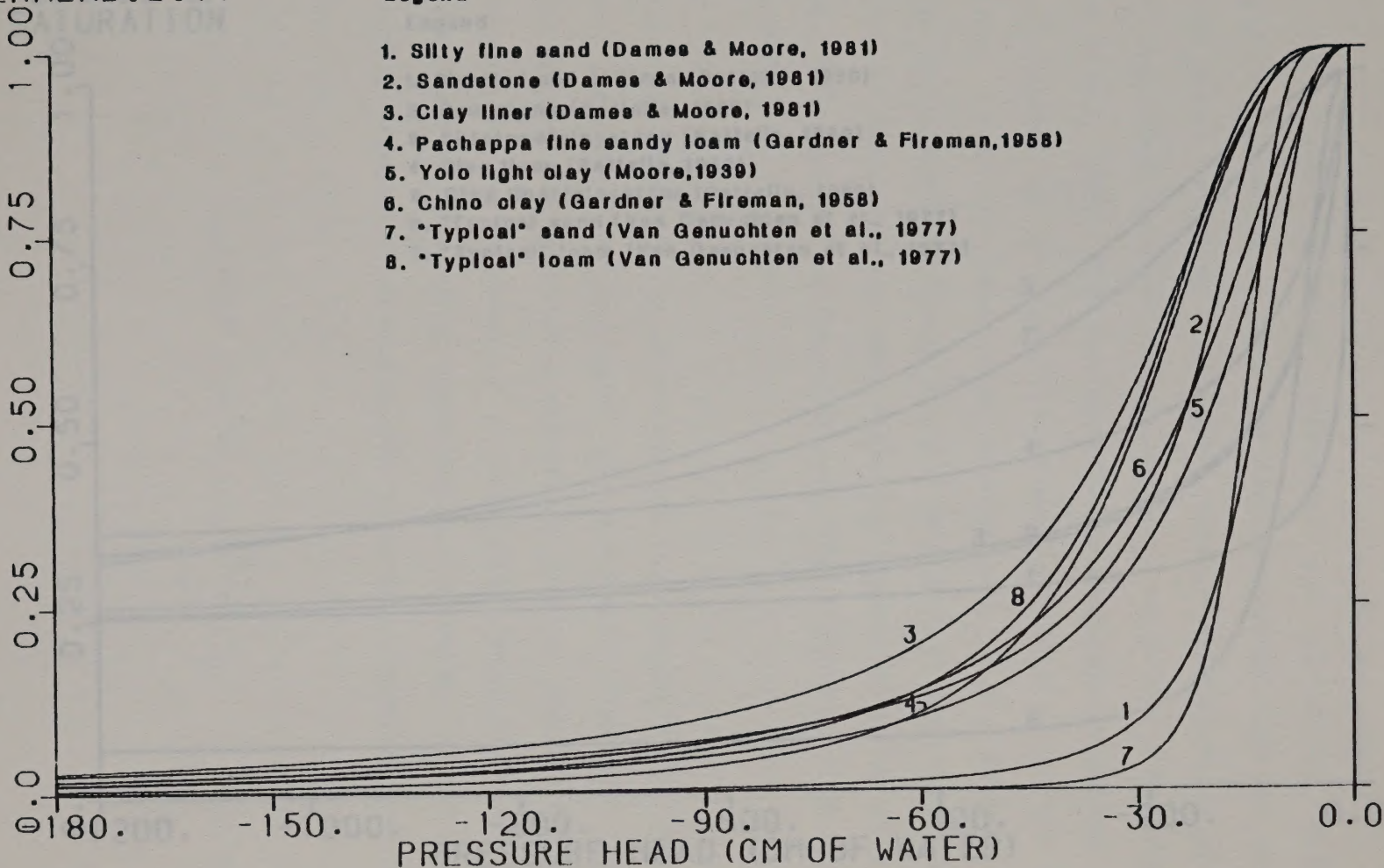
F.2.2 Solute Transport

The model described in this appendix has been designed to simulate the movement of dissolved constituents of similar different density and viscosity than that of ground water, in variably saturated soil and rock. The transport mechanisms incorporated in the model are advection, mech-

RELATIVE
PERMEABILITY

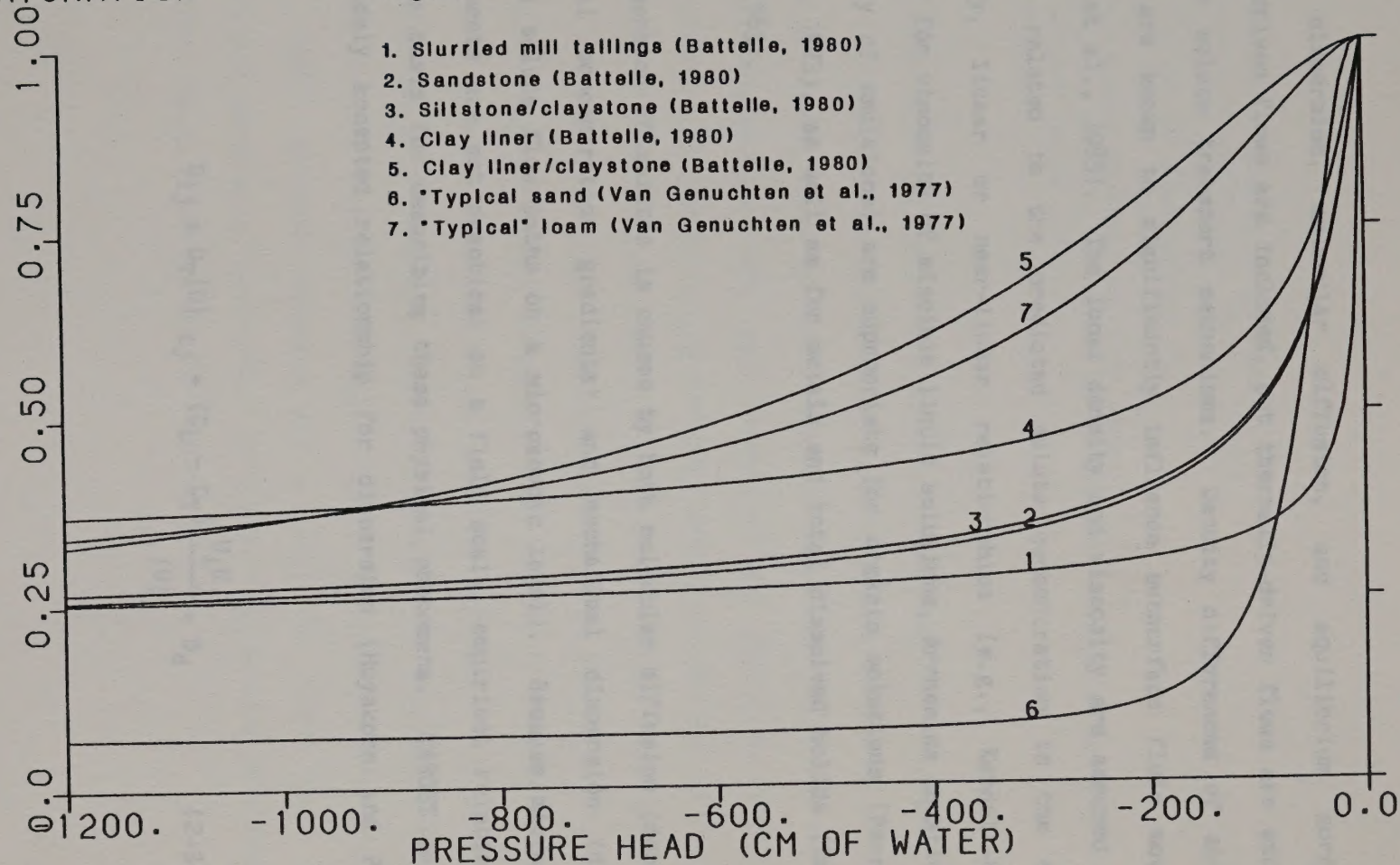
Legend

1. Silty fine sand (Dames & Moore, 1981)
2. Sandstone (Dames & Moore, 1981)
3. Clay liner (Dames & Moore, 1981)
4. Pachappa fine sandy loam (Gardner & Fireman, 1958)
5. Yolo light clay (Moore, 1939)
6. Chino clay (Gardner & Fireman, 1958)
7. "Typical" sand (Van Genuchten et al., 1977)
8. "Typical" loam (Van Genuchten et al., 1977)



**Relationship Between Relative Permeability And
Pressure Head For Various Soils**

DEGREE OF
SATURATION



**Relationship Between Degree Of Saturation And
Pressure Head For Various Soils**

Figure F.2

anical, dispersion, molecular diffusion, and equilibrium sorption. Density-driven flows are included, but thermally-driven flows are excluded from the solute transport mechanisms. Density differences of about 1 percent are known to significantly influence subsurface fluid movement (Mackay et al., 1985). The local density and viscosity are assumed to be linearly related to the predicted solute concentration in the model. Typically, linear or near-linear relationships (e.g., Kendall-Monroe equation for viscosity of miscible liquid solutions, Arrhenius equation for viscosity of emulsions) are appropriate for organic solutions (Perry and Chilton, 1973), as well as for metals and total dissolved solids (Dames & Moore, 1983).

Dispersion of solutes is caused by both molecular diffusion (dependent on local concentration gradients) and mechanical dispersion (due to tortuous solute flow paths on a microscopic level). Because microscopic measurements are not practical on a field scale, empirical relationships form the basis for describing these physical phenomena. TARGET uses the most widely accepted relationship for dispersion (Huyakorn and Pinder, 1982):

$$D_{ij} = D_T |U|_{ij} + (D_L - D_T) \frac{U_i U_j}{|U|} + D_d \quad (2-3)$$

where:

D_d = molecular diffusion coefficient [L^2/T]
 D_{ij} = dispersion coefficient tensor [L^2/T]
 D_T = transverse dispersivity [L]
 D_L = longitudinal dispersivity [L]
 U = magnitude of velocity tensor [L/T]
 U_i = i-direction particle velocity component [L/T]
 U_j = Particle velocity component in a direction perpendicular to i [L/T]
 δ_{ij} = Kronecker delta [-]
 τ = tortuosity [-].

In characterizing the mobility and attenuation of solutes, it is essential to quantify the geochemical mechanisms that influence or control the chemical interactions between subsurface media and the fluids contained in them. Predominant among such mechanisms are mechanical filtration, cation exchange, buffering of pH chemical precipitation due to reactions with the solid matrix as well as with interstitial water, hydrolysis, and oxidation-reduction reactions. The factors that make such a quantification difficult are the kinetic or non-equilibrium nature of certain reactions, competition, between mechanisms and chemical species, and multi-layer adsorption. While a number of adsorption models have been proposed in the literature (e.g., Cameron and Klute, 1977; Valocchi, 1984; Goltz and Roberts, 1984), the best approach for a particular study rests on the solute(s) and geochemical environment involved. The version of TARGET described here uses a linear adsorption isotherm:

$$m_{J,s} = K_d C_J \quad (2-4)$$

where:

$m_{J,s}$ = mass concentration in the solid phase [M/M]
 K_d = adsorption distribution coefficient [L^3/M]
 C_J = volumetric concentration in the liquid phase [L^3/M].

which incorporates two assumptions: (1) that equilibrium is immediately established (or at least reactions occur much faster than ground-water flow) between adsorption and desorption; and (2) that adsorption is reversible. Alternate adsorption isotherms may be readily incorporated in the model if appropriate. Evidence suggests that linear adsorption isotherms are representative of organic contaminant behavior for concentrations up to the aqueous solubility (Chiou et al., 1979), but that adsorption of metal contaminants may be strongly dependent on the local pH (Dames & Moore, 1981).

F.3 MATHEMATICAL FORMULATION

F.3.1 Governing Equations

Three basis equations govern flow and solute transport in variably-saturated porous media. These are:

- o The equation of conservation of ground-water flow (i.e., mass conservation of ground water);
- o Darcy's law; and
- o The equation of conservation of chemical product in solution in ground water (solute), also referred to as the equation of mass transport.

The mathematical derivation below shows how these three basic equations are transformed into two relationships of the primary variables:

ψ (pressure head) and,

m_J (mass concentration of chemical product J).

A three-dimensional cartesian system of coordinates is used in the following derivations and, consequently, the remainder of this appendix is applicable to both three-dimensional and two-dimensional, cross-section (profile) situations.

1. Conservation of Ground-Water Flow

The fundamental three-dimensional mass conservation equation for variably-saturated porous media is expressed as follows (Bear, 1979, p. 213):

$$\underbrace{\frac{\partial}{\partial t} \{nSr\rho\}}_{\text{storage}} + \underbrace{\frac{\partial}{\partial x_i} \{nSr\rho U_i\}}_{\text{in/out flow}} = \underbrace{\dot{m}'''}_{\text{source/sink}} \quad (3-1)$$

where:

- \dot{m}''' = specific mass source rate [M/TL³]
- n = porosity [-]
- Sr = degree of saturation [-]
- t = time [T]
- U_i = i-direction particle velocity [L/T]
- x_i = i-direction coordinate [L]
- ρ = density [M/L³].

2. Darcy's Law

The generalized form of Darcy's law in anisotropic porous media can be expressed as follows (Bear, 1979, p. 64):

$$\underbrace{nSrU_i}_{\text{Darcy velocity}} = -Kr \frac{k_{ij}}{\mu} \underbrace{\left\{ \frac{\partial p}{\partial x_j} + \rho g \frac{\partial Z}{\partial x_j} \right\}}_{\text{total pressure gradient}} \quad (3-2)$$

where:

- g = gravitational acceleration [L/T²]
- k_{ij} = intrinsic conductivity tensor component [L²]
- Kr = relative conductivity [-]
- p = pressure [M/LT²]
- Z = vertical axis [L]
- μ = viscosity [M/LT].

3. Conservation of Chemical Product in Solution

The fundamental three-dimensional conservation equation for a chemical product in solution in ground water is expressed as (Bear, 1979, p. 239):

$$\underbrace{\frac{\partial}{\partial t} \left\{ n S r \rho m_J \right\}}_{\text{storage in mobile phase}} + \underbrace{\frac{\partial}{\partial t} \left\{ (1-n) \rho_s m_{J,s} \right\}}_{\text{storage in immobile phase}} + \underbrace{\frac{\partial}{\partial x_i} \left\{ n S r \rho U_i m_J \right\}}_{\text{advection}} = \underbrace{\frac{\partial}{\partial x_i} \left\{ n S r \rho D_{ij} \frac{\partial m_J}{\partial x_j} \right\}}_{\text{dispersion}} + \underbrace{\dot{m}''' M_J}_{\text{source/sink}} \quad (3-3)$$

where:

- D_{ij} = dispersion coefficient tensor [L^2/T]
 m_J = mass concentration of chemical product of J in liquid phase [M/M]
 $m_{J,s}$ = mass concentration of chemical product of J in solid phase [M/M]
 \dot{m}'''_J = source mass concentration of chemical product of J [M/M]
 ρ_s = soil bulk density [M/L³].

Upon introducing Darcy's law (Equation 3-2) into the equation of mass conservation (Equation 3-1) and transforming the time-dependent term through the use of the concept of specific storage, the mass conservation equation may be expressed as a single equation of the dependent variable, ψ (pressure head):

$$RSrSc \frac{\partial \psi}{\partial t} = \frac{\partial}{\partial x_1} \left\{ RKrK_{1j}M \left[\frac{\partial \psi}{\partial x_j} + R \frac{\partial Z}{\partial x_j} \right] \right\} - Rn \frac{\partial Sr}{\partial t} - nSr \frac{\partial R}{\partial t} + \frac{\dot{m}'''}{\rho_o} \quad (3-4)$$

where:

Pressure head $\psi \equiv \frac{p}{\rho_o g}$

Density ratio $R \equiv \frac{\rho(m_J)}{\rho_o}$

Viscosity ratio $M \equiv \frac{\mu_o}{\mu(m_J)}$

Hydraulic conductivity $K_{1j} \equiv \frac{k_{1j} \rho_o g}{\mu_o}$

Sc = specific storage coefficient [1/L]
 ρ_o = reference density [M/L³]
 μ_o = reference viscosity [M/LT].

The fundamental form of the mass transfer equation (Equation 3-3) requires additional relationships to completely define the problem of transport of a chemical product in variably saturated porous media. These relationships are:

- o Relationship to link the concentration of the chemical product in the solid matrix to that in the ground water; and
- o Relationship to link the coefficients of the dispersion tensor to the longitudinal and transverse dispersivities.

The solid/fluid interaction is assumed to be represented by a so-called linear isotherm (Equation 2-4). Under this assumption the matrix concentration ($m_{J,s}$) can be rewritten as:

$$m_{J,s} = \rho K_d m_J \quad (3-5)$$

Upon introducing the equation for solid/fluid interaction (Equation 3-5) and the relationship for the diffusion coefficients (Equation 2-3) into the fundamental mass transfer equation (2-3), the mass transfer equation may be expressed as:

$$\begin{aligned}
 nSrR \frac{\partial m_J}{\partial t} + R_b R \rho_o K_d \frac{\partial m_J}{\partial t} + nSrU_1 \frac{\partial m_J}{\partial x_1} = \\
 \frac{\partial}{\partial x_1} \left\{ RnSrD_{1j} \frac{\partial m_J}{\partial x_1} \right\} + \frac{\dot{m}'''}{\rho_o} [M_J - m_J] \\
 - m_J \left\{ \frac{\partial}{\partial t} (nRSr) + \frac{\partial}{\partial x_1} (nSrU_1) - \frac{\dot{m}'''}{\rho_o} \right\}
 \end{aligned} \quad (3-6)$$

where:

$$R_b = \frac{\rho_b}{\rho_o} = [1-n] \frac{\rho_s}{\rho}$$

$$\rho_b = \text{soil (grain) density [M/L}^3\text{]}$$

F.3.2 Guess and Correct Algorithm

Prior to the transformation of the partial differential equations into their finite-difference form and implementation in the numerical model, Equations (3-4) and (3-6) are modified using a guess and correct (or predictor/corrector) algorithm. This technique was implemented because of its numerical advantages primarily when solving for variables such as pressure head, with which it is common to encounter relatively large mean values and small but highly significant gradients.

The basis of this algorithm consists in substitution for the dependent variable in the partial differential equations by the sum of a guessed value and a correction to be applied to the guessed value. The terms are then grouped and the resulting equation is expressed in terms of the correction with a distributed source representing the accuracy of the guess value. The converged solution for the dependent variable is thus zero throughout the calculation domain.

F.3.3 Initial Conditions

Initial distribution of the dependent variables (or in the guess and correct nomenclature initial guessed value) of the pressure head, ψ , and of the mass concentrations of the chemical product, m_j , are necessary. These can be derived from observed or postulated field conditions or through the calculation of steady-state distributions with appropriate boundary conditions. Often, partially saturated initial conditions are available, from field data, in the form of the moisture content distribution. It is of particular importance to the correct prediction of transient phenomena to obtain good initial conditions, (i.e., flow field and concentration distributions that obey the conservation principles). Failing to follow these requirements, unwanted pressure redistribution and mass transport may take place in the early stages of a transient calculation. In other words, the initial conditions of a transient calculation are usually the result of a preliminary steady-state or transient calculation.

F.3.4 Boundary Conditions

Boundary conditions for the primary variables are required to complete the problem definition. The various types of boundary conditions encountered in flow and solute transport through porous media are:

1. **Prescribed Boundary Values** - The pressure head or the concentrations are assigned a prescribed value along the entire boundary or sections thereof. This type of boundary condition is also called a Dirichlet boundary condition.
2. **Prescribed Boundary Flux** - On a boundary of this type, the flux of ground water or chemical product perpendicular to the boundary is prescribed. A special case of this type of boundary is the impervious boundary where the flux is zero. This type of boundary condition is also called a Neumann boundary condition.

Other types of boundary conditions, such as a Cauchy (also called mixed boundary conditions), can be represented by combinations of the above two types. Although seepage faces can be represented by the above types of boundary conditions, the correct point of exit has, generally, to be approached through a series of trial-and-error steady-state solutions. All of the boundary condition values may further vary with time.

F.3.5 Internal Sources and Sinks

Often, practical problems require that man-made or natural features such as wells, rivers, lakes, ponds, infiltration, or evaporation be represented. This is generally achieved by the use of internal sink or source terms, or, by the use of prescribed values within the calculation domain as opposed to prescribed values on the boundary of the calculation domain. Sources and sinks may arbitrarily vary with time.

F.4 NUMERICAL METHODS

The numerical calculation procedures employed to solve the equation set described in Section F.3 is of the integrated finite-difference (IFD) variety. A grid system consisting of rectangular cells of arbitrary aspect ratio, with grid nodes located at the geometrical center of each cell, serves as the basis for the derivation of the discretized (i.e., finite-difference) equations. These latter are obtained by integrating the appropriate differential equations over each of the cells in the calculation domain. For this integration, the dependent variables are presumed to vary linearly between adjacent grid nodes. This procedure transforms the partial differential equations into two sets of algebraic linearized equations, one of the calculation of pressure head, ψ , and the other for the calculation of mass concentrations, m_j . In the case of dense chemical products, these two sets are coupled through terms representing gravitational induced fluid motion. Because of this coupling and because of the non-linear nature of the pressure head equation, an iterative Alternating Direction Implicit (ADI) algorithm is used in the solution of the algebraic set of equations. Under-relaxation or over-relaxation of the iterative scheme is permitted to damp or accelerate the convergence rate of the solution.

Indiscriminate use of the finite difference discretization technique for the first and second spatial derivatives can lead to unstable and even to physically meaningless solutions when the problem is advection dominated. This situation may occur when the magnitude of the cell Peclet

number is greater than one. In the present model, such difficulties are overcome by the use of a hybrid differencing scheme in which upstream, downstream or central differencing schemes are employed depending on the local Peclet number and direction of flow.

Particular care is also taken with the evaluation of the local degree of saturation both due to the non-linearity of the S_r relationship and due to the close link between degree of saturation and relative hydraulic conductivity. Because the $S_r(\psi)$ relationship is strongly non-linear, the average degree of saturation of a cell is calculated on the basis of an assumed linear variation of pressure head between nodes along the vertical axis, rather than as a function solely of the pressure at the node. In addition, the formulation of the time-dependent term $\partial S_r / \partial t$ in finite difference form requires particular care as:

- o It is a strongly non-linear term, highly sensitive to changes in pressure head; and
- o It is the dominant term controlling changes in storage in partially saturated cells.

F.5 SOLUTION TECHNIQUES

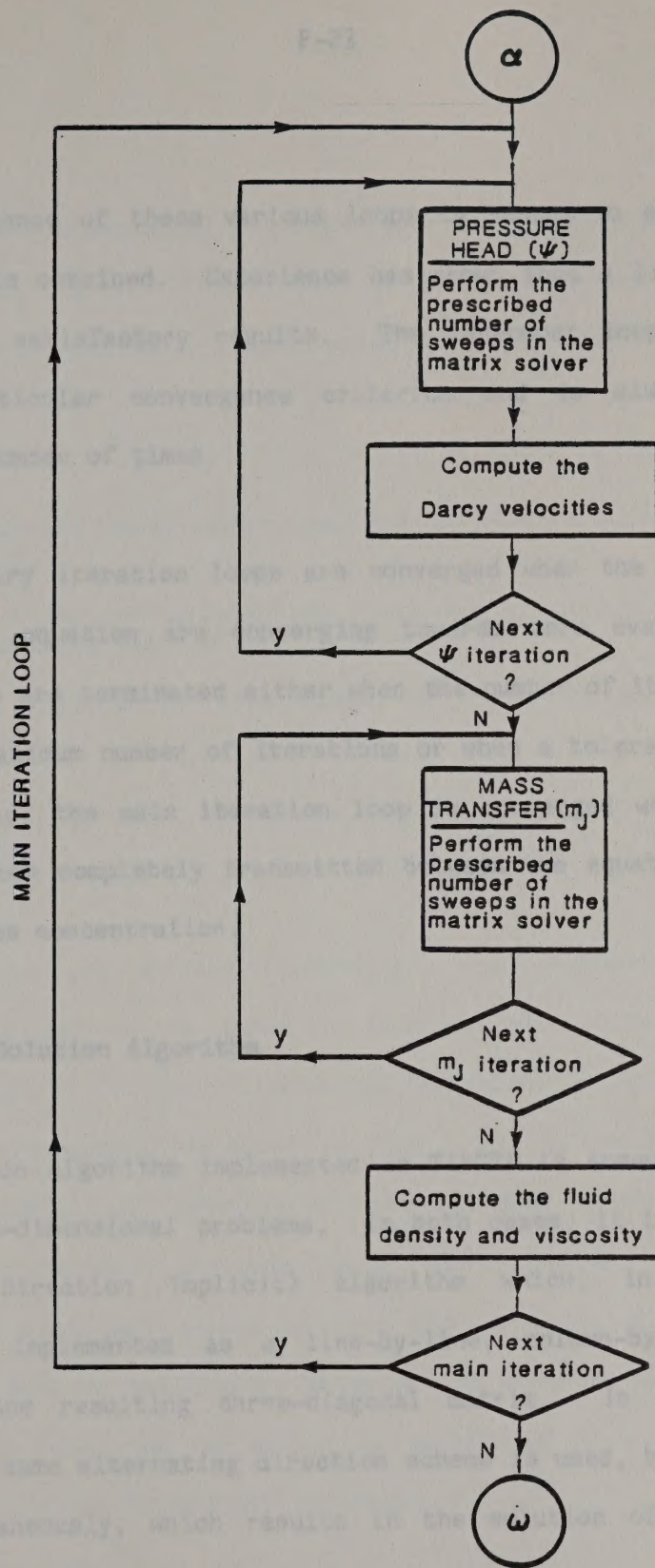
F.5.1 Iterative Method

Since the pressure head equation is non-linear, and since density and viscosity effects create a strong coupling between the pressure head and the mass transfer equations, an iterative solution method is required.

The iteration scheme used in TARGET is composed of three levels of iteration. These levels, discussed below, are also illustrated in Figure F.3:

1. The main iteration loop, over the solution of both the pressure head and mass concentration equations. The objective of this loop is to account for the density and viscosity coupling effects. This loop need not be executed more than once in non-coupled problems, i.e., when the chemical product in solution in ground water has the same density and viscosity as the ground water.
2. The secondary iteration loop over the solution of the equations of pressure head and mass concentration individually. The objective of this loop is to account for the non-linear terms such as relative conductivity and degree of saturation. This loop need not be executed more than once for linear equations such as the mass transfer equation.
3. The innermost iteration loop is the matrix solution loop. The objective of this loop is to obtain a good solution for a given set of coefficients.

ITERATION SCHEME



ITERATION SCHEME

The convergence of these various loops is tested to establish when a good solution is obtained. Experience has shown that a limited number of sweeps produce satisfactory results. The innermost loop is not tested against a particular convergence criterion and is always executed a predetermined number of times.

The secondary iteration loops are converged when the source terms of the correction equation are converging towards zero everywhere. These iteration loops are terminated either when the number of iterations exceeds a prescribed maximum number of iterations or when a tolerance criterion is met. Similarly, the main iteration loop is converged when the coupling effects have been completely transmitted between the equations of pressure head and of mass concentration.

F.5.2 Matrix Solution Algorithm

The solution algorithm implemented in TARGET is somewhat different in two- and three-dimensional problems. In both cases, it is based on a ADI (Alternating Direction Implicit) algorithm which, in two-dimensional problems, is implemented as a line-by-line, column-by-column solution sequence of the resulting three-diagonal matrix. In three-dimensional problems, the same alternating direction scheme is used, but all planes are solved simultaneously, which results in the solution of a five-diagonal matrix.

Taking the two-dimensional solution algorithm as an example, a complete execution of the solver is composed of a line-by-line, followed by a column-by-column solution. Each solution sweep is composed of the following steps:

- o Assemble the three-dimensional matrix through suitable combination of terms.
- o Apply a forward elimination, backward substitution algorithm to the resulting matrix.
- o Repeat sequence an even number of times to achieve a complete solution.

F.5.3 Relaxation

In the guess and correct formulation, the dependent variable is a correction that has to be added to the previous value of the primary variables itself. A fully converged solution is obtained when the correction is everywhere identical to zero. Due to the non-linear nature of the coefficients, the convergence rate can show strong variations from one problem to another. In some cases, the correction starts at a high value and decreases very slowly without sign changes, while in the other cases, it may show an oscillatory pattern. In order to accelerate or damp the convergence rate, the correction is multiplied by a relaxation factor before being added to the primary variables.

Density coupled problems are inherently unstable because the fluid densities calculated after solution of the mass transport equation result in a substantial contribution to the pressure head equation. In order to stabilize this effect, an additional relaxation factor has been introduced on the density term itself. This approach has enabled simulation of otherwise intractable problems.

F.6 VALIDATION CASES

A selection of three validation cases are illustrated on the following pages. They have been chosen to illustrate a range of model features as well as a variety of types of validation:

- o **Case 3** - Comparison with analytical solution for one-dimensional transport problem.
- o **Case 4** - Comparison with laboratory data for two-dimensional falling water table problem.
- o **Case 7** - Comparison with U.S. Geological Survey ground-water model for practical application in a mine pit backfilling investigation.

CASE 3: TARGET_2DU VALIDATION - COMPARISON WITH ANALYTICAL SOLUTION

One-Dimensional Transport
Generated April, 1985

Objective: To compare the results of modeled contaminant transport in one dimension with the exact solution obtained analytically.

Description: The situation is one of uniform flow in one dimension where the specific discharge is constant along the flow axis. At some point in time, a contaminant or tracer of constant concentration is introduced into the system. The distribution of this concentration along the direction of the flow is investigated.

Specification: The initial and boundary conditions are:

if x = distance along the direction of flow;
for time ≤ 0 , tracer concentration, $C = 0$ at $x = 0$

for time > 0 , $C = C_0$, at $x = 0$
Velocity, $u = 1$ ft/day
porosity, $n = 1$

The exact analytical solution to this problem (Freeze and Cherry, 1979) is:

$$\frac{C}{C_0} = \frac{1}{2} \left[\operatorname{erfc} \left\{ \frac{x - ut}{2\sqrt{Dt}} \right\} + \exp \left(\frac{ux}{D} \right) \operatorname{erfc} \left\{ \frac{x + ut}{2\sqrt{Dt}} \right\} \right]$$

The finite-difference grid consists of 100 cells 10 feet long to simulate the 1,000-foot-long medium being modeled.

Two cases are modeled. In the first, the longitudinal dispersivity, $D_L = 10$ feet and the Peclet number, $Pe = 2$. In the second case, $D_L = 100$ feet and $Pe = 0.2$.

Results: The results of the modeled concentrations at various times are plotted in Figures 3-1 and 3-2. The y-axis represents relative concentration (C/C_0) and the x-axis represents a quantity which is a function of distance. This representation is convenient since it allows the exact solution of concentration distribution at any time to fall on the same curve. This exact solution is the curve drawn in each figure.

The analytical solution presented by Bear (1979) is an equation containing only the first item in the above equation. A similar solution has been presented by Freeze and Cherry (1979; see above) which includes a second term in the equation. Freeze, however, indicates that the second term is negligible under certain conditions, but does not give sufficient information with which to evaluate in the general case when the term is negligible. The analytical solution presented in Figures 3-1 and 3-2 does contain the assumption that the second term is negligible.

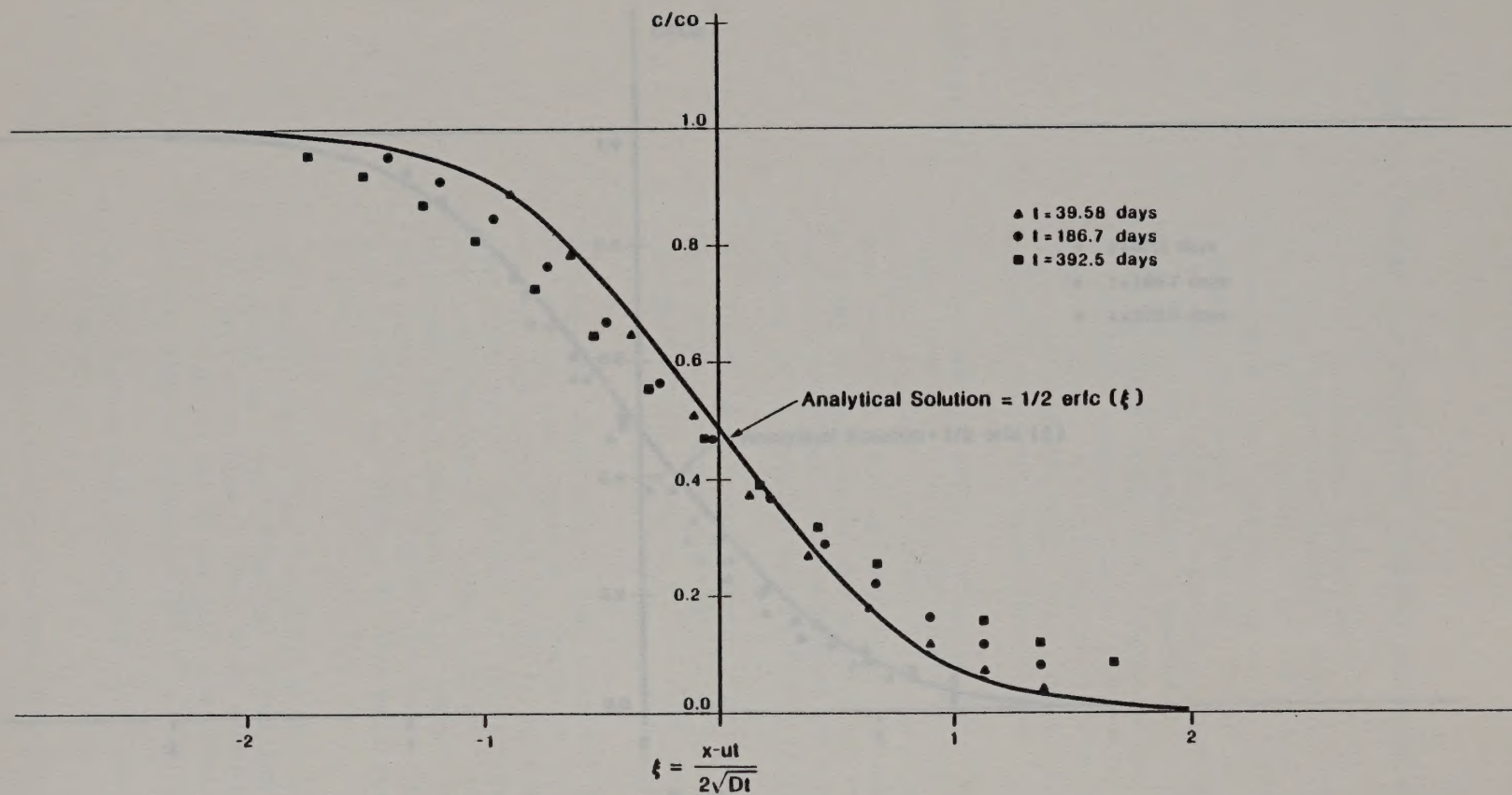
Discussion:

The results of the modeled concentration distributions compare favorably with the exact solution. The fact that the $C/C_0 = 0.5$ point is not predicted to lie exactly on the x-axis where $x = 0$ indicates that the modeled location of the moving concentration "front" is slightly behind the actual location. Since the calculation difference between mass inflow and outflow was very small, the cause of this discrepancy is probably an asymmetrical calculation of the concentration rather than a loss of solute.

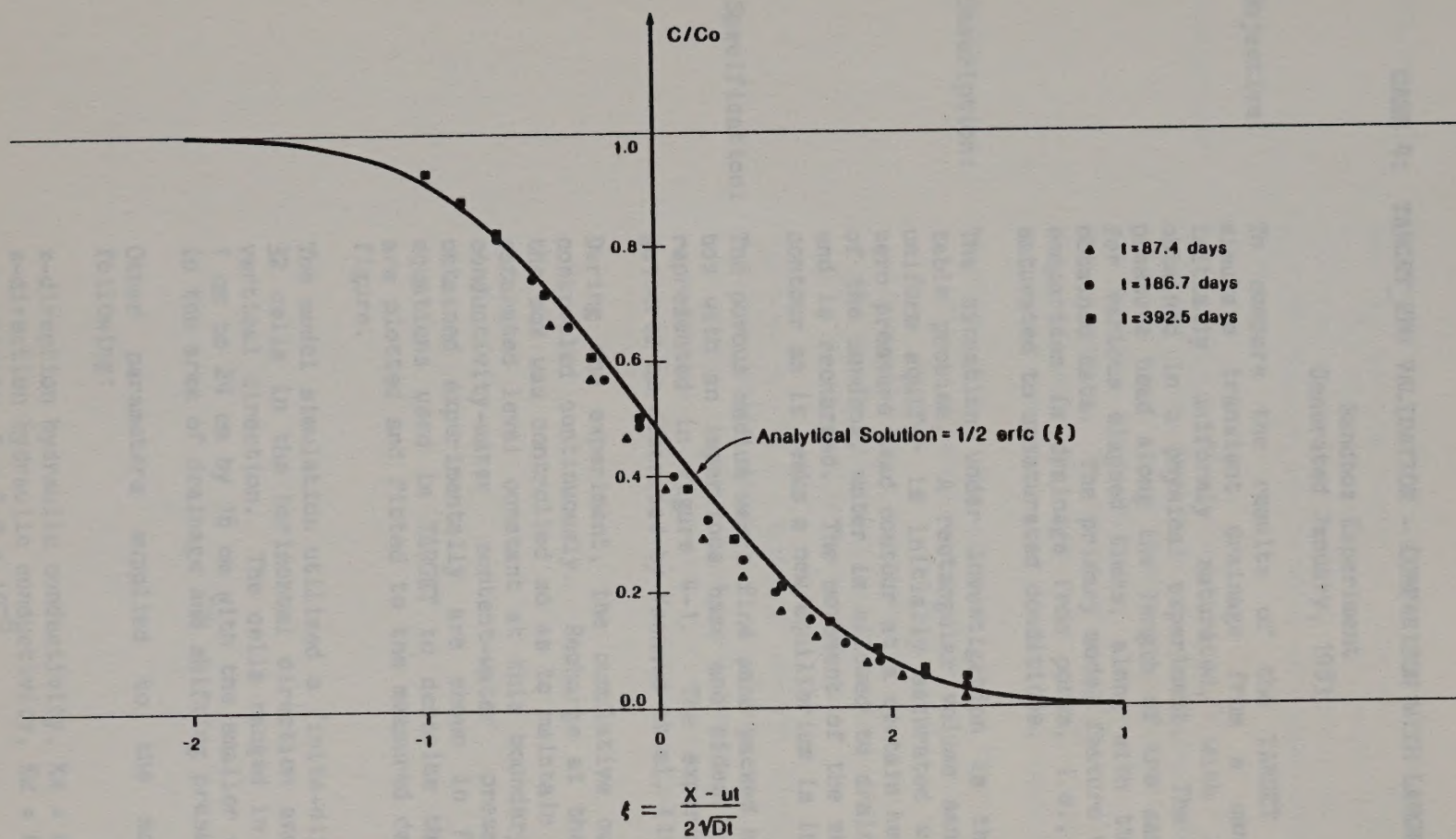
The results shown in Figure 3-2 are a better match to the analytical solution than those in Figure 3-1. The cell Peclet number, which is the ratio between convective and diffusive fluxes, is lower in Figure 3-2. This indicates that diffusion is the more controlling mechanism for the second figure. It is expected that a more dominant molecular diffusion action will result in predictions which more closely follow the exact analytical solution.

References:

- Bear, J. Hydraulics of Ground Water, McGraw-Hill Book Company, 1979, pp. 264-265.
- Freeze, R. A. and J. A. Cherry. Ground Water, Prentice Hall, Inc., 1979, pp. 388-393.



Modeled vs Analytical Solution
 $Pe = 2.0$



Modeled vs Analytical Solution

Pe = 0.2

CASE 4: TARGET_2DU VALIDATION - COMPARISON WITH LABORATORY DATA

Sandbox Experiment
Generated January, 1983

Objective: To compare the results of the TARGET model, used to simulate transient drainage from a sandbox which was initially uniformly saturated, with laboratory data obtained in a physical experiment. The contour of zero pressure head along the length of the sandbox is plotted for various elapsed times, along with the experimentally obtained data. The primary model feature validated in this comparison is drainage from pores, i.e., transition from saturated to unsaturated conditions.

Description: The situation under investigation is the falling water table problem. A rectangular volume sand representing a uniform aquifer is initially saturated with a horizontal zero pressure head contour at a certain height. At one end of the sandbox, water is allowed to drain while the other end is recharged. The movement of the zero pressure head contour as it seeks a new equilibrium is investigated.

Specification: The porous medium was a fine sand packed homogeneously in a box with an impervious base and sides. The situation is represented in Figure 4-1. The experimental data were gathered as described by Vachaud et al. (1971, 1975).

During the experiment, the cumulative outflow volume was controlled continuously. Recharge at the opposite end of the box was controlled so as to maintain the height of the saturated level constant at this boundary. The hydraulic conductivity-water content-water pressure head data obtained experimentally are shown in Figure 4-2. The equations used in TARGET to describe these relationships are plotted and fitted to the measured data points in this figure.

The model simulation utilized a finite-difference grid with 32 cells in the horizontal direction and 31 cells in the vertical direction. The cells ranged in size from 1 cm by 1 cm to 24 cm by 16 cm with the smaller cells concentrated in the area of drainage and shifting pressure head.

Other parameters supplied to the model include the following:

x-direction hydraulic conductivity, $K_x = 0.011$ cm/sec
z-direction hydraulic conductivity, $K_z = 0.011$ cm/sec
storativity, $S = 4.9 \times 10^{-5}$
porosity, $n = 0.3$

Results: The model prediction of the zero value contour of pressure head at various times is plotted in Figures 4-3 through 4-6. The experimentally obtained data for the same contour are also presented in these figures. As can be seen, the modeled results are in good agreement with the laboratory data.

Discussion: The results at four instants in time are presented in the figures. At the earliest instance, the model shows a slightly lower water table than the measured values, with the largest discrepancy at the area of steepest pressure head gradient. By the time of the next displayed instance, the two sets of data are nearly identical, and this agreement remains in the following displayed instances.

References: Vachaud, G.M., M. Vauclin, J.L. Thorny, and D. Khanji (1971). Etude Experimentale du Drainage de la Recharge des Nappes a Surface Libre dans un Modele Bidimensionel. Laboratoire de Mechanique des Fluides, Universite Scientifique et Medicale de Grenoble, Cendex, 53, 38 - Grenoble-Care, France.

Vauclin, M., G.M. Vachaud, and D. Khanji (1975). Two-Dimensional Numerical Analysis of Transient Water Transfer in Saturated-Unsaturated Soils. Institut de Mecanique, Universite Scientifique et Medicale de Grenoble, B.P. 53 - F. 38401 - Grenoble-Cedex, France.

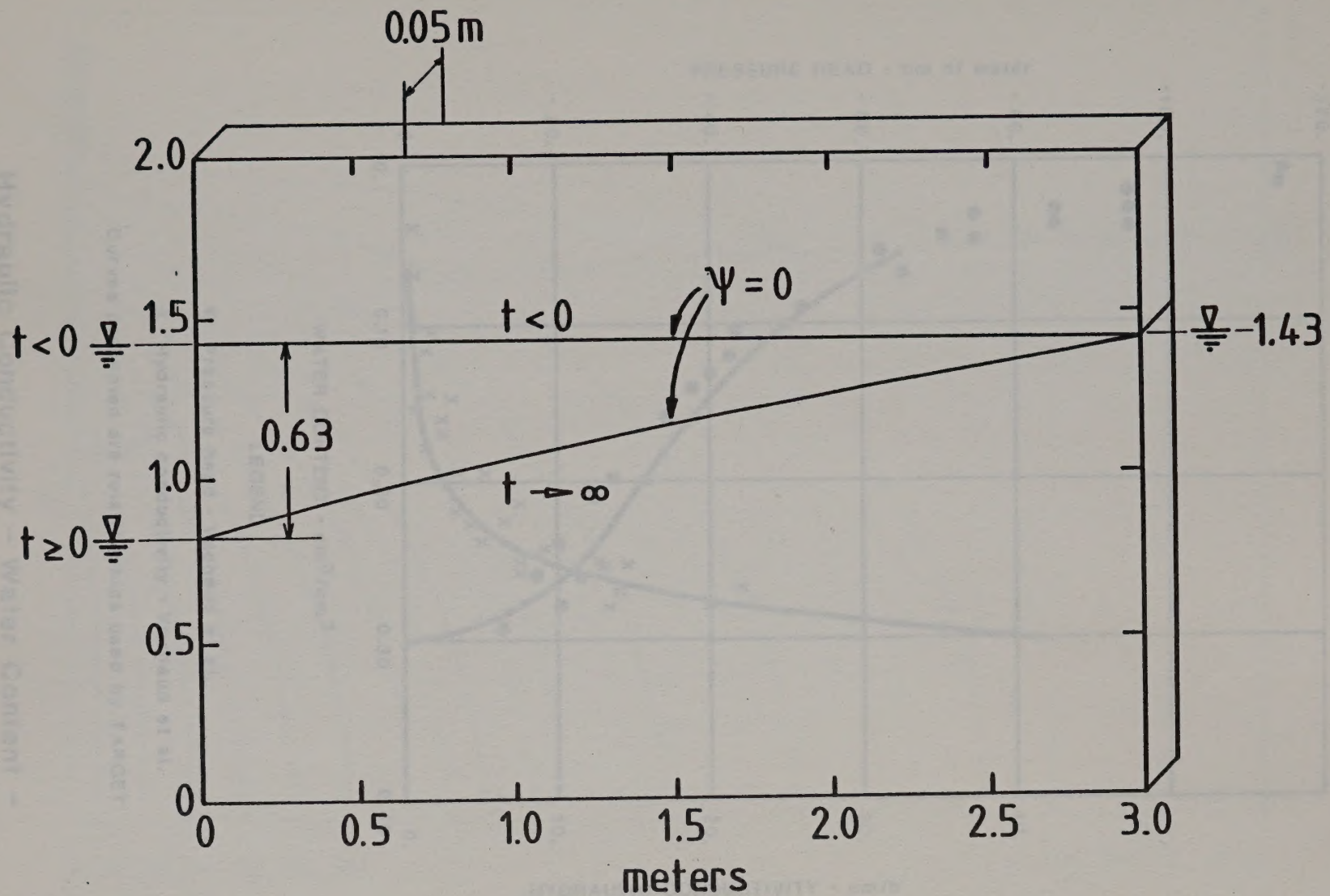
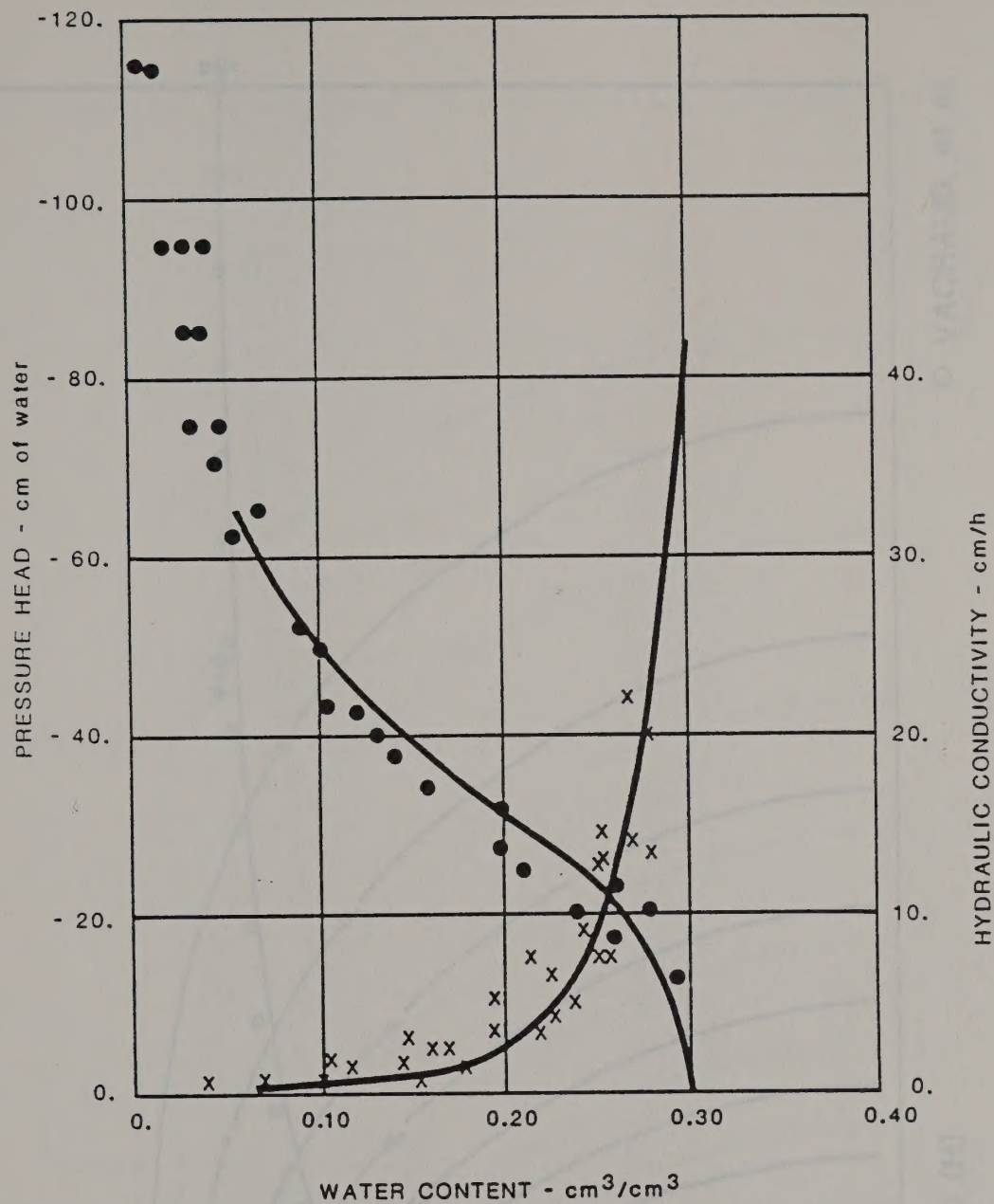


Figure 4-1
Schematic Diagram
Falling Water Table Simulation



LEGEND

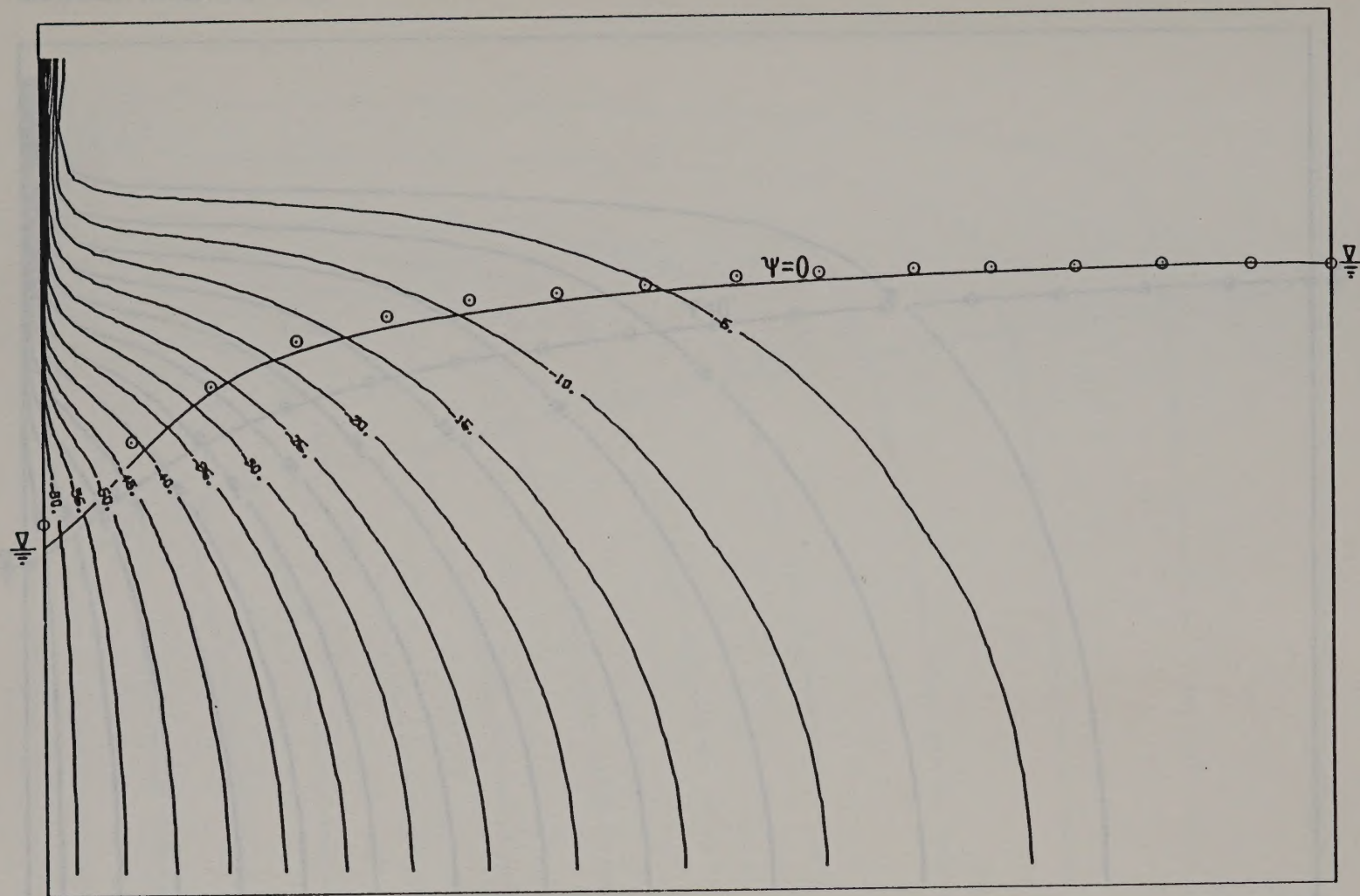
- Pressure head - Vachaud et al.
- x Hydraulic conductivity - Vachaud et al.

Curves presented are relationships used by TARGET

Hydraulic Conductivity - Water Content -
Water Pressure Head Relationships
Comparison of TARGET Model Simulation vs
Experimentally Obtained Data

CONTOUR INTERVAL = 5.

11-JAN-83



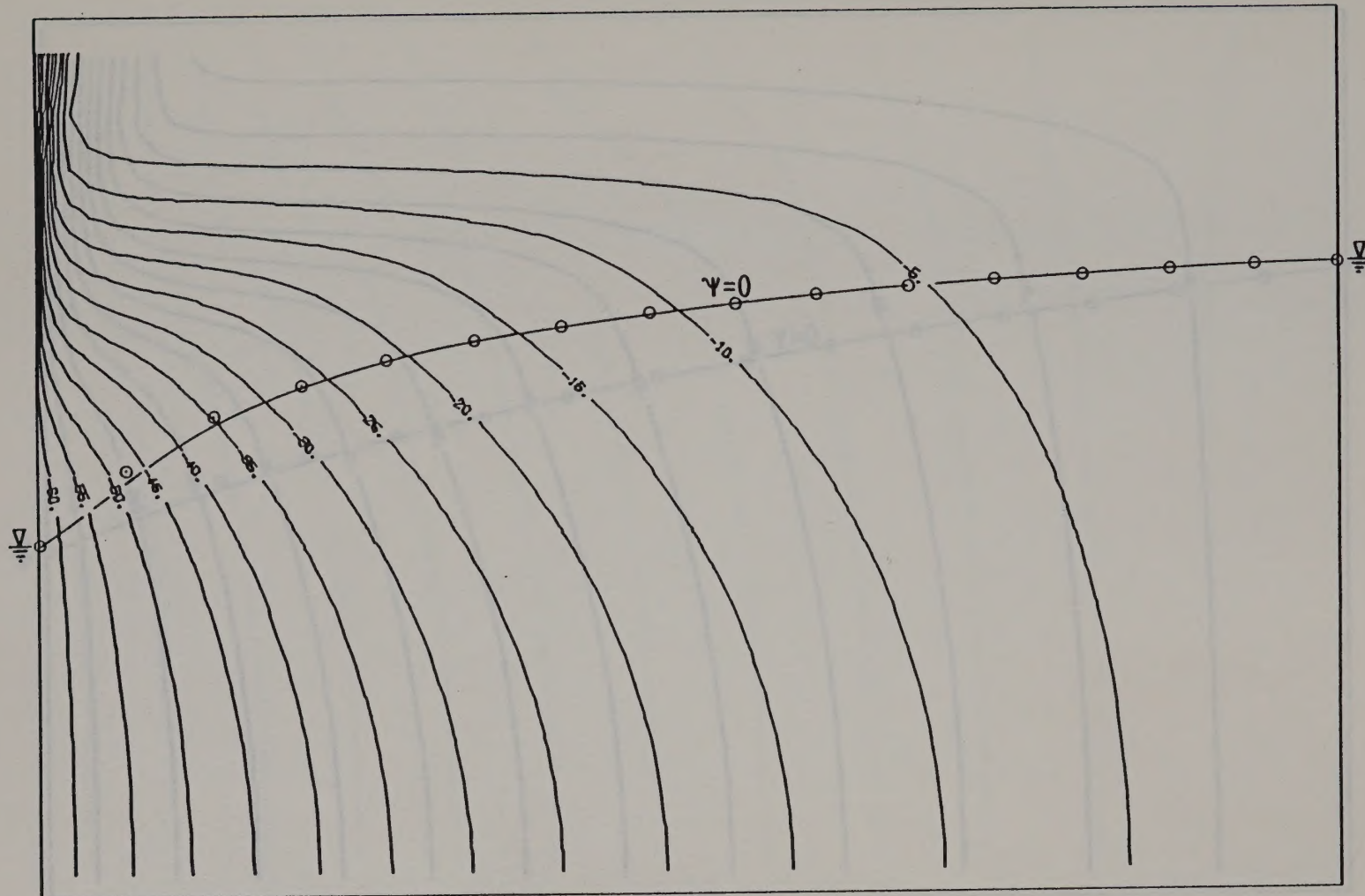
POTENTIAL HEAD (H)

© VACHAUD, et al.

Figure 4-3
Plot at Time = 108 Step = 17

CONTOUR INTERVAL = 5.

11-JAN-83



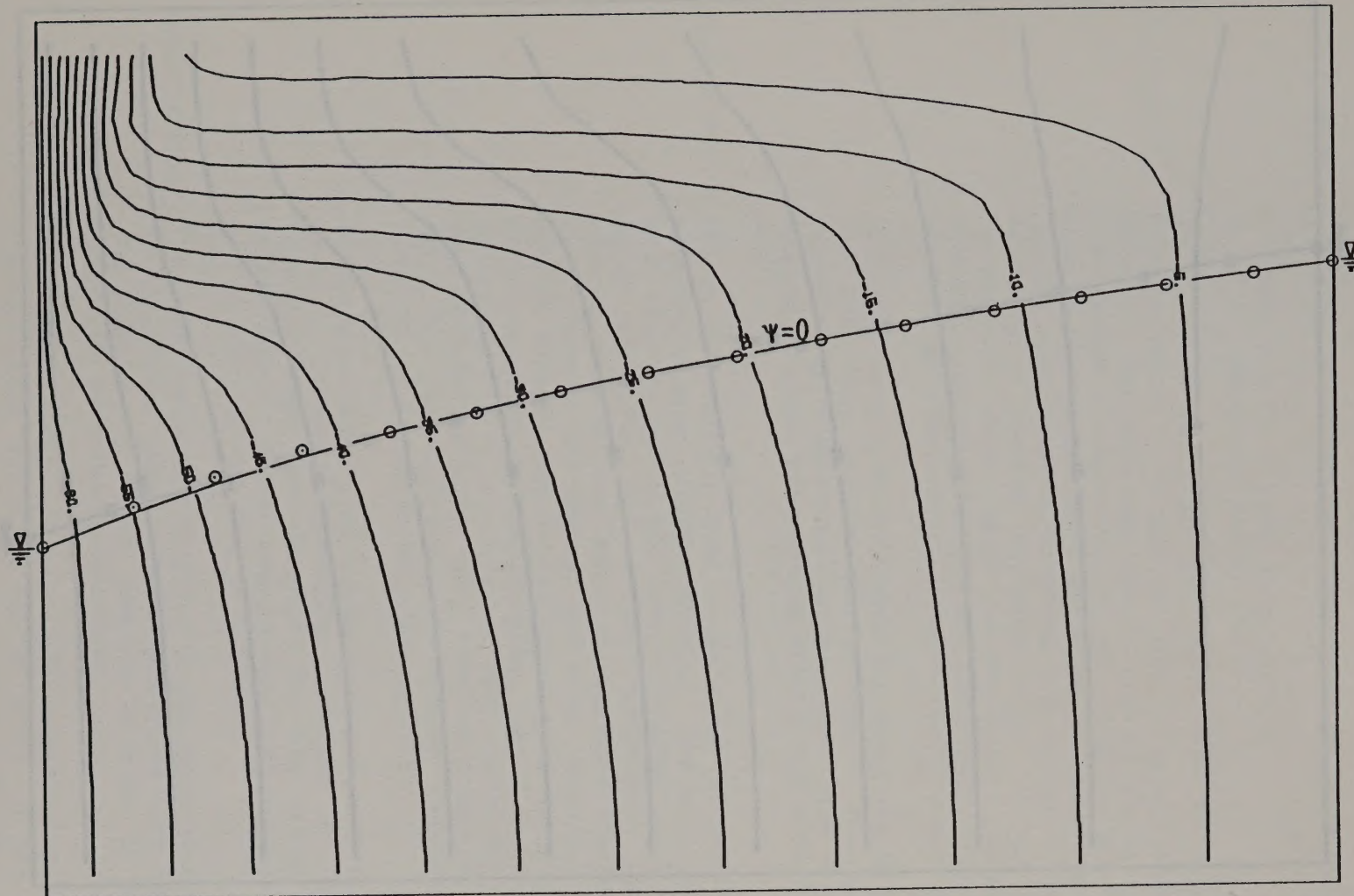
POTENTIAL HEAD (H)

© VACHAUD, et al.

Figure 4-4
Plot at Time = 360 Step = 31

CONTOUR INTERVAL = 5.

11-JAN-83



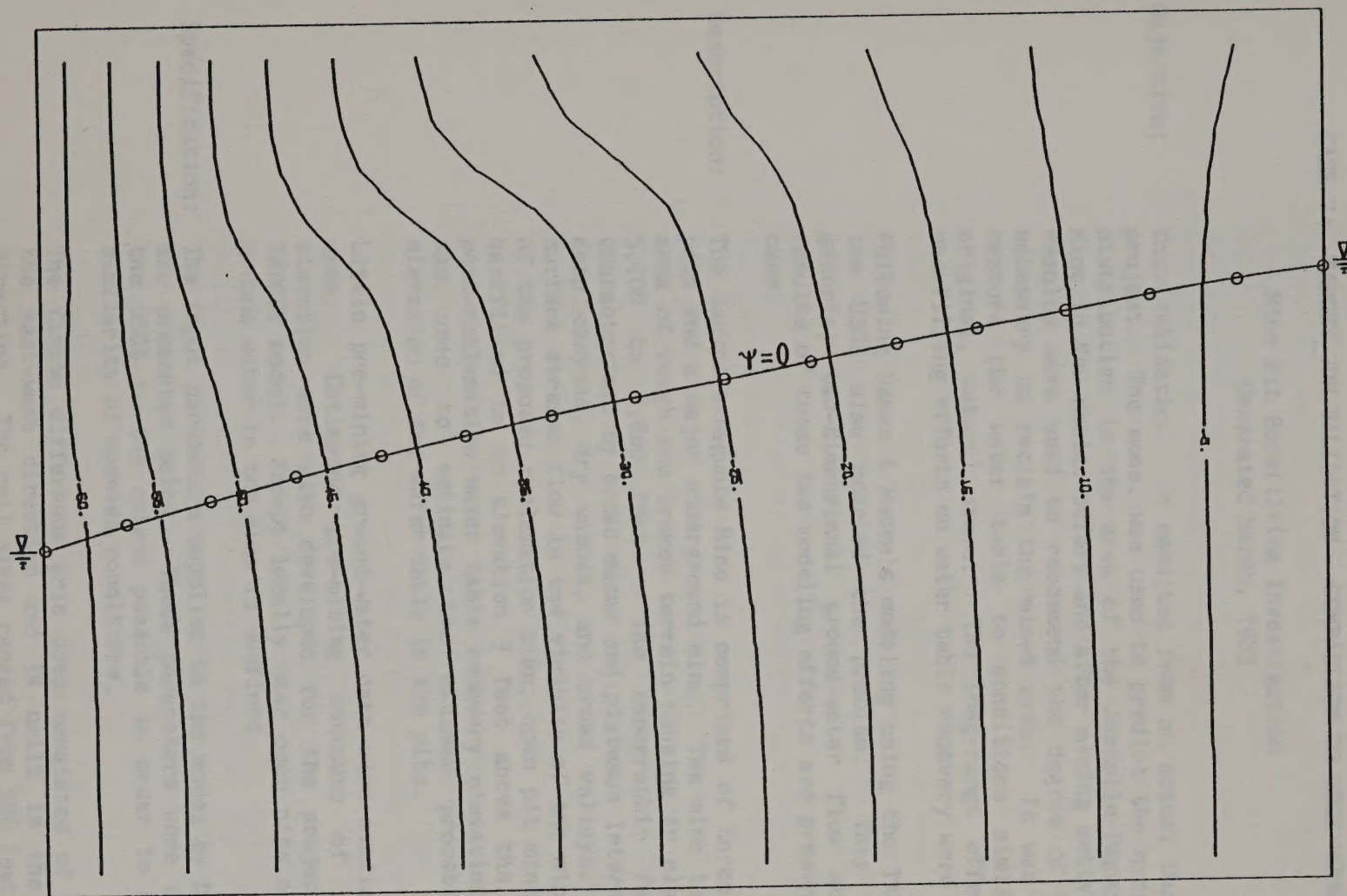
POTENTIAL HEAD (H)

© VACHAUD, et al.

Figure 4-5
Plot at Time = 3,600 Step = 73

CONTOUR INTERVAL = 5.

11-JAN-83



POTENTIAL HEAD (H)

© VACHAUD, et al.

Figure 4-6
Plot at Time = 36,000 Step = 129

CASE 7: TARGET_2DH VALIDATION - COMPARISON TO USGS MODEL

Mine Pit Backfilling Investigation
Generated March, 1983

Objective: This validation was the result of an actual Dames & Moore project. The model was used to predict the hydraulic head distribution in the area of the Jackpile-Paguate Uranium Mine in New Mexico before and after mining activities. The results were used to recommend the degree of backfilling necessary to reclaim the mined area. It was desired to restore the water table to conditions similar to its original, natural state. The long-range effects of the backfilling efforts on water table recovery were predicted.

Following Dames & Moore's modeling using the TARGET model, the USGS also modeled the problem. They used their generic, two-dimensional ground-water flow model. The results of these two modeling efforts are presented in this case.

Description: The Jackpile-Paguate Mine is comprised of three major open pits and a major underground mine. The mine is located in an area of rough and broken terrain ranging in elevation from 5,700 to 7,000 feet. The topographic features are characterized by broad mesas and plateaus interspersed with deep canyons, dry washes, and broad valleys. Two major surface streams flow in the vicinity of the mine. As part of the proposed reclamation plan, open pit mines are to be backfilled to an elevation 3 feet above the anticipated post-reclamation water table recovery elevation. Modeling was used to estimate the maximum probable recovery elevation of the water table in the pits.

Little pre-mining ground-water data were available for the area. Estimated pre-mining contours of ground-water elevation were also developed for the project using the TARGET model. Except locally near open pits and outcrops, ground water in the area is confined.

Specification: The input parameters supplied to the model by Dames & Moore are presented below. These parameters were used only by the USGS to the extent possible in order to maximize the similarity of modeled conditions.

The finite difference grid used consisted of 42 cells in the east-west direction and 34 cells in the north-south direction. The cell sizes ranged from 500 feet by 500 feet to 6,000 feet by 8,000 feet. The smaller cells were concentrated in the area of the mine pits.

The upper boundary of the model, the left boundary, and the right boundary all were set as zero flux (impermeable) boundaries. In order to simulate the outcrop of the Jackpile sandstone and its contact with alluvium along the Rio Paguete and Rio Moquino (the two major streams), an area of high hydraulic conductivity was placed along the lower portion of the grid and a fixed head was placed along the lower edge of the grid. A fixed head was also placed at the upper reach of the Rio Paguete alluvium to allow simulation of the interconnection of the Rio Paguete and the Rio Moquino surface streams along the extent of the alluvium. The fixed head was set at an appropriate elevation in two nodes to simulate ground-water levels in alluvium along the Rio Paguete and its uppermost interconnection with the Jackpile sandstone. By fixing the heads in these nodes, ground-water levels in nodes representing alluvium downgradient closely approximate those encountered in the field. Recharge to the system was simulated by a constant flux over a large areal portion of the aquifer. This combination of boundary conditions allows simulation of ground-water flow from recharge areas to outcrop areas.

The thickness of the Jackpile sandstone was input to the model on a cell-by-cell basis based upon a detailed map showing thickness of the unit at several hundred drill hole sites. The combination of saturated thickness and hydraulic conductivity of the Jackpile sandstone was used in the model to estimate transmissivity on a cell-by-cell basis.

The hydraulic conductivity varied from cell to cell in the model based on actual conditions. The values supplied to the model varied from 0.05 to 22 ft/day, except for backfill material which was modeled as 190 ft/day.

The storage coefficient for confined conditions in the Jackpile sandstone was modeled based upon a specific storage of $2.5 \times 10^{-6} \text{ ft}^{-1}$ and the local thickness of the aquifer. For unconfined conditions, a storage coefficient (specific yield) of 0.20 was used in the model. Total porosity of the Jackpile sandstone was estimated at about 28 percent based upon an in-situ density of 120 pounds per cubic foot.

Total porosity of backfill was estimated at 45 percent. The initial volumetric moisture content was measured at approximately 15 percent. Therefore, an unconfined storage coefficient of 0.30 was utilized in the model. The backfill is never under confined conditions and, therefore, a confined storage coefficient is not required for the backfill material. Virtually no changes occur in water levels in alluvium, therefore, the model is insensitive to the values chosen for storativity of the alluvium.

Recharge to the aquifer was estimated to range between 0.12 to 0.24 in/yr. The total recharge rate to the model was 12,700 ft³/day (66 gpm).

In order for the USGS to perform modeling comparable to that of Dames & Moore, to modifications to the USGS model were incorporated since the numerical solutions employed by the two models are different. First, the TARGET model requires that all cells (including the perimeter boundary) have a finite transmissivity. The USGS model was modified to match the TARGET model's requirement of a minimum transmissivity based on an equivalent thickness of 0.10 foot of saturated aquifer.

The second modification concerns the treatment of the modeled outcrop boundary. The TARGET model's requirement that cells have a finite transmissivity causes a small, steady ground-water flow through outcrop areas. This treatment was abandoned in the USGS model to allow cells to completely desaturate. This change allowed a steady-state simulation to be completed and further improved the agreement between the models for the simulated premining steady-state hydraulic-head distribution.

The USGS modeling effort also varied from the Dames & Moore effort in its simulation of field conditions in the model. The larger cells in the finite-difference grid were split into two cells in order to increase numerical stability in the USGS model.

Results:

The results of the model comparisons are presented in Figures 7-1 through 7-9. Three scenarios are represented in these figures, and are labeled as follows:

- Case 1 - Pre-mining simulation
- Case 2 - Post-mining simulation
- Case 3.5 - Post-mining simulation with recommended in-pit dam installed

The figures present comparisons over the entire modeled area, the immediate mine area, and also presents cross sections along selected grid rows through the mine area. The following is a list of these figures:

Figure 7-1 Case 1, entire area
 Figure 7-2 Case 3, entire area
 Figure 7-3 Case 1, detailed area
 Figure 7-4 Case 3, detailed area
 Figure 7-5 Case 3.5, detailed area
 Figure 7-6 Case 3.5, cross section, entire area, D&M row 14
 Figure 7-7 Case 3.5, cross section, entire area, D&M row 21
 Figure 7-8 Case 3.5, cross section, detailed area, D&M row 14
 Figure 7-9 Case 3.5, cross section, detailed area, D&M row 21

Discussion:

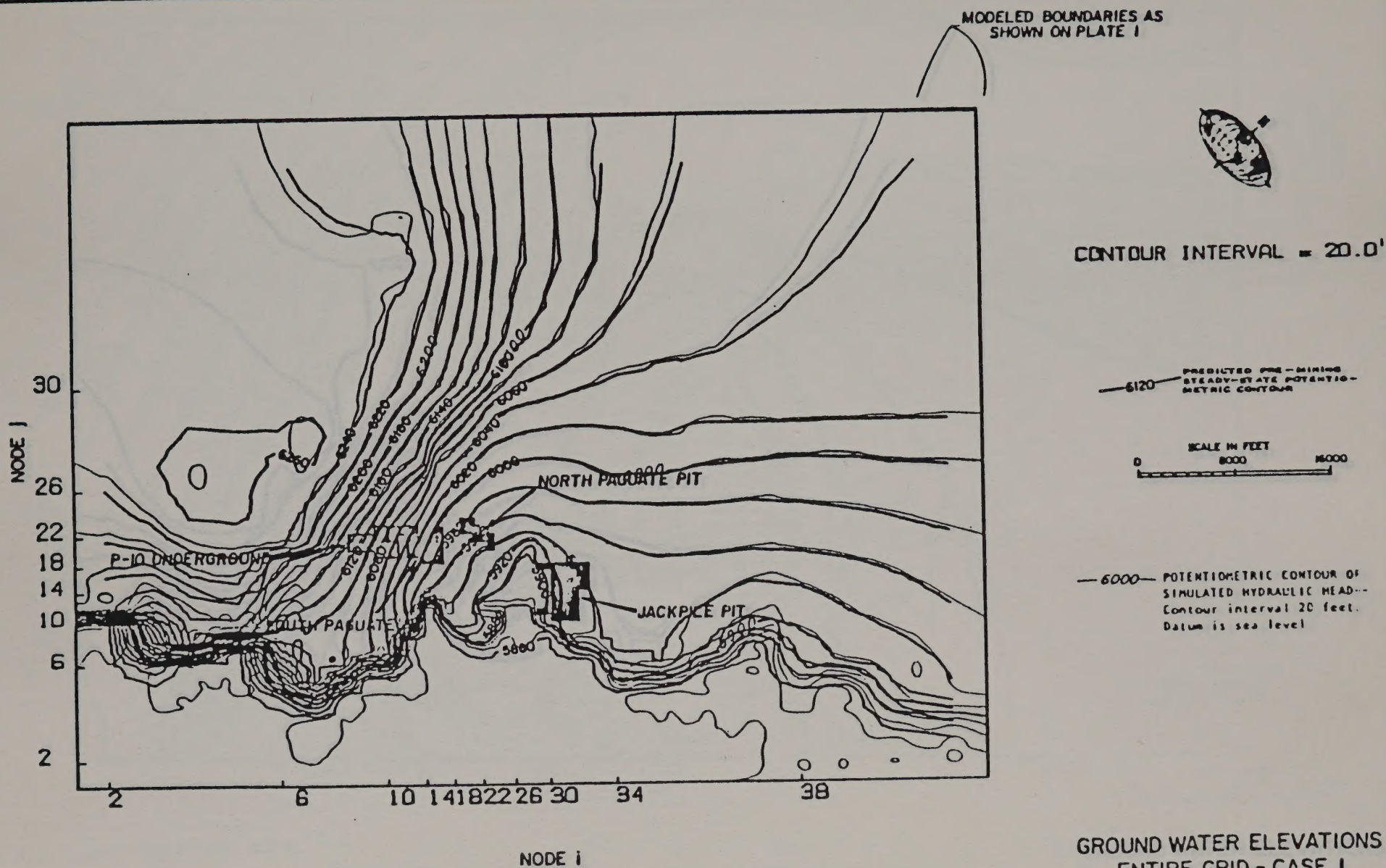
As can be seen in the accompanying figures, the results of simulation of the mine pit backfilling presented herein are consistent. In the simulation of the pre-mining case, the results from the two models are generally within 5 feet in computed heads. For the post-mining simulations, the results also agree closely except in the vicinity of the outcrop of the aquifer, where the USGS model computes heads that are commonly more than 40 feet higher than the TARGET model. These discrepancies diminish rapidly within distance from the outcrop.

In performing the comparison, the USGS stated in the discussion of their report that they found "no inconsistencies" of a mathematical or programming nature which significantly affected its results" when discussing the TARGET model.

References:

Dames & Moore, 1983. Evaluation of Hydrologic Effects Resulting from Pit Backfilling, The Anaconda Company's Jackpile-Paguate Uranium Mine, Valencia County, NM, Consultant Report dated March 23, 1983.

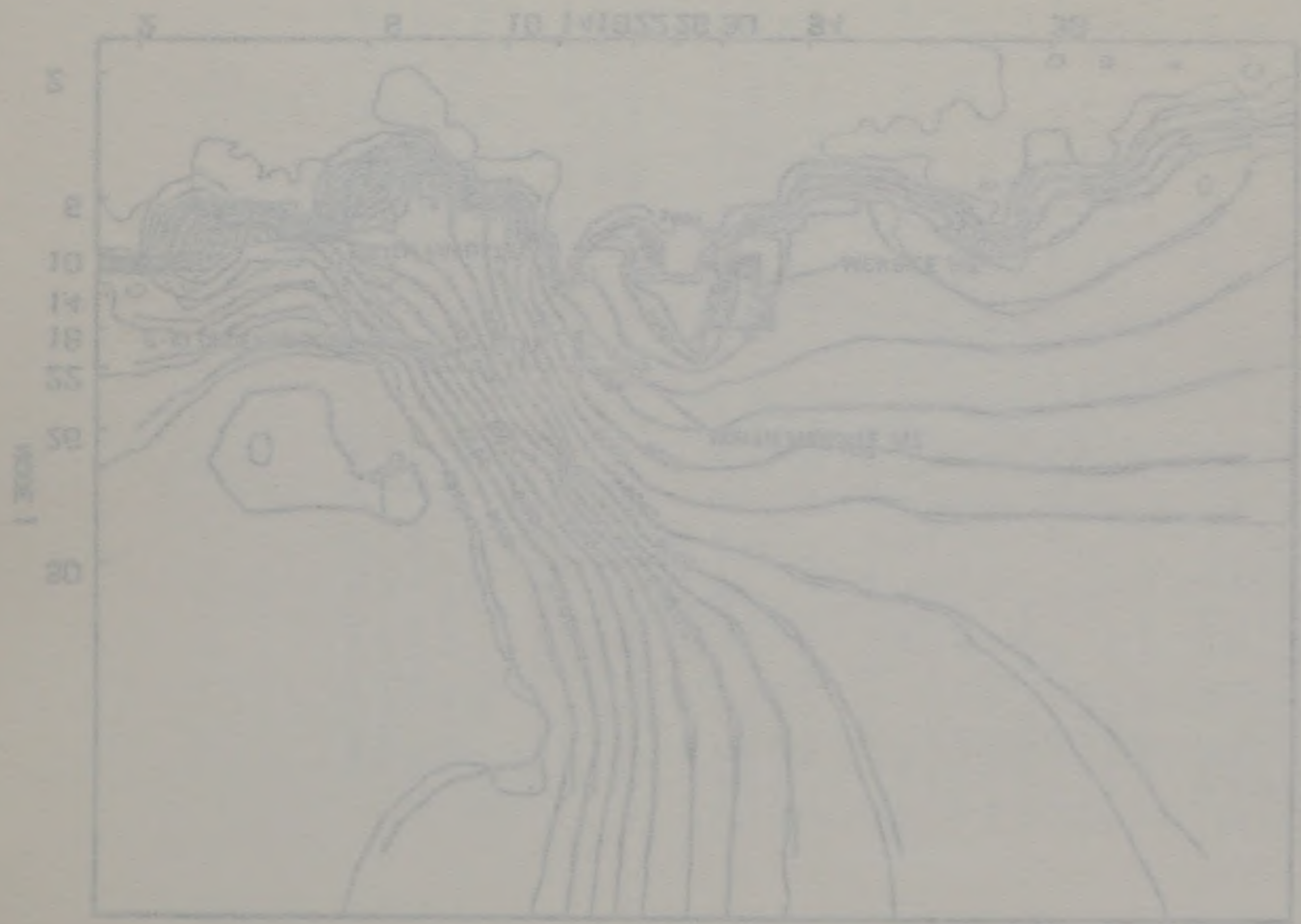
USGS. 1984. Results of Simulations Using a U.S. Geological Survey Generic Two-Dimensional Ground-Water-Flow Model to Process Input Data from the Dames & Moore Ground-Water-Flow Model of the Jackpile-Paguate Uranium Mine, New Mexico, USGS Report Transmitted August 23, 1984.



These elevations are relative to the datum of the 1929 mean low water of the tide.

Scale

ENTIRE SHEET - CASE 1
GROUND WATER ELEVATIONS



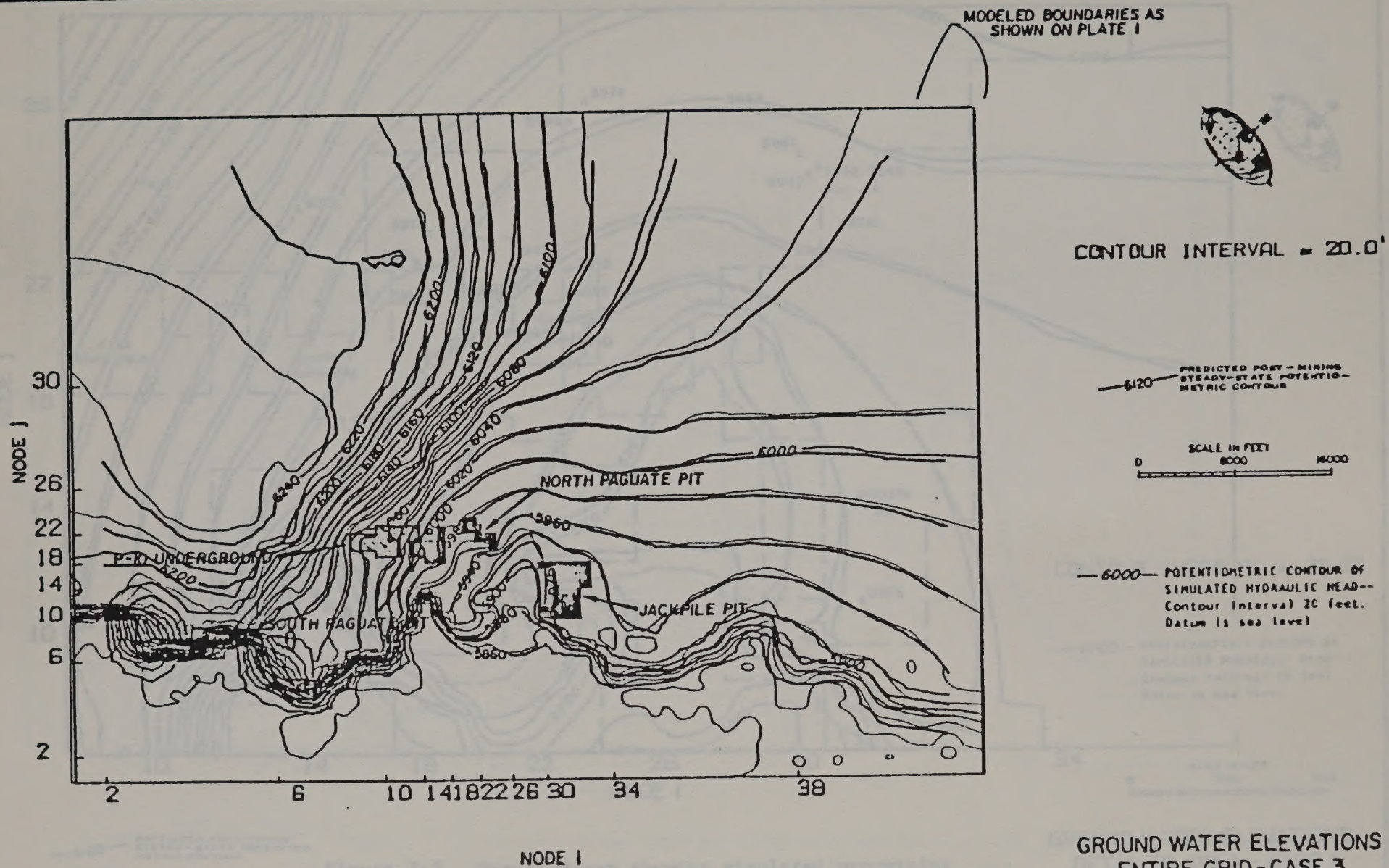


Figure 7-2. Map showing simulated post-mining and post-reclamation potentiometric heads (without artificial hydraulic barrier) in the entire modeled area for the simulation "case3".

in the model used for the simulation "model" (containing the model) and the simulation results are shown in Figure 3.5.

MODE 1

Figure 3.5-2
Simulation Results

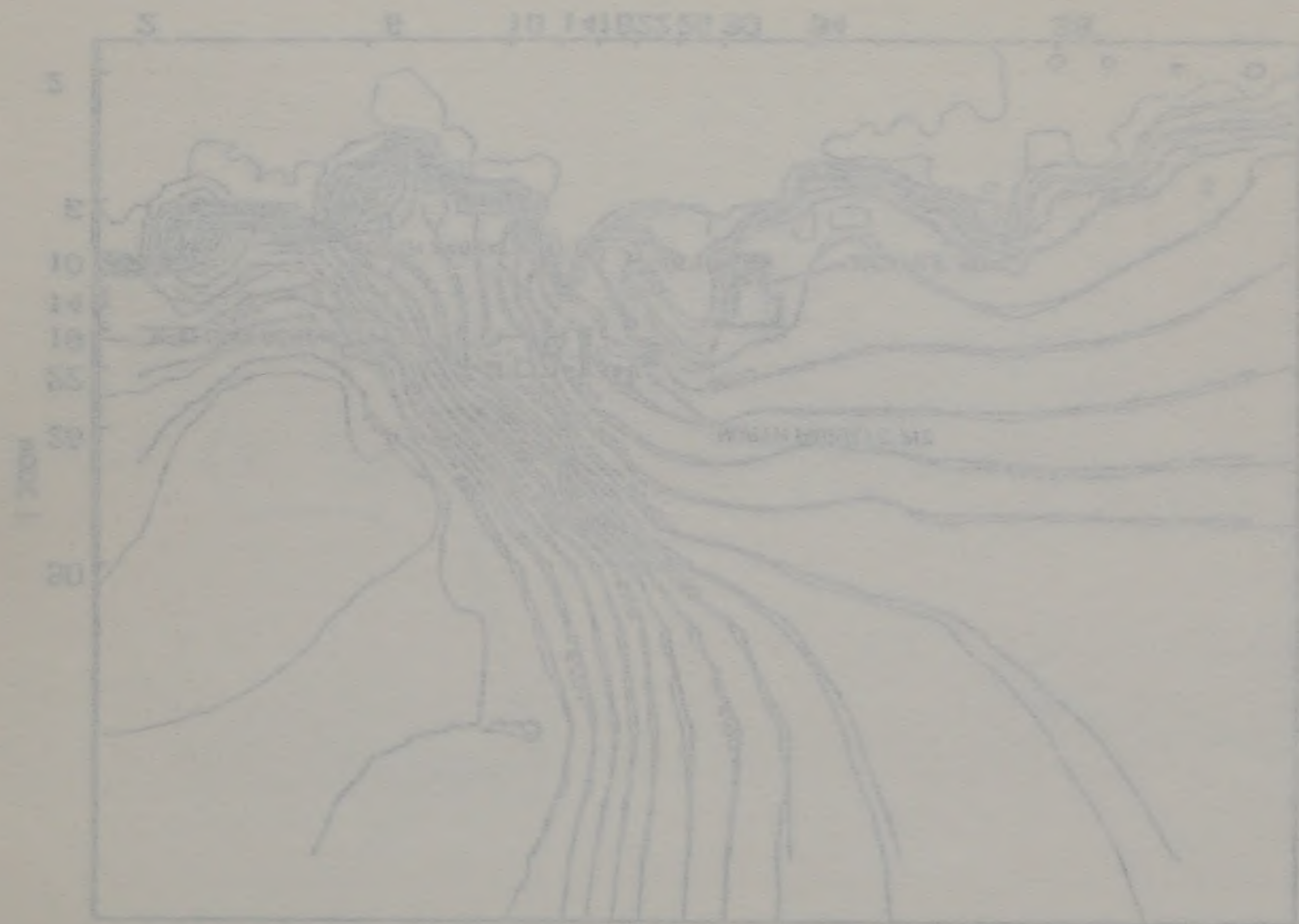


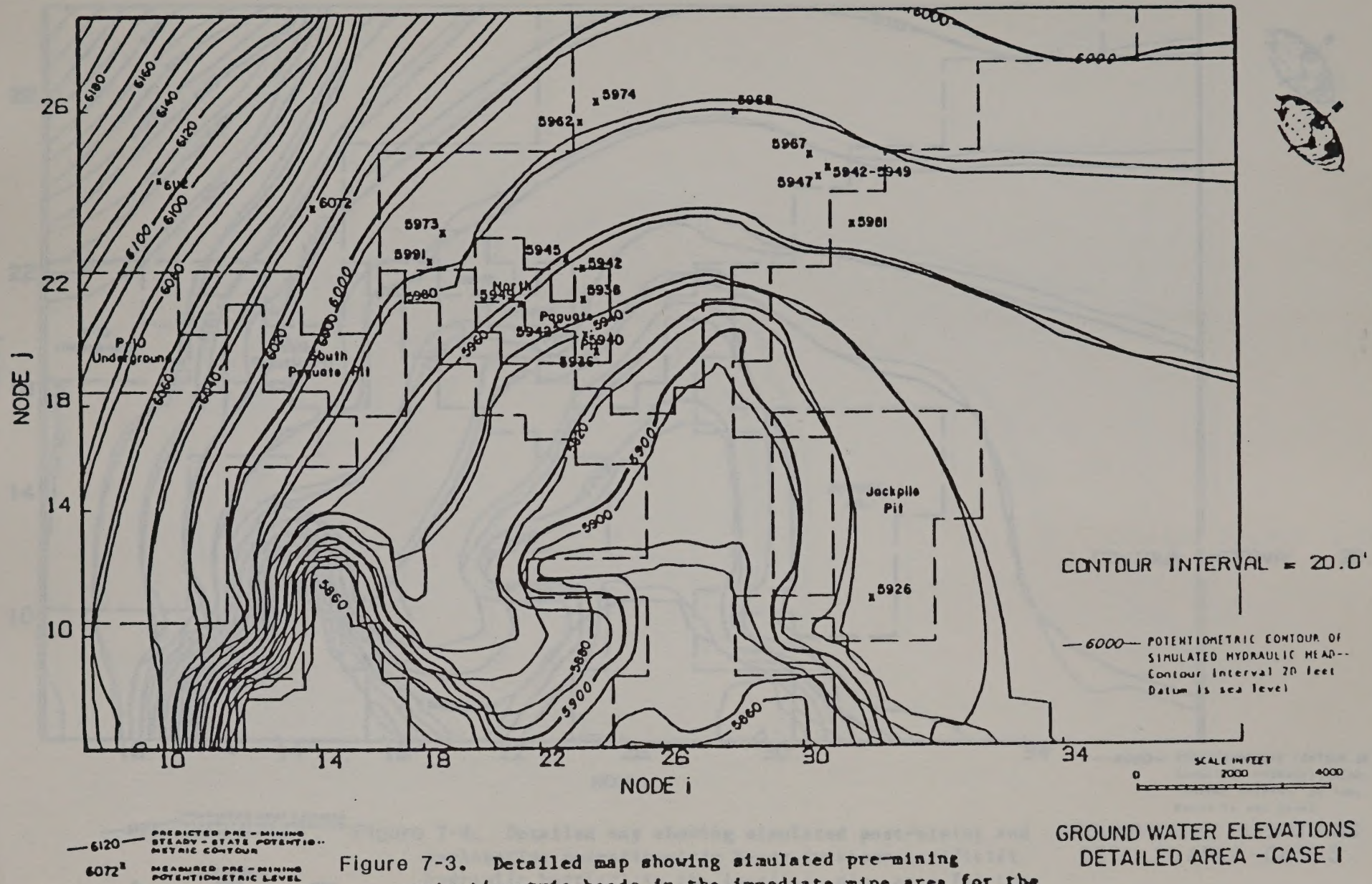
Figure 3.5-2
Simulation Results

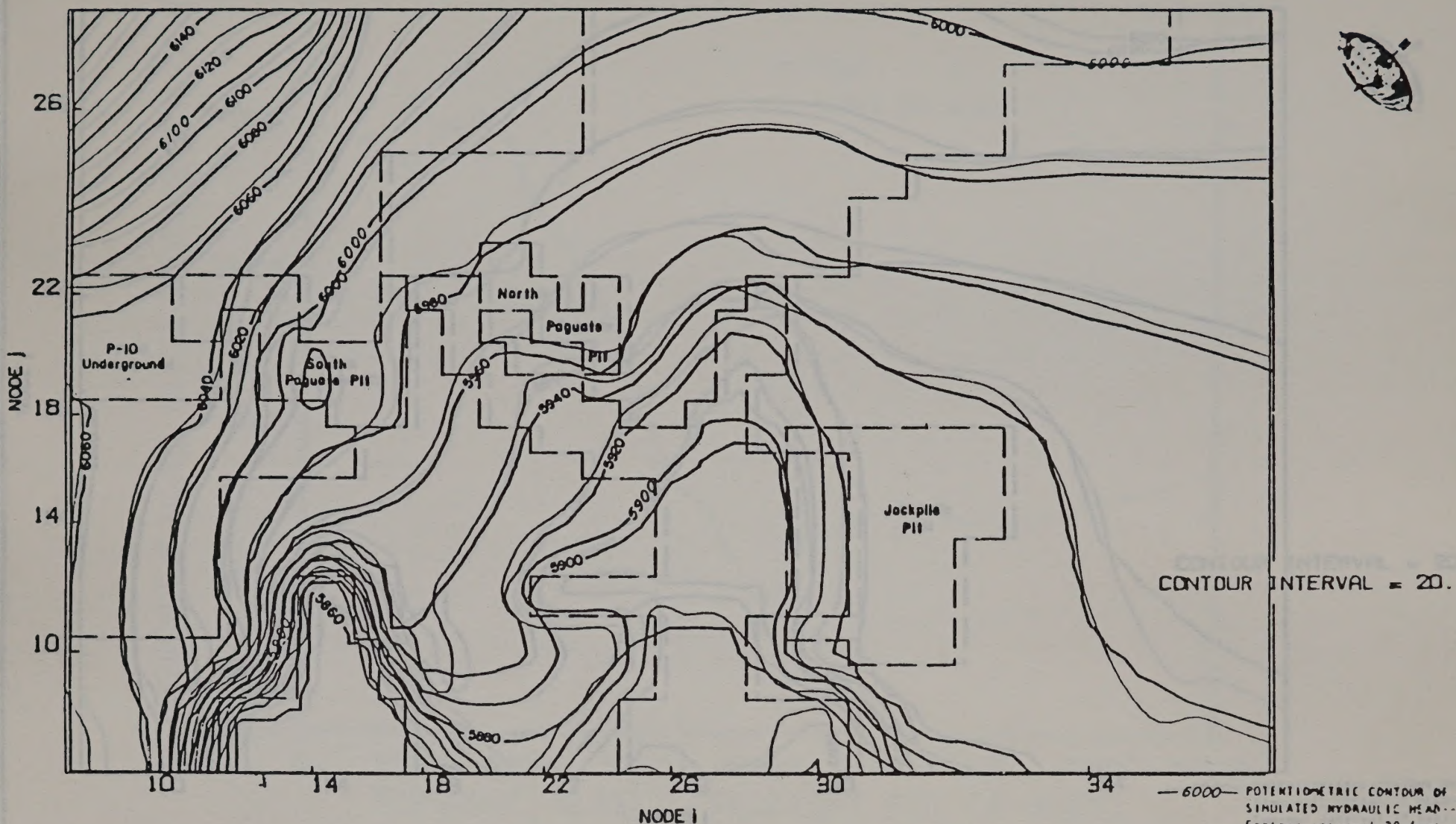
Figure 3.5-2
Simulation Results

Figure 3.5-2
Simulation Results



Figure 3.5-2
Simulation Results



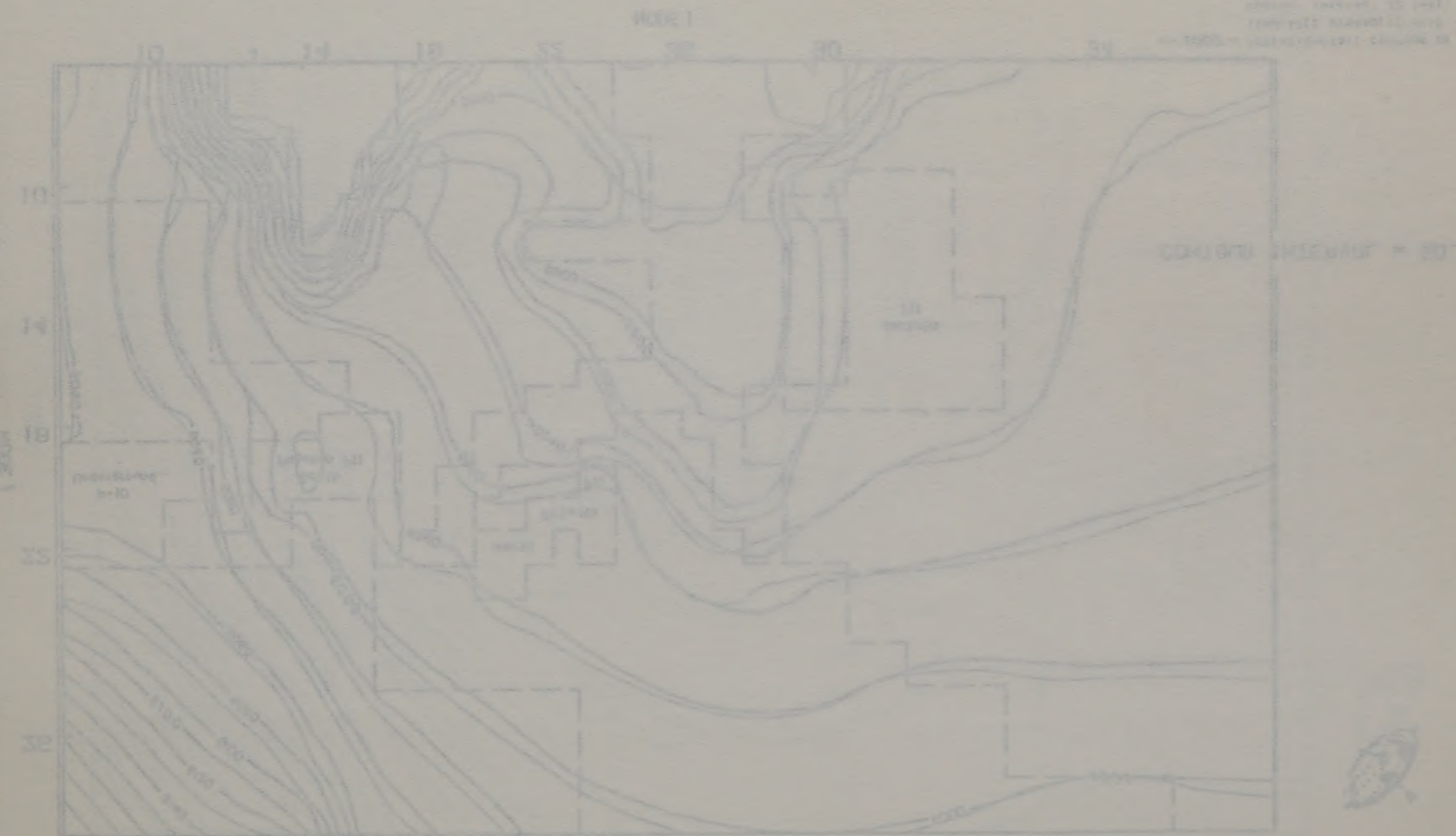
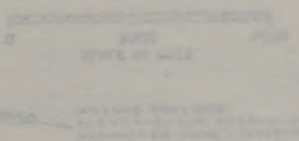


DEVELOPMENT CASE 2 GROUNDWATER EVALUATION

DATE: 10-11-1960
BY: J. H. [illegible]
FOR: [illegible]

The purpose of this evaluation is to determine the groundwater resources available for development of the proposed project. The evaluation is based on the following assumptions:

- 1. The groundwater is confined by an impermeable layer.
- 2. The groundwater is homogeneous and isotropic.
- 3. The groundwater is under steady-state conditions.



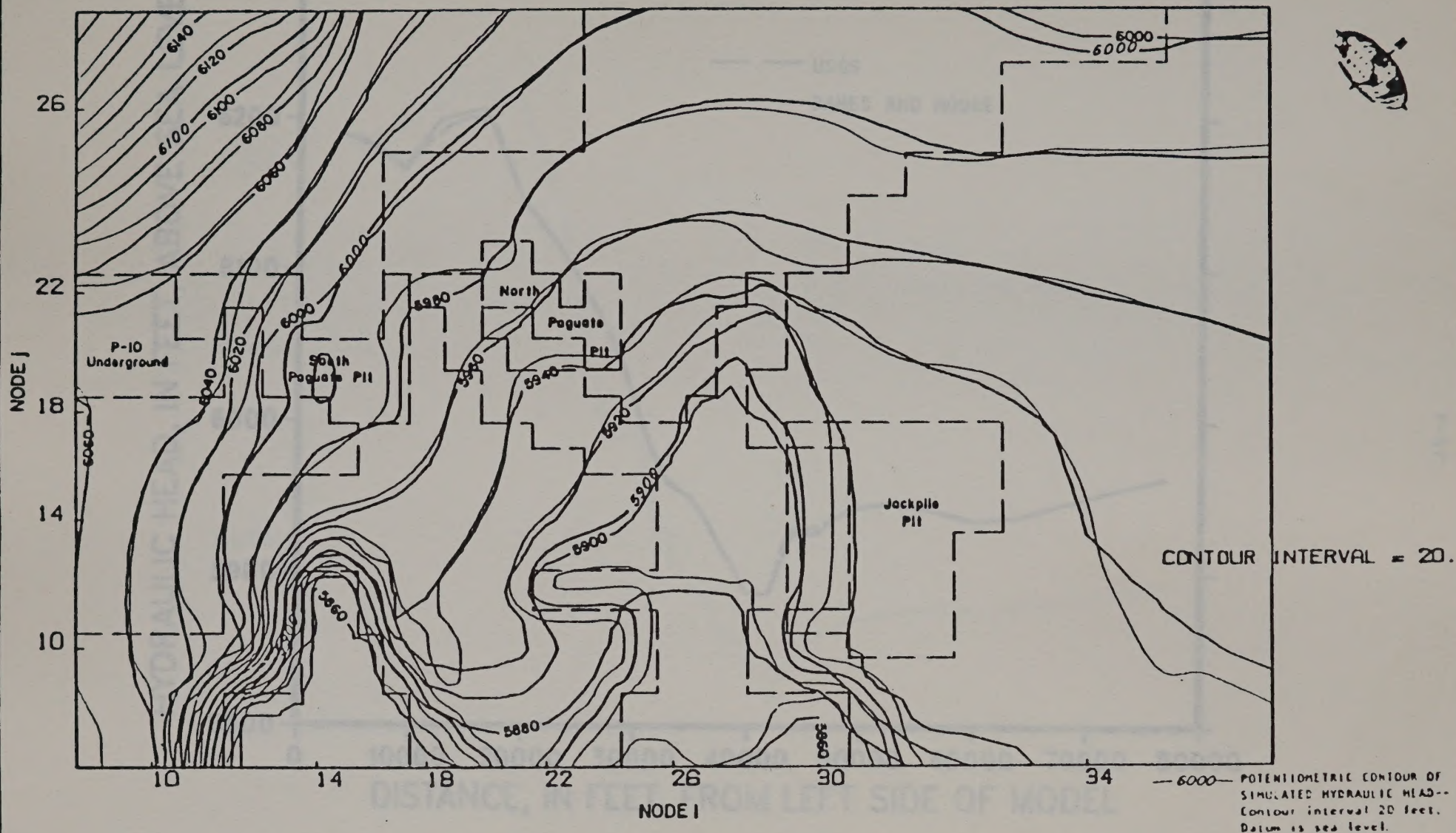
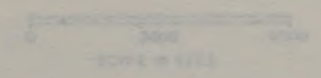


Figure 7-5. Detailed map showing simulated post-mining and post-reclamation potentiometric heads (with artificial hydraulic barrier in the North Paguate pit) in the immediate mine area for the simulation "case3.5".

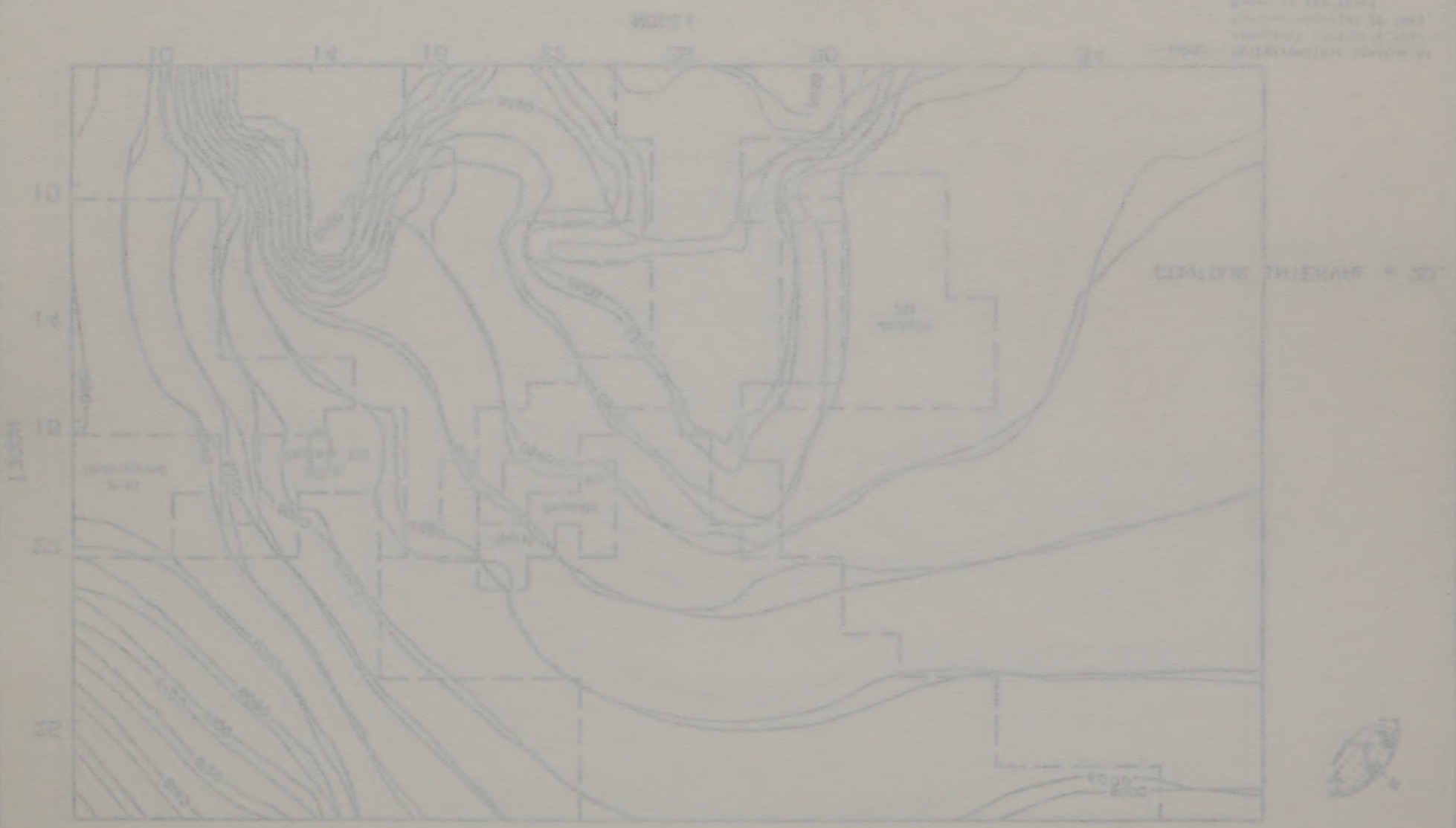
GROUND WATER ELEVATIONS
DETAILED AREA-CASE 3.5



2. The ...
...
...

UNITED STATES DEPARTMENT OF THE ARMY
ENGINEERING DIVISION
WASHINGTON, D. C.

...
...



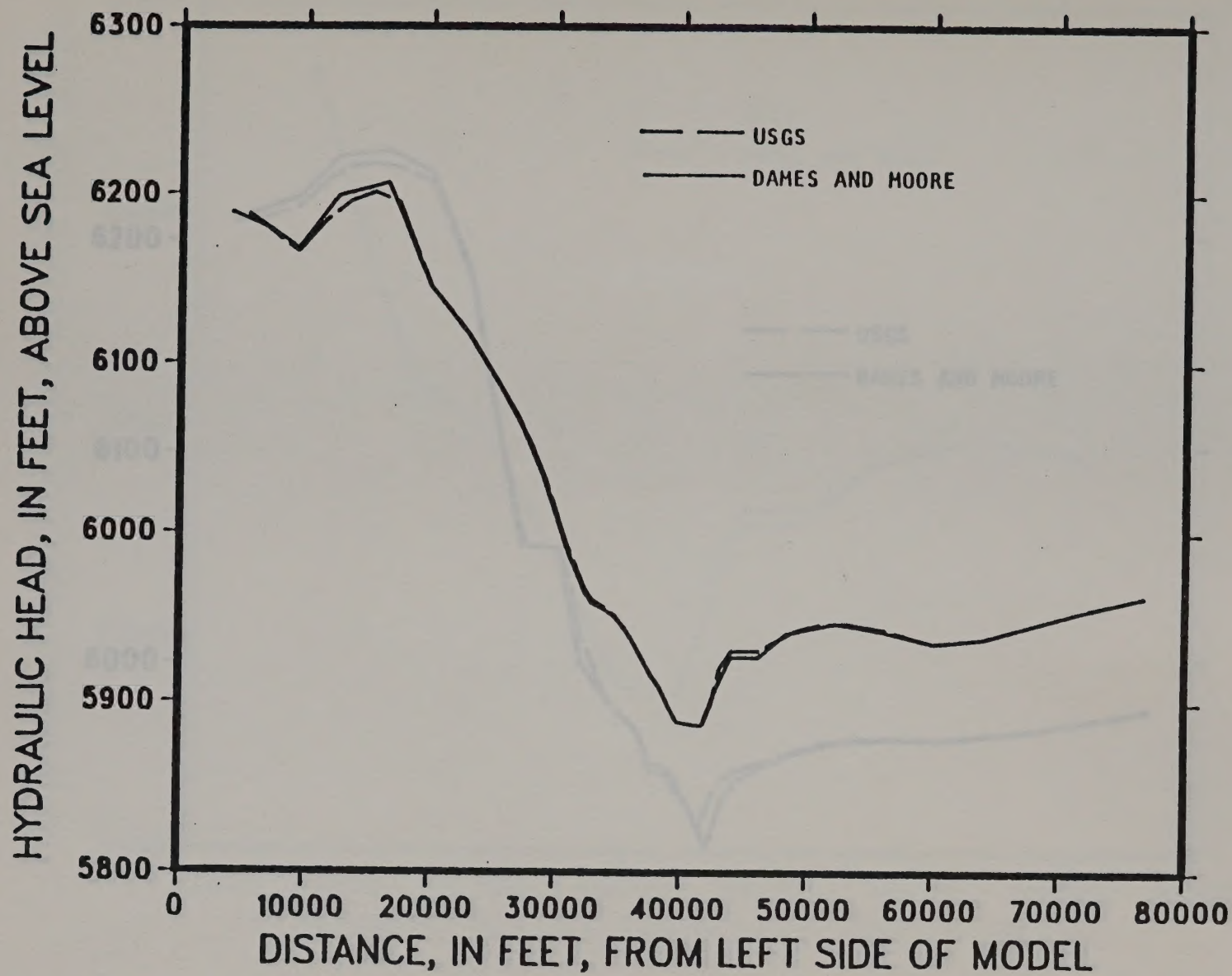


Figure 7-6. Cross-section of the entire modeled area along Dames and Moore model row 14 (USGS model row 28) through the Jackpile mine showing post-reclamation hydraulic heads for the simulation "case3.5".

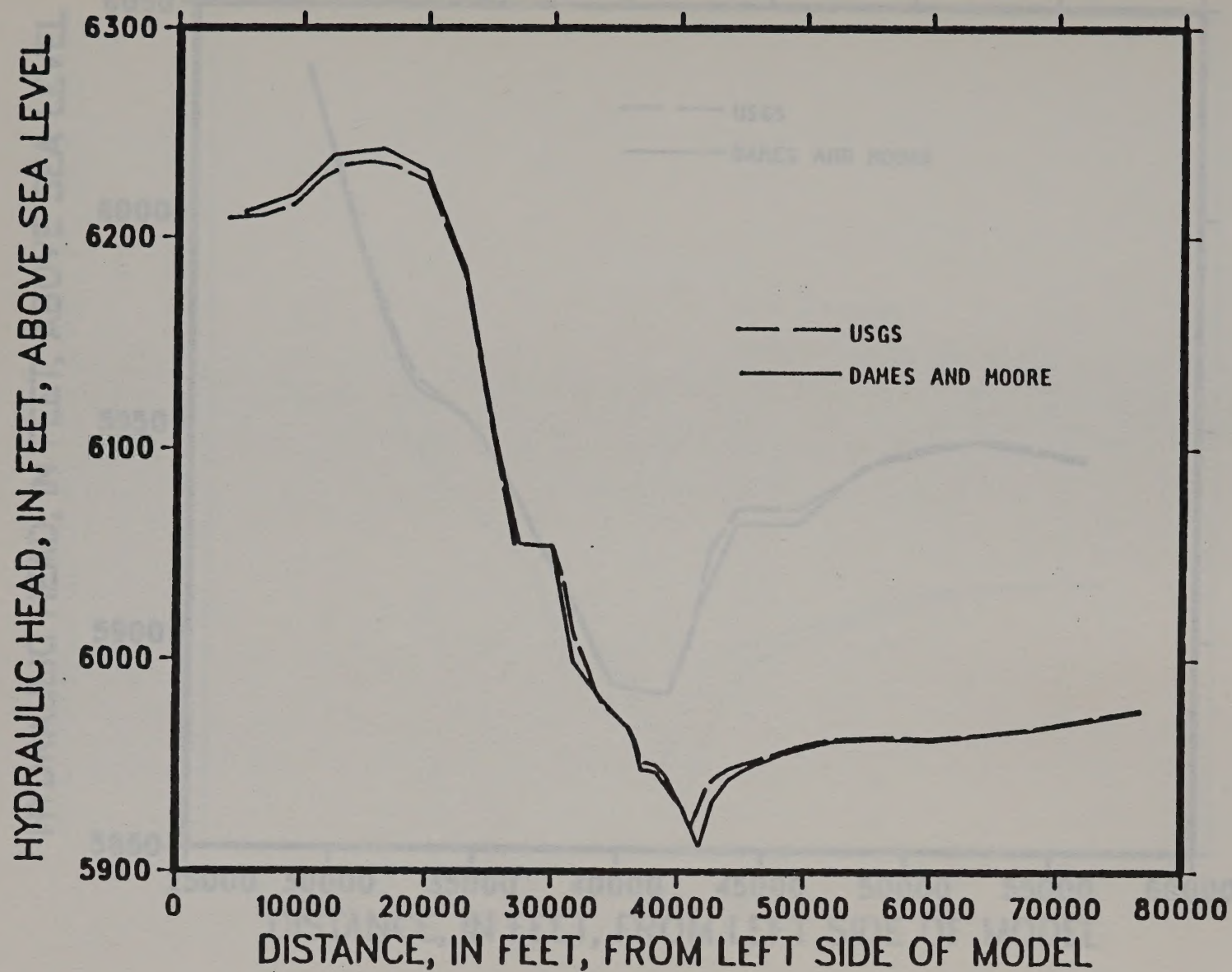
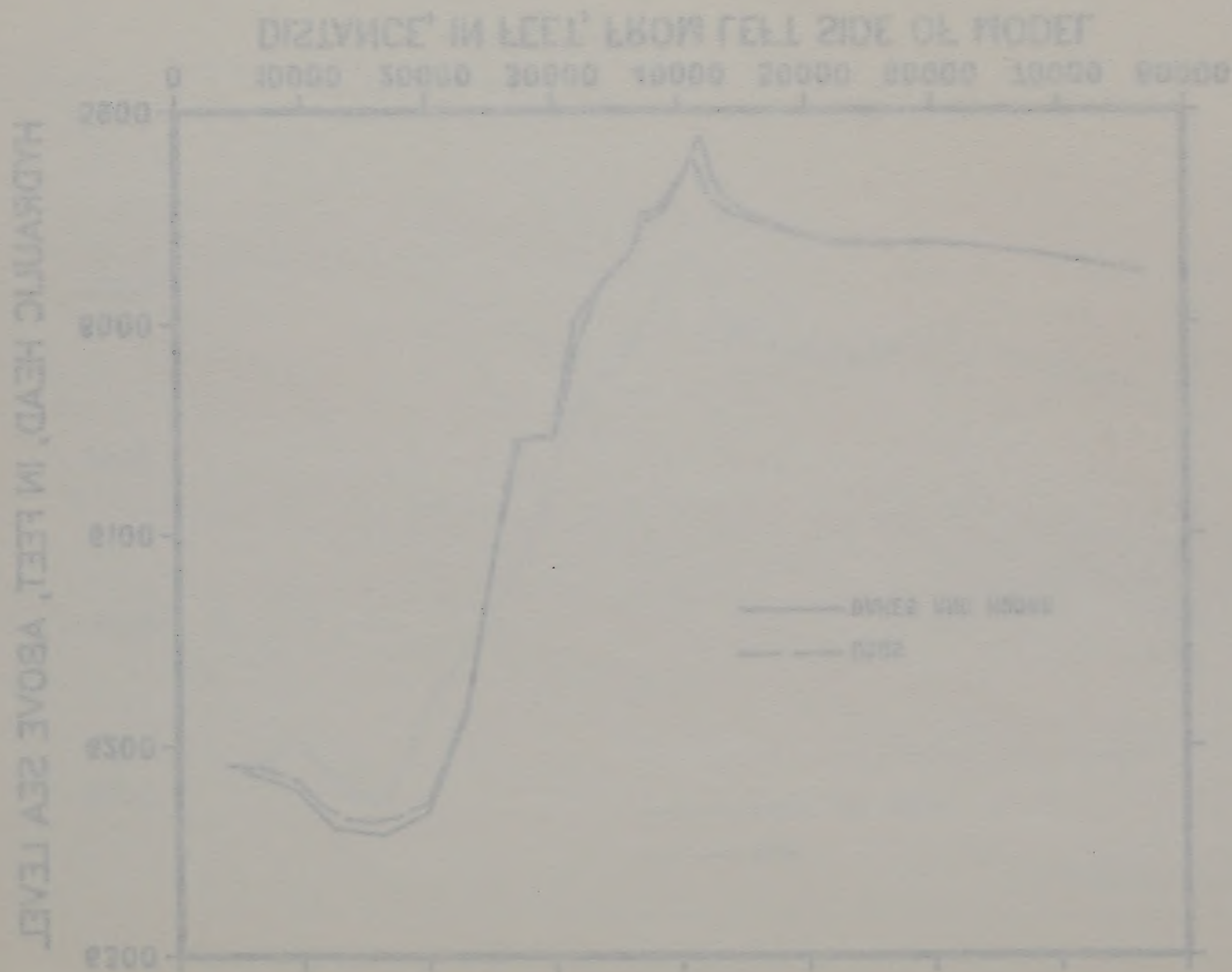


Figure 7-7. Cross-section of the entire modeled area along Dames and Moore model row 21 (also USGS model row 21) through underground mine P10, South and North Paguate mines showing post-reclamation hydraulic heads for the simulation "case3.5".

Figure 1-1. Cross-section of the water table at the station
 between water surface (left) and water table (right).
 The water table is shown as a dashed line. The water surface is shown as a solid line. The distance between the water surface and the water table is shown as a solid line. The distance between the water surface and the water table is shown as a solid line.



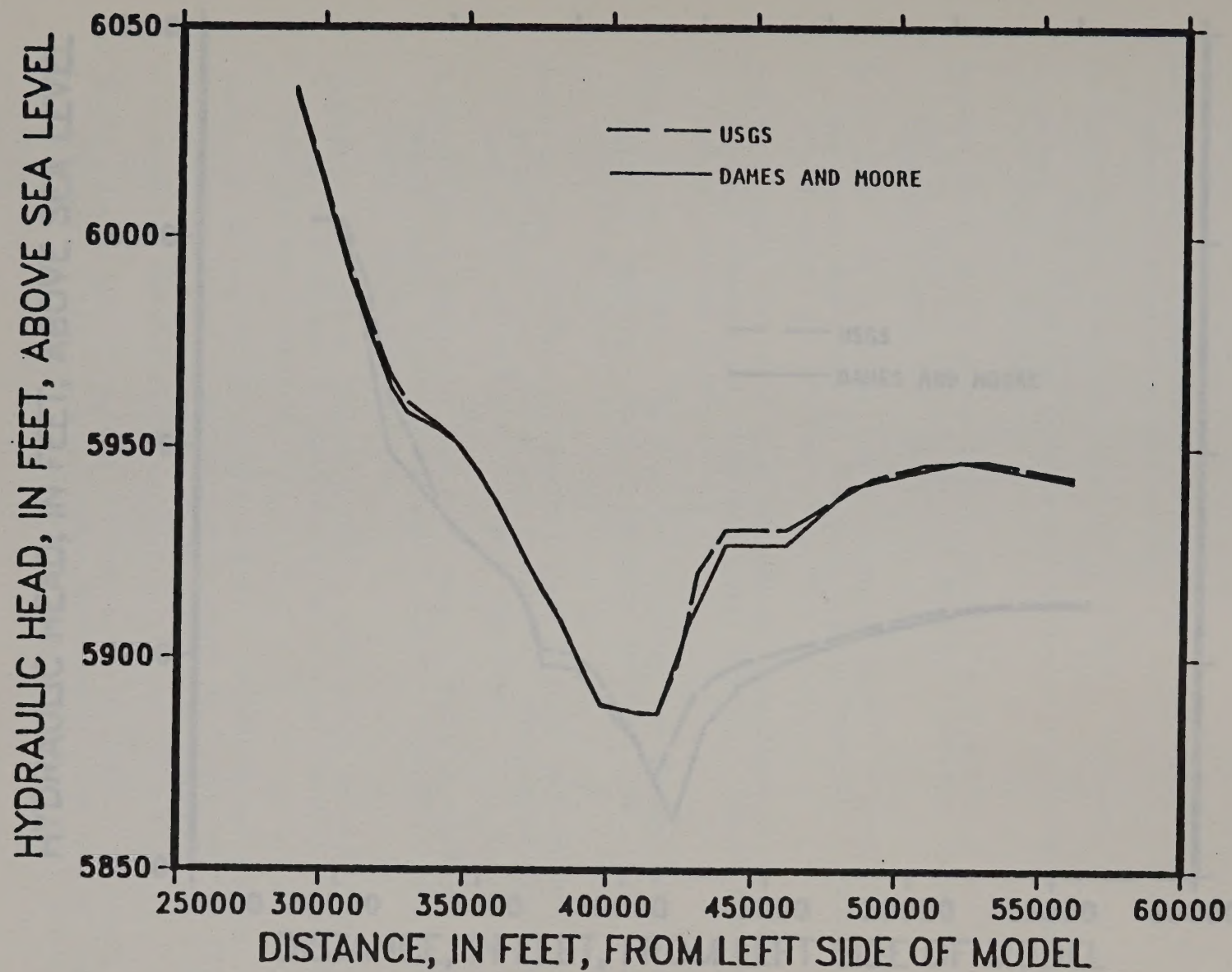
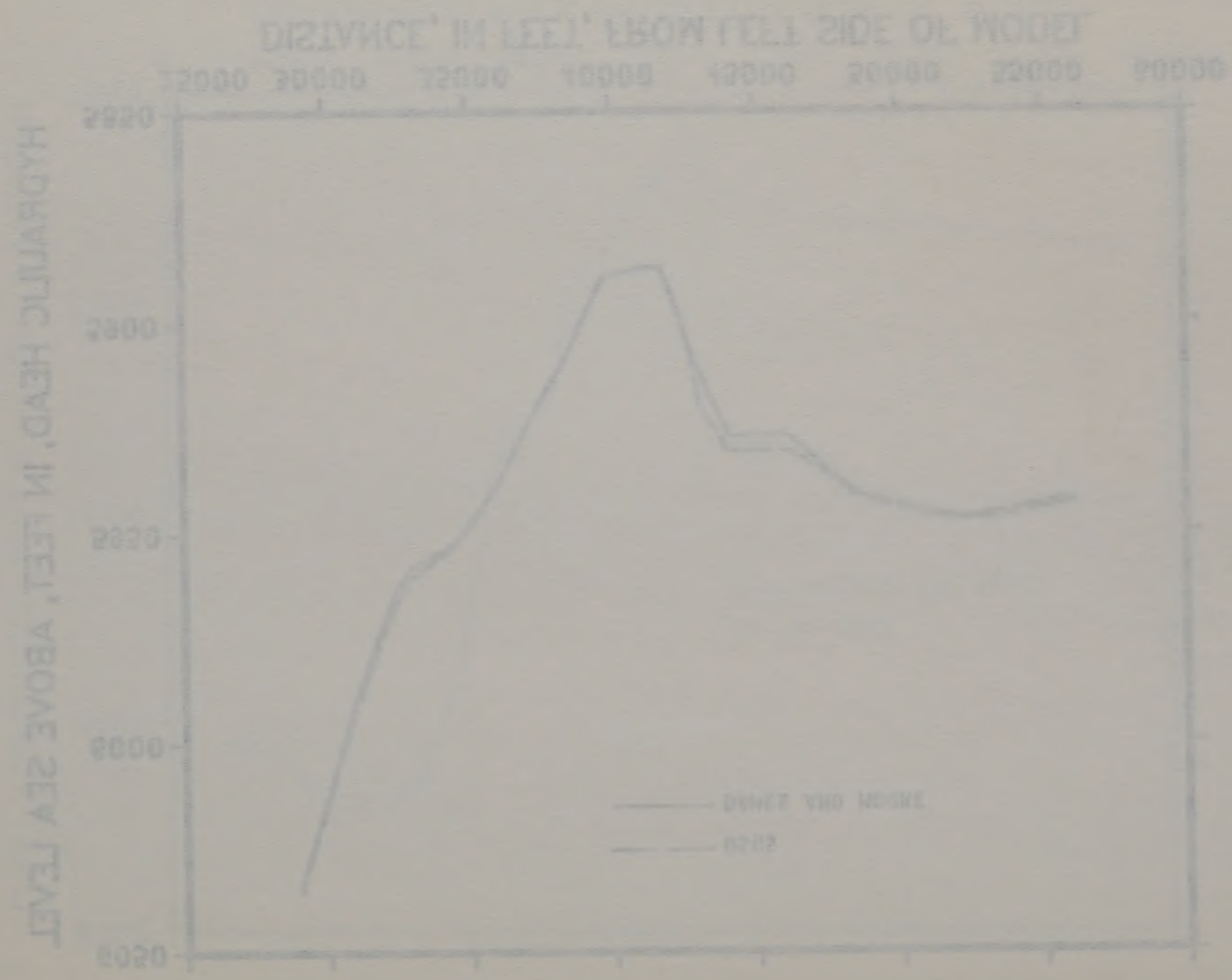


Figure 7-8. Cross-section of the detailed area of the model along Dames and Moore model row 14 (USGS model row 28) through the Jackpile mine showing post-reclamation hydraulic heads for the simulation "case3.5".

Data taken at 20 feet below water surface at 1000 ft. from
 and depth (25 feet below surface) at 1000 ft. from
 and depth (25 feet below surface) at 1000 ft. from
 the station "1000" in the
 "1000" station.



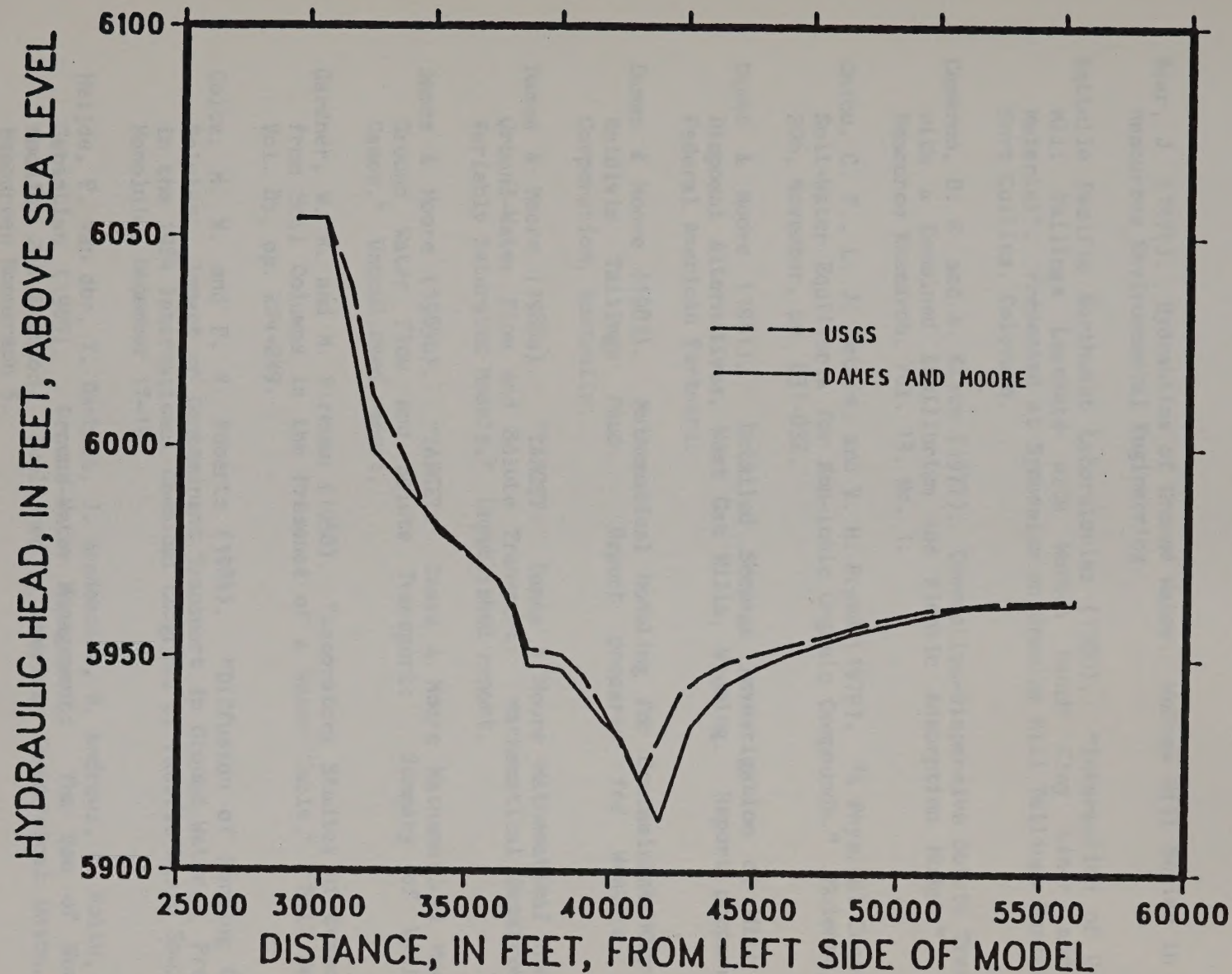


Figure 7-9. Cross-section of the detailed area of the model along Dames and Moore model row 21 (also USGS model row 21) through underground mine P10, South and North Paguate mines showing post-reclamation hydraulic heads for the simulation "case3.5".

F.7 REFERENCES

- Bear, J. (197()). **Hydraulics of Ground Water.** McGraw Hill Series in Water Resources Environmental Engineering.
- Battelle Pacific Northwest Laboratories (1980). "Interaction of Uranium Mill Tailings Leachate with Morton Ranch Clay Liner and Soil Material". Presented at Symposium on Uranium Mill Tailings Management, Fort Collins, Colorado.
- Cameron, D. R. and A. Klute (1977). Convection-Dispersive Solute Transport with a Combined Equilibrium and Kinetic Adsorption Model." **Water Resource Research.** Vol. 13, No. 1.
- Chiou, C. T., L. J. Peters, and V. H. Freed (1979). "A Physical Concept of Soil-Water Equilibria for Non-ionic Organic Compounds." **Science**, Vol. 206, November, pp. 831-832.
- Dames & Moore (1981). **Detailed Seepage Investigation of Mill Waste Disposal Alternatives, West Gas Hills, Wyoming.** Report prepared for Federal American Partners.
- Dames & Moore (1983). **Mathematical Modeling for Contaminant Migration, Baldivis Tailings Pond.** Report prepared for Western Mining Corporation, Australia.
- Dames & Moore (1985a). "TARGET: Dames & Moore Mathematical Model of Ground-Water Flow and Solute Transport: Mathematical Background of Variably Saturated Models." Unpublished report.
- Dames & Moore (1985b). "TARGET: Dames & Moore Mathematical Model of Ground Water Flow and Solute Transport: Summary of Validation Cases." Unpublished report.
- Gardner, W. R. and M. Fireman (1958). "Laboratory Studies of Evaporation from Soil Columns in the Presence of a Water Table." **Soil Science**, Vol. 85, pp. 224-249.
- Goltz, M. N. and P. V. Roberts (1984). "Diffusion of Sorbing Organic Solutes: Impact on Contaminant Transport in Ground Water." Presented in the 1984 International Chemical Congress of Pacific Basin Societies, Honolulu, December 17-19.
- Heijde, P. van der, Y. Bachmat, J. Bredehoeft, B. Andrews, D. Holtz, and S. Sebastian (1985). **Ground-Water Management: The Use of Numerical Models**, 2nd Edition. Published by American Geophysical Union, Water Resources Monograph 5.
- Highland, W. R., P. J. Pralong and D. Sharma (1983). "Evaluation of Ground-Water Contamination with Mathematical Modelling." International Conference on Ground Water and Man, Sydney, Australia.

APPENDIX G

CRITICAL REVIEWS OF
TARGET MODELS

APPENDIX G

TABLE OF CONTENTS

	<u>Page</u>
Summary of Ground-Water Model (TARGET) Reviews	G-1
ATTACHMENT 1 - List of Projects in which TARGET Predictions Were Reviewed and Accepted by State and Federal Agencies.	G-2
ATTACHMENT 2 - Memorandum from Director, U.S. Department of Interior Geological Survey, Reston, VA.	G-3
ATTACHMENT 3 - Memorandum from, Peter M. Onstein, Hydrogeologist, Physical Sciences Section, U.S. Environmental Protection Agency, Washington, D.C.	G-5
ATTACHMENT 4 - Letter from R. Allan Freeze, PhD, P.Eng.	G-7

Two of the model reviews listed in Attachment 1 are included further in Attachments 2 and 3 with the original letters and review comments. Attachments 2, 3 and 4 are available for review on request. Attachment 2 contains the text of a letter from the U.S. Geological Survey (USGS) to the Bureau of Land and Mineral Management concerning verification of model predictions for the Colorado Plateau Aquifer, New Mexico. The conclusions of the USGS study "established that the model used by BLM & MMS contained no inconsistencies of a mathematical or programming nature which significantly affected its results".

Attachment 3 covers an EPA review of model documentation, model guides, validation cases and 30 model listings prior to model application at a hazardous site in Baton Rouge, Louisiana. Review of the technical approach proposed at this site was particularly sensitive due to ongoing litigation. The conclusions of the review state that "the theory and logic presented appear to be suitable to perform reasonably reliable simulations". In addition, it was recommended that the EPA rely on the TARGET only at the site under question, with the provision of a comprehensive sampling and monitoring plan.

Attachment 4 consists of the general review comments on the TARGET package provided by Professor Allan Freeze. This review was solicited by BLM & MMS in the interests of refining the model documentation prior to sale of the TARGET models. Freeze's general comments indicate that "the TARGET package is versatile and powerful" while noting that the level of sophistication in the Physical and Mathematical Background chapter may be beyond the training of typical engineers in soil consulting firms. The specific comments elaborate on the general comments with reference to portions of the documentation, and have not been reproduced here.

APPENDIX G

SUMMARY OF GROUND-WATER MODEL (TARGET) REVIEWS

The purpose of this document is to summarize peer, federal agency, and state agency reviews of the TARGET model in order to clarify the context and outcome of significant reviews. The objective of most of the reviews documented here was to establish validity of the model/assumptions/data for the site in question. Quite frequently the reviews were undertaken with ensuing public review or litigation in mind. Dames & Moore testing and validation of the TARGET models are described in the model documentation and not considered here.

Attachment 1 provides a list of projects in which ground-water modeling formed a significant portion of the study and elicited separate review. A range of different agencies have been involved. In at least one case, an external expert was involved in assisting agency review. In some of the cases listed here, additional model calculations were requested to cover a wider range of site conditions, but at no time have the basic tenets of the model remained under question.

Two of the model reviews listed in Attachment 1 are described further in Attachments 2 and 3 (the original letters and reviews excerpted in Attachments 2, 3 and 4 are available for review on request). Attachment 2 contains the text of a letter from the U.S. Geological Survey (USGS) to the Bureau of Land and Minerals Management concerning verification of model predictions for the Anaconda Minerals Jackpile-Paguate Mine, New Mexico. The conclusions of the USGS study "established that the model used by Dames & Moore contained no inconsistencies of a mathematical or programming nature which significantly affected its results".

Attachment 3 covers an EPA review of model documentation, users guides, validation cases and 3D source listing prior to model application at a Superfund site in Baton Rouge, Louisiana. Review of the technical approach proposed at this site was particularly sensitive due to on-going litigation. The conclusions of the review state that "the theory and logic presented appear to be suitable to perform reasonably reliable simulations". In addition, it was recommended that the EPA rely on the TARGET code at the site under question, with the provision of a comprehensive sampling and monitoring plan.

Attachment 4 consists of the general review comments on the TARGET package provided by Professor Allan Freeze. This review was solicited by Dames & Moore in the interests of refining the model documentation prior to sale of the TARGET models. Freeze's general comments indicate that "the TARGET package is versatile and powerful" while noting that the level of sophistication in the Physical and Mathematical Background chapter may be beyond the training of typical engineers in small consulting firms. The specific comments elaborate on the general comments with reference to portions of the documentation, and have not been reproduced here.

ATTACHMENT 1List of Projects in Which TARGET Predictions Were
Reviewed and Accepted by State and Federal Agencies

Client	Date	Version of TARGET	Agency	Notes On Project Status
Amoco, Salt Lake City	5/85	2DU/2DH	EPA, State of Utah	Project Complete, Permit Pending
Anaconda Blue Water	3/81	2DU	NMEID	Project On Hold
Anaconda Minerals	2/84	2DU	USGS, BLM	Modeling Approved, EIS Being Finalized
Chem-Security	7/84	2DU/2DH	EPA	Modeling Complete
Chevron, Salt Lake City	3/85	2DU	EPA, State of Utah	ACL Petition
Federal American Partners	12/80	1DU/2DU/2DH	Wyoming DEQ	Project On Hold
Motorola, Phoenix	12/83	2DH/2DU/3DS/3DU	ADHS, ADWR, EPA	Continuing
Olean/NYSDEC	3/85	3DS	EPA, NYSDH	RI/FS Being Finalized
Petroprocessors, Inc.	6/85	2DU/2DH	EPA (Washington)	Pre-Project Model Approval Was Required
Phelps-Dodge	5/84	2DU/2DH	NMEID	Permit Approved
UMTRAP	82 & 83	2DU	DOE	Status Unknown
Gulf + Western	10/85	2DU	Colorado DOH, EPA	Continuing
Waste Management, Inc.	11/85	2DU	EPA (Ohio)	Model Approved, Project Continuing
Kentucky Avenue/ NYSDEC	11/85	2DH	EPA, NYSDH	Continuing

ATTACHMENT 2

Memorandum From

United States Department of Interior

Geological Survey, Reston, VA 22092

(Text of Letter Reproduced In Full Below)

August 23, 1984

Memorandum

To: Assistant Secretary -- Land and Minerals Management

Through: Assistant Secretary -- Water and Science

From: Director, Geological Survey

Subject: PUBLICATIONS- Report "Results of simulations using a U.S. Geological Survey generic two-dimensional ground-water-flow model to process input data from the Dames & Moore ground-water-flow model of the Jackpile-Paguete Uranium Mine, New Mexico"

In accordance with the agreement reached at the meeting of May 29, 1984, between yourself, Bureau of Land Management (BLM) Assistant Director Sokoloski, other representatives of BLM, and Philip Cohen, Gordon Bennett, and Roger Wolff of the Water Resource Division, U.S. Geological Survey (USGS), we are pleased to provide the accompanying two copies of the subject report.

In the work summarized in this report, USGS hydrologists of the New Mexico District office carried out a number of numerical simulations of the ground-water-flow system in the vicinity of the Jackpile mine. The simulations were performed using a standard USGS generic model for two-dimensional ground-water flow; they employed hydrologic parameters which in some cases were identical to those used in an analysis by Dames & Moore, Inc., and in some cases were systematically varied from those values.

In all, 14 simulations were carried out by USGS hydrologists. Initially, four simulations were run corresponding to Case 1 of the Dames & Moore analysis, which addressed the pre-mining steady-state condition of the aquifer. These four simulations differed from one another in the subdivision of the model mesh, in the way a particular aquifer outcrop was simulated, and in the way two streams, the Rio Paguate and Rio Moquino, were simulated; the hydraulic conductivity and recharge values used in all four of these simulations were identical to those used by Dames & Moore. Next, two simulations were carried out corresponding to Case 3 of the Dames & Moore analysis, which addressed the final post-reclamation condition, subject to the assumption that no low-permeability barrier would be emplaced in the North Paguate pit during reclamation.

Memo To:

Assistant Secretary--Land and Minerals Management

Page -2-

These two simulations differed from one another only in the way the Rio Paguete and Rio Moquino were represented; the hydraulic conductivity and recharge values were identical to those of Dames & Moore. Finally, eight simulations were carried out corresponding to Case 3.5 of the Dames & Moore analysis, which again addressed the final post-reclamation condition, but with the assumption that a low-permeability barrier would be emplaced in the North Paguete pit during reclamation. Within this group, the first two simulations differed from each other in the way the streams were represented, but again, the hydraulic conductivity and recharge values used by Dames & Moore were retained. The final six simulations of this group, on the other hand, incorporated various combinations of recharge and hydraulic conductivity which differed from those used by Dames & Moore. The variation in recharge consisted of an increase from 0.12 inches to 0.24 inches per year over a relatively small fraction of the modeled area. The changes in hydraulic conductivity involved uniform halving and doubling of the aquifer conductivity, and uniform halving and doubling of the conductivity of the backfill material in the reclaimed mine pits.

The USGS work established that the model used by Dames & Moore contained no inconsistencies of a mathematical or programming nature which significantly affected its results. The analysis further demonstrated that the changes in the method of simulating the outcrop and the streams produced significant water level differences only in the immediate vicinity of those features. Variation in recharge and hydraulic conductivity, on the other hand, caused significant water level differences within the reclaimed mine pits. In one simulation, in which the hydraulic conductivities of the aquifer and the backfill were doubled while the recharge values used by Dames & Moore were unchanged, the USGS results indicated lower post-reclamation ground-water levels in the Jackpile and South Paguete pits, but higher levels in the North Paguete pit. In the five other simulations in which parameters were varied, the USGS results indicated final ground water levels in the reclaimed pits that were higher by at least 20 feet, and commonly by as much as 50 feet, than those computed by Dames & Moore. These results illustrate the sensitivity of computed water levels to the assumed parameters, but do not in any way either corroborate or dispute the parameter values assumed by Dames & Moore. We point out again that to address this latter question a full hydrologic investigation, requiring at least 18 months' time, would be required.

Please call me at (773) 362-2063 if you have any questions or comments.

CONCLUSION

As the purpose of this review is to recommend whether or not EPA may rely upon TACET to produce reasonably reliable results at the Metro Processors' site, portions of the documentation not relevant to this purpose were not critically reviewed. In addition, any confidence in TACET's results must be qualified since the reviewer did not see the data and therefore did not have

ATTACHMENT 3

Memorandum From

United States Environmental Protection Agency

Washington, D.C. 20460

(Text of Covering Memorandum and Conclusions
Reproduced in Full Below)

May 17, 1985

MEMORANDUM

SUBJECT: Review of TARGET Code for use at Petro Processors Site

FROM: Peter M. Ornstein, Hydrogeologist
Physical Sciences Section, OWPE (WH-527)

THRU: Rob Clemens, Acting Chief
Physical Sciences Section, OWPE

TO: Tony Gardner
Region VI

Attached please find my review of Dames & Moore's TARGET computer code. Based on my review, I recommend that EPA accept the use of TARGET at the Petro Processors Site provided that a comprehensive monitoring and sampling plan is implemented. The plan should provide for monitoring contaminant levels in and around the predicted plume in the 40 foot zone to assist in code calibration and also provide for monitoring the 400 foot aquifer in selected locations to assure trigger level credibility.

In light of this recommendation, the Phase 2 review of TARGET does not seem appropriate. At such time as the agency has determined what peer review criteria and procedures will be employed for the selection and use of ground-water models, this and other model codes will, in all likelihood, be evaluated in greater detail on a generic basis.

Please call me at (FTS or 202) 382-2063 if you have any questions or comments.

CONCLUSION

As the purpose of this review is to recommend whether or not EPA may rely upon TARGET to produce reasonably reliable results at the Petro Processor's site, portions of the documentation not relevant to this purpose were not critically reviewed. In addition, any confidence in TARGET expressed herein must be qualified since the reviewer did not run the code and therefore did not have

the opportunity to test or stress the code. Overall confidence in the TARGET code would be substantially improved if the code were in the public domain and used by others within the technical community.

In summary, TARGET employs a non-traditional approach to modeling contaminant transport in ground water by use of its guess and correct algorithm. Given the limited scope of this review, the theory and logic presented appear to be suitable to perform reasonably reliable simulations. No inherent deficiencies either in the guess and correct algorithm or in the way the hydrodynamics and mass transport have been treated are apparent.

It is recommended that EPA rely upon the TARGET code at the Petro Processor's Site. It cannot be overemphasized that use of TARGET must be performed in conjunction with a comprehensive sampling and monitoring plan. The monitoring and sampling is necessary to provide a "safety net" to counter the uncertainty associated with the site's complex hydrogeology as well as uncertainty associated with modeling the site (i.e., quality of data, applicability of generic assumptions to the site, etc.). Since the intended use of TARGET is to establish trigger levels in the 40 foot zone to protect the 400 foot aquifer, both zones should be monitored to enhance confidence in the predicted levels as well as aid in further field calibration and verification of the model.

To reiterate, the scope of this review focused on TARGET's use for a specific purpose at the Petro Processor's site. Until such time as the code has been peer reviewed and tested in the professional community and available in the public domain, evaluation of site by site applications is recommended.

SEVERAL COMMENTS

1. It is clear to me that the TARGET package is a versatile and powerful set of computer programs for the mathematical modeling of groundwater flow and solute transport. The mathematical formulations are sound and the numerical methodology clever and efficient. It is clear that the authors of the program and the documentation are working from a strong technical base.
2. The writing style throughout the report is very clear. I will have some comments about the level and order of presentation, but I must emphasize that the current presentation of each topic, both in their descriptive and mathematical contexts, is very well done.
3. The major area of concern that I can identify lies in the level of explanation in the chapter on the physical and chemical processes and the model. This chapter needs a very thorough revision. The current version is a very advanced notation. As a reviewer, I find it difficult to follow the logic and argument, but my experience in reviewing technical literature tells me that this is a very common problem. I would like to see a more detailed explanation of the physical and chemical processes and the model. I would like to see a more detailed explanation of the physical and chemical processes and the model. I would like to see a more detailed explanation of the physical and chemical processes and the model.

Dr. D. A. Stephenson
July 10, 1985
Page 2

ATTACHMENT 4

Letter From

R. Allan Freeze, Ph.D., P.Eng.

(Text of General Comments Reproduced
in Full Below)

July 10, 1985

Dr. D. A. Stephenson
Dames & Moore
3737 N. 7th Street, Suite 121
Phoenix, Arizona
U.S.A. 85014

Dear Dave:

In response to your letter of June 11, 1985, I reviewed the Dames & Moore TARGET package, giving special consideration to the suitability of the documentation for outside-the-firm release. I have divided my comments into general comments and specific comments.

GENERAL COMMENTS

1. It is clear to me that the TARGET package is a versatile and powerful set of computer programs for the mathematical modeling of groundwater flow and solute transport. The mathematical foundations are strong and the numerical methodology clever and efficient. It is clear that the authors of the program and the documentation are working from a strong technical base.
2. The writing style throughout the report is very clear. I will have some comments about the level and order of presentation, but I must emphasize that the current presentation of each topic, both in their descriptive and mathematical contexts, is very well done.
3. The major area of concern that I can identify lies in the level of sophistication in the chapter on the Physical and Mathematical Background of the models. This chapter uses a very sophisticated mathematical framework and a very advanced notation. As a research scientist in this field I find it compact and elegant, but my experience in dealing with small consulting firms who may provide a primary market for TARGET would lead me to question whether engineers from such firms would be at home with this level of presentation. One must ask to whom this chapter is directed. If it is directed to reviewers such as myself as a kind of base document that lays out the mathematical foundations of the programs for those few who may wish to follow it up, then the current presentation may be suitable. If, on the

other hand, it is intended as a kind of textbook to accompany training sessions for consulting engineers from smaller companies, then I believe it needs to be expanded and the order changed somewhat in order to bring it into line with the backgrounds that such "students" will have. Several of the Specific Comments pertain to this issue, but the more general suggestions are as follows:

- (a) The Introduction should be expanded to include more complete descriptions of the types of boundary-value problems that the programs can handle (and the engineering problems to which they apply). It should include clear definitions of such concepts as steady-state and transient flow, unsaturated and saturated pressure heads, homogeneity and anisotropy, etc.
- (b) Section 2-0 on Physical Mechanisms and Chemical Processes should include detailed positive statements of the capabilities of the models with respect to groundwater flow and solute transport. In the current write-up the basic assumptions of Section 2-1-1 hit the reader without lead in or warning. Some of them are quite sophisticated and required a detailed understanding of the equations of groundwater flow. I would be inclined to save this list until after the primary development of Section 3-0.
- (c) The references provided in the Introduction are a bit obscure. I would refer to the available textbooks by Wang and Anderson, Pinder and Gray, Remson et al, and to the AGU monograph by Bredehoeft et al and the NWWA monograph by Mercer and Faust.
- (d) Much of the descriptive material is too terse. Two examples: (i) Section 2-2 on Solute Transport ought to summarize all the mechanisms of transport noting which ones are included and which ones are not; (ii) The discussion of seepage faces in the 2nd paragraph from the bottom of page 16 does not hint at the complexities associated with their simulation (iterative positioning of the exit point, problems associated with multiple seepage faces, etc.).
- (e) There are many examples in the Specific Comment of cases where the readers first encounter with a concept or notation occurs in the midst of some other explanations. Examples: (i) on p. 26 just below Eqn. (4-38) the reader is first informed that the numerical solution is iterative; (ii) The Peclet number is introduced for the first time on page 3-1 in the Validation Chapter. In all cases, introductory material should have appeared earlier so that the reader is not taken by surprise.
- (f) I would prefer to see variables defined at the point of first encounter as well as in the notation list. It is difficult for the reader to switch back and forth from the text to the list and to locate the particular symbol on the list.

4. In the Introduction it is stated that there are 5 models in the TARGET family, but there are 18 possible contaminations of the properties listed there. The 5 models should be identified clearly and examples of their use described. Model TARGET 2DH does not figure anywhere in the Background chapter or the User's Guides, but it appears in the first two validation cases.
5. The User's Guide to TARGET 2DU and TARGET 3DS are clearly done and should prove easy to follow by prospective clients. The Specific Comments note a few places where clarification is needed. I note, however, that a list clearly relating the computer acronyms to their mathematical notation in the Background chapter would be useful.
- 6.* The chapter on the Summary of Validation Cases is clear and convincing. The only apparent capability of the TARGET family that is not fully validated is a case that involves solute transport in the unsaturated zone. If such a validation is available, it would make a worthwhile addition.

*Note by Dames & Moore:

Since this review was conducted a number of additional model validation cases have been undertaken. A validation case currently being undertaken involves the simulation of water and solute movement in unsaturated conditions (validation data obtained from Pickens, J.F., R. W Gillham and D.R. Cameron (1979)). Finite-Element Analysis of the Transport of Water and Solutes in Tile-Drained Soils. Journal of Hydrology, 40 (1979) 243-264).

APPENDIX H

PREDICTED CONCENTRATION
PLUMES

APPENDIX H

TABLE OF CONTENTS

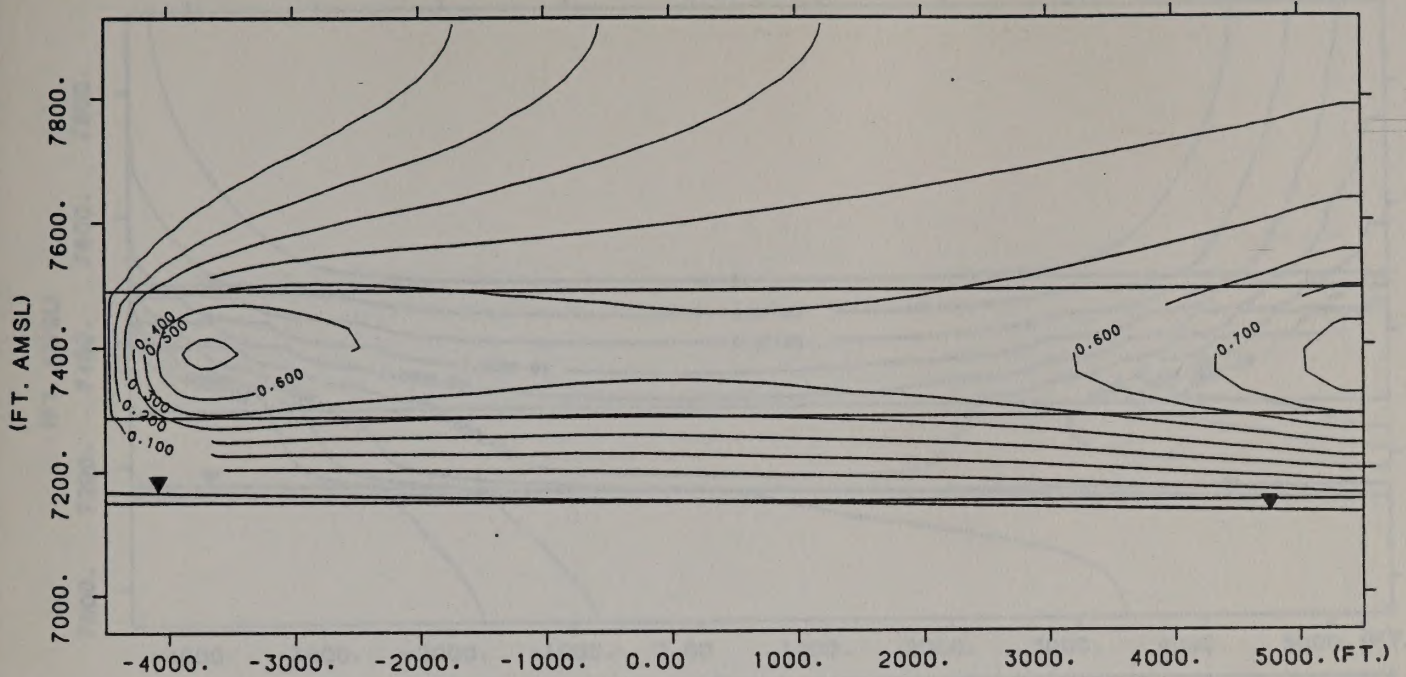
Predicted Concentration Plumes

Figure H-1	Case 2
Figure H-2	Case 3
Figure H-3	Case 4
Figure H-4	Case 5
Figure H-5	Case 6
Figure H-6	Case 7
Figure H-7	Case 8
Figure H-8	Case 9
Figure H-9	Case 10
Figure H-10	Case 11
Figure H-11	Case 12
Figure H-12	Case 13
Figure H-13	Case 14
Figure H-14	Case 15
Figure H-15	Case 16
Figure H-16	Case 5 - with 50 feet of Saturated Thickness
Figure H-17	Case 5 - with 10 feet of Saturated Thickness
Figure H-18	Case 5 - with Original Domain and Expanded Domain
Figure H-19	Case 3 - with 40-Day Initial Time Step

-and-

Case 5 - with 40-Day Initial Time Step

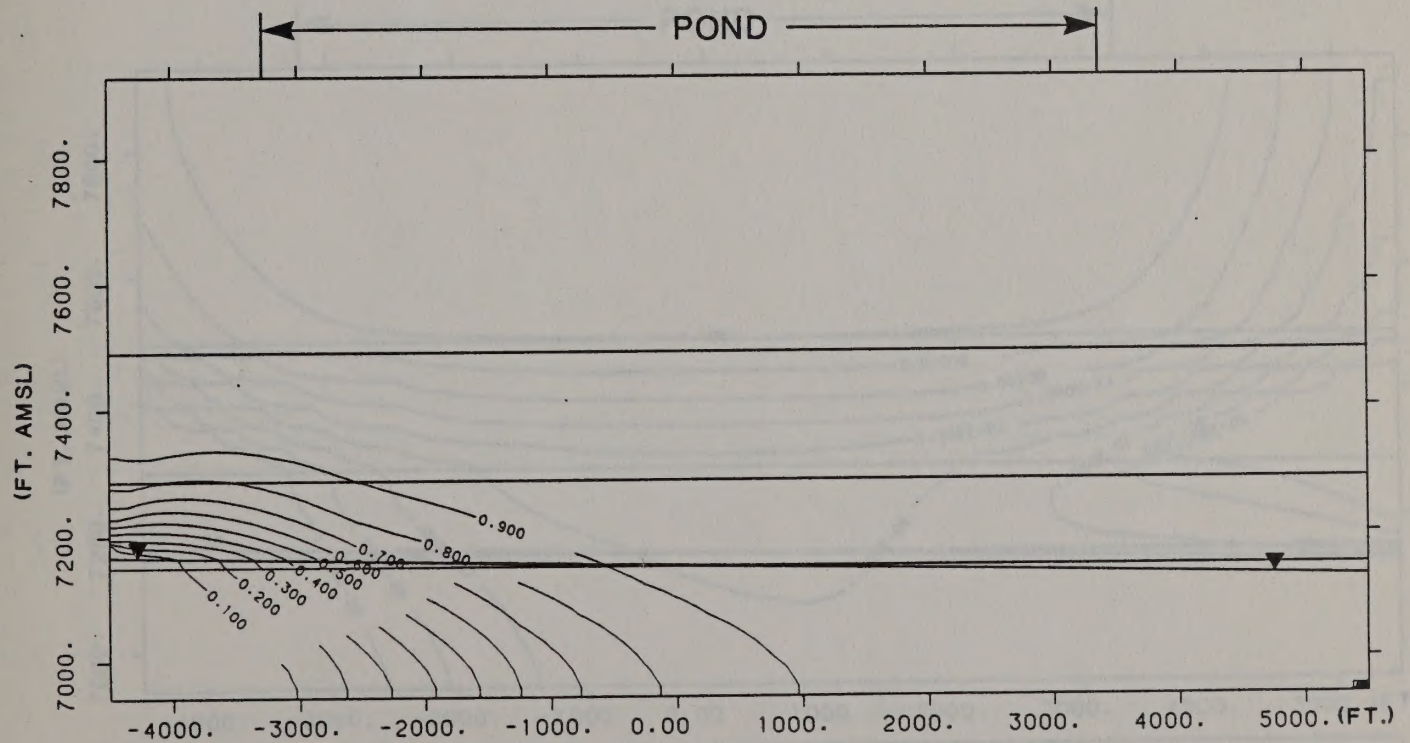
CASE 2



MOLYCORP: METAL TRANSPORT: 1.5 CFS SEEP RATE, $KH:KV=10:1$, ZERO KD CASE

CONTOUR OF NORMALIZED CONCENTRATION

TIME = 80 YEARS



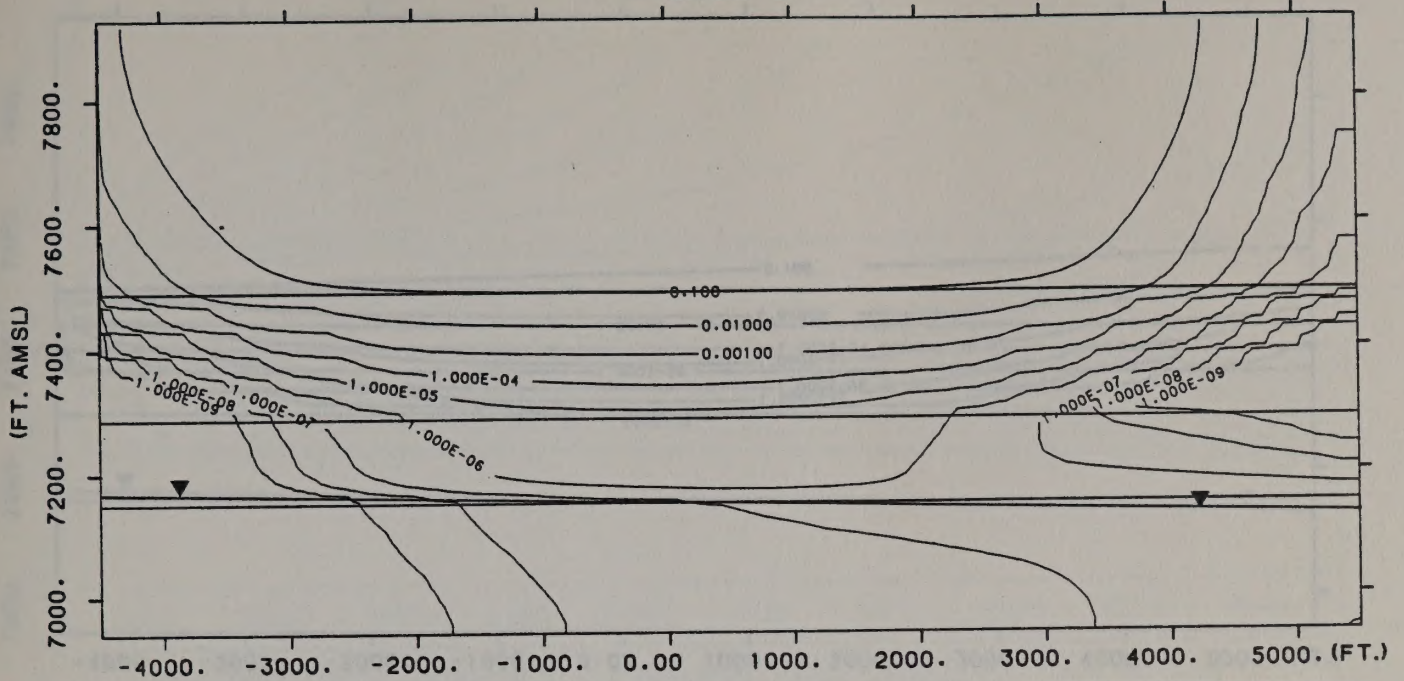
MOLYCORP: METAL TRANSPORT: 1.5 CFS SEEP RATE, $KH:KV=10:1$, ZERO KD CASE

CONTOUR OF NORMALIZED CONCENTRATION

TIME = 27 YEARS AFTER POND STARTUP

Figure H.1

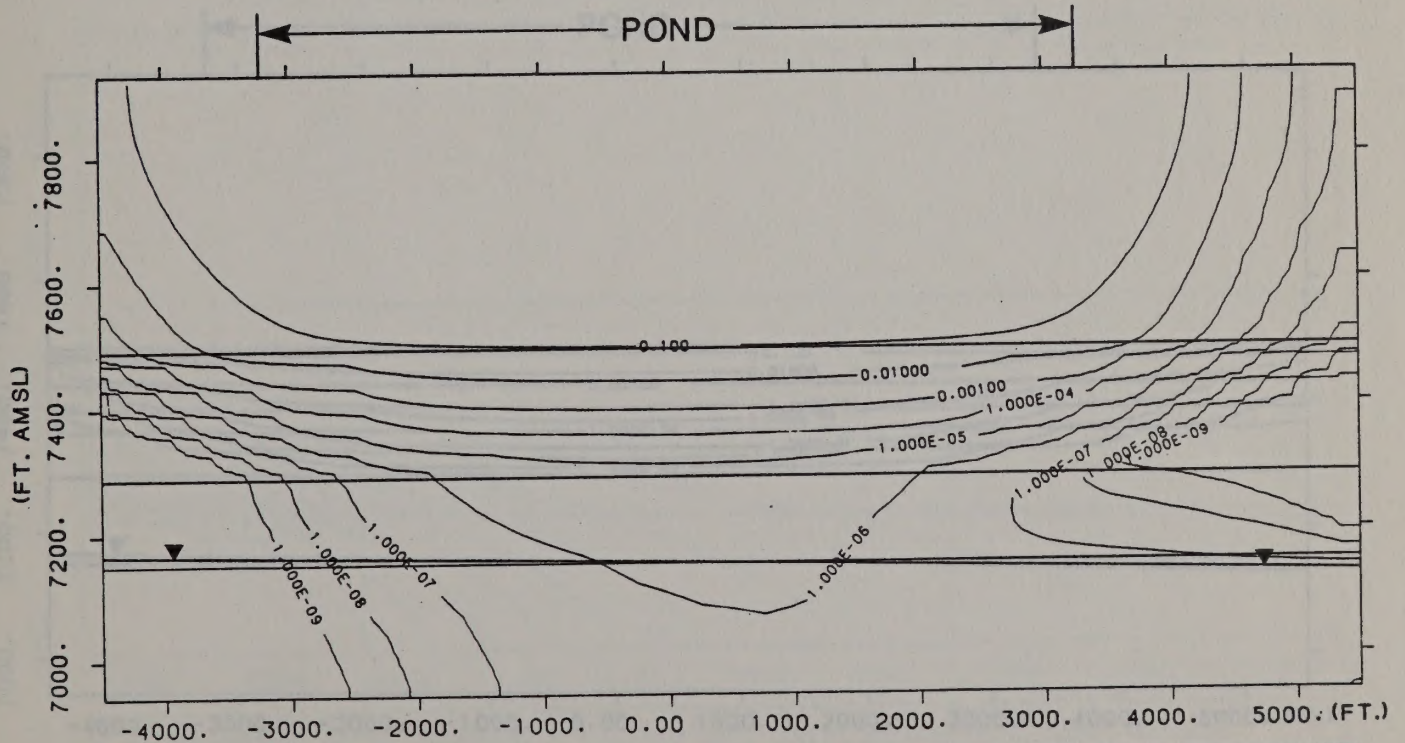
CASE 3



MOLYCORP: METAL TRANSPORT: 1.0 CFS SEEP RATE, $KH:KV=10:1$, MEDIUM KD CASE

CONTOURS OF NORMALIZED CONCENTRATION

TIME = 80 YEARS



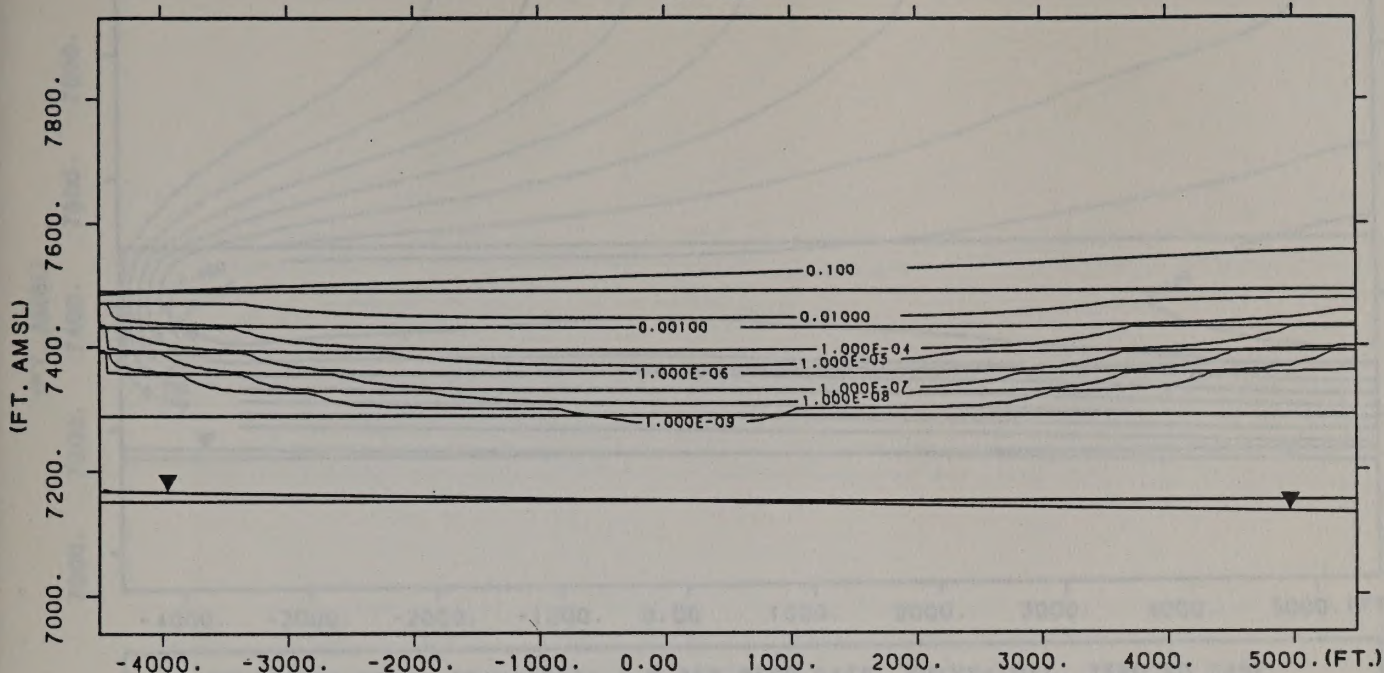
MOLYCORP: METAL TRANSPORT: 1.0 CFS SEEP RATE, $KH:KV=10:1$, MEDIUM KD CASE

CONTOURS OF NORMALIZED CONCENTRATION

TIME = 27 YEARS AFTER POND STARTUP

Figure H.2

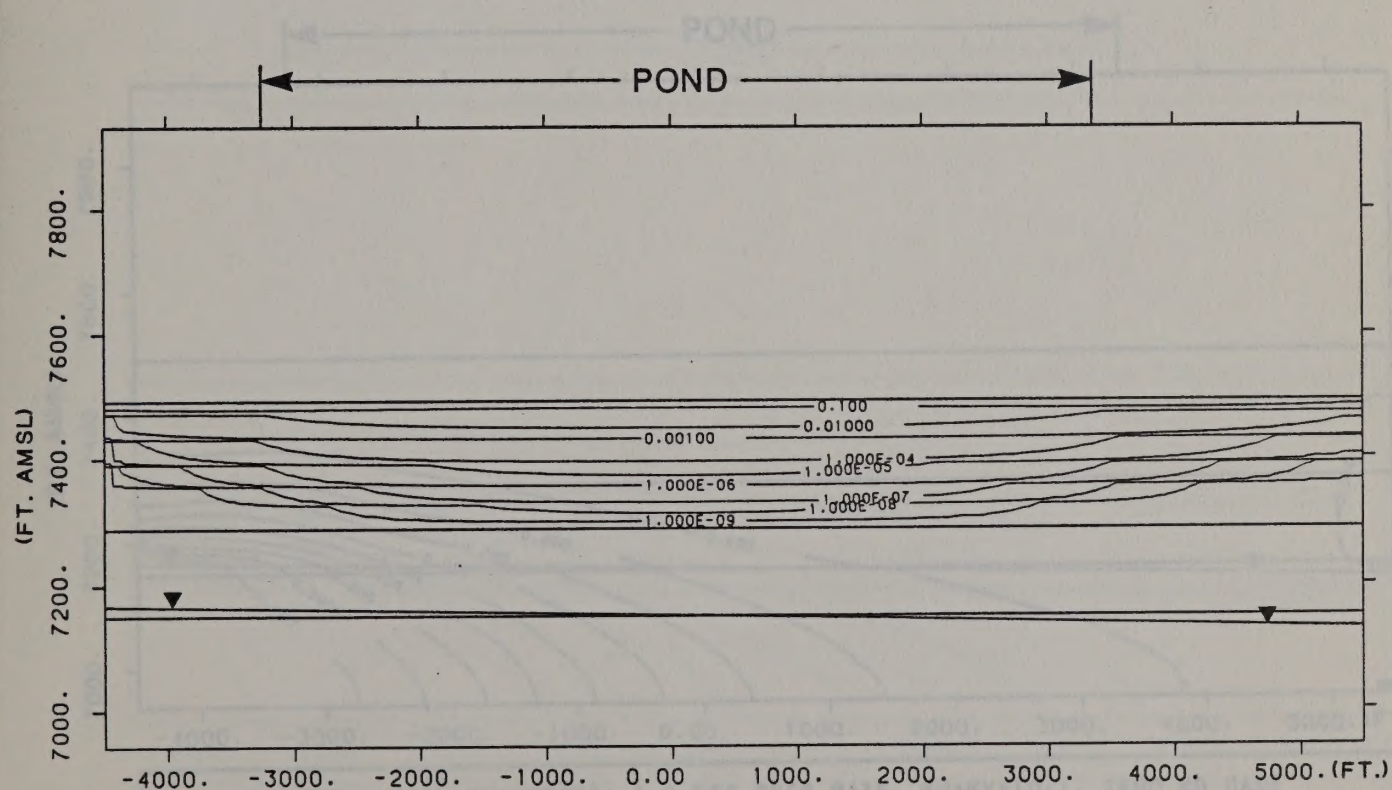
CASE 4



MOLY CORP: METAL TRANSPORT: 1.0 CFS SEEP RATE, KH:KV=10:1, HIGH KD CASE

CONTOURS OF NORMALIZED CONCENTRATION

TIME = 80 YEARS



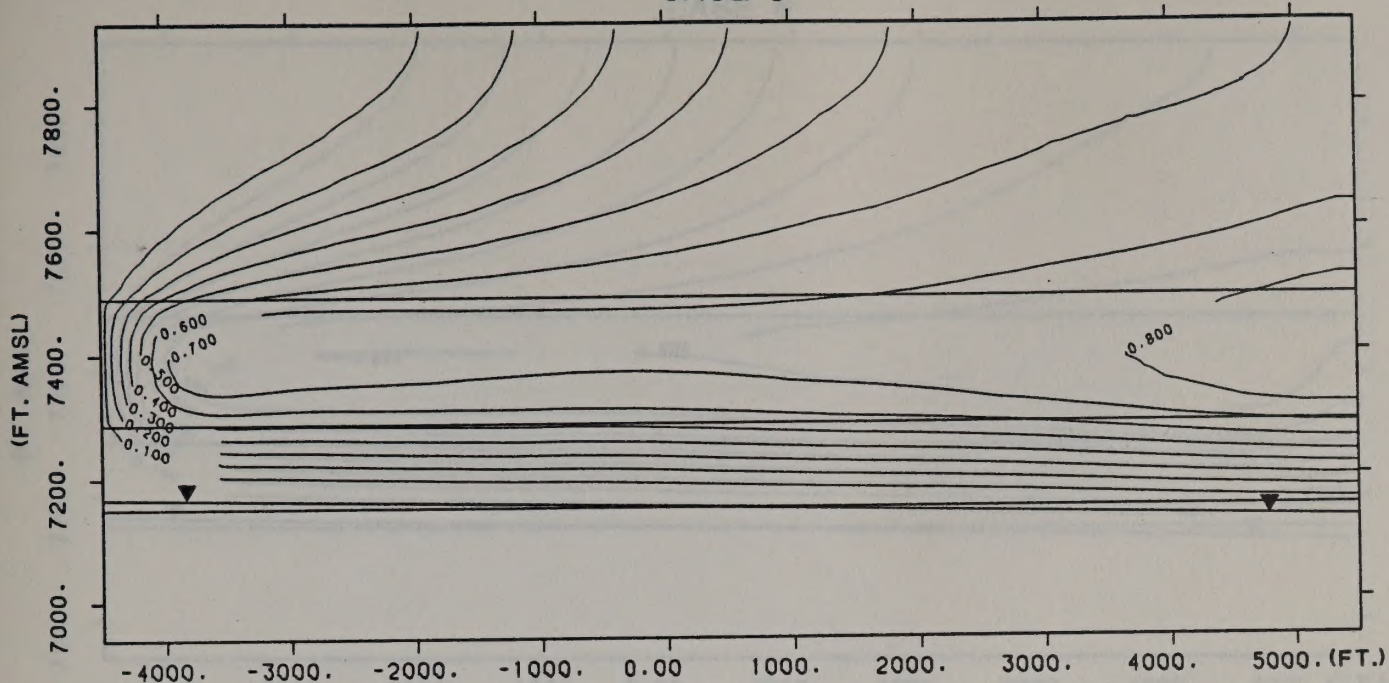
MOLY CORP: METAL TRANSPORT: 1.0 CFS SEEP RATE, KH:KV=10:1, HIGH KD CASE

CONTOURS OF NORMALIZED CONCENTRATION

TIME = 27 YEARS AFTER POND STARTUPT

Figure H.3

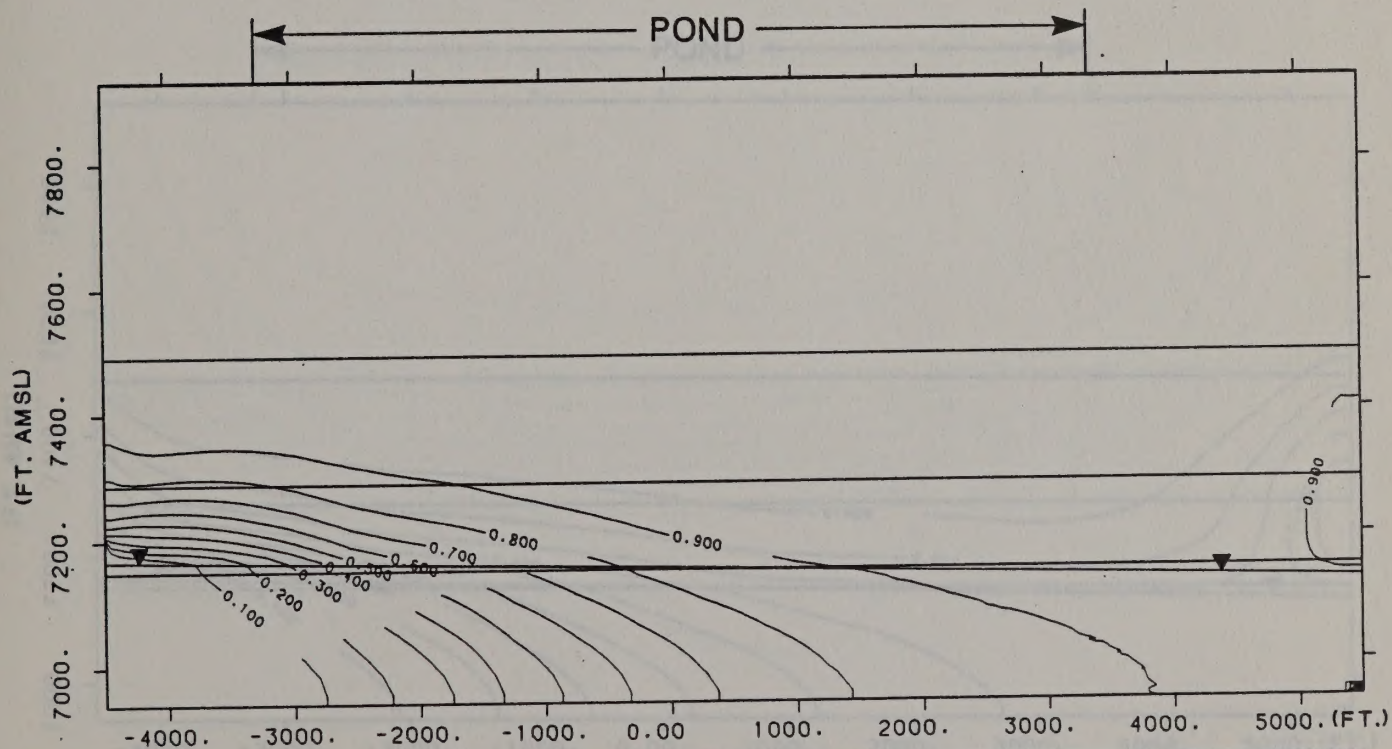
CASE 5



MOLYCORP: METAL TRANSPORT: 1.0 CFS SEEP RATE, $KH:KV=10:1$, ZERO KD CASE

CONTOURS OF NORMALIZED CONCENTRATION

TIME = 80 YEARS



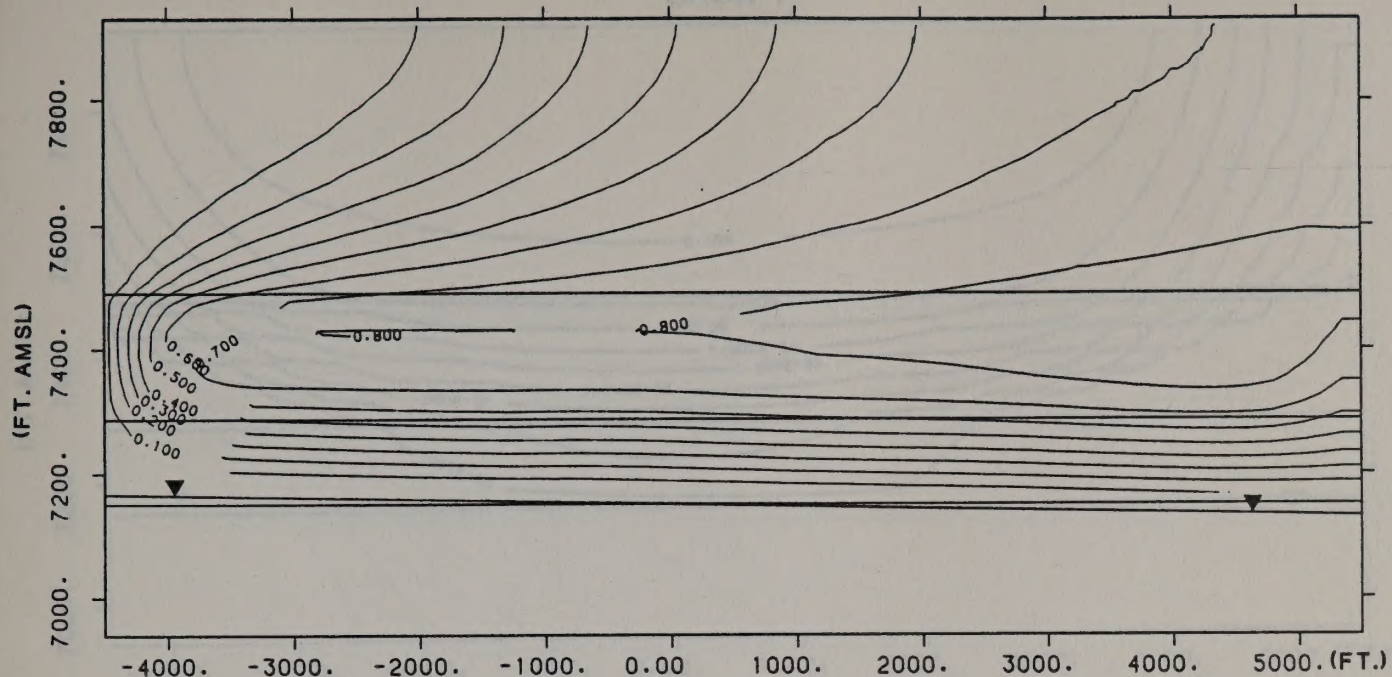
MOLYCORP: METAL TRANSPORT: 1.0 CFS SEEP RATE, $KH:KV=10:1$, ZERO KD CASE

CONTOURS OF NORMALIZED CONCENTRATION

TIME = 27 YEARS AFTER POND STARTUP

Figure H.4

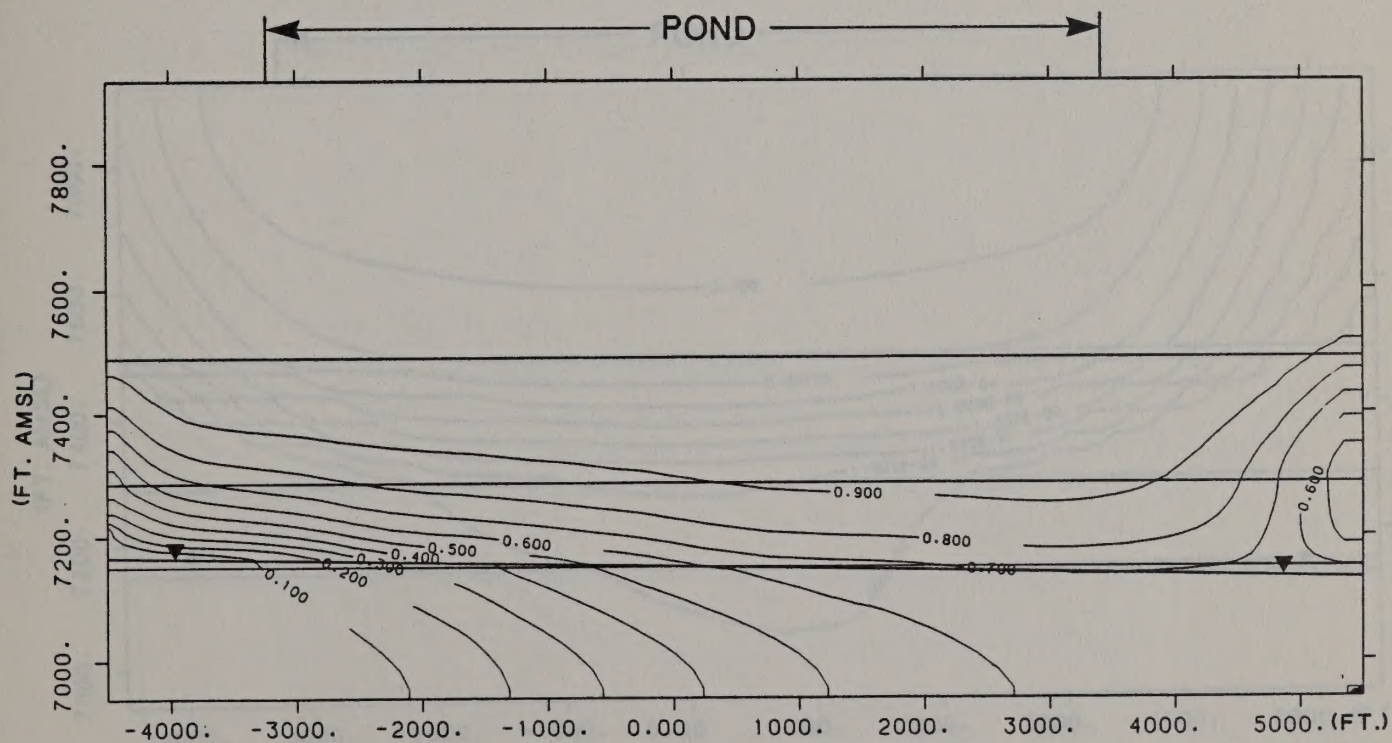
CASE 6



MOLYCORP: METAL TRANSPORT: 0.5 CFS SEEP RATE, $KH:KV=10:1$, ZERO KD CASE

CONTOURS OF NORMALIZED CONCENTRATION

TIME = 80 YEARS



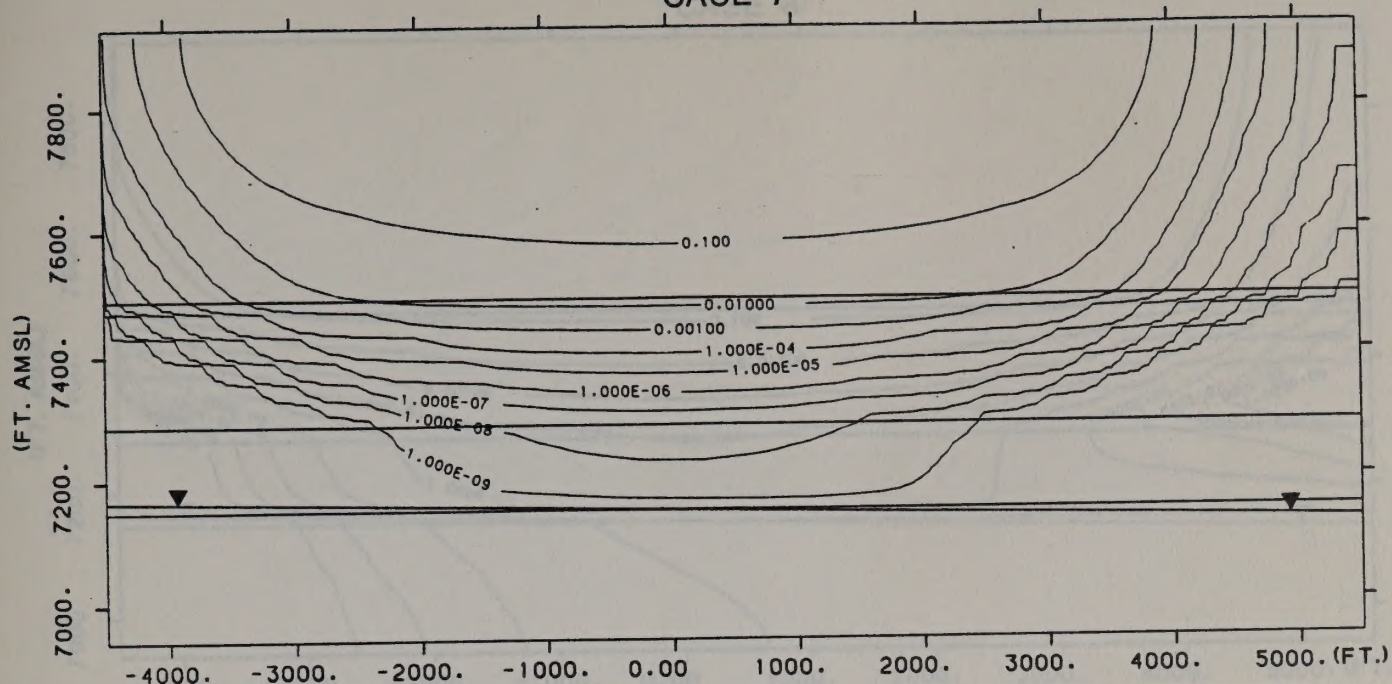
MOLYCORP: METAL TRANSPORT: 0.5 CFS SEEP RATE, $KH:KV=10:1$, ZERO KD CASE

CONTOURS OF NORMALIZED CONCENTRATION

TIME = 27 YEARS AFTER POND STARTUP

Figure H.5

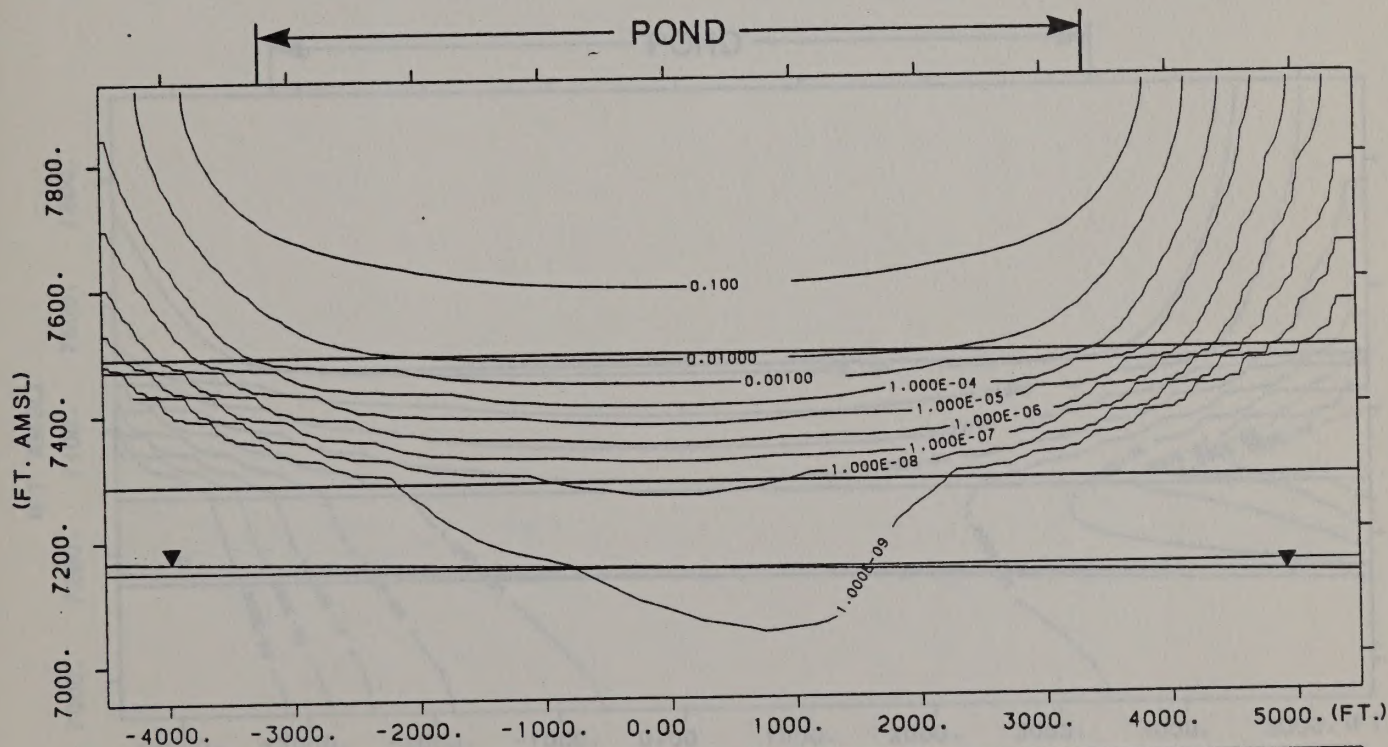
CASE 7



MOLYCORP: METAL TRANSPORT: 0.5 CFS SEEP RATE, $KH:KV=10:1$, MEDIUM KD CASE

CONTOURS OF NORMALIZED CONCENTRATION

TIME = 80 YEARS



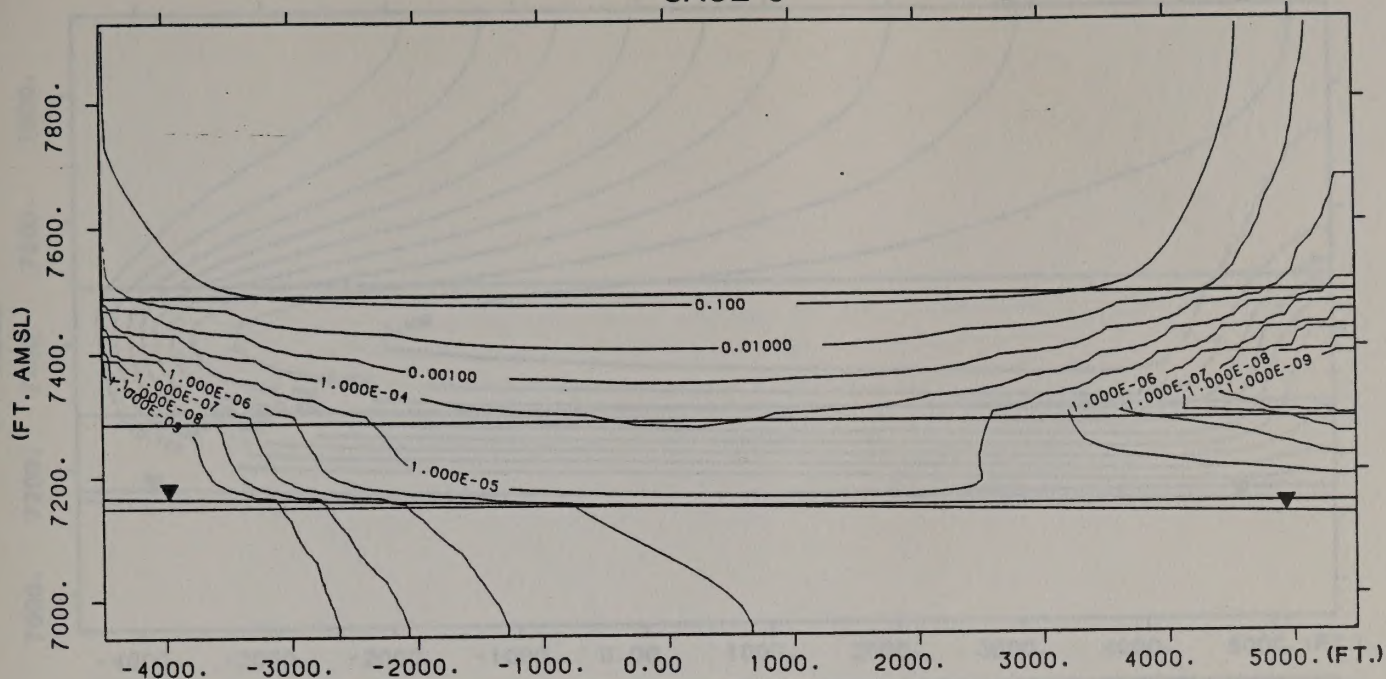
MOLYCORP: METAL TRANSPORT: 0.5 CFS SEEP RATE, $KH:KV=10:1$, MEDIUM KD CASE

CONTOURS OF NORMALIZED CONCENTRATION

TIME = 27 YEARS AFTER POND STARTUP

Figure H.6

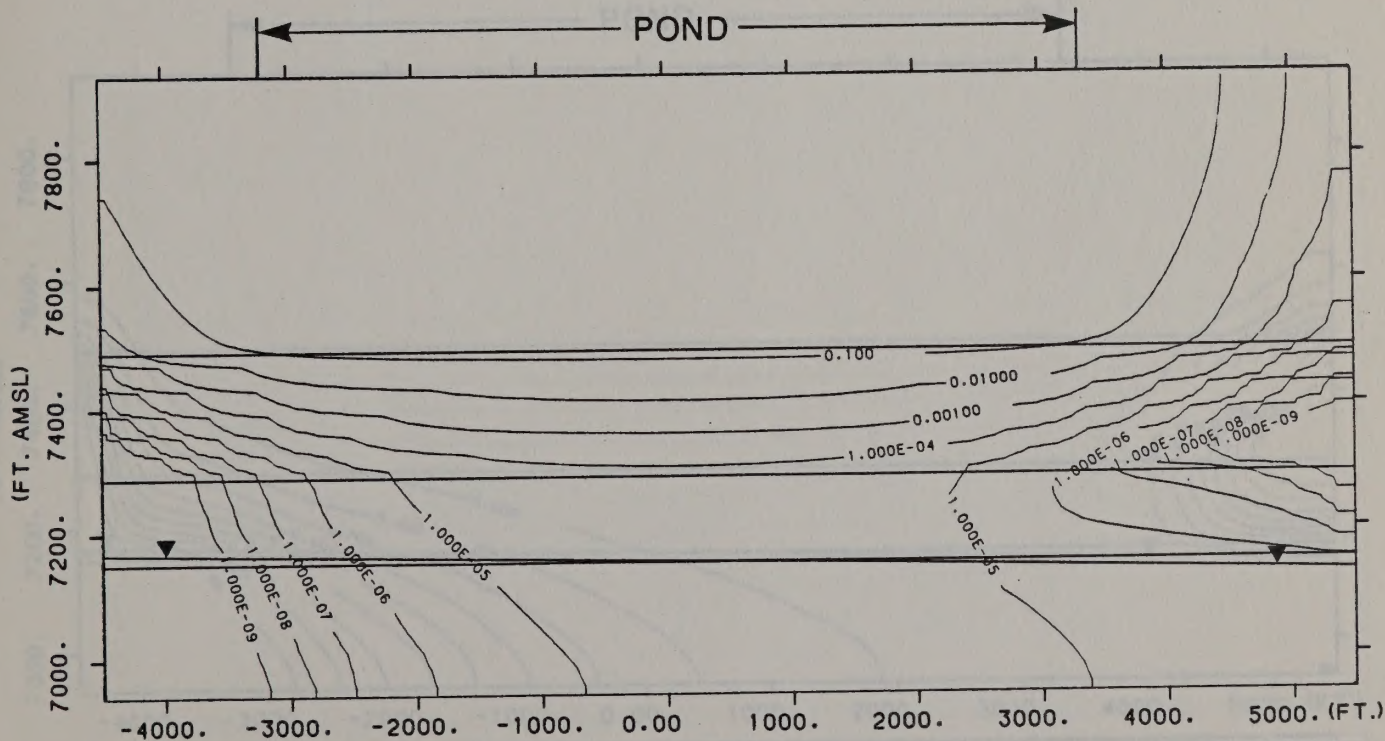
CASE 8



MOLYCORP: METAL TRANSPORT: 1.5 CFS SEEP RATE, $KH:KV=10:1$, MEDIUM KD CASE

CONTOURS OF NORMALIZED CONCENTRATION

TIME = 80 YEARS



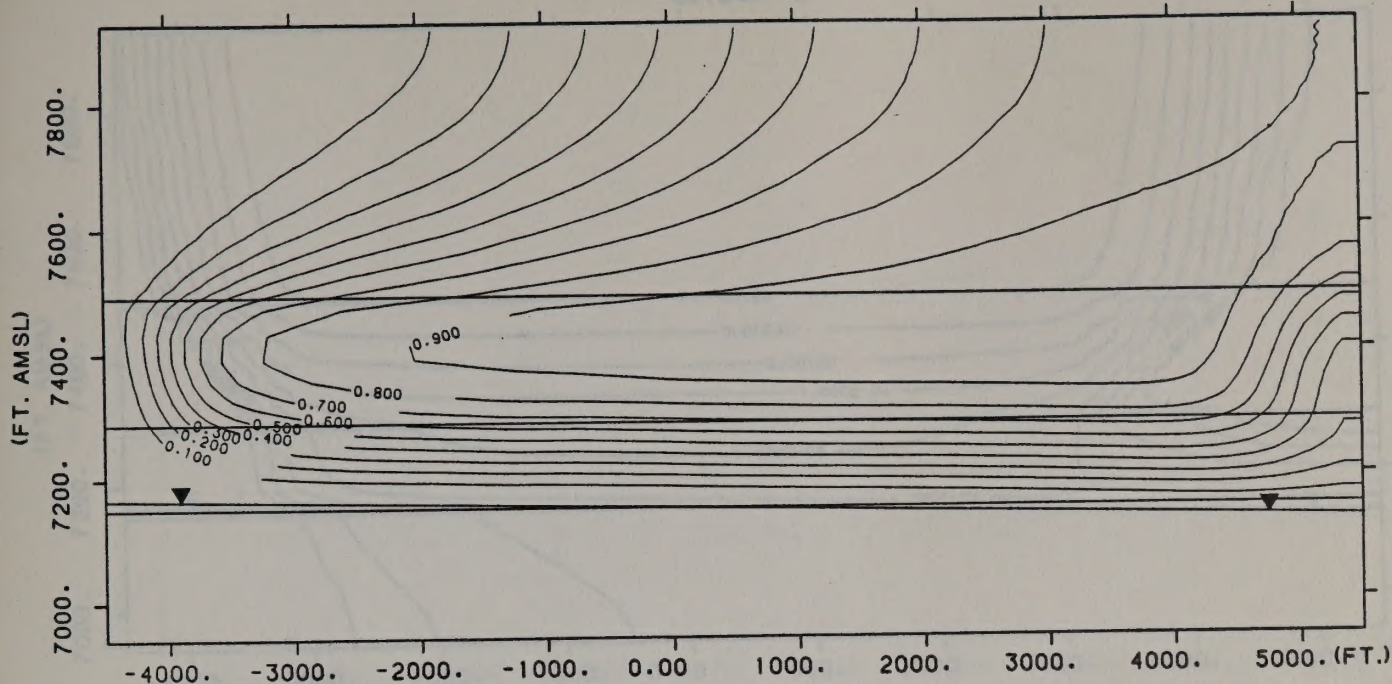
MOLYCORP: METAL TRANSPORT: 1.5 CFS SEEP RATE, $KH:KV=10:1$, MEDIUM KD CASE

CONTOURS OF NORMALIZED CONCENTRATION

TIME = 27 YEARS AFTER POND STARTUP

Figure H.7

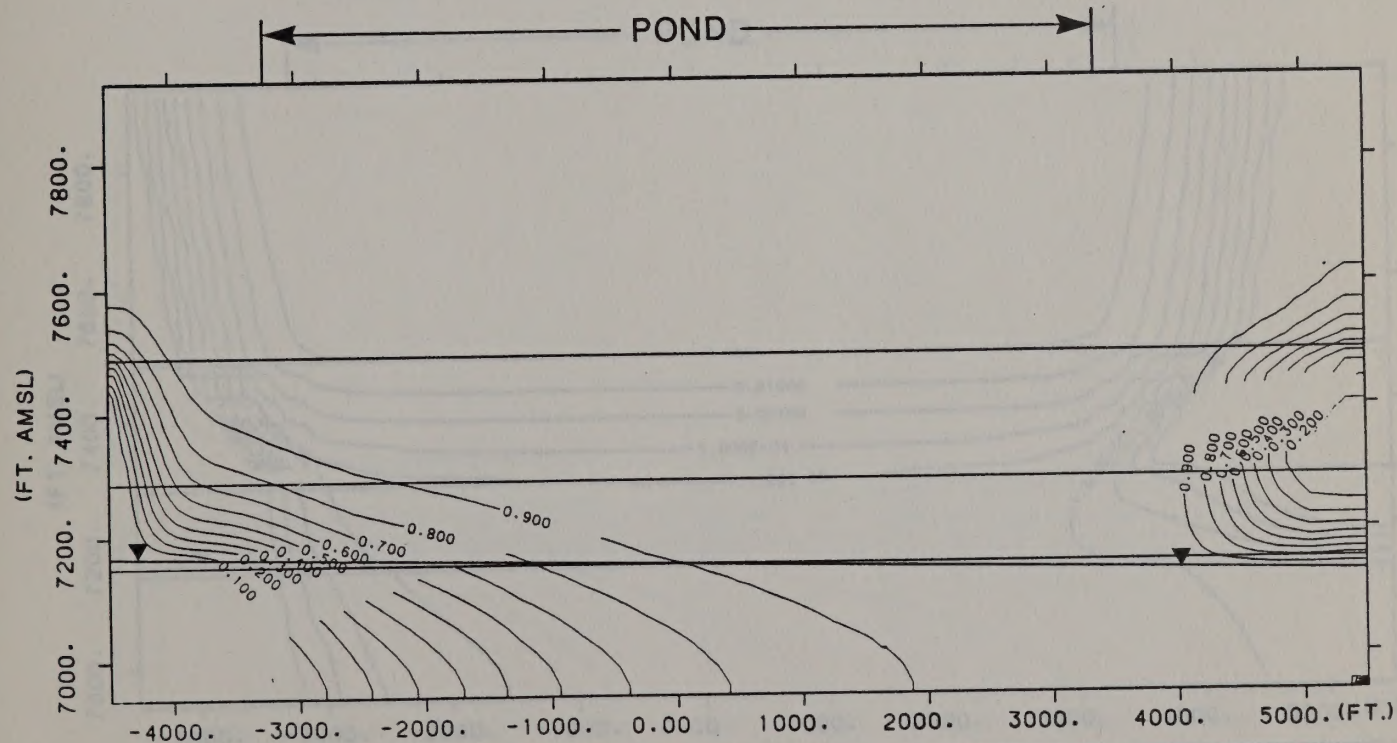
CASE 9



MOLYCORP: METAL TRANSPORT: 1.0 CFS SEEP RATE, $KH:KV=1:1$, ZERO KD CASE

CONTOURS OF NORMALIZED CONCENTRATION

TIME = 80 YEARS



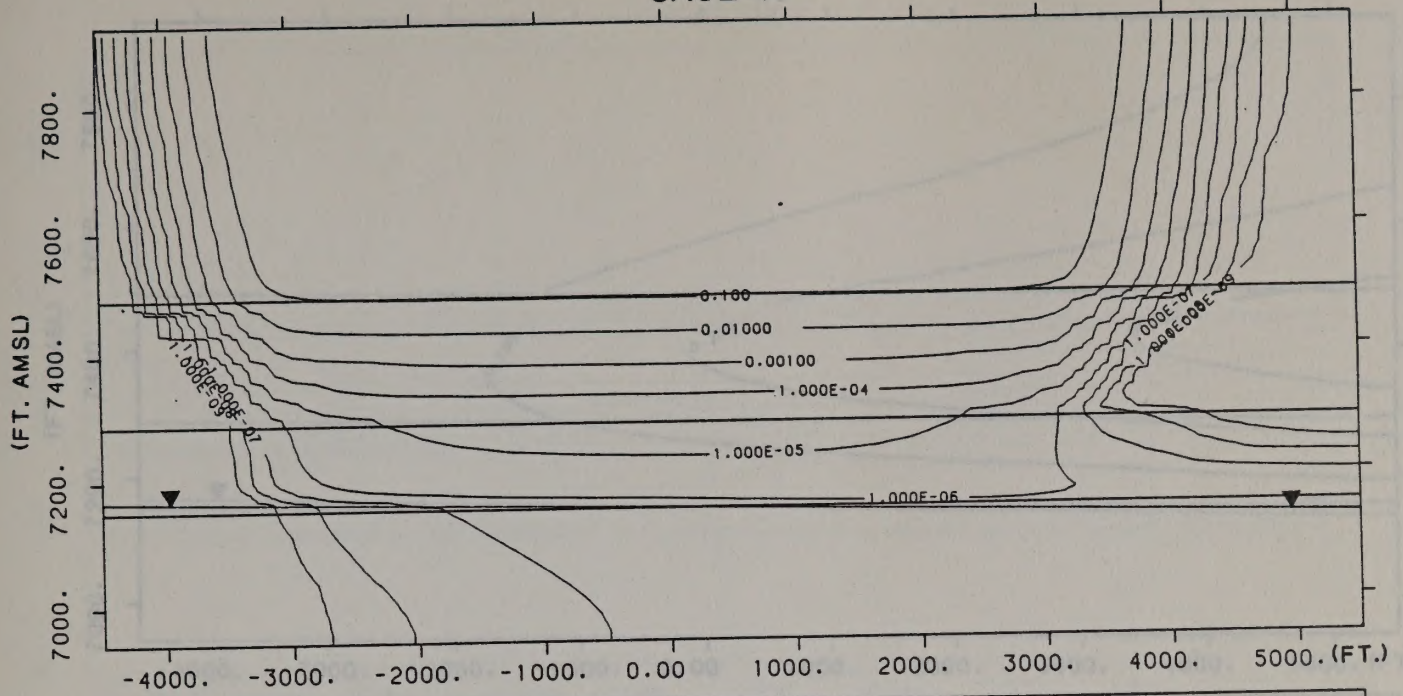
MOLYCORP: METAL TRANSPORT: 1.0 CFS SEEP RATE, $KH:KV=1:1$, ZERO KD CASE

CONTOURS OF NORMALIZED CONCENTRATION

TIME = 27 YEARS AFTER POND STARTUP

Figure H.8

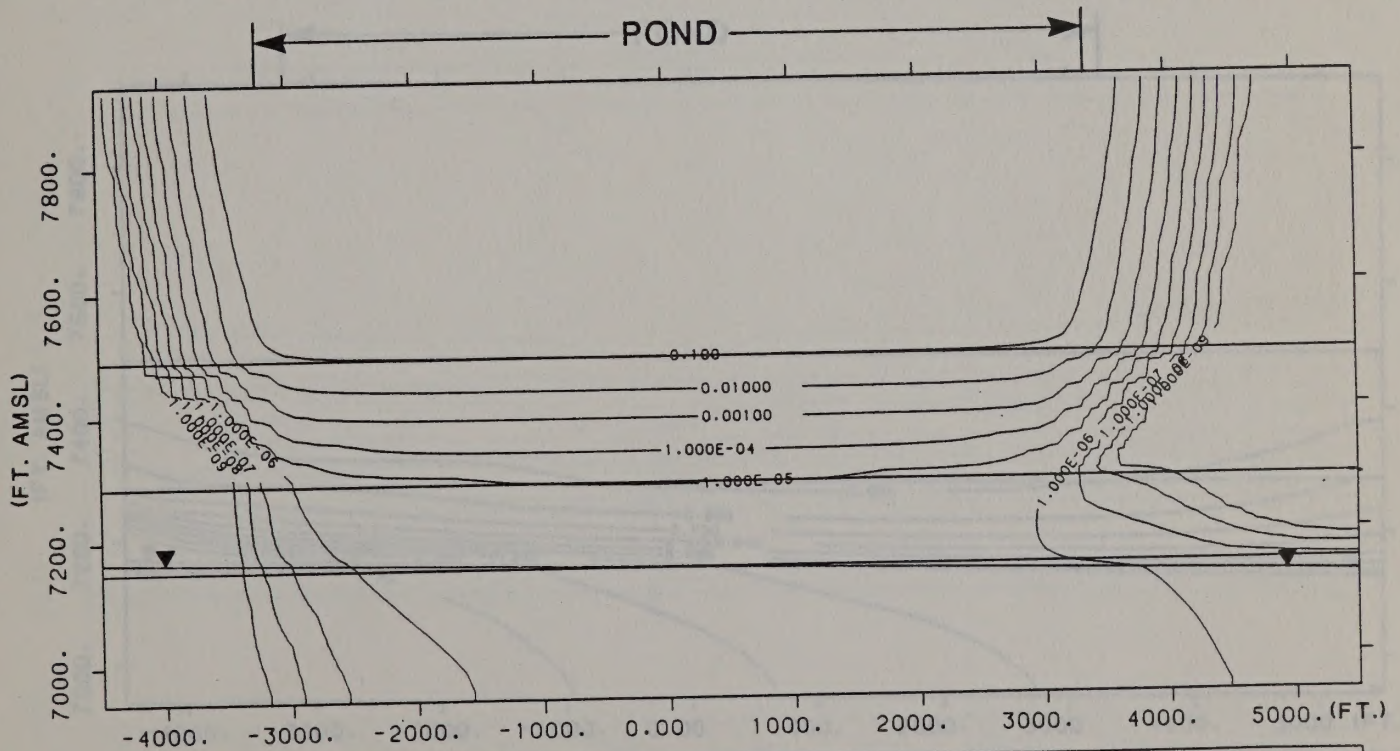
CASE 10



MOLYCORP: METAL TRANSPORT: 1.0 CFS SEEP RATE, $KH:KV=1:1$, MEDIUM KD CASE

CONTOURS OF NORMALIZED CONCENTRATION

TIME = 80 YEARS



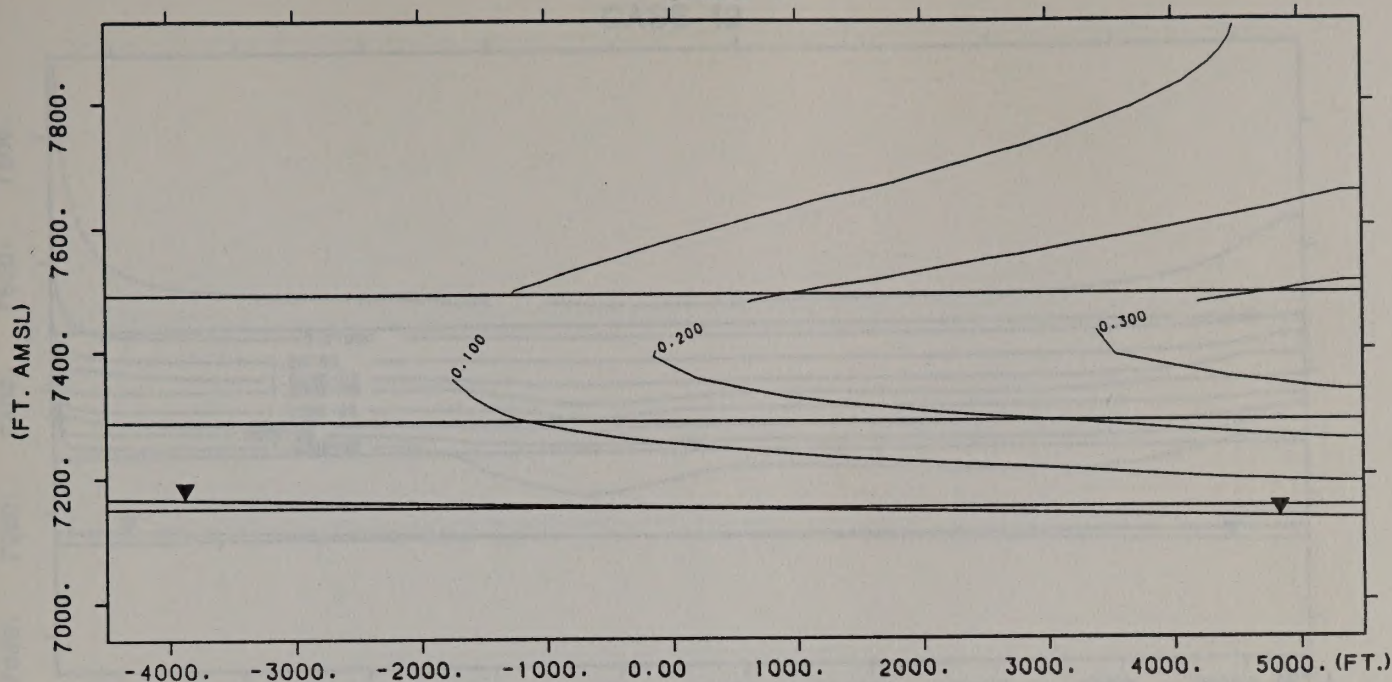
MOLYCORP: METAL TRANSPORT: 1.0 CFS SEEP RATE, $KH:KV=1:1$, MEDIUM KD CASE

CONTOURS OF NORMALIZED CONCENTRATION

TIME = 27 YEARS AFTER POND STARTUP

Figure H.9

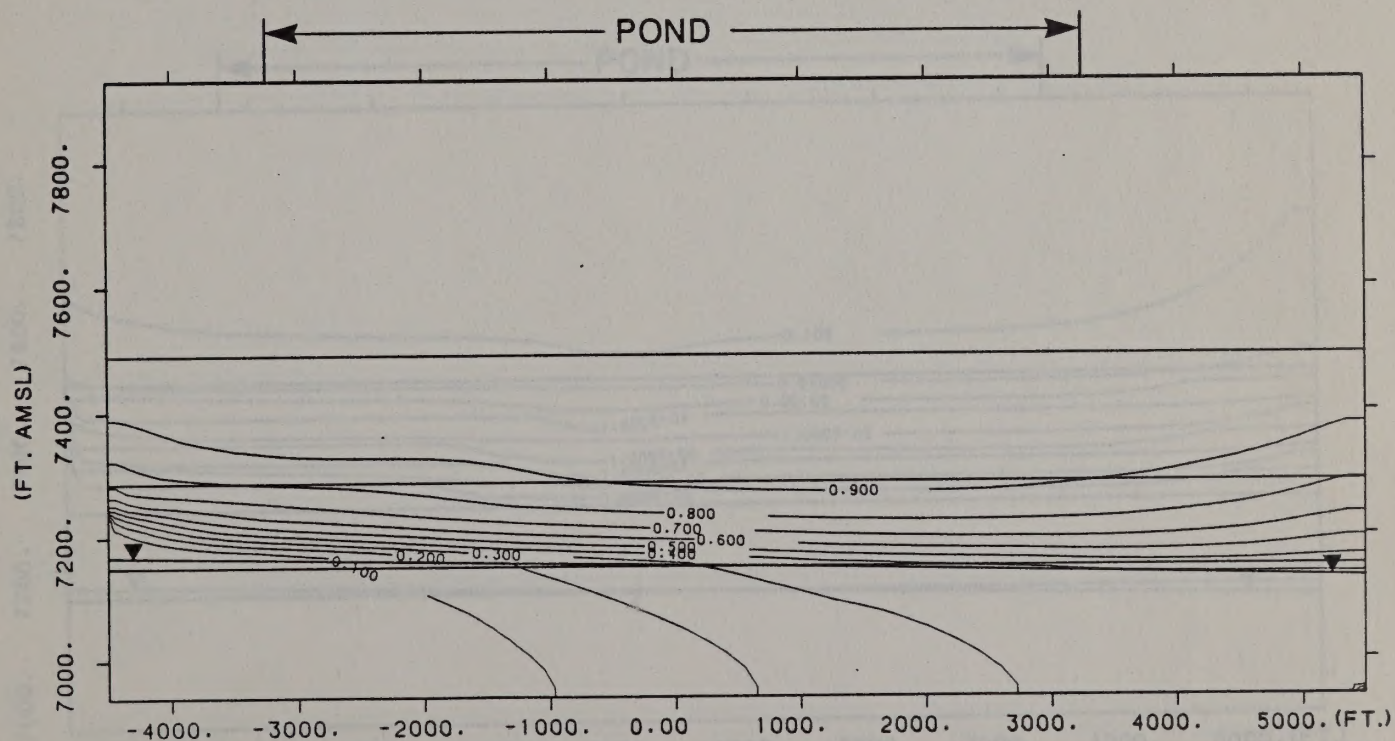
CASE 11



MOLY CORP: METAL TRANSPORT: 1.0 CFS SEEP RATE, $KH:KV=100:1$, ZERO KD CASE

CONTOURS OF NORMALIZED CONCENTRATION

TIME = 80 YEARS



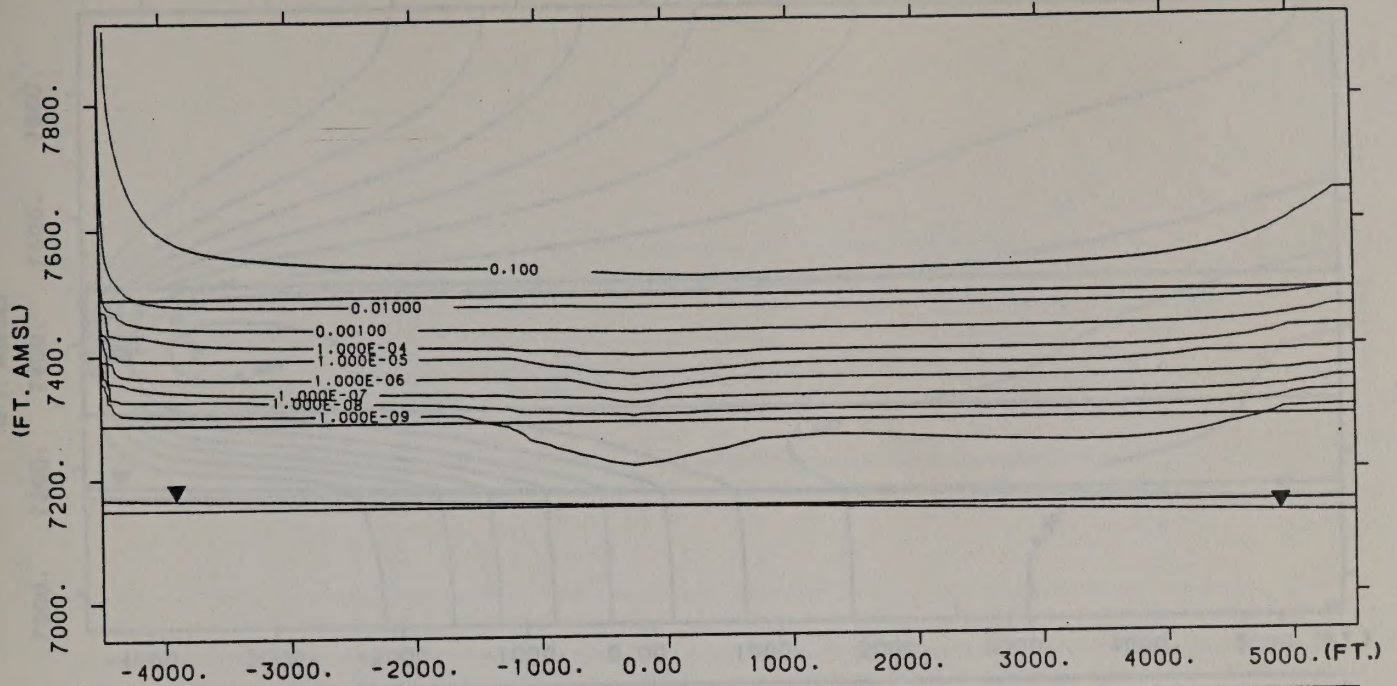
MOLY CORP: METAL TRANSPORT: 1.0 CFS SEEP RATE, $KH:KV=100:1$, ZERO KD CASE

CONTOURS OF NORMALIZED CONCENTRATION

TIME = 27 YEARS AFTER POND STARTUP

Figure H.10

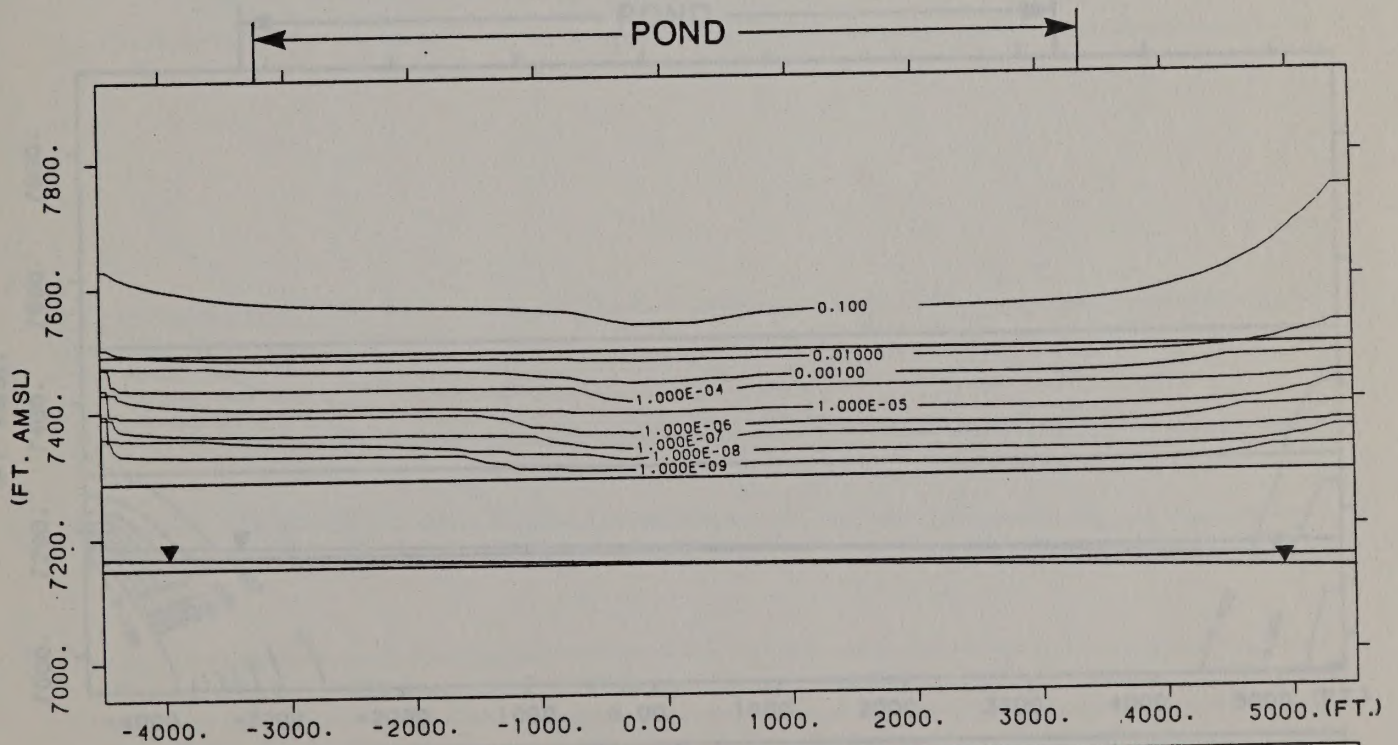
CASE 12



MOLYCORP: METAL TRANSPORT: 1.0 CFS SEEP RATE, $KH:KV=100:1$, MEDIUM KD CASE

CONTOURS OF NORMALIZED CONCENTRATION

TIME = 80 YEARS



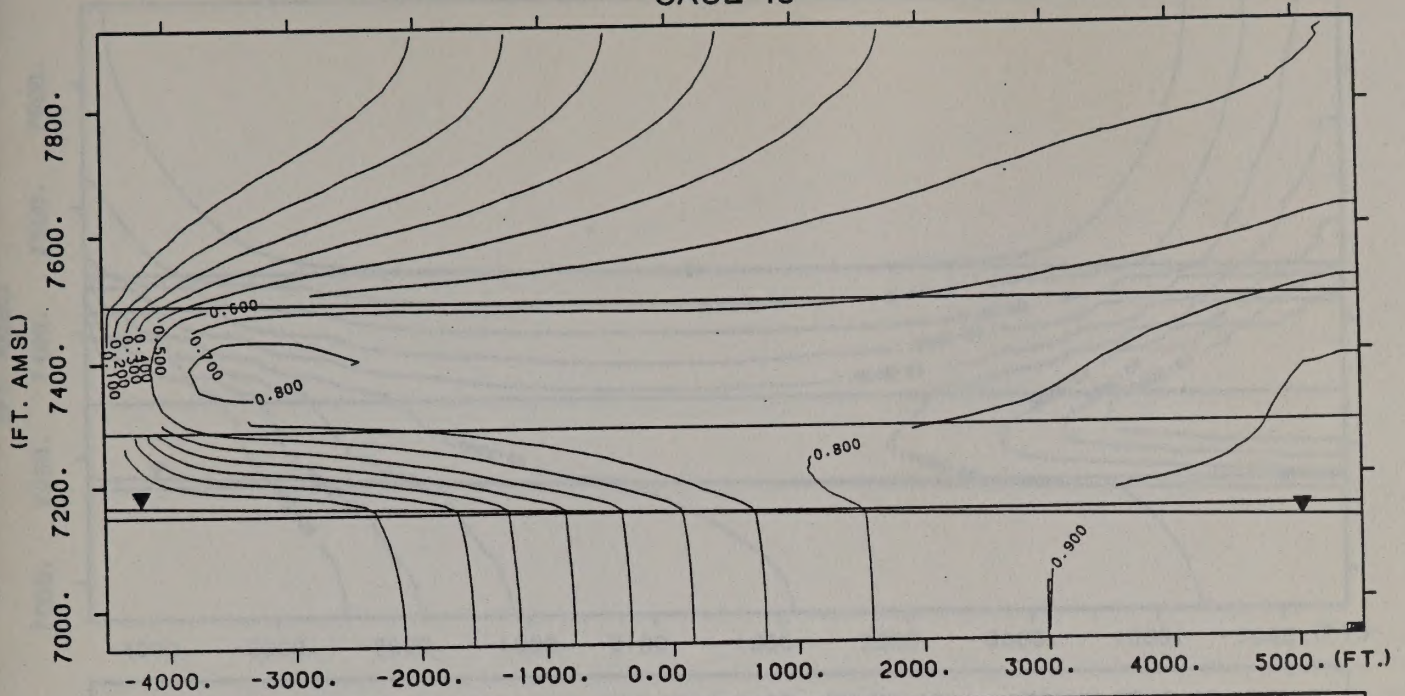
MOLYCORP: METAL TRANSPORT: 1.0 CFS SEEP RATE, $KH:KV=100:1$, MEDIUM KD CASE

CONTOURS OF NORMALIZED CONCENTRATION

TIME = 27 YEARS AFTER POND STARTUP

Figure H.11

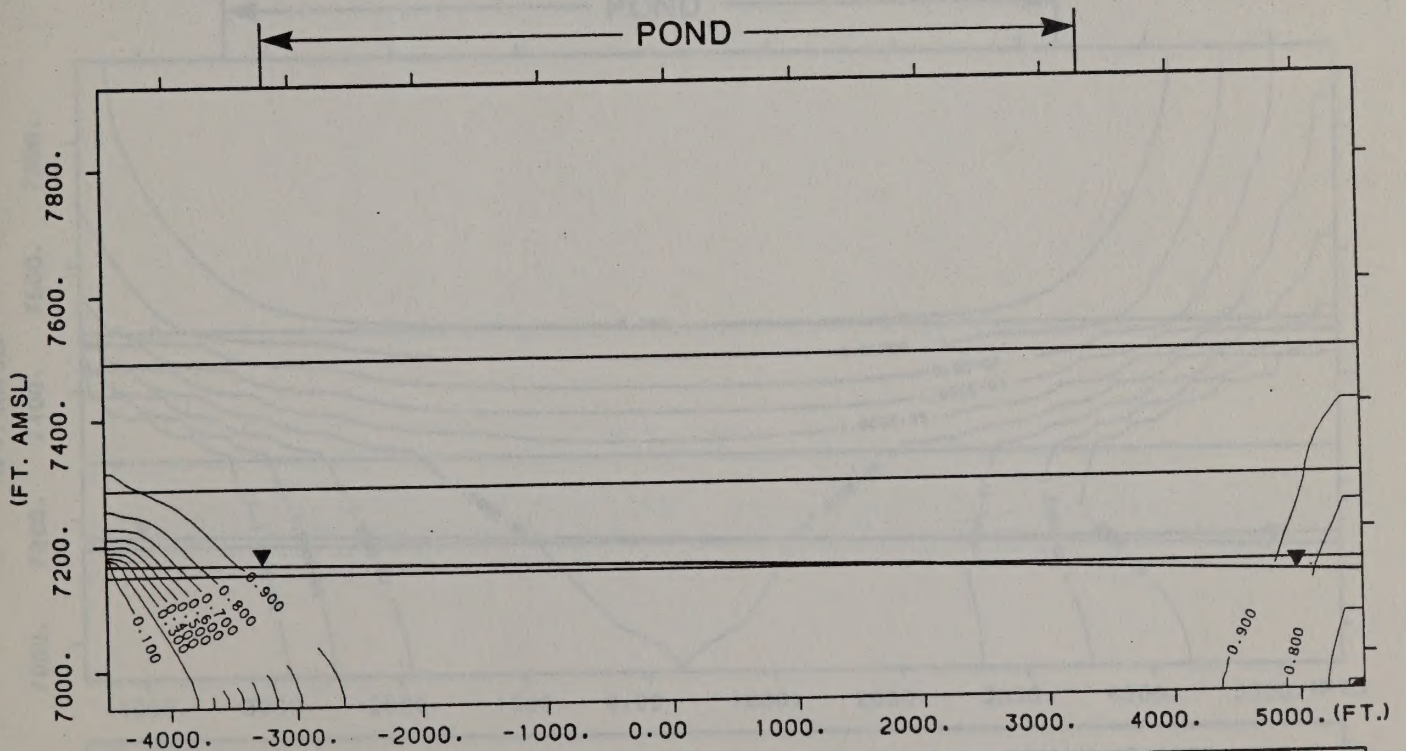
CASE 13



MOLYCORP: METAL TRANSPORT: 1.0 CFS SEEP RATE, $KH:KV=10:1$, ZERO KD CASE, LOW K

CONTOURS OF NORMALIZED CONCENTRATION

TIME = 80 YEARS



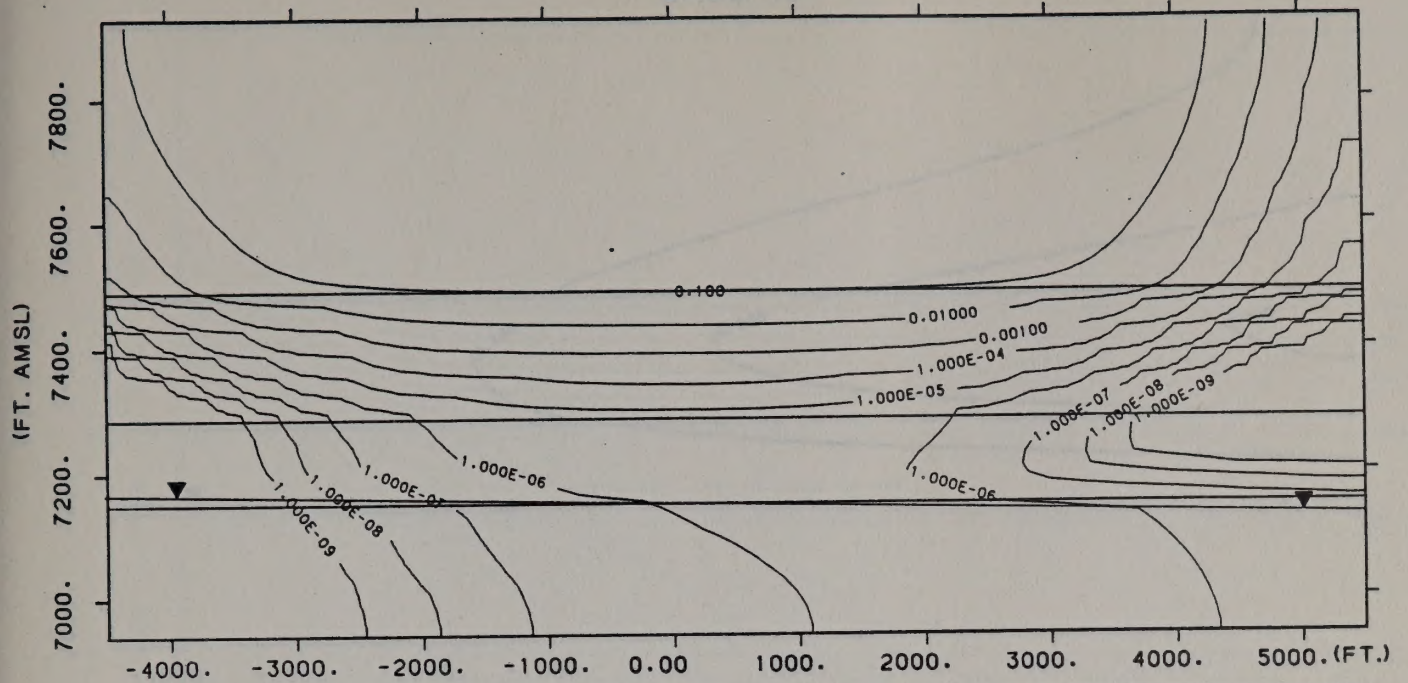
MOLYCORP: METAL TRANSPORT: 1.0 CFS SEEP RATE, $KH:KV=10:1$, ZERO KD CASE, LOW K

CONTOURS OF NORMALIZED CONCENTRATION

TIME = 27 YEARS AFTER POND STARTUP

Figure H.12

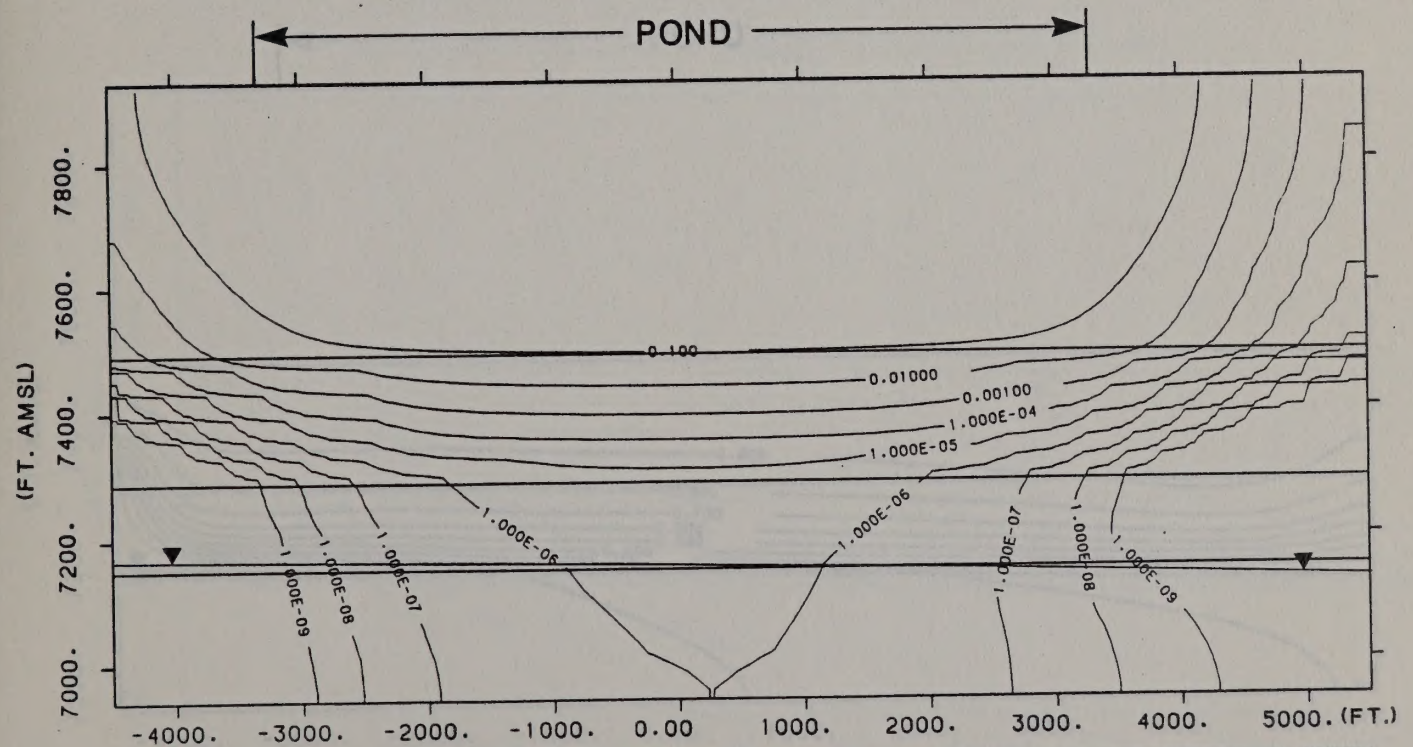
CASE 14



MOLY CORP: METAL TRANSPORT: 1.0 CFS SEEP RATE, KH:KV=10:1, MEDIUM KD CASE, LOW K

CONTOURS OF NORMALIZED CONCENTRATION

TIME = 80 YEARS



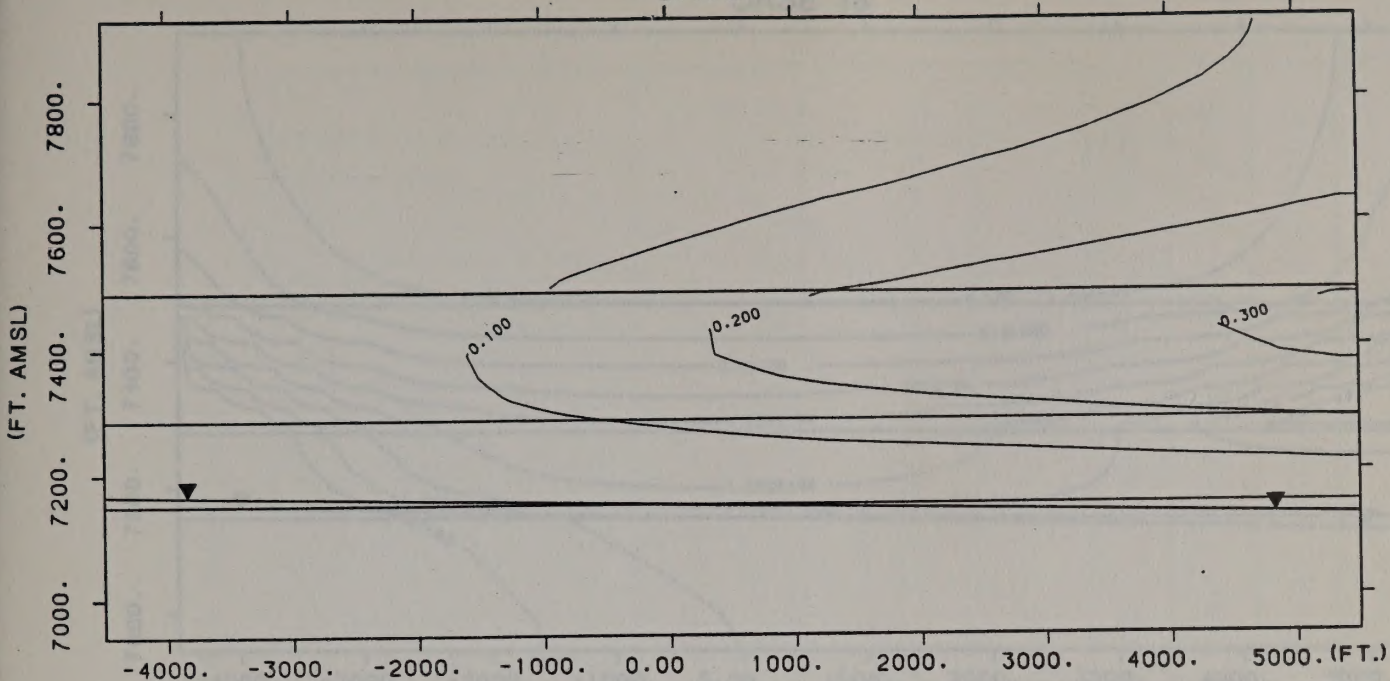
MOLY CORP: METAL TRANSPORT: 1.0 CFS SEEP RATE, KH:KV=10:1, MEDIUM KD CASE, LOW K

CONTOURS OF NORMALIZED CONCENTRATION

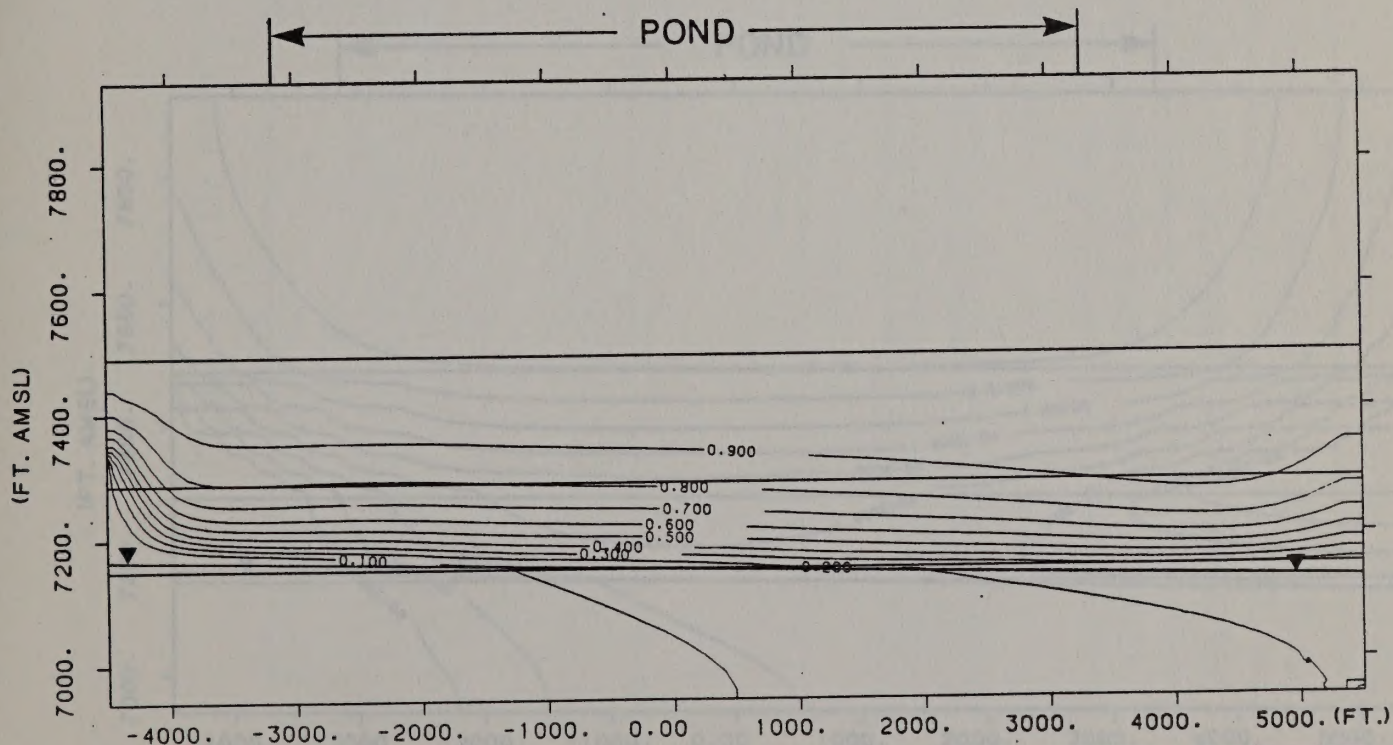
TIME = 27 YEARS AFTER POND STARTUP

Figure H.13

CASE 15



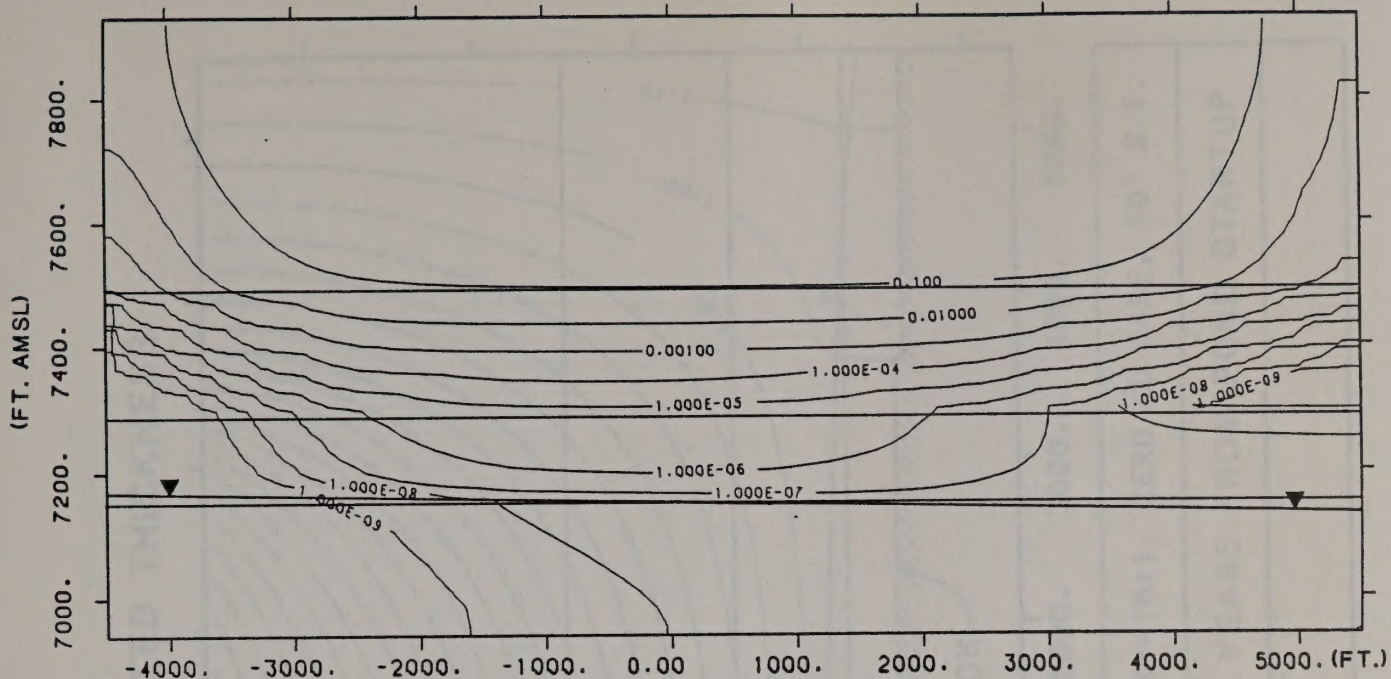
MOLYCORP: METAL TRANSPORT: 1.0 CFS SEEP RATE, $KH:KV=10:1$, ZERO KD CASE, HIGH K	
CONTOURS OF NORMALIZED CONCENTRATION	TIME = 80 YEARS



MOLYCORP: METAL TRANSPORT: 1.0 CFS SEEP RATE, $KH:KV=10:1$, ZERO KD CASE, HIGH K	
CONTOURS OF NORMALIZED CONCENTRATION	TIME = 27 YEARS AFTER POND STARTUP

Figure H.14

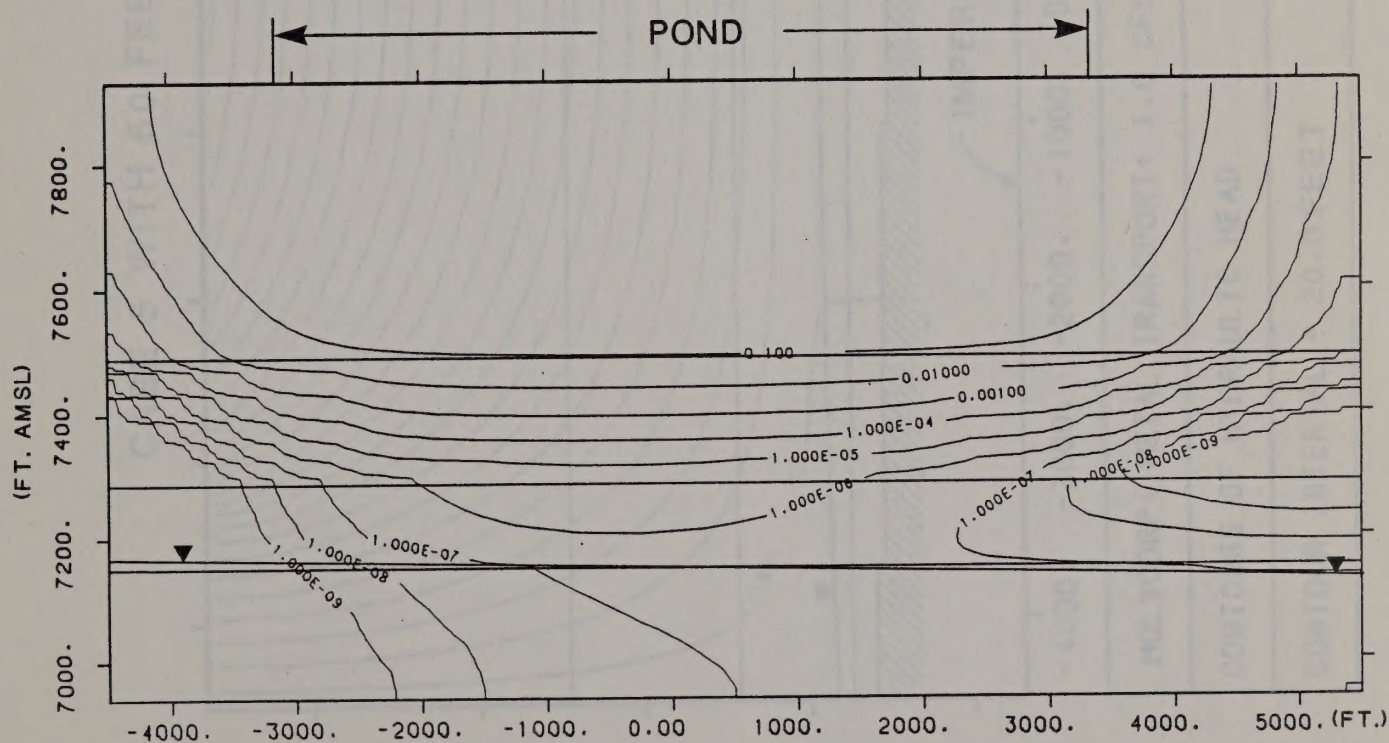
CASE 16



MOLY CORP: METAL TRANSPORT: 1.0 CFS SEEP RATE, KH:KV=10:1, MEDIUM KD CASE, HIGH K

CONTOUR OF NORMALIZED CONCENTRATION

TIME = 80 YEARS



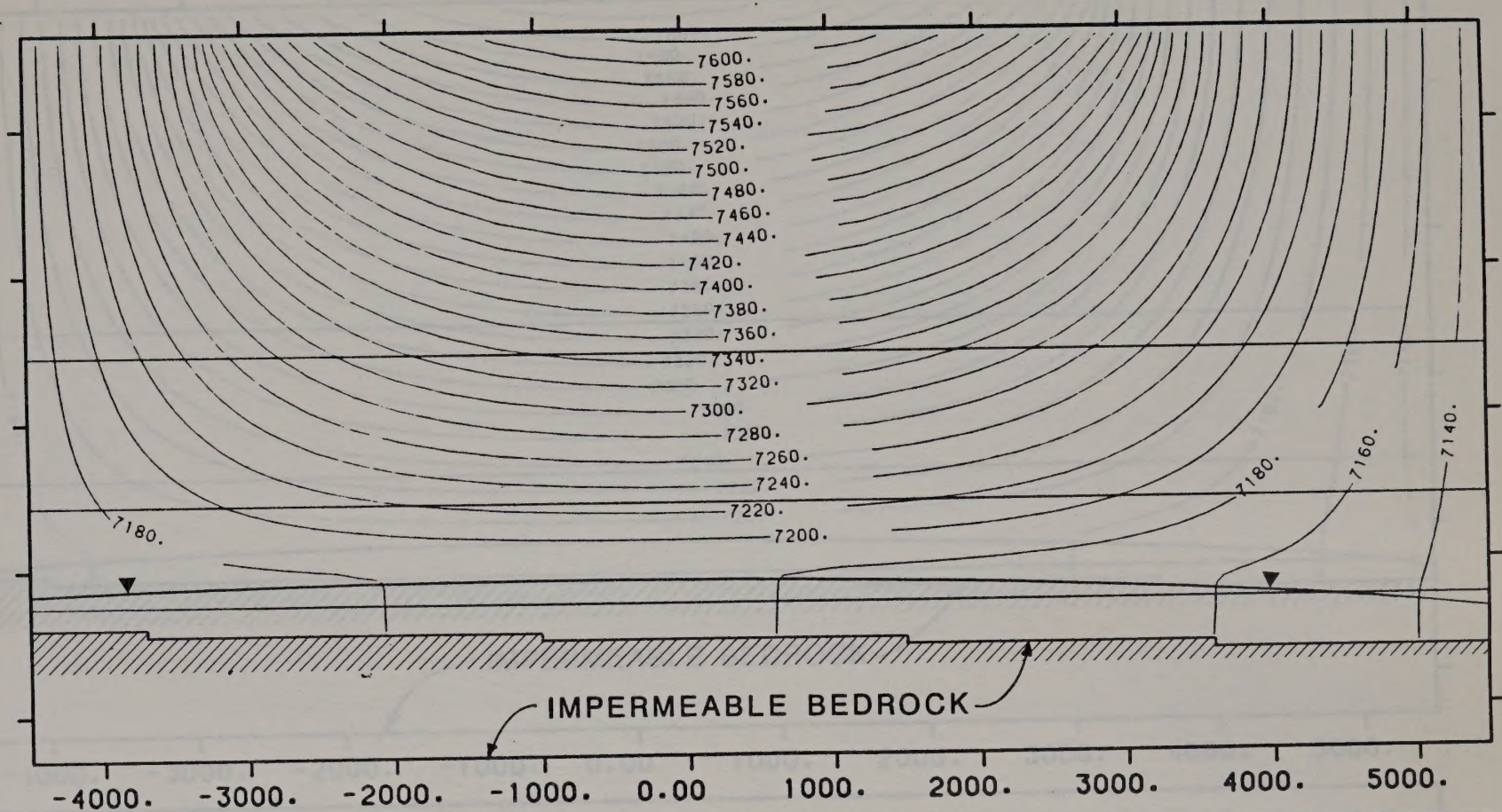
MOLY CORP: METAL TRANSPORT: 1.0 CFS SEEP RATE, KH:KV=10:1, MEDIUM KD CASE, HIGH K

CONTOUR OF NORMALIZED CONCENTRATION

TIME = 27 YEARS AFTER POND STARTUP

Figure H.15

CASE 5 WITH 50 FEET OF SATURATED THICKNESS



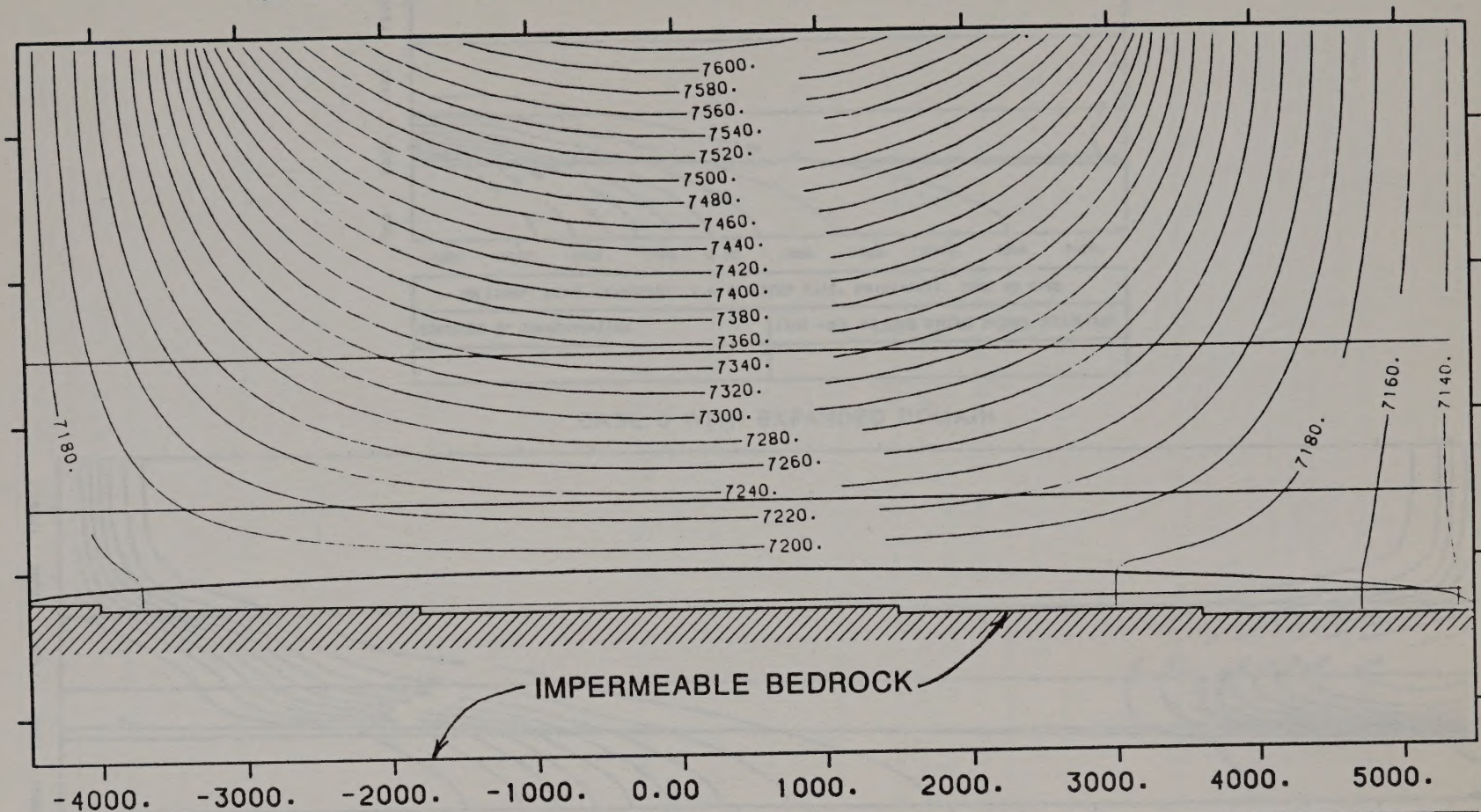
MOLYCORP: METAL TRANSPORT: 1.0 CFS SEEP RATE, $KH:KV=10:1$, ZERO KD CASE, 50' S.T.

CONTOURS OF HYDRAULIC HEAD

TIME = 27 YEARS FROM POND STARTUP

CONTOUR INTERVAL = 20.0 FEET

CASE 5 WITH 10 FEET OF SATURATED THICKNESS



MOLYCORP: METAL TRANSPORT: 1.0 CFS SEEP RATE, $KH:KV=10:1$, ZERO KD CASE, 10' S.T.

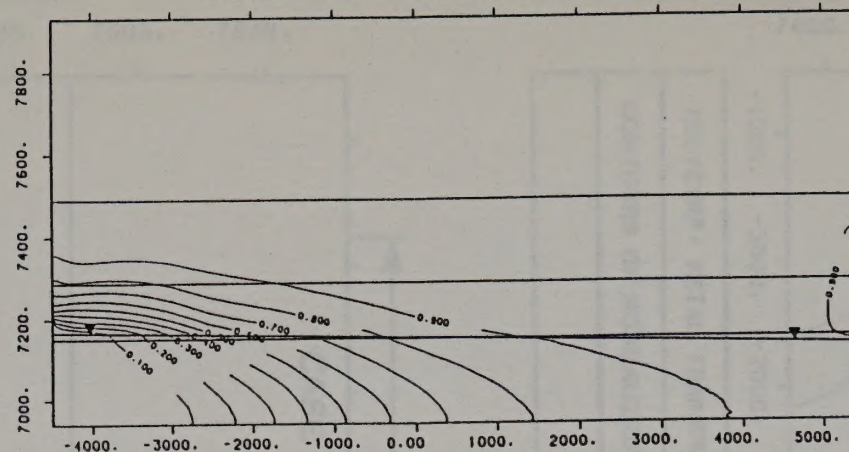
CONTOURS OF HYDRAULIC HEAD

TIME = 27 YEARS FROM STARTUP

CONTOUR INTERVAL = 20.0 FEET

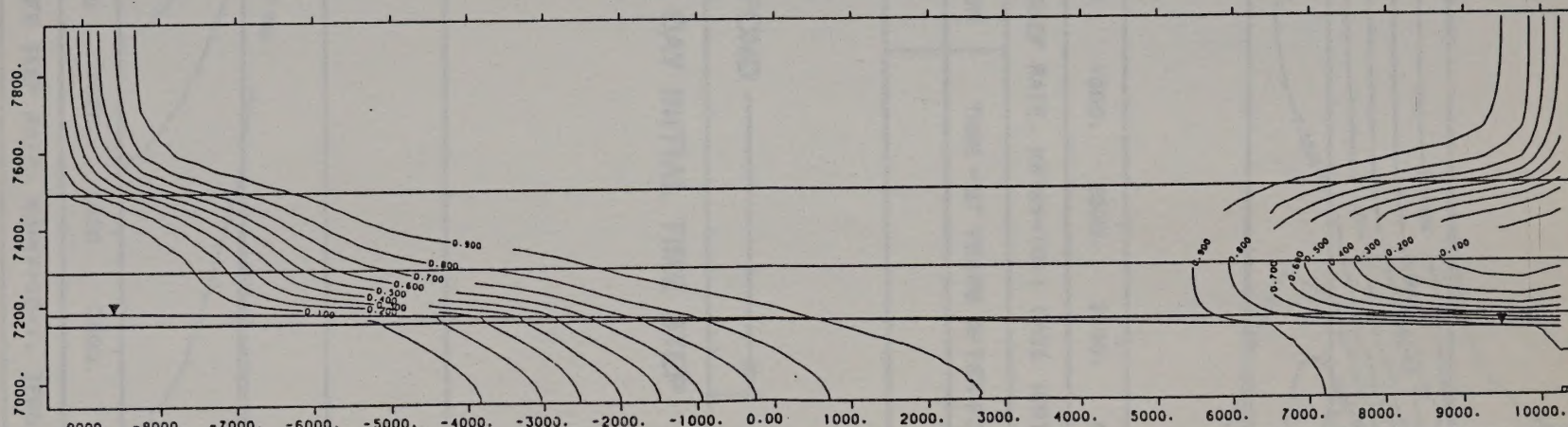
2-FEB-87 14:08:03 JOB1303

CASE 5 WITH ORIGINAL DOMAIN



MOLYCORP: METAL TRANSPORT: 1.0 CFS SEEP RATE, $KH:KV=10:1$, ZERO KD CASE	
CONTOURS OF CONCENTRATION	TIME = 27 YEARS FROM POND STARTUP

CASE 5 WITH EXPANDED DOMAIN



MOLYCORP: REVISED DOMAIN: TRANSIENT ANION TRANSPORT: $KH:KV=10:1$ ZERO KD (MOLY5-2)	
CONTOURS OF NORMALIZED CONCENTRATION	TIME = 27 YEARS FROM POND STARTUP

Figure H.18

CASE 3 WITH

10000 10000 10000 10000 10000 10000 10000 10000 10000 10000

METAL TRANSPORT 1.0 CFS SEEP RATE, CHLORIDE CASE

CONCENTRATION OF NORMALIZED CONCENTRATION

TIME - 21 YEARS AFTER POND

POND

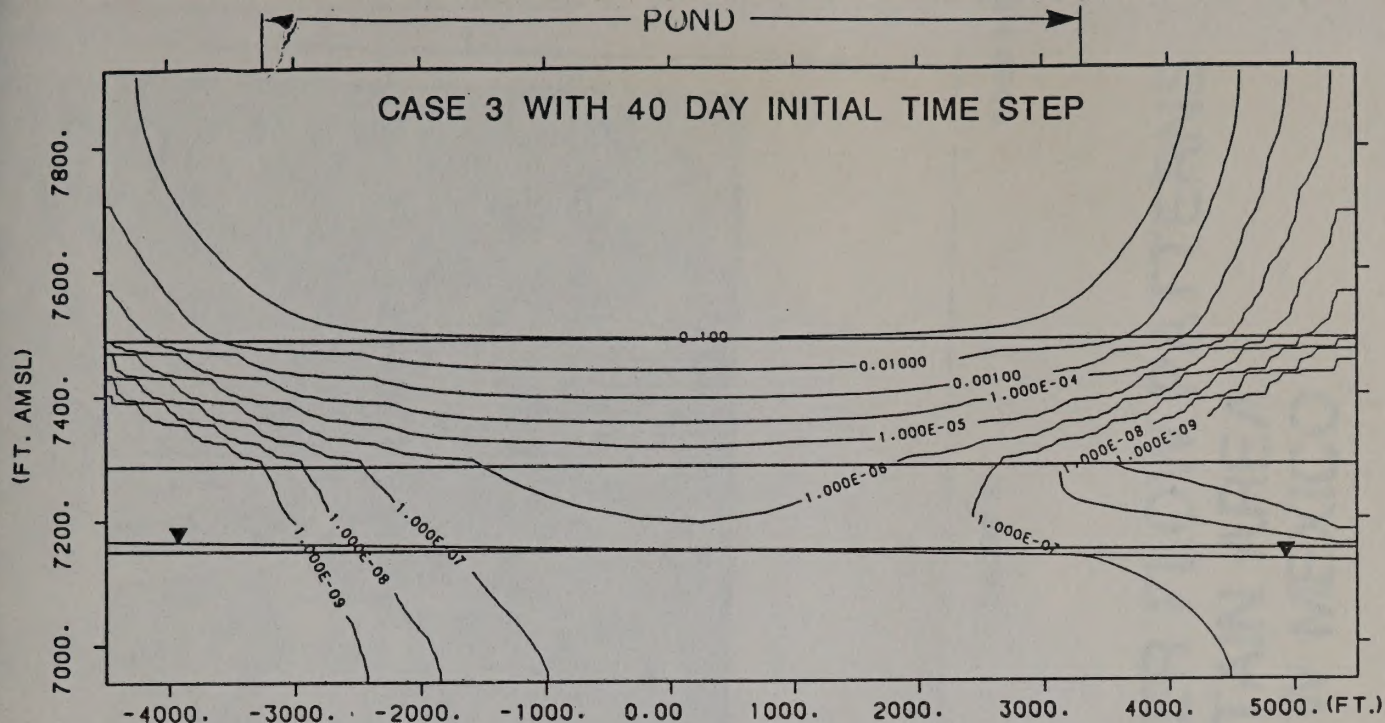
CASE 3 WITH 40 DAY INITIAL TIME STEP

10000 10000 10000 10000 10000 10000 10000 10000 10000 10000

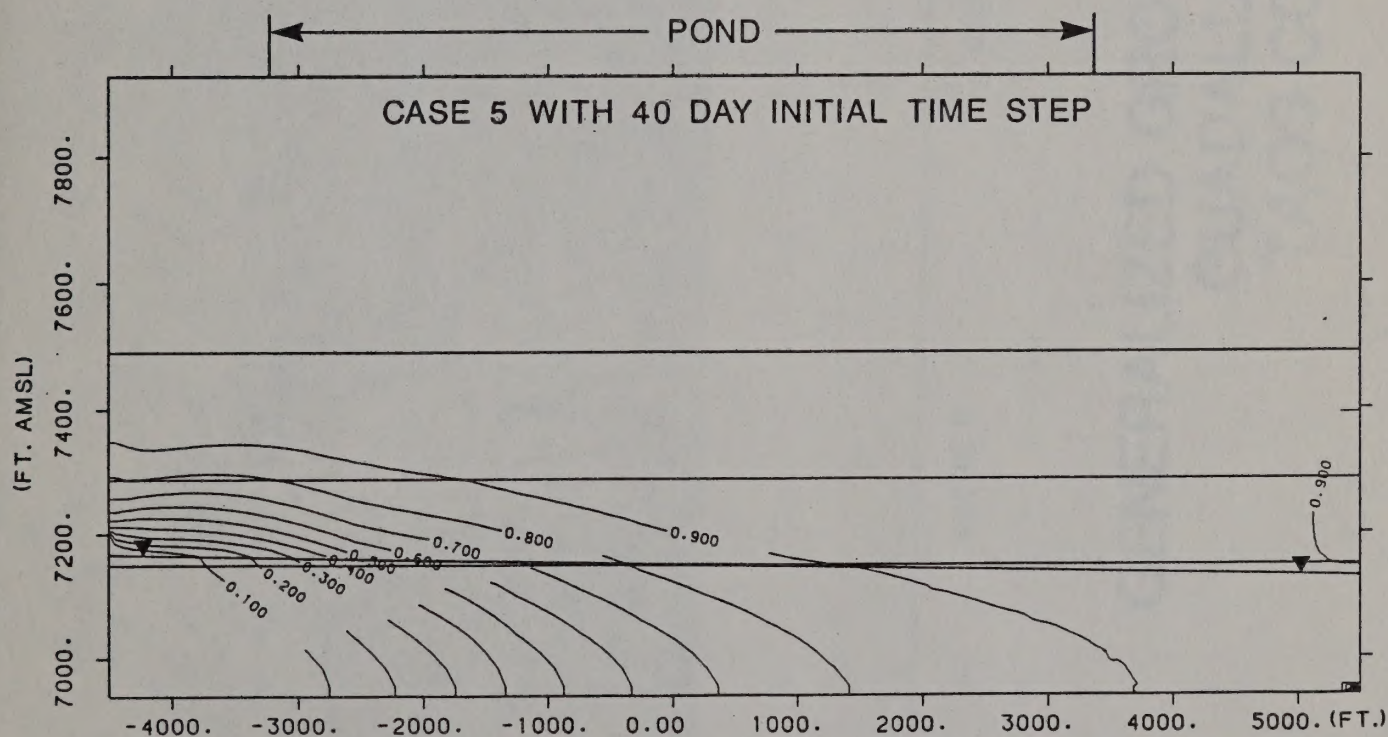
METAL TRANSPORT 1.0 CFS SEEP RATE, CHLORIDE CASE

CONCENTRATION OF NORMALIZED CONCENTRATION

TIME - 21 YEARS AFTER POND



MOLYCORP: METAL TRANSPORT: 1.0 CFS SEEP RATE, KH:KV=10:1 CASE (UNITS FT DAYS)	
CONTOURS OF NORMALIZED CONCENTRATION	TIME = 27 YEARS AFTER POND STARTUP



MOLYCORP: METAL TRANSPORT: 1.0 CFS SEEP RATE, KH:KV=10:1, ZERO KD CASE	
CONTOURS OF NORMALIZED CONCENTRATION	TIME = 27 YEARS AFTER POND STARTUP

Figure H.19



Plate 1
GEOLOGIC MAP OF THE GUADALUPE MOUNTAIN AREA
 TAOS COUNTY, NEW MEXICO
 SCOTT G. VAIL
 1987

0 5000 10,000
 FEET

EXPLANATION

- | | | | |
|--|--|--|---|
| al | Alluvium: interflow, surficial and older alluvial deposits. | | contact, dashed where approximate |
| sb | Servilleta basalt: tabular flood basalt flows, undifferentiated. | | fault, dashed where approximate or inferred; dotted where buried. |
| gv | Volcanic Rocks of Guadalupe Mountain: lobate, dacite flows and minor olivine andesite. | | volcanic vent area. |
| ql | Quartz latite of Cerro Chiflo: flow dome and small pyroclastic cone exposed in Rio Grande Gorge. | | average flow direction, of volcanics |

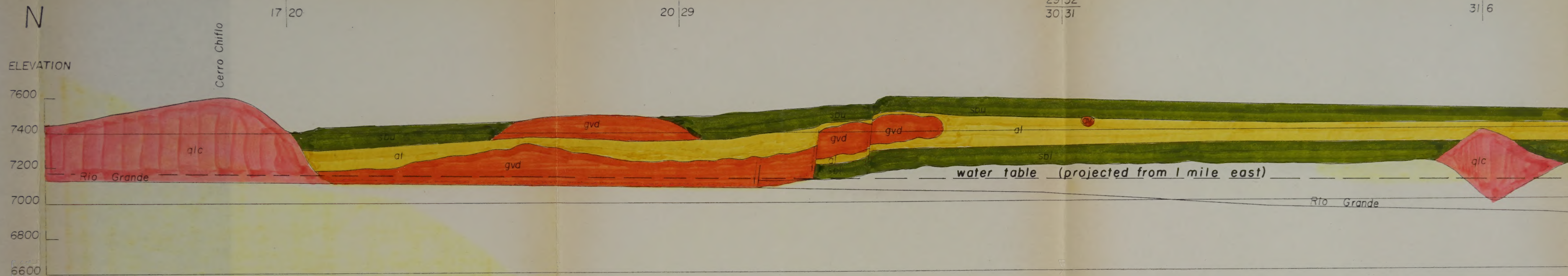
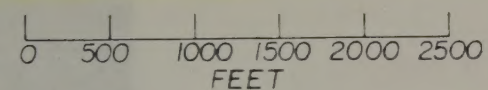


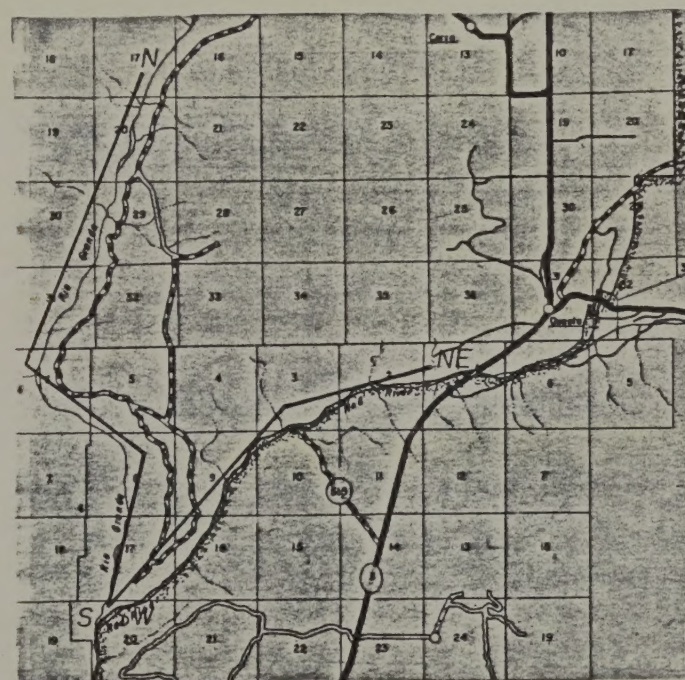
Plate 2

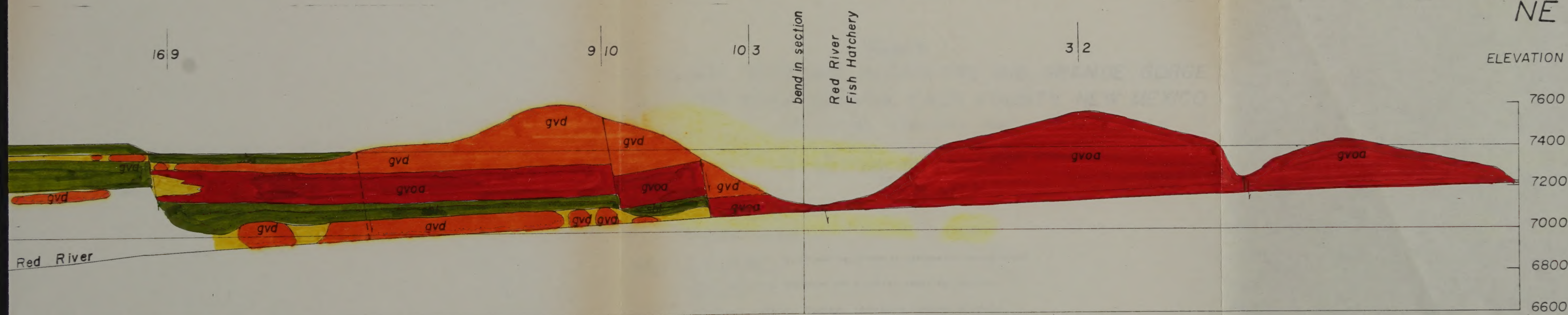
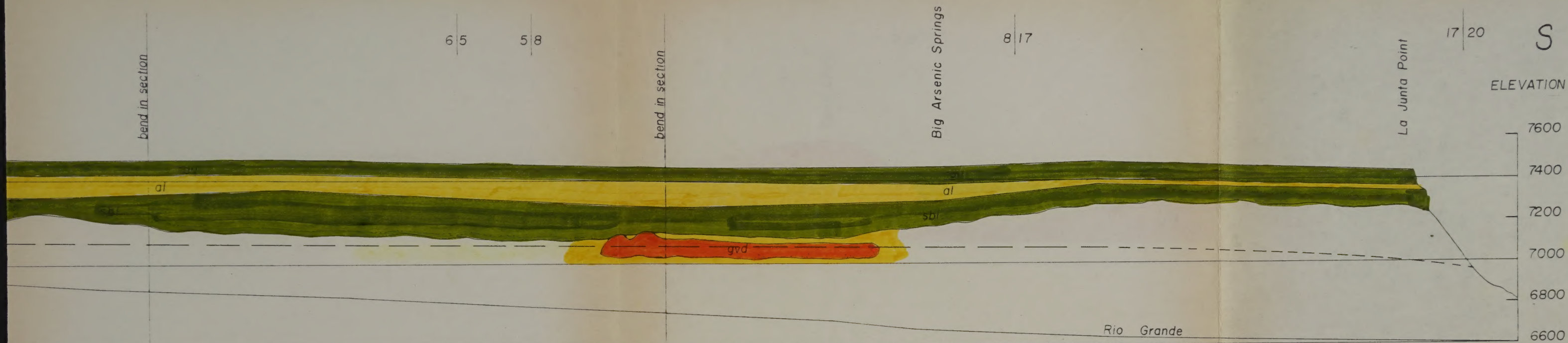
GEOLOGIC SECTIONS ALONG THE RIO GRANDE GORGE
AND RED RIVER CANYON, TAOS COUNTY, NEW MEXICO

SCOTT G. VAIL FEBRUARY, 1987



- Cover: talus and slump blocks.
- Serrillita flood basalt; olivine-bearing; grouped as upper (sbu) and combined middle and lower (sbl) members.
- Alluvium: conglomerate, sandstone, and siltstone; mostly derived from mountains to east.
- Volcanic flows of Guadalupe Mountain; lobate dacite flows (gvd) and olivine andesite.
- Quartz latite of Cerro Chiflo.





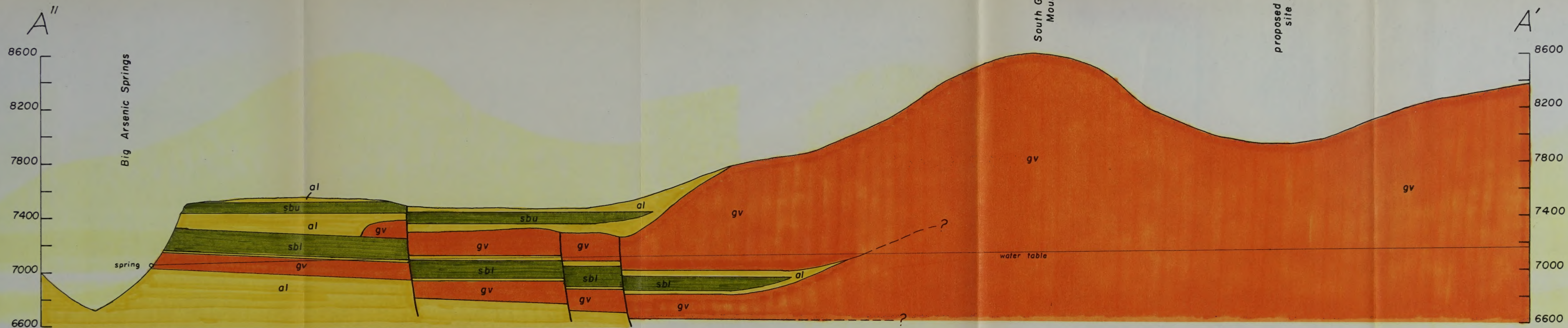


- al interflow and surficial alluvial deposits.
- sbu Servilleta Basalt, upper (sbu) and combined middle and lower (sbi) units.
- gv volcanic flows of Guadalupe Mountain: dacite and olivine andesite, undifferentiated.

"Cross Section From Rio Grande Gorge North of Arsenic Springs to Guadalupe Mountain Saddle."

Plate 3
GEOLOGIC CROSS SECTION
GUADALUPE MOUNTAIN AREA
TAOS COUNTY, NEW MEXICO
 SCOTT G. VAIL MARCH 1987

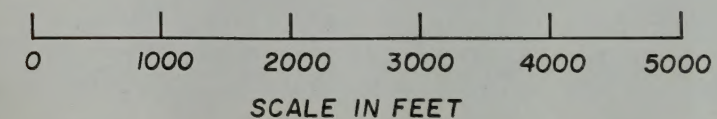
0 1000 2000 3000 4000 5000
 SCALE IN FEET



- al interflow and surficial alluvial deposits.
- sbu Servilleta Basalt, upper (sbu) and combined middle and lower (sbl) units.
- gv volcanic flows of Guadalupe Mountain: dacite and olivine andesite, undifferentiated.

"Cross Section From Big Arsenic Springs to Guadalupe Mountain Saddle."

Plate 4
GEOLOGIC CROSS SECTION
ARSENIC SPRINGS AREA
TAOS COUNTY, NEW MEXICO
 SCOTT G. VAIL MARCH 1987



55000 N

50000 N

45000 N

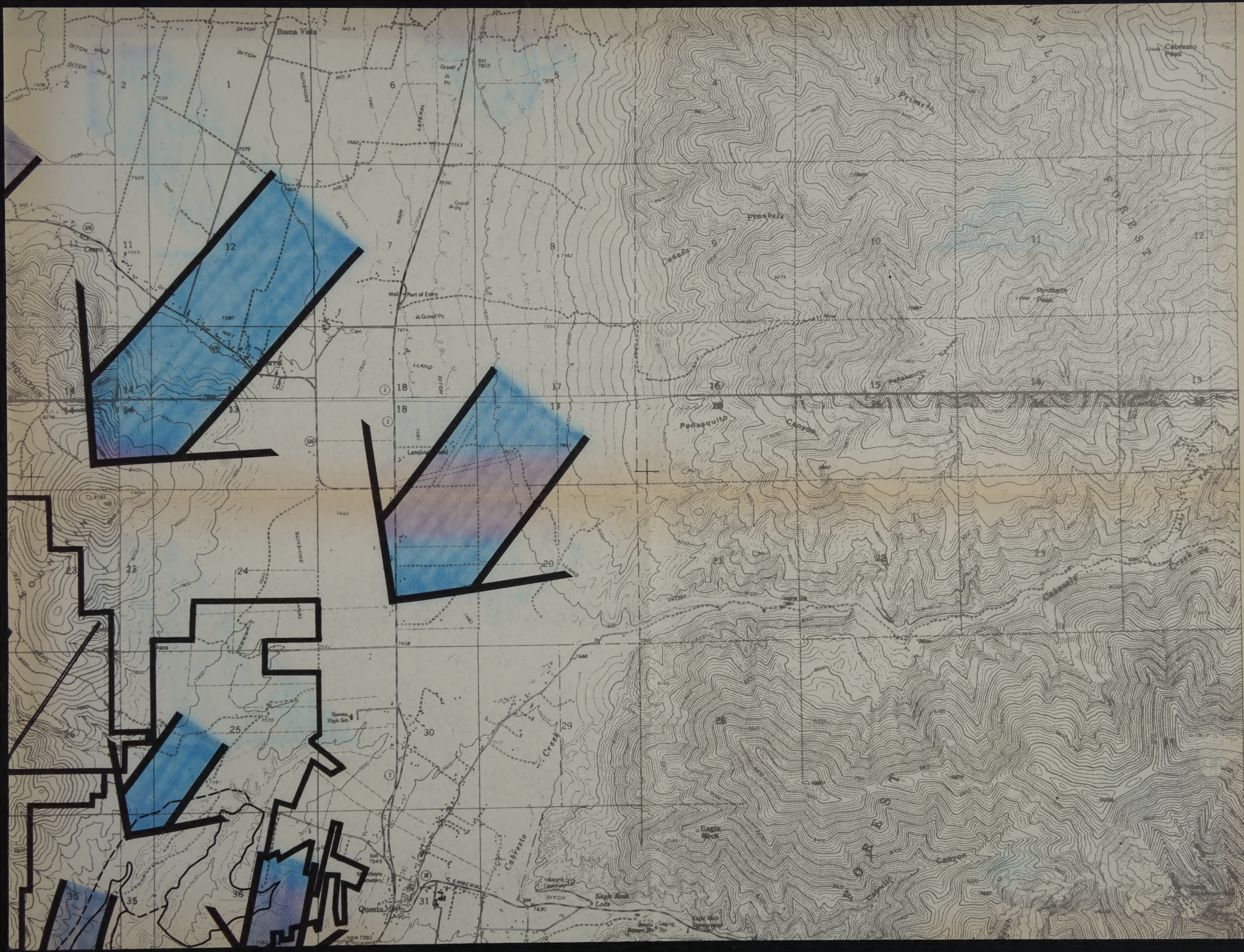
40000 N

35000 N

30000 N

25000 N





20000 N

15000 N

10000 N

5000 N

0
10000 W

5000 W

0

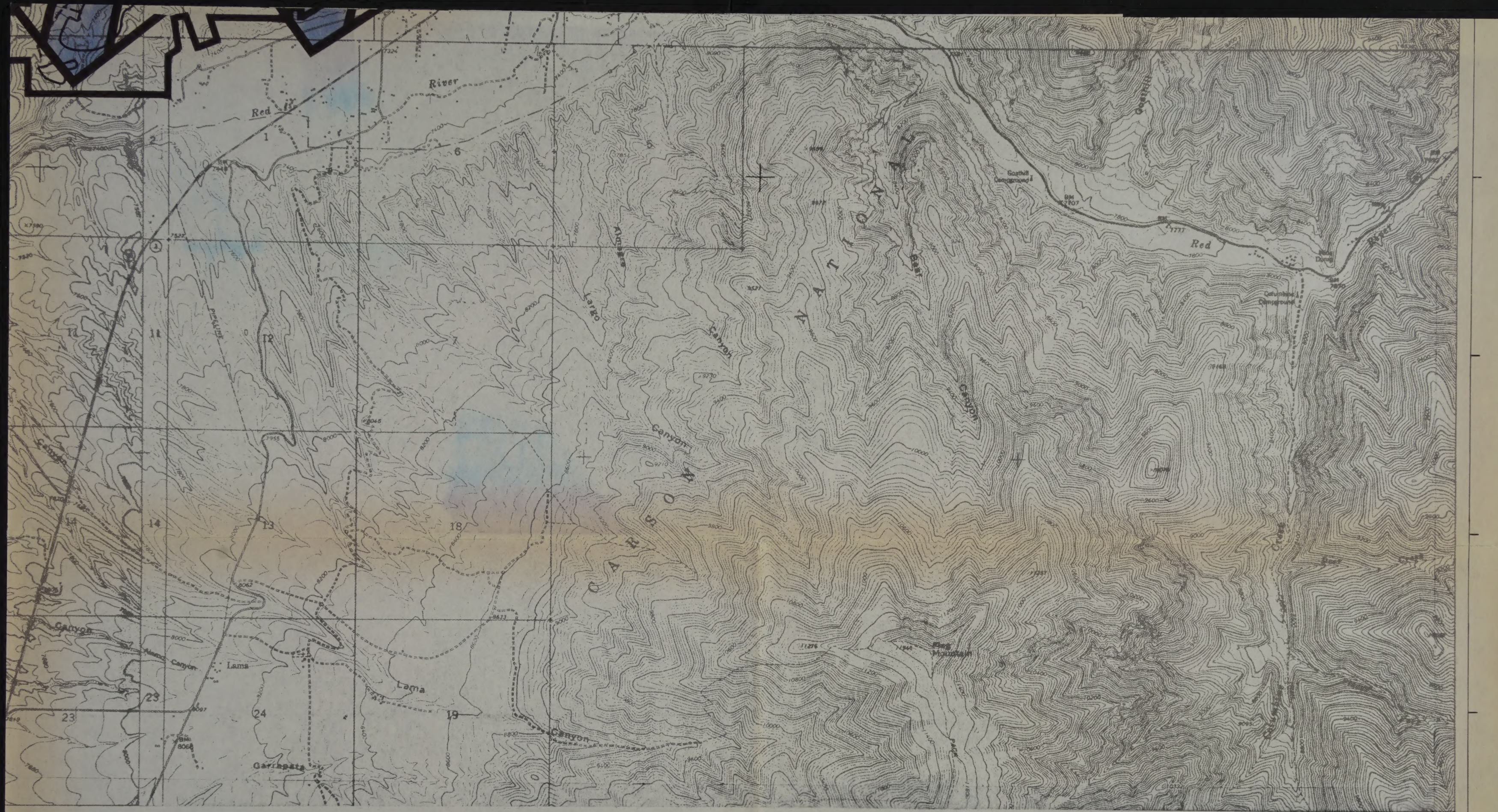
5000 E

10000 E

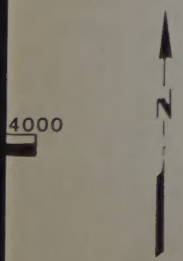
15000 E

SCALE
2000
FEET





20000 E 25000 E 30000 E 35000 E 40000 E 45000 E 50000 E 55000 E 60000 E



GENERALIZED GROUND-WATER FLOW PATTERNS
GUADALUPE MOUNTAIN AREA
TAOS COUNTY, NEW MEXICO

